Developing multiplex molecular diagnostics for tropical pathogens

Witchayoot Huangsuranun

Christ Church

University of Oxford

A thesis submitted for the degree of

Doctor of Philosophy

April 2025

Abstract

Acute undifferentiated fevers are illnesses with generalised symptoms, making clinical diagnosis difficult. Diagnosis largely depends on laboratory tests, however, access to these tests can be limited in rural areas of low- and middle-income countries (LMICs) due to the remoteness of these areas as well as the high cost of the tests.

This thesis explores the theme of diagnostics for acute undifferentiated fever (AUF) in rural South and Southeast Asia, making them more accessible and economical both for service providers/patients and as a surveillance tools. Three diagnostic tests were developed around this concept. Oligonucleotides for real-time PCR assays were designed to detect multiple targets from a single specimen. A rapid test based on CRISPR technology was developed as a point-of-care (POC) test that can be done outside laboratory settings. A protocol for a molecular detection of viruses was developed to evaluate using dried blood spots (DBS), a more convenient specimen type, on the automated BD MAX™ instrument. Lastly, the Chembio DPP® Fever Panel II Asia System, consisting of an antigen and IgM antibody cassette was evaluated both in the laboratory and at site using patient whole blood samples.

This thesis is part of the South and Southeast Asia Community-based Trials Network (SEACTN) research programme which aims to investigate the morbidity and mortality in rural communities across South and Southeast Asia. The real-time reverse transcriptase (RT) PCR tests for whole blood and DBS will be used to detect pathogens in patient samples collected in SEACTN.

Dedicated to the memory of Dr Andy Porter

Acknowledgement

I would like to express my deepest appreciation to my supervisory team, Dr Elizabeth Batty, Dr Janjira Thaipadungpanit, Professor Yoel Lubell, and Dr Chaiyasith Uttamapinant for their continuous support throughout my DPhil studies in both scientifically and emotionally. Thank you also to my mentor, Dr Yanin Pittayasathornthun, for her encouragement over the years.

This project was made possible by the support from three funding bodies: SEACTN, The Mahidol-Oxford Translational Innovation Partnership (MOTIP) Technical Support Accelerator (TSA) Award, and The Nuffield Department of Medicine Tropical Network Fund. I would like to express my gratitude for their support.

I would also like to thank Panuvit Rienpradub and Saranya Wongrattanapipat among others from the Molecular Microbiology Laboratory for Diagnosis and Epidemiology (MoMiLDE) team at MORU for their help in and out of the laboratory as well as being incredible colleagues and friends. This gratitude is extended to my other peers at MORU/Oxford Tropical Network including but most definitely not limited to Watcharintorn Thongpiam and Professor Stuart Blacksell as well as my colleagues at the Chiangrai Clinical Research Unit (CCRU), led by Dr Carlo Perrone. Much appreciation also to the Department of Paediatrics, Faculty of Tropical Medicine, Mahidol University for their support in scientific advice and help with culturing the viruses used for this project. Special thanks go to Dr Maturada Patchsung at the Vidyasirimedhi Institute of Science and Technology (VISTEC) as well as the MORU postgraduate studies team; Dr Leigh Jones and Pawadee Boonyakanjanapon.

A heartfelt thank you to my family, most of all to my mothers who let me pursue my dreams and continuously supported me even if they still don't quite understand what exactly it is that I do, and to my partner, Buranee Chinotaikul for always having my back. Thank you to all my friends and colleagues both old and new for the company and encouragement over the years.

Declaration

I hereby declare that this thesis is of my own work with the guidance and support of my supervisory team; Dr Elizabeth Batty, Dr Janjira Thaipadungpanit, Professor Yoel Lubell, and Dr Chaiyasith Uttamapinant.

I also declare that, to the best of my knowledge, this thesis contains no previously published materials nor materials submitted or awarded a degree at any university or institution. The content of this thesis is the product of my own work, of which the majority of the laboratory experiments was conducted by myself. It is also important to acknowledge the contributions of the Molecular Microbiology, SEACTN, and CCRU teams at MORU, as well as the School of Biomolecular Science & Engineering team at VISTEC including in routine laboratory work, scientific guidance, and logistical aid.

Impact of the COVID-19 pandemic

This project was impacted by the COVID-19 pandemic as a travel restriction was placed in Bangkok, Thailand from July 12th to September 1st, 2021. The Faculty of Tropical Medicine, Mahidol University, and by extension, MORU, also disallowed use of any facilities between July 20th and September 5th, 2021. Without access to the lab, the project was halted during this time until restrictions slowly eased up.

The work originally planned for this period includes optimising the DENV real-time RT-PCR assay as well as optimising the rapid extraction protocol using the QuickExtract DNA extraction solution as suggested by Lucigen's technical support team. Initial isothermal amplification testing with LAMP was also planned, with the reagents already ordered and received. Unfortunately, they were near their expiry date by the time restriction lifted. Instead of the aforementioned lab work, this period was focused on literature review and the start of writing the introduction and methods of this thesis. LAMP and RPA primers were also sought after in literature and by designing from scratch.

Overall, while most of the planned lab work was able to be completed within the timeframe, the pandemic did delay lab work by several months.

List of abbreviations

Abbreviation	Definition
ABS	Acrylonitrile butadiene styrene
ADE	Antibody-dependent enhancement
AMR	Antimicrobial resistance
AUC	Area under the curve
AUF	Acute undifferentiated fever
BHQ	Black Hole Quencher
BIP	Backward internal primer
BSC	Biosafety cabinet
BSL	Biosafety level
C	Capsid
Cas	CRISPR associated
CCRU	Chiang Rai Clinical Research Unit
cDNA	Complementary DNA
CHIKV	Chikungunya virus
COVID-19	Coronavirus disease 2019
CPS	Capsular polysaccharide antigen
CRISPR	Clustered regularly interspaced short palindromic repeats
crRNA	CRISPR RNA
CSF	Cerebrospinal fluid
DBS	Dried blood spot
DENV	Dengue virus
DF	Dengue fever
DHF	Dengue haemorrhagic fever
DI	De-ionised
dNTP	Deoxynucleotide Triphosphates

dsDNA	Double-stranded DNA
DSS	Dengue shock syndrome
DTT	Dithiothreitol
E	Envelope
ECSA	Eastern/Central/Southern Africa
eDST	Electronic decision-support tool
EDTA	Ethylenediaminetetraacetic acid
ELISA	Enzyme-linked immunosorbent assay
FDM	Fused deposition modelling
FIP	Forward internal primer
GBS	Guillain-Barré syndrome
Hcp1	Hemolysin-coregulated protein 1
HIV	Human immunodeficiency virus
HR	Homologous recombination
HRLMP	Hamilton Regional Laboratory Medicine Program
HRPII	Histidine-rich protein II
IFA	Immunofluorescent antibody
IgG	Immunoglobulin G
IgM	Immunoglobulin M
IO	Indian Ocean
JEV	Japanese encephalitis virus
LAMP	Loop-mediated isothermal amplification
LB	Luria-Bertani
LFT	Lateral flow tests
LMIC	Low- and middle- income countries
LOD	Limit of detection
MAT	Microscopic agglutination test
MAYV	Mayaro virus

MoMiLDE	Molecular Microbiology Laboratory for Diagnosis and Epidemiology
MORU	Mahidol-Oxford Tropical Medicine Research Unit
NAAT	Nucleic acid amplification test
NHEJ	Non-homologous end-joining
NS	Non-structural
nsP	Non-structural protein
NTC	No template control
ONNV	O'nyong'ngyong virus
PBS	Phosphate-buffered saline
PCR	Polymerase chain reaction
PETG	Polyethylene terepthalate glycol
PLA	Polylactic acid
pLDH	*Plasmodium* lactate dehydrogenase
POC	Point-of-care
prM	Precursor membrane
qPCR	Quantitative polymerase chain reaction
RAA	Recombinase-aided amplification
RDT	Rapid diagnostic test
RFI	Rural febrile illness
RFU	Relative fluorescence unit
ROC	Receiver operating characteristic
RPA	Recombinase polymerase amplification
RRV	Ross River virus
RSV	Respiratory syncytial virus
RT	Reverse transcriptase
RT-PCR	Reverse-transcriptase polymerase chain reaction
SBT	Sample buffer tube
SEACTN	South and Southeast Asia Community-based Trials Network

SHERLOCK	Specific high-sensitivity enzymatic reporter unlocking
SNP	Single nucleotide polymorphism
ssDNA	Single-stranded DNA
ssRNA	Single-stranded RNA
STOP	SHERLOCK testing in one pot
SVG	Scalable vector graphics
TB	Terrific broth
TBE	Tris/Borate/EDTA
T_m	Melting temperature
TNA	Total nucleic acid
URS	Unitized reagent strip
UTR	Untranslated region
VHW	Village healthcare worker
VISTEC	Vidyasirimedhi Institute of Science and Technology
WHO	World Health Organization
WP-A	Work package A
WP-B	Work package B
WP-C	Work package C
ZIKV	Zika virus
ZNA	Zip nucleic acid

Table of Contents

List of figures

List of tables

List of appendices

CHAPTER 1

Introduction

This chapter outlines the theme of this thesis, discussing the burden of acute undifferentiated fever, key pathogens of interest and currently available diagnostics for them. The aims of this thesis will be presented with background information on dried blood spots, Chembio DPP® Fever Panel II Asia system, and CRISPR technology.

1.1. Acute undifferentiated fever

Acute undifferentiated fever (AUF) describes a febrile illness whether organ-wise or system-wise, that is conventionally defined as lasting under two weeks in which the cause cannot be determined through clinical evaluation (1). With the decline of malaria, mainly due to better access of effective treatment, more testing in patients, and guidelines from the World Health Organization (WHO) concerning treatment, non-malarial AUF has become the leading cause of illness and mortality in low- and middle-income countries (LMICs) (2, 3). Major diseases contributing to AUF include dengue fever, scrub typhus, influenza, Japanese encephalitis (JE), and leptospirosis (4). Diagnosis of non-malarial AUF is difficult because of the non-specific symptoms such as headache, chills, sweating, and/or fatigue (5). Due to the difficulties in clinical diagnosis, definitive diagnosis largely depends on laboratory tests such as nucleic acid amplification tests (NAATs) or serological tests. However, the availability of these tests can be limited or severely delayed especially in rural areas of LMICs due to the remoteness from healthcare facilities and high cost of these tests (6).

Treatment, as with clinical diagnosis, has proven to be difficult. Without knowing the cause of the illness, treatment is typically supportive care, treating patients by what symptoms are present. Some patients can be misdiagnosed, leading to misuse of medication, such as prescribing antibiotics for a viral infection or antivirals for bacterial infections. Not only does this not improve the course of disease, it also contributes to antimicrobial resistance (AMR) (7). Furthermore, some diseases such as dengue can become life-threatening if the disease is not correctly diagnosed and the patient given sufficient supporting care (8).

AUF incidence is often high in tropical regions where both wildlife and pathogen biodiversity are typically rich. This is associated with higher disease burden as high diversity means higher chance of presence and high abundance of a potential vector. Within these regions, rural areas have the highest disease burden as urbanisation has shown to lower disease burden due to better sanitation, public health campaigns, and closer proximity to healthcare facilities (9).

The following sections describes prevalent and noteworthy pathogens that cause non-malarial AUF in South and Southeast Asia.

1.2. The South and Southeast Asian Community-based Trials Network

As cases of malaria continues to decline, the causes of AUFs in LMICs today remain largely unknown. This makes the appropriate management of patients difficult which leads to further issues such as treatable illness being missed or the overuse of antibiotics. Determining the causes and incidences of AUFs in different rural areas can help village healthcare workers (VHWs) better understand and be better equipped to manage AUF patients in their respective areas (4).

The South and Southeast Asian Community-based Trials Network (SEACTN) research programme aims to understand the causes of morbidity and mortality in rural communities across South and Southeast Asia, and then establish a network of healthcare workers to trial new interventions to improve health outcomes in these underserved populations (10). The first project in the SEACTN programme, of which this thesis is a part, is the Rural Febrile Illness (RFI) project. This project aims to determine the epidemiology of AUFs in selected areas in Bangladesh, Cambodia, Laos PDR, Thailand, and Myanmar and use this information to design novel interventions that could improve their management. The RFI project is divided into three work packages (11).

Work package A (WP-A) concerns the incidence and causes of AUFs in lower-level healthcare facilities such as primary healthcare centres. Capillary blood samples, stored as DBS, were collected to be tested by molecular and serological methods. Household health surveys and verbal autopsies were also conducted to determine the health-seeking behaviour and causes of mortalities in these communities respectively (12, 13). Work package B (WP-B), which was conducted in parallel with WP-A, focuses on the epidemiology of AUFs in higher-level healthcare centres such as clinics and hospitals. Patient venous blood samples were taken, along with nasopharyngeal swabs to be tested by molecular and serological diagnostics. Lastly, work package C (WP-C) aims to develop electronic decision-support tools (eDST) and POC tests that will later be implemented and evaluated across the network.

1.2.1. Chikungunya

Chikungunya virus (CHIKV) is an arbovirus in the family *Togaviridae*, and genus *Alphavirus*, which also contains other disease-causing viruses such as O'nyong-nyong virus (ONNV), Mayaro virus (MAYV) and Ross River virus (RRV). Vectors of CHIKV are mosquitoes in the genus Aedes, namely *A. aegypti* and *A. albopictus*. Four CHIKV genotypes have been identified: Western Africa, Eastern/Central/Southern Africa (ECSA), Asian and Indian Ocean (IO) lineages (14). Although endemic to the tropics, cases and outbreaks of chikungunya are found worldwide (15).

CHIKV is a positive sense, single-stranded RNA (ssRNA) virus. The CHIKV genome is approximately 11.8 kb long and encodes five structural proteins (capsid protein [C], two envelope glycoproteins [E1 and E2], and two accessory proteins [E3 and 6K]), as well as four non-structural proteins (nsP1-4) with the two ends terminating with a 5' 7-methylguanosine cap and 3' poly(A) tail as shown in Figure 1 (16). CHIKV circulates between an urban cycle (human – mosquito – human) and sylvatic cycle (animal – mosquito – animal) with cross-overs when infected animals come into contact with human (17). The virus infects human epithelial cells, endothelial cells, fibroblasts and macrophages before moving to the lymphatic and circulatory systems. Other viral replication sites include lymphoid organs, skin and muscles (18).

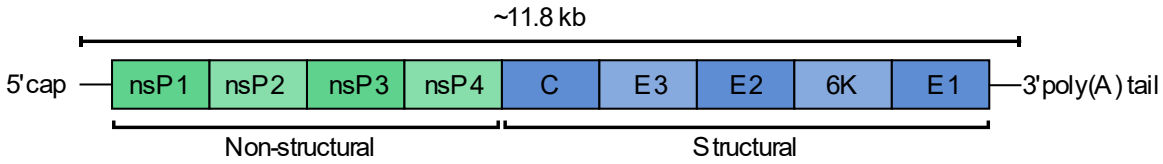

Figure 1: CHIKV genome structure encoding four non-structural proteins (nsP1 – 4) and five structural proteins consisting of the capsid protein (C), envelope proteins (E1 and E2), and accessory proteins (E3 and 6K). The genome is flanked by a 5' cap and 3' poly(A) tail.

1.2.1.1. Chikungunya fever

Chikungunya fever is characterised by high fever and arthralgia that manifest after a 2-7 days incubation period. Other symptoms also include myalgia and rash. The name 'Chikungunya' is derived from the Bantu language translates to 'to be contorted', which describes the contorted posture of CHIKV patients due to joint pain (19). Because these symptoms are relatively non-

specific, CHIKV is often misdiagnosed as another febrile illness such as dengue fever. CHIKV infection is generally separated into three phases; acute, post-acute and chronic (20).

The acute phase takes place in the first three weeks of symptom manifestation. The resulting pain is generally symmetric and very intense, often accompanied by stiffness of joints (21). Other non-specific symptoms such as nausea, vomiting or diarrhoea are also commonly found (22). The acute phase is generally self-limiting and resolves within two weeks of symptom onset (23).

The post-acute phase begins after approximately 3-4 weeks after symptom onset and can last for three months. This phase is characterised by a persistent polyarthralgia with constant intensity. The symptoms usually slowly resolve over the course of approximately three months. Other non-specific symptoms can also manifest during this phase such as fatigue, change in skin colour, hair loss and hypertension (24).

If symptoms are still present past three months, the infection is considered chronic. This phase mostly has the same symptoms as the post-acute phase but the duration can vary from several months to several years. The symptoms can also fluctuate in intensity over the course of the chronic phase. Additional complications that can occur in this phase include other musculoskeletal symptoms such as symmetric tenosynovitis in the wrists or ankles (25).

1.2.1.2. Diagnosis of chikungunya fever

CHIKV is a risk group 3 virus and requires a biosafety level 3 (BSL-3) laboratory. Because of the low availability of BSL-3 laboratories, strategies have been developed to work with the virus at a lower safety level laboratory such as heat inactivation at 56°C for 30 minutes to 2 hours (26). Virus culture for diagnosis of CHIKV is done by infecting the *A. albopictus*-derived C6/36 cell line or the African green monkey-derived Vero cell line, although the former is more common because it is more easily infected (27). NAATs for CHIKV uses RNA extracted from patient serum or plasma and are much more rapid and very sensitive although the patient samples need to be taken within the first 4-5 days of symptom onset, therefore patients that are not able to reach a clinic within this timeframe could result in a false negative (28).

Antigen detection methods for CHIKV are mostly in development and usually rely on the detection of the viral E1 protein in patient serum. However, not only do these tests have moderate sensitivities with an overall sensitivity of 76.9%, they are not able to reliably detect certain lineages of CHIKV, with a sensitivity of 33.3% for Asian lineage (29). Serological methods for CHIKV uses the detection of IgM and IgG. These methods usually use enzyme-linked immunosorbent assay (ELISA) with several commercially available kits (30), however some of these tests have cross-reactivity with other alphaviruses such as ONNV and MAYV, compromising their specificity (31). Moreover, patient samples must be collected between 4-20 days after symptom onset to be reliably detected making early diagnosis difficult. Antibodies can also linger in the body for months post-infection so a patient with another infection with a recent CHIKV fever can be misdiagnosed with the latter, also affecting the tests' specificity (32).

1.2.2. Dengue

Dengue virus (DENV) is an arbovirus that is also transmitted by *A. aegypti* and *A. albopictus*, and is the biggest cause of arboviral diseases endemic throughout most of the tropical and subtropical areas of the world and spreading to more (33). The virus is in the family *Flaviviridae* and genus *Flavivirus* and is divided into four serotypes (DENV1-4) (34). Estimates of infections per year can be as high as 390 million cases worldwide, 96 million of which are symptomatic (35). The estimates for Southeast Asia alone are approximately 2.9 million cases with clinical manifestation and 5,906 deaths annually. Economically, the annual dengue burden cost in Southeast Asia is at approximately US$950 million with Indonesia, Thailand and Malaysia having the highest burden respectively (36).

The virus itself is a positive sense, single-stranded ssRNA virus. Its genome is approximately 10.7 kb long and encodes three structural proteins (capsid [C], precursor membrane [prM] and envelope [E]) and seven non-structural (NS) proteins (NS1, NS2A, NS2B, NS3, NS4A, NS4B, and NS5) as shown in Figure 2 (37). The genome is flanked by two untranslated regions (UTR) which while untranslated, are necessary for viral replication and translation and are relatively conserved among the serotypes (38). Upon entry into the host, dengue virus initiates its infection

by infecting the skin Langerhans cells and dendritic cells (DCs) (39). Using these cells, the infection then spreads into the lymph nodes where it infects monocytes and macrophages (40).

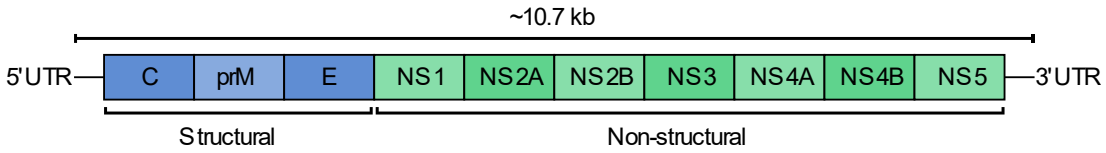

Figure 2: DENV genome structure encoding seven non-structural proteins (NS1, NS2A, NS2B, NS3, NS4A, NS4B, and NS5), as well as three structural proteins consisting of the capsid protein (C), precursor membrane (prM), and envelope (E). The genome ends on both the 5' and 3' termina with untranslated regions.

A noteworthy property of dengue and dengue infection is antibody-dependent enhancement (ADE). Dengue, as well as viruses such as influenza A, respiratory syncytial virus (RSV), Ebola virus, and the human immunodeficiency virus (HIV), are able to use the host's immune system to enhance infectivity (41-44). In the case of dengue, infection by one serotype grants the host immunity for that serotype but if a secondary infection occurs from any of the remaining three serotypes, the chances of the patient developing more severe dengue haemorrhagic fever (DHF) dramatically increase. Antibodies produced by the primary infection have reduced or lack of neutralising properties against subsequent infections (45). While not completely understood, the current hypothesis suggests that these antibodies facilitate cell binding and entry as well as modifying the immune response to increase virus production in infected cells (46). Due to ADE, vaccine development for dengue has proven to be difficult as the ideal vaccine should be able to induce a tetravalent immunity to each serotype. Currently, there are two licenced vaccines, Dengvaxia® (CYD-TDV) and Qdenga® (TAK-003), both live attenuated tetravalent vaccines. CYD-TDV was the first to be licenced and shows a low to moderate efficacy against DENV infections. However, the efficacy is higher in people with previous dengue fever compared to dengue naïve individuals. Furthermore, cases of hospitalisation of previously naïve vaccinated children ages 2 - 5 were reported. Because of these reports, the vaccine is only recommended for people with previous confirmed dengue fever in endemic areas (47, 48). TAK-003 has been shown to have 80.9% efficacy in the general population and 74.9% efficacy in dengue naïve individuals.

The safety of TAK-003 is still being investigated but no serious complications have been reported so far (49-51).

1.2.2.1. Dengue fever and dengue haemorrhagic fever

Dengue fever (DF) and dengue haemorrhagic fever (DHF) present with similar symptoms initially, which manifests after a 3-7 days incubation period, although many dengue infections are non-symptomatic. DF is generally non-fatal and manifests as a febrile period with other nonspecific symptoms such as nausea, rash or body aches. After 3-7 days of illness, most patients will make a full recovery. DHF, on the other hand, can be fatal, depending on the severity of the disease. DHF manifestation is divided into three stages; febrile, critical and recovery (52).

The febrile phase is mainly characterized by, as the name suggests, high fever of more than 38.5°C. Other symptoms in this phase include headache, erythema, and arthralgia. Because these symptoms are common among febrile illnesses, clinical diagnosis is difficult during early infection. Furthermore, during this phase, it is very difficult to differentiate DF and DHF. Enlarged liver and mild haemorrhagic symptoms are also sometimes observed and are a better clinical indication of dengue infections (53). The febrile phase lasts for approximately 3-7 days and patients with DF make a full recovery.

In cases that do not make a full recovery, generally in children under 15 years old, the patient moves into the critical phase of DHF. This phase is characterized by increased vascular permeability, thrombocytopenia and worsened symptoms with the exception of a decrease in fever (54). High vascular permeability in turn causes plasma leakage which results in a drop in blood pressure and increase in blood concentration. Conditions generally improve 24-48 hours after the critical phase and the patients enter the recovery phase. This phase sees the improvement of vascular permeability and reabsorption of extravascular fluids. The patient will gradually improve over a period 48-72 hours although certain symptoms such as headache, insomnia or fatigue may remain for several weeks after recovery (55). Some cases might experience mild rash or prolonged fatigue (56).

If vascular permeability does not improve, the patient becomes at risk of dengue shock syndrome (DSS). The WHO describes DSS as manifestation of: rapid, weak pulse, narrow pulse pressure of less than 20 mmHg or hypotension for patient age, and cold, clammy skin and restlessness in addition to DHF symptoms (57). Shock usually results from plasma leakage, myocarditis, renal failure, and death is caused by haemorrhage and multiple-organ failure (58-60).

1.2.2.2. Diagnosis of dengue fever

DENV is a risk group 2 pathogen and requires a biosafety level 2 (BSL-2) laboratory. DENV is diagnosed with all the methods mentioned above for CHIKV. For virus isolation, patient serum or whole blood is collected within 7 days of symptom manifestation to be grown in tissue culture or live mosquitoes. The most common cell lines are C6/36 and Vero cell lines, as with CHIKV (61). NAATs for dengue also require patient samples to be collected within 7 days of symptom manifestation. An advantage of NAATs for dengue diagnosis is the ability to do multiplex PCR, detecting and differentiating between the four serotypes (62). Due to the requirement of acute patient samples, virus isolation and NAATs are not effective if patients are not able to reach a clinic or hospital within the first week of symptoms.

For later diagnosis, antigen detection and serological methods are favoured. The most common antigen detection method is the detection of the dengue NS1 protein with ELISA or lateral flow tests (LFTs) (63). Serological methods rely on the detection of patients' Immunoglobulin M (IgM) and G (IgG). This method has the advantage of being able to differentiate between primary and secondary infections by measuring the concentrations of IgG. However, because antibodies tend to be present in low levels for months after an infection, there is the chance of false positives (64). Antigen and antibody detection require patient samples to be collected approximately 5-9 days after symptom manifestation, so while these methods are much cheaper than virus isolation and PCR, they are not suitable for early diagnosis.

1.2.3. Zika

Zika virus (ZIKV) is an arbovirus in the family *Flaviviridae* and genus *Flavivirus* first isolated from the Zika Forest in Uganda (65). It is endemic to various regions across tropical and

subtropical areas of Asia and Africa and is transmitted by mosquitoes in the genus Aedes such as the aforementioned *A. aegypti* and *A. albopictus*, but also other species such as *A. africanus*, *A. apicoargenteus* and *A. luteocephalus* (66). There has also been reports of sexual transmission and vertical transmission from mother to foetus (67). Phylogenetically, ZIKV is divided into three lineages; West Africa, East Africa and Asia (68). ZIKV is naturally maintained in primates, transmitted by mosquitoes although anti-ZIKV antibodies have been found in other mammals such as sheep and goats (69).

The virus itself is a positive sense, single-stranded ssRNA virus with a genome approximately 10.8 kb long. The genome codes for one structural polyprotein, which is processed into the capsid (C), precursor membrane (prM) and the envelope (E) proteins, and seven non-structural proteins (NS1, NS2A, NS2B, NS3, NS4A, NS4B and NS5) as shown in Figure 3. The two ends of the genome terminate in a 5' and 3' UTR (70).

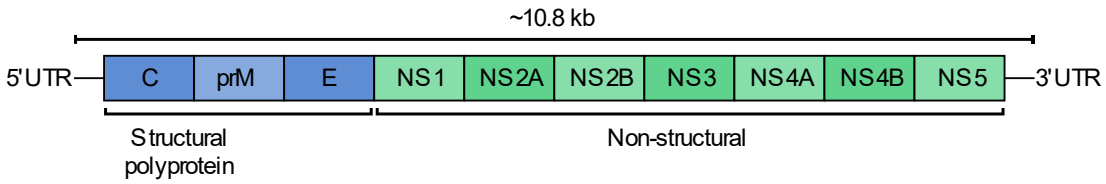

Figure 3: ZIKV genome structure

1.2.4. Zika fever

Symptoms typically manifest after a 3-12 days incubation period, although up to approximately 80% of cases are asymptomatic. Symptomatic cases are generally mild and nonspecific such as low fever, rash, arthralgia, myalgia, fatigue, and headache. Again, this makes definitive diagnosis difficult without laboratory testing. Symptoms usually resolve within 2 weeks of onset (71). While ZIKV itself is generally self-limiting, it is associated with neurological disorders.

During the 2013 outbreak of ZIKV in French Polynesia, an increase of Guillain-Barré syndrome (GBS) was reported. GBS is an autoimmune, acute polyradiculoneuropathy that

manifests as areflexia, muscle weakness and neuromuscular paralysis (72). Serological testing showed that all patients who developed GBS during the outbreak had been infected with ZIKV and 88% of patients reported illnesses with symptoms correlating with ZIKV shortly before GBS symptom manifestation, suggesting the causation of GBS by ZIKV infection (73). Another disorder associated with ZIKV is microcephaly, the abnormal development of infant brains. In 2015, during an outbreak of ZIKV in Brazil, an increase in new born microcephaly cases was observed. Most women who gave birth to these cases reported symptoms correlating with ZIKV during the first months of pregnancy. Furthermore, ZIKV was also detected in amniotic fluid and foetal brain (74).

1.2.5. Diagnosis of Zika fever

ZIKV is a risk group 2 pathogen and requires a BSL-2 laboratory. It is usually diagnosed by NAATs and antibody detection, as there are currently no available antigen-based diagnostics for ZIKV. As opposed to CHIKV and DENV, ZIKV is very difficult to isolate from patient samples, most likely due to the low viral load in the samples (75). NAATs detect viral RNA in patient whole blood or serum using RT-PCR and provide the most accurate results. As before, the sample should be collected within the first week of symptom manifestation (76). Additionally, because of the non-specific symptoms, many NAATs detects ZIKV in a multiplex with CHIKV and DENV (77).

Antibody detection is the most common diagnosis method for ZIKV. Again, the patient sample must be collected approximately 4-7 days after symptom manifestation and can be detected up to 12 weeks. Antibody detection relies on ELISA to detect IgM in patient serum (78). A big limitation with this method is the cross-reactivity. Anti-ZIKV antibodies are highly cross-reactive with other flaviviruses, especially DENV. This is problematic because these viruses are endemic in the same regions of the world, making misdiagnosis common. Because of this, and the lower sensitivity of antibody detection compared to RT-PCR, these tests generally require additional conformational tests (79).

An interesting phenomenon regarding flavivirus antibody is the 'original antigenic sin'. This phenomenon describes the immunological reaction of the body towards secondary infections of viruses. Normally, a primary viral infection will induce the formation of B and T cells against the infecting pathogen. Upon secondary infection, clonal expansion of the previously acquired B and T cells would be able to contain the infection. However, if an infection from a variant of a previously encountered virus occurs, instead of treating it as a primary infection, the body could treat it as a secondary infection and induce the clonal expansion of the previously acquired B and T cells. These responses would not be sufficient enough to neutralize the infection and can lead to a more severe disease (80). Therefore, if a patient has immunity for other flaviviruses, either from a previous infection or vaccination, upon ZIKV infection, the detectable antibody would be towards the previously exposed virus, not the current one (81).

1.2.6. Orientia tsutsugamushi

Orientia tsutsugamushi are Gram-negative bacteria belonging to the family Rickettsiaceae. Its name is derived from the Japanese "tsutsuga" and "mushi" meaning illness and insect respectively. It is endemic to but not limited to an area termed the "tsutsugamushi triangle" which spans across East and Southeast Asia (Figure 4) (82). *O. tsutsugamushi* are obligate intracellular parasites in mites, mainly those of the genus *Leptotrombidium*. Infections in humans occur through bites of the larval stage (called chiggers) of these mites, typically causing eschars at the bite sites (83). There are more than 30 antigenically distinct strains of *O. tsutsugamushi* based on the variations in the 56-kDa type-specific antigen (84)

Figure 4: Tsutsugamushi triangle.

1.2.6.1. Scrub typhus

Scrub typhus is a neglected tropical disease caused by *O. tsutsugamushi* and is among the leading cause of AUFs. It is typically found in rural areas within the tsutsugamushi triangle, but cases are also reported in urban areas. Symptoms manifest early in the infection and include fever, myalgia, headache, gastrointestinal disturbances, and diarrhoea. Macular or maculopapular rash may develop approximately one week after onset of fever. The characteristic symptom is the formation of the aforementioned eschars, appearing as black lesions at the site of the chigger bite. If left untreated, scrub typhus can be fatal as patients can develop pneumonia, meningoencephalitis, cardiac failure, or septic shock among others (85). Scrub typhus is treatable using antibiotics such as doxycycline or azithromycin (86).

1.2.6.2. Diagnosis of scrub typhus

While scrub typhus has the tell-tale sign of eschar formation, not all patients develop them. Because of the life-threatening nature of the disease, early diagnosis is key to treating patients. The main method for scrub typhus diagnosis is by serological methods with indirect immunofluorescent antibody (IFA) tests being the gold standard (87). Other serological tests include Weil-Felix testing and IgM antibody ELISA tests. PCR testing is also done with the

advantage of being able to detect the bacteria before serological methods can. However, it is not typically used routinely due to its high cost. Bacteria culture can also be done but generally not used for diagnosis, because *O. tsutsugamushi* culture requires a BSL-3 laboratory and the process takes many days. As intracellular parasites, culturing *O. tsutsugamushi* also requires mammalian cell culture, making it impractical in a clinical setting (88).

1.2.7. Rickettsia

Rickettsia is a genus of Gram-negative bacteria with many species causing AUF. Members of this genus are obligate intracellular parasites and are transmitted by the bites of mites, ticks, fleas, or lice found across the world (89). The genus is divided into four groups, the spotted fever, typhus, transitional, and ancestral groups (90). Most *Rickettsia* species target the endothelial cells of the host (91). Table 1 shows selected *Rickettsia* species along with the diseases caused by each respective species.

Table 1: Selected Rickettsia species from the different groups along with the diseases caused by the respective species.

Group	*Rickettsia* species	Diseases
Spotted fever group	*R. rickettsii*	Rocky Mountain spotted fever
	R. conorii	Mediterranean spotted fever
	R. parkeri	Mild-moderate spotted fever
Typhus group	*R. typhi*	Murine typhus
	R. prowazekii	Epidemic typhus
Transitional group	*R. felis*	Flea-borne spotted fever
	R. australis	Tick-borne Queensland tick typhus
	R. akari	Mite-borne rickettsialpox
Ancestral group	*R. bellii*	Non-pathogenic
	R. canadensis	Non-pathogenic

1.2.7.1. Rickettsiosis

As with other AUFs, rickettsiosis manifests with non-specific symptoms such as fever and myalgia. Rickettsiosis can be mild or fatal from multi-organ failure depending on the infecting species (92, 93). The characteristic symptom of rickettsiosis is the presence of macular or maculopapular rash with eschars also being reported in many cases, the locations of which can aid in identifying the species causing the disease (94). The spotted fever group typically causes fever for approximately 1-2 weeks while infections from the typhus group can cause a longer fever (95). However, disease severity is higher in the spotted fever group, particularly the Americas native *R. rickettsii (96).*

1.2.7.2. Diagnosis of rickettsiosis

The main methods of diagnosis are similar to those for scrub typhus with serological methods being preferred, specifically IFA detection of IgG antibodies (97). This is because IgM antibodies against *R. rickettsii* can sometimes be detected in patients with no recent *Rickettsia* infection. Other serological methods such as ELISA detection of antibodies are also used. As with many serological methods samples should be taken during the acute and the convalescent stages to compare antibody levels for a definitive diagnosis, albeit for a retrospective diagnosis as the patient would have already recovered. PCR and other NAATs are also available for Rickettsiosis from whole blood, plasma, or eschar specimens. However, apart from the cost, the low concentration of bacteria in samples can limit the sensitivity, especially if whole blood or serum is used as the bacteria infects endothelial cells and doesn't typically circulate in the bloodstream outside of acute infection (98). As with *O. tsutsugamushi*, *Rickettsia* culture is possible but requires a BSL-3 laboratory. The time-consuming process makes bacterial culture impractical for clinical diagnosis. Treatment of rickettsiosis is done by antibiotics such as doxycycline or chloramphenicol with regimens between a few days to up to a week depending on the infecting species (97). It is noteworthy that many common antibiotics such as penicillin and cephalosporins are not effective for the treatment of rickettsiosis (99).

1.2.8. Leptospira

Leptospira is a genus of motile aerobic Gram-negative spirochaetes. The genus is endemic in tropics across the world, specifically in rural areas. *Leptospira* species can be classified into three main groups: pathogenic, intermediate (causing mild infection), and non-pathogenic. Mammals serve as reservoirs for the disease, particularly rats, in which the bacteria will be present in the host's urine. Infection occurs from bacteria entry through open wound or mucosa from contact with contaminated water or soil (100).

1.2.8.1. Leptospirosis

Leptospirosis is the disease caused by *Leptospira* spp. and is a major neglected tropical disease, infecting over 1 million and causing approximately 60,000 deaths per year (101). Clinical manifestation typically occurs 7-12 days after infection and include symptoms such as fever, chills, headaches, and myalgia. The disease can be self-limiting or fatal with more severe symptoms such as renal failure, jaundice, haemorrhage, and multi-organ failure. With appropriate treatment, patients typically make full recoveries with minimal persistent symptoms (102).

1.2.8.2. Diagnosis of leptospirosis

Diagnosis of leptospirosis are usually done using serological methods, with the gold standard being the microscopic agglutination test (MAT) in which live antigens are reacted with patient serum sample before being inspected via microscopy (103). Other serological diagnosis methods are also available such as ELISA tests to detect IgM and IgG antibodies (104). Molecular methods such as PCR can also be done to directly detect the bacteria from a wide range of samples including serum, whole blood, CSF, urine, and bacteria culture, although blood samples give higher sensitivity than bacteria culture (105). Bacterial isolation and culture can also be done relatively easily by inoculating a few drops of patient blood into a specialised growth media and then identified either by serological or molecular methods. Again, this method is too time consuming for practical clinical diagnosis. While most leptospirosis cases spontaneously resolve, antibiotics such as penicillin, ampicillin, or doxycycline are sometimes used to prevent patients from developing more severe disease (106).

1.2.9. Other acute febrile illness-causing pathogens

Apart from the pathogens described above, other pathogens that cause AUF in South and Southeast Asia include other viruses such as those causing hepatitis, herpesviruses, and enterovirus as well as bacteria such as *Salmonella* spp. and *Burkholderia pseudomalle*i (107). *B. pseudomallei*, the pathogen that causes melioidosis, in particular is a major cause of sepsis in Thailand, with as much as 20% of community-acquired cases in the northeastern region attributed to melioidosis (108). Most cases of infections are acquired from the environment in contaminated settings (109).

1.3. Current approaches of AUF diagnosis

Accurate clinical diagnosis of AUFs is difficult due to the undifferentiated nature of the symptoms. Definitive diagnosis relies on laboratory-based methods. In cases in which laboratories are not available, preliminary diagnosis relies on clinical symptoms and patient travel history. Laboratory diagnosis include virus isolation, nucleic acid amplification tests (NAATs), antigen detection and serological detection. Each method of detection has its own advantages and disadvantages (110).

1.3.1. Pathogen isolation

Pathogen isolation has been previously considered the 'gold standard' diagnosis method but due to some major drawbacks, have mostly been phased out of diagnosis, and is currently mainly used for research. Patient samples are collected and cultured in appropriate cell lines or organisms such as mosquitoes. Identification is then done using staining, sequencing, or microscopy. Out of all diagnosis methods, pathogen isolation is the most time consuming, because each pathogen has to be grown, therefore diagnosis can take up to several weeks. It also requires a laboratory with facilities for cell culture and/or an insectary, along with well-trained personnel all of which adds up to a high cost. The high risks of some pathogens also require BSL-2 (DENV, ZIKV, and *Leptospira* spp.) or BSL-3 (CHIKV, *Rickettsia* spp., and *O. tsutsugamushi*) to safely handle the virus cultures. Despite that, isolation is considered highly sensitive and has the added advantage of producing material from pathogens for further study if so desired (111).

1.3.2. Antigen detection

Antigen detection relies on immunological assays such as ELISA to detect bacterial or viral antigen in patient samples. Generally, viral antigens are captured using enzyme-linked antibodies and detected by adding a substrate that reacts to the enzyme and causes a colour change. If a serially diluted standard is also used, the test can also be quantitative (112). Antigen detection is much cheaper compared to pathogen isolation or PCR, with many viruses having commercially available diagnostic kits. However, it is not as sensitive as the previously mentioned methods and viruses from the same genus can have cross-reactivity which can make interpretation difficult (113).

1.3.3. Serological methods

Serological methods use immunological assays to detect the presence of antibodies in the patient's serum. Generally, IgM and IgG antibodies are the target of these methods as they appear relatively early in the infection. Serological testing is among the most rapid and cheapest methods and in many cases, does not require laboratories nor specially trained personnel. However, it is also the least sensitive, usually requiring multiple tests over a period of time, or another separate test for confirmation (114). Also, due to the nature of antibodies, it can be difficult to distinguish between an ongoing infection and a previous one. Furthermore, because the tests target antibodies, the samples used are limited to whole blood, plasma and serum (115).

1.3.4. Molecular methods

Molecular detection of viruses is based around nucleic acid amplification tests (NAATs), with the primary one for RNA viruses being reverse transcription-polymerase chain reaction (RT-PCR). In RT-PCR, viral RNA is extracted from patient sample and reverse transcribed into cDNA. Primers with complementary sequences to specific regions of the virus genome then binds to the cDNA and initiate amplification. Over multiple cycles of denaturing and elongation, the amount of target cDNA exponentially increases (116). The product can then be analysed using agarose gel electrophoresis for identification. Newer methods use real-time detection using real-time PCR, also called quantitative PCR (qPCR). There are generally two methods in real-time PCR: using an intercalating dyes and fluorescent probes. The former uses molecules that get bind to amplifying double-stranded DNA (dsDNA) and fluoresce once incorporated. The latter uses molecular

probes, DNA fragments complementary to the target labelled with a fluorescent dye and a quencher. These probes get cleaved as the DNA strand elongates. In both methods, the resulting fluorescence is then detected and quantified. The main difference between the two methods is that intercalating dyes are non-specific and will detect any DNA that is amplified in the reaction while using probes only detect DNA with the target sequence. Over repeating cycles of denaturation and elongation, the fluorescent signal increases. The number of cycles at which the signal crosses a set threshold is called the quantification cycle (Cq) or threshold cycle (Ct). The higher the initial target's concentration in a reaction, the less cycles would be required for the signal to cross the threshold, and the lower the Cq value would be.

A multiplex reaction can be done by using multiple primers and probes with different fluorescent dyes within a single reaction to detect different targets simultaneously. This is advantageous in cases such as identifying diseases causing similar symptoms such as CHIKV and DENV (117). However, because it is very sensitive, preparation must be done in a suitably clean environment. It also requires specific instruments and specially trained personnel, which makes PCR diagnosis relatively costly (118).

An alternative NAAT to PCR is isothermal amplification. As the name suggests, isothermal amplification operates at a single constant temperature which eliminates the need for a thermal cycler. Isothermal amplification actually predates PCR, with the first method using bacteriophage-derived RNA polymerase being published by Spiegelman et. al. in 1965 (119). Some isothermal amplification methods include helicase-dependent amplification and strand displacement amplification (120, 121).

Arguably the most popular isothermal amplification method is loop-mediated isothermal amplification (LAMP) developed by Notomi et. al. (122). LAMP operates at 60-65°C and uses four to six primers, as opposed to two in conventional PCR. Three or four binding sites flanks the target sequence and are used to design the primers named F1-F3 and B1-B3 in addition to the forward (FL) and backward loop (BL). The main LAMP primers are assembled from the sequences of these binding sites; the F3, B3, FL, and BL have the same sequence as the binding sites of the same

names. The forward and backward inner primers (FIP and BIP) contain sequences of the F2/B2 and the complementary sequence of F1/B1 (Figure 5).

Figure 5: Binding sites for LAMP and primer design. Complementary sequences are denoted by being the same colours and the letter c at the end of the name.

LAMP works by first having the FIP and BIP binding and elongating the target. The F3 primer then binds and elongates, and because LAMP uses *Bst* polymerase, which has strand displacement activity, the previously elongated strand is separated. The structure of the FIP/BIP allows for the ends of the now displaced strand to loop onto itself on both sides. Exponential amplification then begins, both continuing from the 3' end of the self-bound primer and by a FIP or BIP binding to the loop regions. By adding the loop primers (FL and BL), the reaction is accelerated by binding to the loop regions and prime more strand displacement synthesis (123). As the reaction continues, some of the amplified sequences are separated out by the strand displacement activity of the *Bst* polymerase, eliminating for the need of a melting step like in PCR (124). The mechanism of amplification can be seen in Figure 6. The resulting products are a mixture of amplicons with multiple sizes which can be seen from the characteristic ladder-like structure when visualising LAMP product by agarose gel electrophoresis.

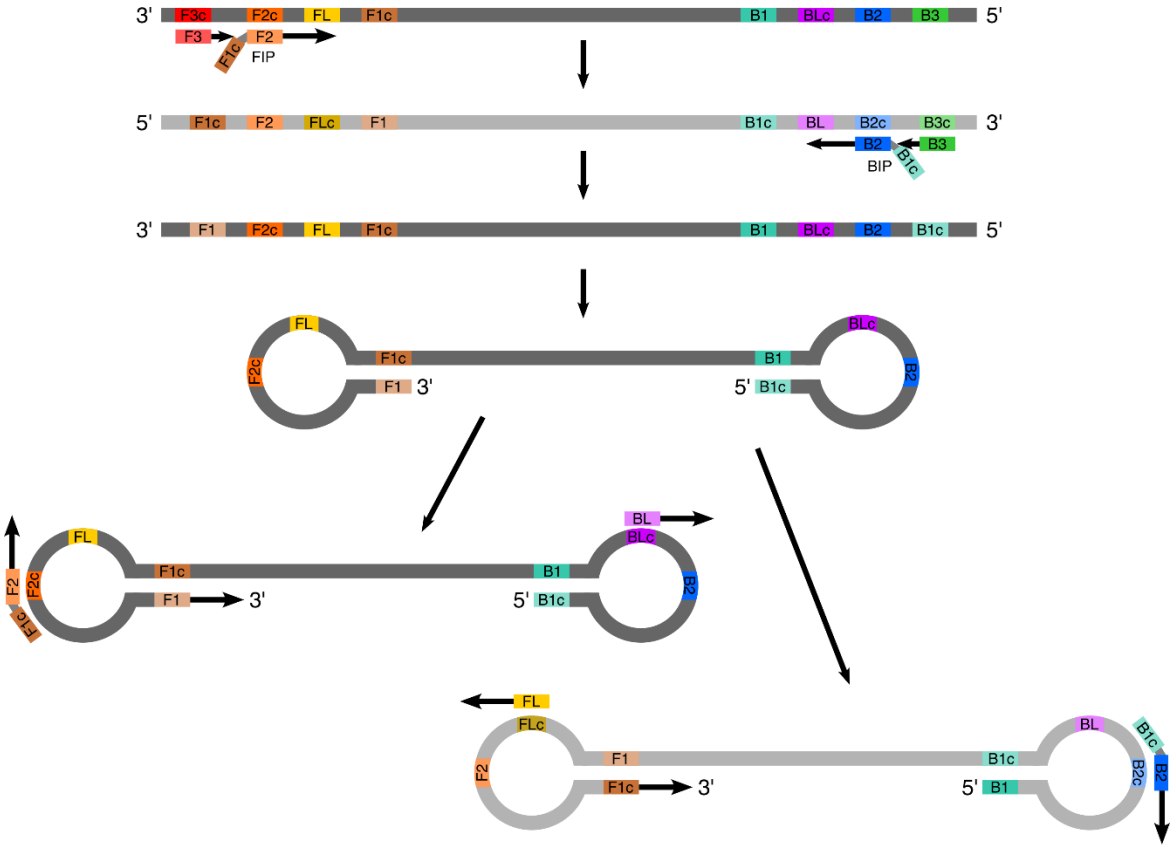

Figure 6: Mechanism of nucleic acid amplification by LAMP.

One limitation of LAMP is its sensitivity to cross-contamination. Small amounts of LAMP products spread through aerosol can cause false-positives (124). Because of how stable LAMP products are, in assays that requires opening the reaction tube after amplification such as LFTs, the area is required to be cleaned thoroughly before and after performing the reaction to prevent carry-over contaminations. Post-amplification applications such as cloning are also limited, as LAMP product is a mixture of different length amplicons (125). Designing primers for LAMP can also be challenging. Because it requires a minimum of 6 conserved regions, 3 flanking each side of the target gene, it can be difficult to design a LAMP assay for highly variable regions.

An alternative isothermal amplification method is recombinase polymerase amplification (RPA) (126). In RPA, only two primers are required as for PCR, albeit much longer, requiring 30 - 35 bases. The optimal amplicon size is around 100 - 200 bp as longer amplicons require longer

incubation time which risks non-specific amplification. The ΔG of hairpins are kept above -3 $\frac{kcal}{mol}$ while the ΔG of both homo- and heterodimers are kept above -6 $\frac{kcal}{mol}$. Because of this, designing primers for RPA is much simpler than LAMP with the main challenge being finding conserved regions of at least 30 bases.

The primers first bind to recombinase protein uvsX which has strand displacement activity. This allows the primers to bind to their targets while the latter still remain double-stranded. The separated strands are stabilised by single-stranded DNA (ssDNA) binding proteins and prevents the template strand from re-annealing and ejecting out the primers. The polymerase, usually derived from *Bacillus subtilis* or *Staphylococcus aureus* is also strand-displacing and starts elongation. Figure 7 shows the mechanism of RPA. RPA operates at much lower temperatures compared to other amplification, working best between 37 and 42°C but can still occur at even lower temperatures. This allows the reaction to be done without any equipment if the ambient temperature is high enough, or even using body heat (127, 128). Another advantage of RPA is its robustness regarding inhibitors, with the presence of haemoglobin or ethanol only having an effect near the limit of detection (LOD) (129). However, RPA is inhibited by high concentrations of DNA, specifically background DNA from whole blood specimens (130).

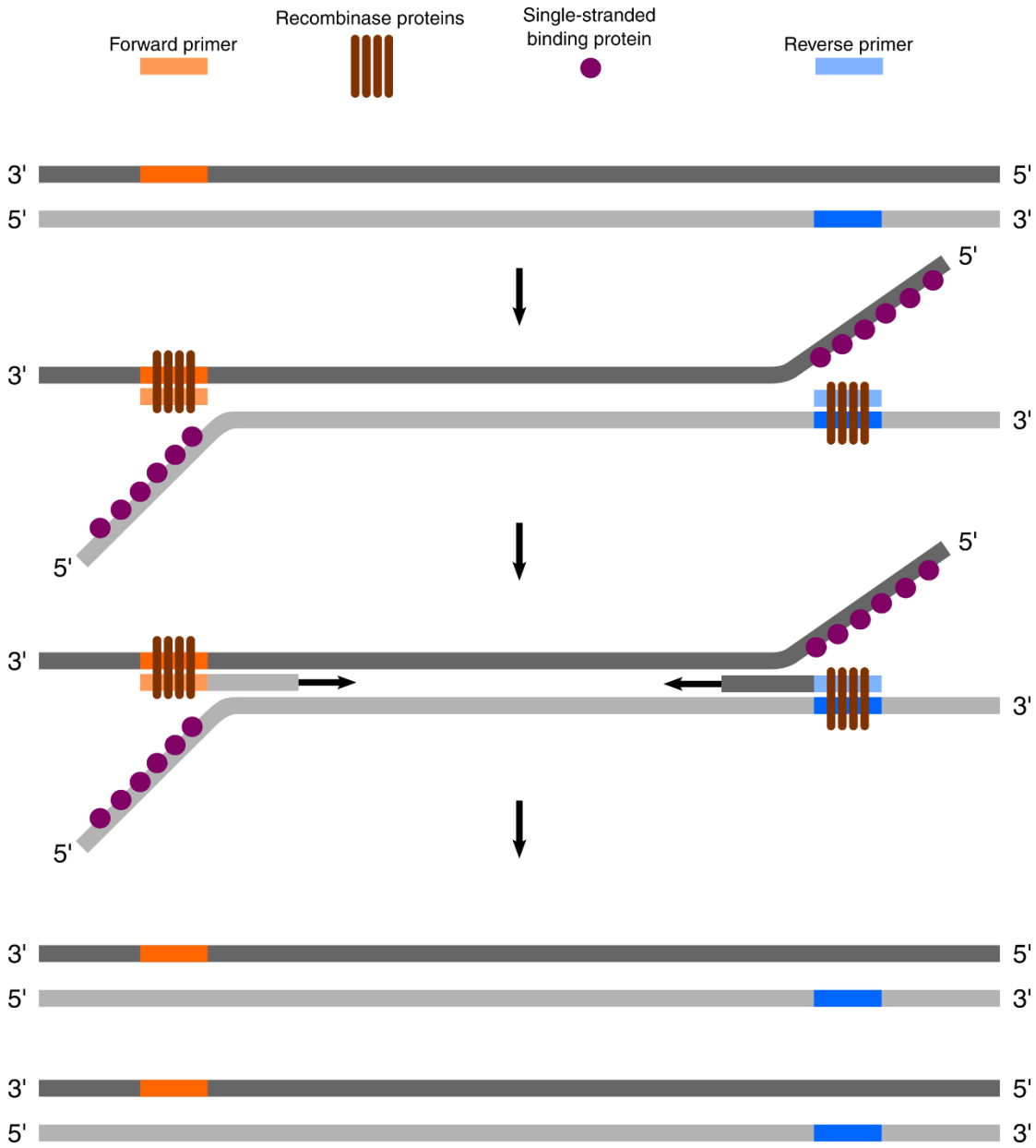

Figure 7: Mechanism of nucleic acid amplification of RPA.

A limitation of RPA is a high false-positive rate, similar to LAMP. Non-specific signal can also be an issue from primer-dependent artifacts if the template concentration is low and the reaction conditions are not optimised (126). RPA is also relatively costly and currently does not have a product that includes a reverse-transcriptase, meaning that assays targeting RNA will have to separately purchase the protein.

Recombinase aided amplification (RAA) is a derivative of RPA and is an improvement in many ways. The main difference between RAA and RPA is the source of the recombinase proteins,

RPA uses a T4 bacteriophage-derived recombinase while RAA uses an *Escherichia coli*-derived recombinase (131). A RT-RAA kit that contains reverse transcriptase is also commercially available, which allows for the detection of RNA as well as DNA. Both RPA and RAA are available in lyophilised forms, which makes storage and transport simpler.

1.3.5. Rapid diagnostic tests

Rapid diagnostic tests (RDT) are tests designed to be simple and quick to perform, generally aiming for use in lower resource settings or at the patient bedside (132). They are also robustly made and are able to be stored unrefrigerated for long periods of time. Because of this, they are mainly used as point-of-care (POC) tests. The REASSURE set of criteria was published by the WHO and give the essential criteria that RDTs should fulfil: real-time connectivity, ease of specimen collection, affordable, sensitive, specific, user-friendly, rapid and robust, equipment free or simple/environmentally friendly, and deliverable to end-users (133).

RDTs are particularly useful for tropical areas where clinical presentation of the endemic diseases can be hard to distinguish from each other. Moreover, RDTs typically have very few requirements regarding equipment, training, and facility which has made them widespread in low resource settings. About 415.5 million RDTs for malaria were sold in 2022 alone with a cumulative sale of 3.9 billion RDTs between 2010 to 2022 which has led to a reduction in malaria deaths (134). Single-plex RDTs are common place and routinely used not only for malaria, but also for other diseases such as dengue fever, enteric fever, and leptospirosis (135). The most common form of RDTs are the LFTs as they are cheap, simple to use, and have a relatively short wait time.

Despite its advantages, RDTs generally have a lower sensitivity compared to laboratory-based diagnostics such as real-time PCR (136). Another pitfall of RDTs is the potential cross reactivity between different pathogens. For example, the NS1-based RDTs for DENV are prone to also detect other flaviviruses such as ZIKV, leading to the overestimation of the prevalence of the latter (137). Cross reactivity has also been reported between DENV and COVID-19 in COVID-19 RDTs (138).

1.3.5.1. Multiplex RDTs for AUF

To increase screening efficiency, some RDTs are able to detect multiple targets in one reaction. One such test is the DPP® Fever Panel II Asia systems, an RDT kit for diagnosing common pathogens causing febrile illnesses developed by Chembio Diagnostics Inc. The kit consists of two multiplex cassettes, one for detecting microbial antigens, and one for detecting IgM. The cassettes are based on the principle of LFTs and contains two detection strips per cassette as shown in

Figure 8.

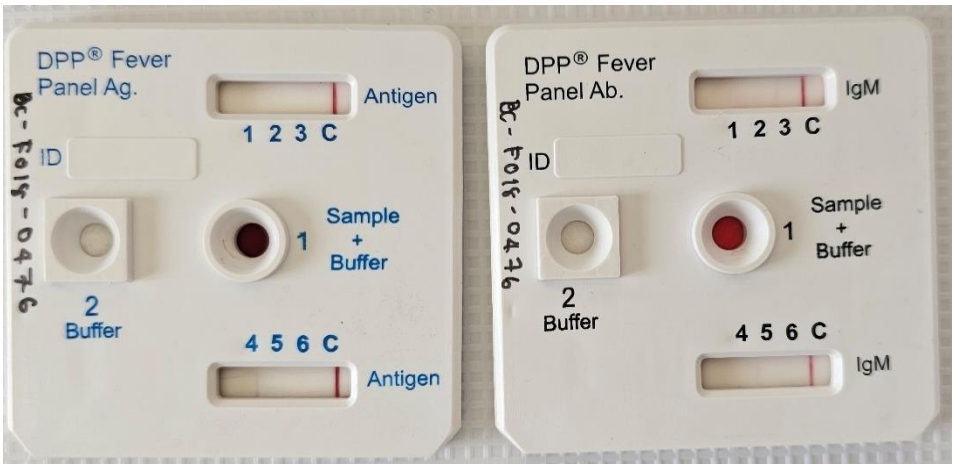

Figure 8: DPP® Fever Panel II Asia Antigen (left) and IgM antibody (right) systems.

Samples are dropped into well 1 and transported via capillary action to the test area where antigens/antibodies specific to each target are immobilised in discrete bands, capturing any target molecules present in the sample (Figure 9A). Next, a running buffer is introduced and hydrates the antigen/antibody-binding coloured conjugate, another set of either antigen or antibody specific to each target conjugated with gold nanoparticles (Figure 9B). These conjugates travel to the test area and binds to the captured target molecules, causing a change in colour of the bands. The intensity of the test bands is read with the DPP® Micro Reader 2 which outputs each band's intensity as a numerical value. The diseases and specific targets for the DPP® Fever II Asia systems are described in Table 2.

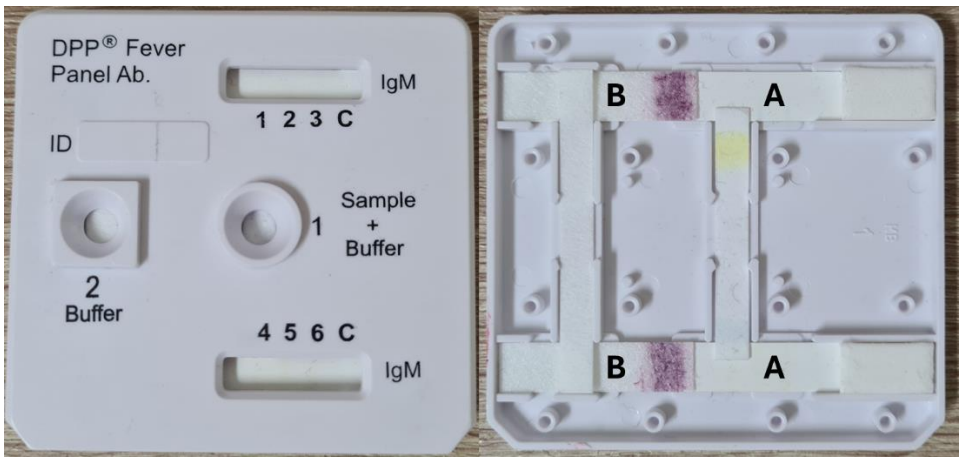

Figure 9: The interior of the DPP® Fever Panel II Asia IgM antibody cassete. A) The test area where antigens specific to each antibody target are immobilised. B) Pathway in which the running buffer passes and hydrates the antibody-binding coloured conjugates, gold nanoparticles conjugated to antibodies specific to the target antibodies.

Table 2: List of targets detected by the DPP® Fever Panel II Asia systems.

Antigen system
CHIKV E1 and E2
Pan-*Plasmodium* lactate dehydrogenase (pLDH)
DENV NS1
ZIKV NS1
Plasmodium falciparum histidine-rich protein II (HRPII)
B. pseudomallei capsular polysaccharide antigen (CPS)
IgM antibody system
CHIKV
ZIKV
Pan-*Leptospira*
Orientia tsutsugamushi
Rickettsia typhi
DENV

To determine whether a sample is positive or not in a test with numerical results, a threshold or cut-off value is required. What the threshold value is will affect the sensitivity of the assay, the higher the threshold, the lower the sensitivity. A common way to assess and determine the threshold value of a diagnostic test is the receiver operating characteristic (ROC) curve. The ROC curve is obtained by plotting the 'sensitivity' against '1 - specificity' (false positives) for all threshold values. The area under the curve (AUC) is then calculated as a general interpretation of the assay itself with an ideal diagnostic test having an AUC of 1 (139). A method to determine the threshold itself is the Youden Index. The Youden index is calculated by the following equation.

$$Youden\ Index = Senstivity + Specificity - 1$$

For each potential threshold value, the Youden Index is calculated to find the threshold with the highest Youden Index which offers the best trade-off between sensitivity and specificity (140).

As the DPP® Fever Panel II Asia systems are currently under development, a threshold for calling positive and negative results is not given for any of the targets. Deciding on a threshold value is a balance between sensitivity and specificity, too high and many cases will be missed, too low and many cases will be falsely flagged as positive. Another issue is the background seropositivity across different populations, therefore applying the same test in different populations can require using different thresholds (141).

A previous study assessed the DPP® Fever Panel II Asia systems' capabilities in detecting malaria, dengue, and melioidosis using serum samples collected from northeast Thailand and assays performed in the lab (142). Nested PCR was used to diagnose malaria while melioidosis was diagnosed by blood culture. The threshold values for each target were chosen so that a sensitivity of approximately 95% is reached. It was shown that while the Fever Panel II Asia systems performed similarly to other RDTs, their performance compared to the reference tests, nested PCR and blood culture, are much lower. Another study also evaluated the performance of the Fever Panel II Asia systems in patient whole blood and serum specimens, finding the DPP® system comparable to RTDs typically used for each target (143).

1.3.6. Automated multiplex diagnostics

An emerging type of diagnostic are the automated multiplex instruments. These instruments are designed to simultaneously detect multiple targets straight from clinical specimens while having an emphasis on ease of use and speed. An example of an automated multiplex system is the BioFire® FilmArray® Torch System (BioMérieux, Marcy-l'Étoile, France). This system uses multiplex real-time PCR to detect pre-selected pathogens. Different panels are made available to users, with each panel specialising in different pathogen groups (respiratory, gastrointestinal, joint infection, etc.). Handling is minimal and users are only required to inject clinical sample into a pouch provided in each panel and insert these pouches into the instrument. These panels have been shown to be highly specific and sensitive to its target pathogens with the main limitation being the test's limited catalogue of targets (144). As this is a closed system, users are only able to detect the targets as provided by the manufacturer, and is not able to adapt their own assay onto the platform. Furthermore, the price of these panels are relatively high so not every demographic will be able to afford them.

1.4. Dried blood spots

The use of whole blood for diagnostics has posed a challenge in areas with limited resources. Collection of whole blood is invasive which affects patient compliance, potentially expensive with the required consumables, and is difficult to store. Dried blood spots (DBS) are an alternative method of sample collection that addresses these points. DBS are prepared by dropping patient whole blood, typically via finger or heel prick, onto filter papers and dried at room temperature before storage. Because DBS require lower blood volumes, they have also been used for collecting samples from neonates (145). Storage and transport of DBS not only require less space, it can also be done at room temperature whereas whole blood storage and transport requires freezing temperatures (146). Applications of DBS are extensive including PCR, detection of antibodies and antigens, and biomarkers (147-150).

1.5. CRISPR

1.5.1. CRISPR technology

Clustered regularly interspaced short palindromic repeats (CRISPR) are DNA sequences found in prokaryotic organisms. These repeated spacers are derived from virus genomes such as bacteriophages, and together with the CRISPR-associated (Cas) proteins, act as an adaptive immunity system in these cells by targeting and destroying the foreign DNA or RNA (151). CRISPR systems are categorised into two major classes depending on whether it requires multiple effector proteins (class 1) or only one endonuclease (class 2). Each class is then further divided into three types; types I, III, and IV in class I and types II, V, and VI in class 2 (152).

The general mechanism for CRISPR-Cas systems contains three main stages; adaptation, expression and maturation, and interference. During adaptation, certain Cas proteins incorporate any foreign DNA into the cell's genome, creating a new spacer sequence. In expression and maturation, the entire CRISPR array is transcribed and processed into individual CRISPR RNAs (crRNAs), each containing one spacer sequence. The crRNAs then form a complex with Cas proteins. In the interference stage, the Cas-crRNA complex is targeted to any foreign nucleic acid whose whole sequences are complementary to the crRNA. This binding activates the Cas protein, which is an RNA-guided endonucleases and creates either single-stranded or double-stranded breaks and destroys the foreign nucleic acid (153).

Perhaps the most understood and well-known Cas protein is Cas9. Cas9 has been shown to be directly involved only in the interference stage and is responsible for the cleavage of foreign nucleic acids (154). The main restraint of Cas9 is the crRNA must be approximately 20 bp and contains a protospacer adjacent motif (PAM), which is an 5'-NGG-3' directly on the 3' end of the crRNA (155). Because of its relative simplicity, CRISPR/Cas9 has been extensively used as a gene editing tool. By inducing a targeted DNA break, the host cell can repair the strand with either non-homologous end-joining (NHEJ) or homologous recombination (HR) (156). NHEJ is the more prevalent method of repair and works by joining the two broken DNA ends directly without any template. This can often lead to insertion/deletion (indel) which effectively knocks out the gene

(157). HR, on the other hand uses a repair template to ensure the resulting sequence is correct (158). An external DNA template can be introduced to be used in HR and the repaired sequence will be that of the template, allowing for gene editing or knock-ins (159).

1.5.2. CRISPR diagnostics

A more recent application for CRISPR technology is for diagnostics. This is made possible by a property present in some type V and type VI CRISPR systems which involves Cas12 and Cas13 respectively. Unlike Cas9, which only cleaves its target according to the crRNA sequence, these two Cas protein groups exhibit 'collateral activity' in which upon activation, they will also cleave other ssDNA (Cas12) or ssRNA (Cas13) outside of the crRNA's target sequence (160, 161). By introducing fluorescently labelled ssDNA or ssRNA reporters, a fluorescent signal can be produced from the cleavage of these reporters in the presence of the target DNA/RNA sequence (162).

A molecular platform was developed by combining the highly specific Cas13a detection with a pre-amplification step, increasing the sensitivity of the assay. This platform, Specific High Sensitivity Enzymatic Reporter unLOCKing (SHERLOCK), uses RPA to pre-amplify the template before detection with a Cas13a ortholog found in *Leptotrichia wadei* (LwaCas13a). The assay was able to detect template concentrations as low as 2 aM and can differentiated sequences with a single-base single nucleotide polymorphism (SNPs). Moreover, for developing the assay for field use, the Cas13a-crRNA complex was also shown to be able to be lyophilised and rehydrated (163).

While the different Cas12 and Cas13 cleave 'bystander' nucleic acids not specifically targeted, the sequences cleaved are not completely random. Different Cas proteins have a preference of which sequence it cleaves. An update to SHERLOCK uses three Cas13 proteins, each with different reporter sequence preferences, along with a Cas12a protein which detects dsDNA targets to create a multiplex assay detecting up to four targets. This assay was also adapted for a visual readout using LFT. By using a reporter labelled with FAM and Biotin, the cleavage of the reporter can be visualised on a commercial LFT strip (164). The single temperature condition of RPA and CRISPR reactions, ability to be lyophilised and stored at room temperature, and

visualisation through LFT while keeping the sensitivity and specificity high makes SHERLOCK a very attractive technology for POC diagnostics.

During the COVID-19 pandemic, a SHERLOCK assay was developed called SHERLOCK Testing in One Pot (STOP). This assay aimed to minimise the amount of liquid handling and combine the extraction, amplification, and detection into a single incubation step and read out was done by LFT (165). STOP test for COVID-19, or STOPCovid, used LAMP instead of RPA and AapCas12b from *Alicyclobacillus acidiphilus*. The reason given was that LAMP reagents are more commercially available and AapCas12b is thermally stable at the higher temperature that LAMP is operated at (55-65°C) (166). The STOPCovid assay was able to detect SARS-CoV-2 concentrations of as low as 100 copies without any cross-reactivity with the related SARS-CoV or MERS-CoV.

A SHERLOCK assay for COVID-19 was clinically validated using nasopharyngeal (NP) and throat swabs from suspected SARS-CoV-2 positive patients in Siriraj Hospital, Bangkok, Thailand (167). A total of 154 clinical samples, 81 of which are SARS-CoV-2 positive as verified by RT-qPCR with a wide range of Cq values from 11 – 37, were tested on both fluorescence and LFT readouts. The fluorescence readout had both a specificity and a sensitivity of 100% while the LFT readout had a sensitivity of 97% for samples with Cq values of less than 32. This test was also deployed as a screening test for pre-operative surgical patients to protect the healthcare worker at Siriraj hospital using the fluorescence readout. The visualisation was simply done by a blue LED and smart phone camera. A multiplexed variation of this assay was also developed to detect two different SARS-CoV-2 genes (S and N genes) to not only detect the virus, but to also differentiate between the Delta (B.1.617.2) and Omicron (B.1.1.529) variants (168).

1.6. Thesis overview, aims and objectives

The overarching theme of this thesis is the enhancement of diagnostic approaches for pathogens causing AUFs in South and Southeast Asia with an emphasis on low resource areas, for both research and clinical purposes. The aims of this thesis are the development of molecular assays

for detecting selected pathogens, the evaluation of DBS as a specimen format for molecular detection, and validating a novel POC test. The objectives of this thesis are as follows.

1. Design oligonucleotides for *Rickettsia* spp. and CHIKV to be assembled into multiplex real-time (RT-)PCR assays for the detection of bacterial (*Rickettsia* spp., *Leptospira* spp., *O. tsutsugamushi*, and other Eubacteria) and viral (DENV, CHIKV, and flaviviruses including JEV and ZIKV) pathogens from whole blood specimens.
2. Development of a CRISPR-based assay to detect DENV, CHIKV, and ZIKV in whole blood specimens with the purpose of being used in a low resource setting, requiring minimal equipment to perform from extraction to detection.
3. Evaluate DBS as a specimen platform to be used in molecular diagnosis for viral pathogens. This includes development of an elution protocol and real-time PCR assay on the automated BD MAX™ system as well as evaluating the effects of storage temperature on the efficiency of the real-time PCR assay.
4. Validate and determine appropriate thresholds for the Chembio DPP® fever panel II Asia systems in patient specimens for detecting pathogenic antigen and IgM antibody. Real-time PCR and serological assays will be used as reference tests.

CHAPTER 2

Materials and methods

This chapter describes the materials and methods used and applied in the chapters to come. Generalised protocols are given here along with the recipes and preparation of chemicals and reagents used in this thesis. Specific protocols are given in their respective chapters.

2.1. Chemical and reagent preparation

2.1.1. Terrific broth (TB)

Terrific broth and agar were used to culture *E. coli* in order to produce plasmids. Two solutions are prepared as follows:

Solution A (0.17 M potassium dihydrogen phosphate (KH_2PO_4) & 0.72 M potassium dihydrogen phosphate (K_2PO_4)):

- 90 mL deionised (DI) water
- 2.31 g KH_2PO_4 (104873.1000, Merck, Darmstadt, Germany)
- 12.54 g K_2PO_4 (105104.1000, Merck, Darmstadt, Germany)

Adjust to 100 mL with DI water

Solution B:

- 400 mL DI water
- 6 g tryptone (T7293-250G, Merck, Darmstadt, Germany)
- 12 g yeast extract (RM027-500G, HiMedia Laboratories, Maharashtra, India)
- 2 mL glycerol (A16205.AP, Thermo Fisher Scientific, Waltham, MA, US)
- (If preparing solid media) 7.5 g Oxoid™ Agar Bacteriological (LP0011B, Thermo Fisher Scientific, Waltham, MA, US)

Adjust to 450 mL with DI water

After the two solutions were sterilised via autoclave, they were left to cool down to approximately 60°C. 50 mL of solution A was then added to solution B to make a mixture solution of 500 mL. If solid media were being prepared, the plates were poured immediately into 15 mm petri dishes after mixing and allowed to cool in a biosafety cabinet (BSC). The plates were stored in sealed plastic bags at 4°C.

2.1.2. Luria-Bertani (LB) broth

Luria-Bertani broth was used to culture *E. coli* in order to produce competent cells. To prepare a 1 L LB broth stock, a mixture was prepared as follows:

- 950 mL DI water
- 10 g tryptone
- 10 g sodium chloride (NaCl)
- 5 g yeast extract

The mixture was sterilised by autoclave and stored at 4°C until use.

2.1.3. Oligonucleotide annealing buffer

The annealing buffer was used for annealing ssDNA crRNAs in preparation for *in vitro* transcription. Table 3 shows the recipe used.

Table 3: Recipe for the oligonucleotide annealing buffer.

Component	Final concentration
Tris, pH 7.5	10 mM
NaCl	50 mM
Ethylenediaminetetraacetic acid (EDTA)	1 mM
Sterile water	Adjust to 1000 μL

2.1.4. Cas13 protein storage buffer

The Cas13 storage buffer was prepared with the recipe shown in Table 4.

Table 4: Recipe for Cas13 storage buffer.

Component	Final concentration	Amount
Tris, pH 7.5 (400 mM)	50 mM	1.25 g
NaCl	0.6 M	0.35 g
Glycerol	5% (v/v)	500 μL
Dithiothreitol (DTT) (1 M)	2 mM	20 μL

The mixture was then adjusted to 10 µL with sterile water and aliquoted into 1.5 mL tubes, 350 µL per tube. The buffer is kept at -80°C for long-term storage and -20°C for short-term storage or as a working stock.

2.2. Nucleic acid amplification and manipulation

2.2.1. Real-time polymerase chain reaction

Primers and probes were ordered from U2Bio (South Korea). The lyophilised stocks were resuspended in DNase and RNase-free water at 100 µM and stored at -20°C. Working dilutions were made by diluting the stock to a concentration of 10 µM with sterile water. For each assay, the oligonucleotides were combined for convenience when preparing the PCR premix. The bacterial assay contains the oligonucleotides for ***R****ickettsia* spp., **E**ubacteria, ***L****eptospira* spp., and ***O****. tsutsugamushi* (RELO). The viral assay contains oligonucleotides for **JE**V, **C**HIKV, **D**ENV, and **Z**IKV (JeCDZ). The list of concentration of each oligonucleotide is shown in Table S 1. The sequences for each oligonucleotide are shown in Table S 7. To carry out a reaction, a pre-PCR master mix containing the primers, probes, and enzyme was prepared in a PCR hood as shown in Table 5. An 8% extra volume was always prepared to compensate for volume loss during pipetting. The enzyme used for all PCR reactions was the qScript XLT 1-Step RT-qPCR Toughmix (95132-500, Quantabio, Beverly, MA, US). After preparation, appropriate volumes of the pre-mix (typically 18-20 µL) was aliquoted into each well of a Hard-Shell® 96-well PCR plate (HSP9601, Bio-Rad, Berkeley, CA, US).

Table 5: General real-time (RT-)PCR pre-mix.

Component	Volume per 1 reaction
Sterile water	Adjust to 15 µL
Primer/probes	Up to the required concentration
qScript XLT 1-Step RT-qPCR Toughmix (2x)	10 µL
Total	15 µL

To add the template, the plate was moved to another PCR hood and appropriate amounts of template was added (typically 2-5 µL). The plate was then sealed with microseal 'B' PCR plate sealing film (MSB1001, Bio-Rad, Berkeley, CA, US) and centrifuged at 1000 rcf for 2 minutes at 4°C in a refrigerated centrifuge (5430R, Eppendorf, Hamburg, Germany). The plate was placed in either a CFX Opus 96 Real-Time PCR System (12011319, Bio-Rad, Berkeley, CA, US) or a CFX96 Touch Real-Time PCR Detection System (10010424, Bio-Rad, Berkeley, CA, US).

2.2.2. Loop-mediated amplification

LAMP primers were first resuspended at 100 M with sterile water before being further diluted to its working concentration. The primer stocks were stored at -20°C. A 10X combined primer mixture was then prepared as shown in Table 6. Two versions of the primer mixture were used, one including the FIP with a T7 promotor and one without. The primer sequences are shown in Table S 2.

Table 6: Preparation of 10X combined LAMP primer mix.

Mix	Oligonucleotide	Final concentration	Volume
With T7 promotor	F3	0.2 μM	1.0 μL
	B3	0.2 μM	1.0 μL
	FIP	0.53 μM	2.7 μL
	BIP	1.6 μM	8.0 μL
	LF	0.4 μM	2.0 μL
	LB	0.4 μM	2.0 μL
	FIP with T7 promotor	1.07 μM	5.4 μL
	Sterile water		28.0 μL
	Total		50 μL
	Oligonucleotide	**Final concentration**	**Volume**
Without T7 promotor	F3	0.2 μM	1.0 μL
	B3	0.2 μM	1.0 μL
	FIP	1.6 μM	8.0 μL
	BIP	1.6 μM	8.0 μL
	LF	0.4 μM	2.0 μL
	LB	0.4 μM	2.0 μL
	Sterile water		28.0 μL
	Total		50 μL

After all work areas were cleaned with 1,000 ppm troclosene sodium solution the LAMP reaction was then prepared on ice as shown in Table 7. The enzyme used for the reaction was the WarmStart® Colorimetric LAMP 2X Master Mix with UDG (M1804S, NEB, Hitchin, UK). When preparing the reaction, the amount prepared was 10% more than necessary to account for loss during pipetting.

Table 7: Reaction pre-mix for LAMP.

Component	Volume for 1 reaction
Sterile water	2 μL
2X LAMP master mix	5 μL
10X combined LAMP primer mix	1 μL
Total	8 μL

The reaction mix was then aliquoted into 8-strip tubes, 8 μL per tube. 2 μL of template DNA/RNA was then added and the reaction mixture was mixed by flicking and spun down. Incubation was done in a T100 thermal cycler (1860196, Bio-Rad, Berkeley, CA, US) at 60°C for 30 minutes. Once incubation was complete, the tubes were photographed and visually inspected. The pink solution turned in the presence of the target DNA/RNA. The amplified products were visualised on a 2% agarose gel or stored at 4°C.

2.2.3. Recombinase-aided amplification

Primers for RAA were ordered from U2Bio (Seoul, South Korea). The primer sequences can be found in Table S 3. After resuspension at 100 μM, working stocks were prepared at 10 μM. The RT-RAA nucleic acid amplification kit (B00R00, Jiangsu Qitian Gene Biotechnology, Wuxi, China) was used with a slightly altered protocol. The protein mixes of the kit were lyophilised inside reaction tubes. The manufacturer's protocol used one tube per one reaction. To save both cost and kit, we used one tube per two RAA reactions.

The reaction mix was first prepared as shown in Table 8: Reaction pre- mix for RAA.. For every 2 reaction, 41 μL of the mix was added to a reaction tube. After mixing by hand, all of the rehydrated contents were pooled together and mixed again by hand. 20.5 μL of the pre-mix was aliquoted into individual wells of an 8-strip tube with snap cap (EX-P-02X8-CF, ExtraGene, Taichung, Taiwan). 2.5 μL magnesium acetate I was added to the lid of each tube before 2 μL template was added into each tube. Sterile water was used for the no template control. After a brief spin down to pull the magnesium acetate I into the mixture, the tubes were mixed by hand and

spun down again. The reaction was then incubated at 39°C for 40 minutes. The products were stored at room temperature for short-term storage (less than 24 hours) or at -20°C for long term storage.

Table 8: Reaction pre- mix for RAA.

Component	Volume for 2 reactions
Buffer V	25 μL
Forward primer (10 μM)	2 μL
Reverse primer (10 μM)	2 μL
Sterile water	4 μL
Total	41 μL

2.2.4. Gel electrophoresis

PCR and isothermal amplification product were visualised via agarose gel electrophoresis. 2% agarose gels were prepared by adding UltraPure™ Agarose (16500100, Thermo Fisher Scientific, Waltham, MA, US) to 0.5% TBE buffer. 5 μL of the sample was vigorously mixed with 1-2 μL Gel Loading Dye, Purple (6X) (B7024S, NEB, Hitchin, UK) before loading into each well. 100 bp DNA Ladder (N3231S, NEB, Hitchin, UK) was also similarly mixed with dye and loaded into the first well of each gel. The gel was immersed in 0.5% TBE buffer and electrophoresis run at 70V until the DNA marker reached approximately 1-2 cm away from the edge of the gel. The gel was then immersed in 1x gel stain prepared by diluting 10 μL SYBR™ Safe DNA Gel Stain (S33102, Thermo Fisher Scientific, Waltham, MA, US) in 100 mL tap water. After 25 minutes, the gel was visualised with the Gel Doc™ EZ System (1708270, Bio-Rad, Berkeley, CA, US) using the UV sample tray.

2.2.5. T7 transcription

T7 transcription was done using the HiScribe™ T7 High Yield RNA Synthesis Kit (E2040S, NEB, Hitchin, UK) following manufacturer's protocol for amplicons shorter than 0.3 kb. Briefly, a reaction was setup at room temperature as shown in Table 9. The reaction was incubated at 37°C for 4 hours in an Eppendorf™ Thermomixer™ Comfort (5361 000.015,

Eppendorf, Hamburg, Germany). Both the pre-transcribed and post-transcribed reactions were quantified using the Qubit™ RNA High Sensitivity (HS) Assay Kits (Q10210, Thermo Fisher Scientific, Waltham, MA, US) to compare the amount of RNA present in the mixtures.

Table 9: Reaction mix for T7 transcription reaction.

Component	Amount for one reaction
Sterile water	Adjust to 20 μL
10X reaction buffer	1.5 μL (0.75X final concentration)
ATP (100 mM)	1.5 μL (7.5 mM)
GTP (100 mM)	1.5 μL (7.5 mM)
UTP (100 mM)	1.5 μL (7.5 mM)
CTP (100 mM)	1.5 μL (7.5 mM)
Template DNA	1 μg
T7 RNA Polymerase	1.5 μL

2.2.6. In Vitro Transcription

crRNAs and their reverse complements were first ordered as ssDNA (Table S 6). The respective pairs were then annealed together by preparing the reaction shown in Table 10 and heating at 95°C for 2 minutes followed by a decrease of 1°C every minute until the reaction reached 25°C.

Table 10: crRNA annealing reaction.

Component	Volume for one reaction
Annealing buffer	40 μL
ssDNA with the crRNA sequence (100 μM)	5 μL
ssDNA with complementary sequence to the crRNA (100 μM)	5 μL
Total	50 μL

The annealed oligonucleotides were then first amplified using the Q5® High-Fidelity DNA Polymerase (M0491S, NEB, Hitchin, UK) in Table 11 and the "crRNA_AMP" cycling condition (Table S 8). After amplification, the products were cleaned up using the DNA Clean & Concentrator-5 kit using manufacturer's protocol (D4014, Zymo Research, Irvine, CA, US). 250 μL DNA binding buffer was added to 50 μL amplified product and mixed by vortex. The mixture was transferred to a spin column which was then turn placed in a collection tube. The column was centrifuged at 11,000 rcf for 30 seconds and the flowthrough was discarded. 200 μL was added to the column before another centrifugation and discarding the flowthrough. This was repeated once more before the column was centrifuged at 18,000 rcf for 3 minutes. The column was placed on in fresh collection tube and 20 μL 60°C nuclease-free water was added before a final centrifugation at 18,000 rcf for 1 minute, collecting the eluent.

Table 11: Reaction mixture for amplifying crRNA before in vitro transcription.

Component	**Volume for one reaction**
Q5® reaction buffer	10 μL
dNTPs (10 mM)	1 μL
T7 primers (10 μM each)	2.5 μL
Annealed DNA with the crRNA sequence (10 μM)	2.5 μL
Q5® DNA polymerase	0.5 μL
Sterile water	Adjust to 50 μL

In vitro transcription was done using the HiScribe™ T7 High Yield RNA Synthesis Kit as described above. The products were further treated with DNase I (M0303s, NEB, Hitchin, UK) as shown in Table 12 before inactivation by adding 1 μL EDTA and incubation at 75°C for 10 minutes. Clean-up was done using the RNA Clean & Concentrator-25 kit (R1017, Zymo Research, Irvine, CA, US) following manufacturer's protocol. 100 μL of RNA binding buffer was added to 50 μL of the RNA product. 100 μL absolute ethanol was then added and mixed before the mixture was transferred into a Zymo-Spin™ IICR column on a collection tube. The column was centrifuged at 11,000 rcf for 30 seconds before the flowthrough was discarded. 400 μL RNA prep

buffer was then added before another centrifugation. Two rounds of washing with RNA wash buffer was done, first by adding 700 µL of the buffer and centrifuging as before. The second round was done by adding 400 µL wash buffer and centrifuging at 11,000 rcf for one minute. A fresh collection tube was added and the product was eluted with 25 µL nuclease-free water.

Table 12: Reaction mix for DNase I treatment of transcribed crRNA.

Component	Volume for one reaction
RNA product (~10 µg)	20 µL
10X DNase I reaction buffer	5 µL
DNase I	1 µL (2 units)
Nuclease-free water	Adjust to 50 µL

2.3. Whole blood extraction

2.3.1. Roche MagNA Pure 24 operation

Whole blood extraction was done using the fully-automated MagNA Pure 24 instrument (07290519001, Roche, Rotkreuz, Switzerland) using the MagNa Pure 24 Total Isolation Kit (07658036001, Roche, Rotkreuz, Switzerland). Before and after every run, the instrument and its accessories were thoroughly cleaned by wiping down all surfaces with once with 1,000 ppm troclosene sodium solution, followed by twice with 70% ethanol. If frozen blood was used, it was first thawed in a water bath set at 37°C and immediately put on ice. In the case of freshly drawn blood, it was kept on ice and used immediately. Roughly 500 µL of whole blood was aliquoted into each well of 3 MagNA Pure 24 processing cartridges (07345577001, Roche, Rotkreuz, Switzerland). Each cartridge has 8 wells and the MagNA Pure 24 can process up to 3 cassettes, totalling a maximum of 24 samples per run. Once the reagents, consumables, and samples were loaded, the run was started following the manufacturer's protocol using the protocol "Pathogen 1000". The program was setup for an input volume of 500 µL and elution volume of 50 µL. Once the run has finished, the extracted nucleic acid samples were placed on a magnetic stand. After any leftover magnetic bead adhered to the tubes' walls, the remaining liquid was aspirated into fresh tubes. The

magnetic beads were removed as they can interfere with PCR reactions down the line. After a short time, the eluent was aspirated and stored in 8-strip tubes at -80°C.

2.3.2. QuickExtract DNA Extraction Solution

Whole blood was drawn into VACUETTE® EDTA tubes (456038, Greiner Bio-One, Kremsmünster, Austria). If plasma was needed, the tube was allowed to sit on ice until the blood cells separate at the bottom. The plasma layer was then carefully pipetted off. The sample was spiked with virus culture at this point if needed.

200 μL whole blood or plasma was added to 1800 μL QuickExtract™ DNA Extraction Solution (QE0905T, Biosearch Technologies, Hoddesdon, UK) for a dilution of 1:10. It was then diluted once more in the DNA Extraction Solution to the final dilution of 1:100. The tubes were incubated at 65°C for 6 minutes followed immediately by 98°C for 2 minutes. The extracted products were either used immediately, stored at -20°C, or purified using AMPure XP beads.

2.3.3. Manual extraction/Nucleic acid purification

DNA extraction from bacteria culture was done by first centrifuging the cells into a pellet. The pellet was then resuspended in 100 μL PBS and approximately 80 μL acid-washed 425-600 μm glass beads (G8772, Merck, Darmstadt, Germany) were added. The tubes were then vortexed at maximum speed for ten minutes to sheer the cell walls. After centrifugation at 16,000 x g for 10 minutes, the supernatant was collected and measured.

Purification of extracted samples or post-PCR products are also performed as follows. Equal volume of room temperature AMPure XP beads (A63881, Beckman Coulter, Indianapolis, IN, US) were added to the PCR product and the tube was incubated at room temperature for 10 minutes on an Eppendorf™ Thermomixer™ Comfort mixing intermittently at 300 rpm every 3 seconds before letting sit still for 2 more minutes. The tubes were then placed on a magnetic stand for 5 minutes or until the mixture became clear. The supernatant was discarded and the beads were washed twice by adding roughly 500 μL 70% ethanol and pipetting it out after 20 seconds. After the second wash, the tubes were briefly spun and any remaining ethanol was pipetted out. To elute the extracted nucleic acid, sterile water was added and the tube was incubated at 35°C for 10

minutes. The tubes were placed back on a magnetic rack for 5 minutes or until the mixture became clear. The supernatant was then collected and quantified by Qubit™ fluorometer 3.0 (Q33216, Thermo Fisher Scientific, Waltham, MA, US).

2.4. Positive control production

2.4.1. Competent cell preparation

Competent cell production was done using the calcium chloride ($CaCl_2$) method (169). A seed culture was prepared by inoculating *E. coli* into LB broth and incubated overnight. 1 mL of the *E. coli* culture was added to 99 mL fresh LB media and incubated on a shaking incubator at 37°C for 3-4 hours, shaking at 200 rpm. The OD_{600} of the culture was measured regularly until the measurement reaches 0.4, at which point the culture was incubated on ice for 20 minutes. The cells were then centrifuged at 4000 rpm for 10 minutes before the supernatant was discarded. The pellet was resuspended in 20 mL ice-cold 0.1 M $CaCl_2$ and incubated on ice for 30 minutes. The cells were then centrifuged again at 4000 rpm for 10 minutes and the supernatant was discarded. The pellet was resuspended in 5 mL ice-cold 0.1 M $CaCl_2$ with 15% glycerol. The cells were then divided into 100 µL aliquots and stored at -80°C.

2.4.2. Molecular cloning

Plasmids were ligated with PCR amplicons using the TOPO™ TA Cloning™ kit (K4575J10, Thermo Fisher Scientific, Waltham, MA, US) following manufacturer's protocols. In short, for each reaction, 4 µL purified PCR product and 1 µL each salt solution (containing 1.2 M NaCl and 0.06 M $MgCl_2$) and TOPO vector was combined in a 1.5 mL tube and incubated at room temperature for 5 minutes before the reaction was stopped by placing the tube on ice.

2.4.3. Transformation and screening

Competent cells were thawed on ice before 6 µL ligated plasmids mixture was added and gently mixed. The cells were then incubated on ice for 30 minutes and heat shocked in a 42°C water bath for exactly 45 seconds and placed back on ice for 2 minutes. After incubation, 250 µL room temperature 0.4% glucose-LB media was added. The cells were then incubated on a thermomixer at 37°C and 500 rpm for 1 hour. 150 µL of the cell culture was then spread onto TB

agar plates containing 100 μg/mL ampicillin. The plates were sealed with parafilm and incubated overnight at 37°C. Selected clones were inoculated in 1.5 mL TB media and incubated overnight at 37°C in a shaking incubator. Once grown, 0.5 mL cell culture was mixed with 0.5 mL sterile glycerol and stored at -80°C.

2.5. CRISPR-Cas13a detection

Prior to preparing the CRISPR reaction, the following reagents were first prepared:

- 10 ng/μL crRNA
- 120 mM $MgCl_2$
- 126 μg/mL LwaCas13a
- 2 μM Poly-U FAM RNA reporter
- 400 mM Tris, pH 7.4
- LwaCas13a storage buffer

All reagents were diluted with sterile water except for the LwaCas13a proteins which was diluted with its storage buffer. LwaCas13a protein stocks were stored at -80°C but after dilution, it was stored at 4°C for up to 9 days. The guide RNAs and reporter were synthesised by Integrated DNA Technologies (IDT, Coralville, IA, US). The poly-FAM reporter has the following sequence; 5' - 56-FAM/UUUUU/3IABkFQ - 3'. The sequences of the crRNA used in this project are shown in Table S 5.

The reaction pre-mix for a CRISPR reaction is shown in Table 13. The reagents were added in the order they appear in the table and everything was prepared on ice. An 8% extra volume is always prepared to compensate for volume loss during pipetting.

Table 13: LwaCas13a CRISPR reaction pre-mix.

Component	Volume for 1 reaction
Sterile water	7.1 μL
400 mM Tris, pH 7.4	2 μL
Ribonucleotide solution mix (N0466S, NEB)	0.8 μL
T7 RNA polymerase (M0251S, NEB)	0.6 μL
126 μg/mL LwaCas13a	1 μL
10 ng/μL crRNA	2 μL
2 μM Poly-u FAM reporter	2.5 μL
LwaCas13a Storage buffer	1 μL
120 mM $MgCl_2$	1 μL
Total	18 μL

18 μL of the premix was aliquoted into a well on a 96-well plate before 2 μL of the template was added. The plate was sealed and placed into the Bio-Rad CFX Opus 96. The program "CRISPR-Cas13" was selected which is essentially a 2-hour incubation at 37°C while reading the signal every 2:30 minutes (Table S 8).

2.6. Dried blood spots

2.6.1. Dried blood spot preparation

To avoid having to use patient samples during optimisation, mock DBS specimens were produced by either spiking healthy whole blood with either virus culture or transformed *E. coli* to be used during the optimisation processes. To prepare the former, DENV and CHIKV viruses were cultured in Vero cells by the Department of Tropical Paediatrics, Faculty of Tropical Medicine, Mahidol University as we do not have access to a BSL-3. For the *E. coli* spiked blood, the amplicon of each target was cloned into a plasmid as detailed earlier which was in turn transformed into competent *E. coli* cells. These *E. coli* cultures were then grown in terrific broth overnight. Virus or *E. coli* culture was diluted ten-fold in PBS before being spiked into healthy

EDTA whole blood at a ratio of 1:10. After thorough mixing, each dilution was dropped onto separate Whatman® 903 Proteinsaver cards, 50 µL per spot, four spots per card (Figure 10). Any remaining spiked whole blood was stored at -80°C to be used as controls while the blood spots were left to dry in a BSC for at least 6 hours or up to overnight. Once dried, each card was placed in separate airtight bags along with desiccant packs and stored either at room temperature, -20°C, or -80°C.

Figure 10: Example of a filled DBS card

Before further processing, the DBS need to be excised from the filter paper to be eluted. In a BSC, a square was carefully cut around each blood spot, being careful to not touch the blood spot directly. Between each blood spot, the scissors and forceps used for handling were sterilised via dipping in absolute ethanol and flaming. After cutting, each spot was placed face-up in separate wells of a 12-well plate (83.3921-C, Sarstedt, Nümbrecht, Germany).

2.6.2. Dried blood spot elution

The entire contents of a BD MAX™ ExK™ TNA-2 samples buffer tube (SBT), roughly 1.5 mL sample buffer, was then poured into each well. The plates were incubated on a Stuart™ microtitre plate shaker (TSSM5, Cole-Parmer, Vernon Hills, IL, US) at 1,100 rpm for 3 hours before the supernatant was pipetted back into the SBT.

2.7. BD MAX™ operation

The protocol for the BD MAX™ instrument is based on the respiratory assay for SEACTN, which in turn is based on a protocol for detecting viral respiratory pathogens from the Hamilton Regional Laboratory Medicine Program (HRLMP) using the BD MAX™ ExK™ TNA-2 (442825, BD, Franklin Lakes, NJ, US). Three different types of tests were used; extraction only,

PCR only, and full process in which the instrument automatically performs the extraction and PCR in a single program.

For the full process run, the PCR mix has to be prepared prior to the run. Primers and probes were mixed into a solution with 50X the concentration of the final reaction. A general reaction mix is shown in Table 14.

Table 14: Reaction mix for BD MAX™ full process PCR pre-mix.

Component	Volume for 1 reaction
Sterile water	Adjust to 12.5 µL
Primer/probe mix	0.5 µL each
qScript XLT One-Step RT-qPCR Toughmix	10.6 µL
Total	12.5 µL

Once mixed, the solution was aliquoted into BD MAX™ conical tubes (437016, BD, Franklin Lakes, NJ, US), 12.5 µL per tube and sealed with the BD MAX™ 5-color seal sheets (21174679, BD, Franklin Lakes, NJ, US) by using the PlateMax® (HS-1230, Corning, Corning, NY, US) set at 185°C for 8 seconds. The sealed tubes were stored at -20°C until use.

To perform a run, the BD MAX™ instrument and BD MAX™ system rack was cleaned first with 1000 ppm troclosene sodium solution, followed by twice with 70% ethanol. The unitized reagent strip (URS) was then assembled onto the rack. Two types of full process run can be performed; single master mix and dual master mix. For the single master mix run, in which the extracted sample is only added to a single reaction, the silica tube from the ExK™ TNA-2 kit and a sealed PCR pre-mix tube was snapped into positions 1 and 3 on the URS respectively. For a dual master mix run, in which the extracted sample is added to two different reactions, functionally doubling the number of targets possible for a single specimen, two sealed PCR pre-mix tubes were added to positions 2 and 4 of the URS, keeping the silica tube in position 1. Figure 11A and B illustrates the setup of the URS for the full process runs.

In the case of an extraction only run, the silica tube is snapped into position 1 again, but an empty conical tube was snapped into position 3 as shown in Figure 11C. The instrument will elute 10-12.5 μL of the extracted product into this tube. Once the run is finished, the products were quickly moved into an 8-strip tube and immediately used or stored at -80°C. The loaded rack was placed at 4°C to keep the PCR mix cool while preparing the samples.

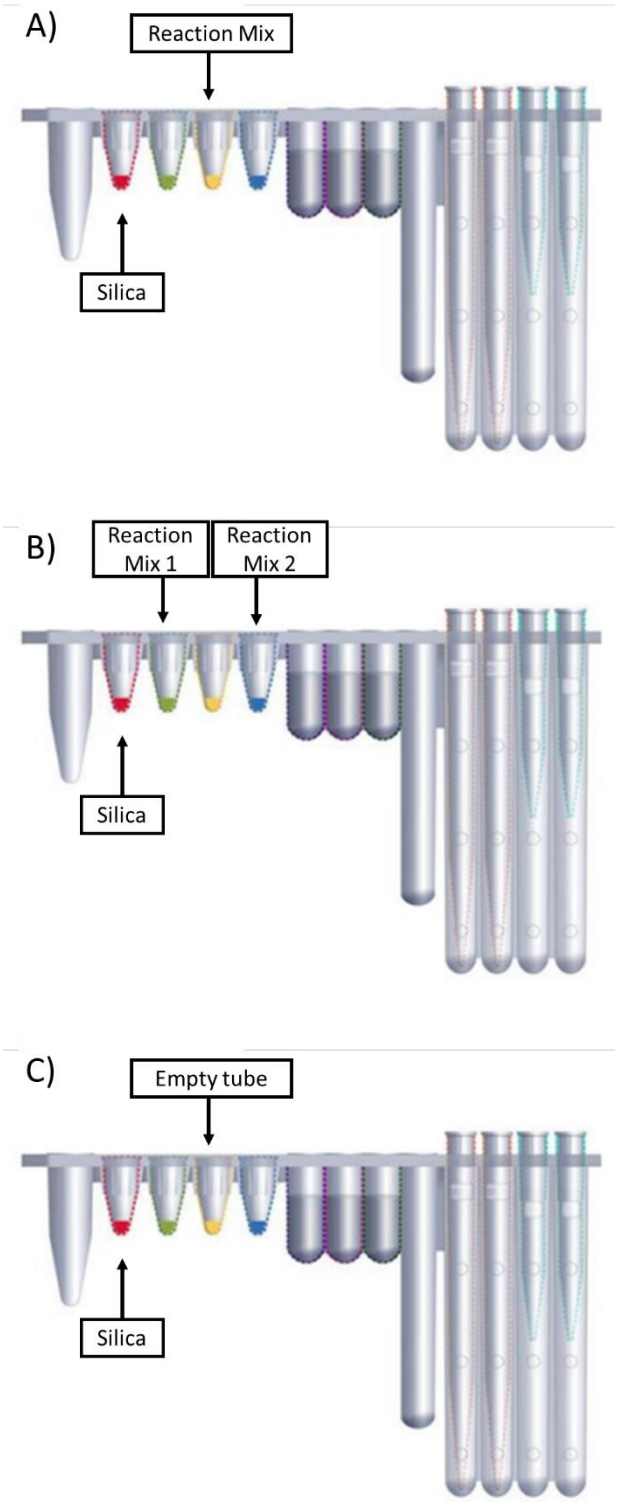

Figure 11: Position of the reagents snapped into a BS MAX™ URS for different types of tests. A) Full process runs with one master mix. B) Full process runs with dual master mix. C) Extraction only runs.

To prepare the sample, SBTs were prepared and labelled for each sample. The barcode on each SBT was then scanned alongside the sample IDs of the respective samples, making sure the correct test was chosen for each sample. Either 50 μL whole blood or eluted DBS was added to each SBT before being mixed by vortex and loaded into the previously assembled system rack. The rack(s) were then loaded into the BD MAX™ instrument and the run stared.

To perform a PCR only run, a pre-mix was first prepared as shown in Table 15 typically with an 8% extra to account for volume loss during pipetting. 5 μL of the pre-mix was then aliquoted into separate tubes and 5 μL of template was added. After a brief vortex and spin-down, the entire mixture was pipetted into separate chambers on a BD MAX™ PCR cartridge (437519, BD, Franklin Lakes, NJ, US). Up to two cartridges can be loaded into the BD MAX™ instrument per run for a total of 42 samples. The PCR only test was chosen on the instrument and the run begins.

Table 15: Components in a general PCR pre-mix for a PCR only run of the BD MAX™ instrument.

Component	Volume per 1 reaction
Sterile water	Adjust to 5 μL
Primer/probes	Up to the required concentration
qScript XLT 1-Step RT-qPCR Toughmix (2x)	4.24 μL
Total	5 μL

2.8. Chembio DPP® Fever Panel II Asia system

2.8.1. Laboratory testing

Initial testing of the DPP® kits were done in the laboratory using fever patients' EDTA whole blood samples from children (age 1 months to 5 years old) in Bangladesh that were collected for Spot Sepsis, a similar project to SEACTN focusing on AUFs in children across South and Southeast Asia, and stored at -80°C (N = 216). Due to difficulties in performing the assays, the commercially available DPP® ZCD IgM/IgG System was used for the last 168 samples as

comparison. These tests are only able to detect DENV, CHIKV, and ZIKV antibodies. Real-time PCR assays for bacteraemia and viraemia were also done on these samples as reference.

During processing, 24 samples were processed at a time in three batches of 8. Because there are multiple incubation periods during processing, subsequent batches can start during the previous batch's incubation step to save time. Before starting processing, the DPP® Micro Reader 2 was loaded with the respective RFID card (antigen or IgM antibody). The blood samples were thawed by immersing the tubes in a water bath at 37°C and immediately put on ice once thawed. 8 DPP cartridges were opened at a time and labelled with the patient ID. The work area is divided into three zones to separate each batch. Each assay was performed as described in the manufacturers protocol, albeit with EDTA venous whole blood rather than freshly drawn capillary blood.

A control was also performed as a comparison to the patient whole blood specimens. Healthy venous whole blood was drawn into EDTA tubes before inverting at least 20 times before they were kept on ice. The collected blood was pooled into a 50 mL tube before storage at -80°C overnight. The DPP® tests were done identically to the patient samples.

For the antigen system, 50 μL of the sample was added to well 1 as labelled on the antigen cartridge before 4 drops of the sample buffer was added to the same well at which point a timer was started. At the 5-minute mark, 12 drops of the running buffer were added to well 2 of the cassettes before letting the cartridge sit for 15 more minutes. During this time, processing the next batch could begin. After the incubation, the signal was read in the DPP® Micro Reader 2.

For the IgM antibody system, 10 μL of blood was first mixed with 600 μL sample buffer before 100 μL of the mixture was added to well 1 of each IgM cartridge and a timer was started. The remaining steps follows the antigen cartridge with a 5-minute waiting before 300 μL of the running buffer was added to well 2 of the cartridges. A 15-minute waiting period follows in which processing the next batch can start. After waiting, the signal is ready to be read.

The ZCD IgM/IgG system was processed similarly to the Fever Panel II Asia IgM antibody panel and was performed after the two Fever Panel II Asia systems. 2 drops of sample

buffer were added to the remaining whole blood sample before 100 μL of that mixture was added to well 1 of each ZCD cassette. After 5 minutes, 9 drops of running buffer were added to well 1 and the cassettes were left for 15 minutes before reading.

To read the signal the cartridges were first visually inspected and the presence of the control bands were noted. If either of these bands are missing, the test is considered invalid and the cartridge is discarded. The presence of the six test bands was also noted and recorded. Each cartridge was then inserted into the DPP® Micro Reader 2 which reads the intensity of each band as a numerical value which was recorded. The ZCD system was read using the older version of the DPP® Micro Reader. A photo was also taken of each cartridge and DPP® Micro Reader 2 in case of any discrepancies in the written data. The cartridges and were disposed of in red biohazardous waste bags for incineration. Any contaminated waste was disinfected with Virkon® before discarding in to red biohazard bags.

2.8.2. Field testing

Performance of the DPP® Fever Panel II Asia tests on patients' capillary blood in Chiang Rai, Thailand was coordinated by the Chiang Rai Clinical Research Unit (CCRU). The tests were performed for patients recruited in SEACTN WP-B at two sites, Mae Chan Hospital and Mae Suai Hospital (N = 520). Criteria for enrolment were fever patients, axillary temperature ≥ 37.5°C, or history of fever less than 24 hours within presentation, aged > 28 days. Exclusion criteria include presentation caused by trauma, presentation less than 3 days after immunisations, or the healthcare worker in charge of the patient decided to send the patient home after the initial assessment. Sample collection was done over the course of four months, from July to November 2023. A total of 269 and 269 patients were tested at Mae Suai Hospital and Mae Chan respectively. During routine whole blood sample collection for SEACTN, capillary blood was taken via finger prick and tested on the DPP® kits immediately.

Prior to starting performing the tests on patients, a training session was held at Mae Suai Hospital and the CCRU office for the research nurses. A booklet for running the tests was made to give to the research nurses (Appendix 9.3). These booklets served several purposes, mainly as

an illustrated guide for the nurses with a checklist for each step of the process to make following the protocol more intuitive rather than having to read the more verbose Chembio manual. This was especially helpful as nurses could keep track of the process even while working on multiple tests or multiple patients simultaneously. The front page of the booklet also served as a data entry point with a table to record the signal value, as well as the presence of each respective band as well as the control bands. Again, if either of the control bands were missing, the test was considered invalid although the nurses were instructed to continue to fill in the entire form regardless. Furthermore, a QR code on the front page led to a google form documents for the nurses to input the data once they had the time to do so, serving as another data entry point. As the test benefits from having multiple timers running simultaneously, QR codes linking to a free timer application for smartphones, MultiTimer (Persapps), were also included in the booklet.

Some minor adjustments were made to make running multiple tests simultaneously simpler as both the antigen and IgM antibody system were used for each patient. Each of the test kits included a sample buffer bottle and a running buffer bottle which are virtually identical, except for the labels. To prevent confusion and accidentally using the wrong bottle, the nurses were instructed to label the sample buffers' lids with brightly coloured stickers to differentiate them from running buffer bottles.

Used cassettes were collected in airtight bags to be sent back to MORU Bangkok, along with the booklets for cross-checking any discrepancies that might be present in the digital data. Any booklet without a corresponding digital data entry was discarded, as without the digital form, there were no photographic evidence.

2.9. Data analysis and visualisation

Statistical analysis and data visualisation was done in the R programming language (R 4.2.3) (170) inside RStudio (Build 563). Data manipulation was done primarily with the `dplyr`, `reshape2`, `tidyverse`, and `tidyr` packages (171-174). Other packages used include `lubridate` and `stringi` for processing dates and strings respectively (175, 176). Data

visualisation was done using `ggplot2` and figures were exported as scalable vector graphics (SVG) using the built-in export function (177).

CHAPTER 3

Design of a multiplex real-time PCR assays for detecting bloodborne pathogens

This chapter describes the design of multiplex real-time PCR assays to detect bacterial and viral pathogens from whole blood specimens. The targets for the bacterial assays are *Rickettsia* spp., pathogenic *Leptospira* spp., *O. tsutsugamushi*, and other Eubacteria while the targets for the viral assay are CHIKV, and members of the genus flavivirus DENV, JEV, and ZIKV. The details of designing the probes and primers of each target are presented here. This assay was developed for use in SEACTN and was a collaboration effort of the laboratory. I was responsible for the design of the *Rickettsia* and CHIKV oligonucleotides in their entirety while aiding in the design of the remaining oligonucleotides as well as analysing the compatibility of the oligonucleotides in each assay. I also performed optimisation for the CHIKV assay.

3.1. Methods

3.1.1. Real-time PCR probes and primers design

After the target organisms to be included in the assays were finalised, primers and probes were sought from literature to identify conserved genes (178-180). Selected gene (bacteria) or whole genome (virus) sequences were obtained from NCBI, with an emphasis on sequences originating in South and Southeast Asia, then aligned in MEGA X using ClustalW to identify conserved loci within the genes (181). The human housekeeping *rnaseP* gene, which codes for ribonuclease P (RNase P), was chosen as the internal control for both assays (182). The list of target organisms and their respective target genes can be found in Table 16. Existing primers and probes were mapped onto the alignments to assess whether there were SNPs in their regions. If any SNPs are present, the location of the primer or probe would be changed to avoid them. In cases that this was not possible, such as in a highly variable region where there is an unavoidable SNPs, a degenerate base would be used in that location.

3.1.2. Bacterial real-time PCR assay

The citrate synthase (*gltA*) was selected for the *Rickettsia* spp. target as it contains a variable region that is flanked by two conserved regions (183). Designing a primer set in the conserved regions allows for species identification by sequencing the amplicons. Sequences from *Rickettsia* species of the typhus, spotted fever, and transitional groups were selected as shown in Table S 9 (184). Non-pathogenic species such as *R. bellii* and *R. canadensis* were omitted (185). After alignment, the oligonucleotides for *Rickettsia* were designed using the SkyNet's EasyPrimer tool which allows for primer design from an aligned FASTA file and is designed to find conserved regions that flanks variable ones (186).

The oligonucleotide for *O. tsutsugamushi*, *Leptospira* spp., and other Eubacteria targets were similarly designed from alignments by other members of the laboratory. For these targets, the 16S rRNA gene was chosen with the designs based on sequences found in literature (179, 180, 187, 188). Sequences used for designing the *O. tsutsugamushi*, *Leptospira* spp., and Eubacteria are shown in Table S 10, Table S 11, and Table S 12 respectively.

3.1.3. Viral real-time PCR assay

To reduce the number of oligonucleotides in each reaction, the three prime untranslated region (3'UTR) was chosen as the target as it is conserved across the flavivirus genus which includes DENV and JEV. This allows for having the two targets to share a primer. The E gene and E1 gene of ZIKV and CHIKV were chosen for their conserved nature and to reduce the chance of heterodimers forming. The CHIKV oligonucleotides were designed based on an existing oligonucleotide set (189). The sequences used for designing the viral assay is shown in Table S 13.

The other targets: DENV, ZIKV, and JEV were designed in the same manner by other members of the laboratory. The shared flavivirus forward primer was based on sequences from Xu et. al. while the DENV specific reverse primer was based on sequences from Mishra et. al. (190, 191). The remaining flavivirus-specific oligonucleotides were newly designed for this assay.

Table 16: List of genes chosen as the PCR target for each organism.

Target organism	Target gene	References
Rickettsia spp.	gltA	-
O. tsutsugamushi	16s rDNA	(188)
Leptospira spp.	16s rDNA	(105, 179)
Eubacteria	16s rDNA	(187)
DENV	3'UTR	(190, 191)
JEV	3'UTR	(190, 191)
ZIKV	E	-
CHIKV	E1	(189)
Homo sapiens (internal control)	*rnaseP*	(182)

After satisfactory primer and probe sequences were obtained, each oligonucleotide was analysed using either Primer3Plus or IDT's OligoAnalyzer tool (192) for its melting temperature (T_m), GC content, and potential dimers. To compare heterodimers, a matrix was made to compare the Gibbs free energy (ΔG) of each oligonucleotide against every other oligonucleotide involved in the same reaction. The T_m of each primer was kept around 60°C and the probes' Tm was aimed

to be approximately 5°C higher than the primers if possible. The GC content was set between 30% and 80% and repeat/palindromic sequences were avoided. Furthermore, any potential hairpin formation was minimised and the ΔG was limited to no less than -3 $\frac{kcal}{mol}$ while the ΔG of homo- and heterodimers among the other oligonucleotides in the same assay were kept -7.5 $\frac{kcal}{mol}$. If a primer or probe did not comply to the above criteria, the sequence was modified and analysed again.

Primer3Plus also analyses the T_m of each hairpin, homodimer, or heterodimer. If the T_m of an oligonucleotide is lower than the temperature the reaction uses, the oligonucleotide is considered adequate as the binding will dissociate in the reaction. Also because of the requirement of a template sequence in Primer3Plus, to assess heterodimers between sequences, the sequences of every probe and primer as well as its reverse complement were joined together for the analyses. Because Primer3Plus does not accept degenerate bases, to analyse any oligonucleotide that contain them, each of the possible bases were substituted and the one with the lowest ΔG was used for the analysis.

Once the oligonucleotides' sequences were finalised, they were ordered and tested separately in singleplex reactions. Genomic RNA from CHIKV culture was serially diluted and used as the template of the CHIKV assay. Initial testing was done using a gradient PCR cycling profile, from 51 to 61°C to determine the optimum annealing temperature. Optimising the primer and probe concentrations, reactions were setup with varying concentrations (0.2, 0.4, 0.6 pmol/μL) of the forward and reverse primer with a probe at a constant concentration of 0.2 pmol/μL.

3.2. Results

3.2.1. Bacterial assay oligonucleotides

Most of the first iteration of the primers and probes have properties within the set criteria. The oligonucleotides that fall outside of these criteria are the *Rickettsia* spp. probe and the entire *Leptospira* probe and primer set, all having a lower ΔG than -7.5 $\frac{kcal}{mol}$. The list of all the first iteration of the bacterial primers is shown in Table 17. Upon creating the matrix for the primers, many heterodimers had ΔG lower than -7.5 $\frac{kcal}{mol}$, with some exceeding -10.0 $\frac{kcal}{mol}$ as shown in Table 18.

After modifying the primers as described in Chapter 3.1.1 and updating the matrix, it became apparent that it is very difficult to eliminate all ΔG lower than -7.5 $\frac{kcal}{mol}$ as reducing a heterodimer between one pair of oligonucleotides generally introduces another between a different pair. Because of this, some heterodimers with ΔG as low as -12.9 $\frac{kcal}{mol}$ such as the dimer between the forward primer and probe of the Eubacteria oligonucleotide set were allowed if there was no way to increase it without affecting another heterodimer. The matrix of the ΔG of heterodimers between each oligonucleotide is shown in Table 18.

In some targets, achieving high enough T_m while keeping the remaining properties satisfactory was found to be difficult. This could be due to highly variable sequences which prevent designing in a new locus or the conserved region is a low GC-region. To counter this, the 3' ends of these primers were modified with zip nucleic acids (ZNA®, Metabion) which are able to increase the T_m by up to 10°C by decreasing the electrostatic repulsion between oligonucleotides and thus increasing the affinity (193).

Table 17: List of the first iteration on the oligonucleotides in the bacterial real-time PCR assay. The data given was analysed by IDT's OligoAnalyzer tool.

Target	Name	Sequence	Type	T_m	GC%	ΔG ($\frac{kcal}{mol}$)	
						Hairpin	Homodimer
	WH_RicGlt-F	ATCGAGGATATGATATTAAAGACTTAGCT	Forward	62.4°C	31.0%	0.27	-6.76
Rickettsia spp.	WH_RicGlt-R	CGCAAGCATAATAGCCATAGGA	Reverse	62.4°C	45.5%	-0.53	-3.14
	WH_RicGlt-P	ACTAATGMATGATGAGCAAYCT	Probe	68.1°C	36.4%	0.28	-9.21
	OT3-F	CCCATCAGTACGGAATAACA	Forward	60.0°C	45.0%	0.23	-3.65
O. tsutsugamushi	OT1-R	CTCTCAGACCAGCTACAGATCACA	Reverse	64.9°C	45.0%	0.66	-6.34
	OT-P	TAAGTGCTAATACCGTATGCCCTCTA	Probe	64.7°C	45.0%	0.11	-3.78
	Lepto-F	CCCGCGTCCGATTAG	Forward	59.3°C	66.7%	-1.12	-10.36
Leptospira spp.	Lepto-R	TCCATTGTGGCCGRACAC	Reverse	64.3°C	58.3%	-1.08	-9.28
	Lepto-probe-FAM	CTCACCAAGGCGACGATCGGTAGC	Probe	70.2°C	62.5%	-1.66	-11.85
	341F	CCTRCGGGRGGCWGCAG	Forward	67.6°C	76.5%	0.35	0.35
Eubacteria	803R	CTACCRGGGTATCTAATCC	Reverse	57.5°C	50.0%	-0.56	-0.56
	KB_Eub16s-P	GTGCCAGCAGCCG	Probe	67.6°C	76.9%	-1.08	-5.09

Table 18: Matrix of the Gibbs free energy of heterodimers between the bacterial PCR primers and probes.

ΔG ($\frac{kcal}{mol}$)	***Rickettsia*-F**	***Rickettsia*-R**	***Rickettsia*-P**	**OT-F**	**OT-R**	**OT-P**	***Leptospira*-F**	***Leptospira*-R**	***Leptospira*-P**	**Eubacteria-F**	**Eubacteria-R**	**Eubacteria-P**
***Rickettsia*-F**	-											
***Rickettsia*-R**	-5.34	-										
***Rickettsia*-P**	-4.67	-6.57	-									
***O. tsutsugamushi*-F**	-5.00	-3.07	-6.96	-								
***O. tsutsugamushi* -R**	-5.00	-5.70	-5.33	-3.07	-							
***O. tsutsugamushi* -P**	-4.5	-6.21	-7.27	-5.02	-6.37	-						
***Leptospira*-F**	-6.66	-4.64	-5.98	-8.26	-3.14	-9.82	-					
***Leptospira*-R**	-4.64	-8.16	-5.38	-6.59	-5.25	-5.02	-4.56	-				
***Leptospira*-P**	-6.66	-6.21	-5.38	-3.61	-7.04	-8.31	-9.73	-5.02	-			
Eubacteria-F	-3.61	-7.81	-6.26	-6.14	-6.69	-6.69	-12.89	-4.64	-4.74	-		
Eubacteria-R	-6.12	-4.64	-3.92	-6.68	-4.65	-7.55	-9.75	-5.02	-10.58	-6.68	-	
Eubacteria-P	-3.61	-5.09	-5.09	-6.68	-4.74	-9.82	-3.61	-8.16	-6.68	-12.90	-5.12	-

3.2.2. Viral assay oligonucleotides

The resulting primer set contains 13 oligonucleotides across 4 targets; DENV, JEV, ZIKV, and CHIKV. DENV and JEV shares the same forward primer. ZIKV was originally planned to also share this forward primer, as well as share the probe with JEV as a pan-flavivirus target, however, high variation between different ZIKV sequences in the 3'UTR made oligonucleotide design very difficult. As such it was decided to separate the ZIKV primers and probe using the E gene while labelling the probe with the same fluorescent dye as JEV. DENV and ZIKV each has two reverse primers.

In DENV, one reverse primer (Den_Wu_SWmod-R1) detects DENV1-3 while the other (Den_Wu_SWmod-R2) detects DENV4. In ZIKV, the two reverse primers were necessary as the region contains a SNP. While most sequences contain an adenine in this position, some sequences from Thailand, Malaysia, and China contains a cysteine. Because these sequences are the minority, one of the reverse primers (ZikE_JT-R2) was designed with a degenerate base, K, in the SNP while the other (ZikE_JT-R1) contains thymine, as appropriate for the more common adenine. By doing so, the majority of the primer's population will be specific to the more common variant.

In analysing the oligonucleotides, the Tm of each dimer has been very informative on the potential behaviour of each oligonucleotide in a reaction. While most dimers have ΔG within the -7.5 $\frac{kcal}{mol}$ criterion, some does exceed it such as the heterodimers caused by the CHIKV probe. However, the T_m of these dimers are much lower than the PCR cycling condition (around 25°C) so in a reaction, most of the dimer will dissociate. On the other hand, dimers with high T_m such as the homodimers from the ZIKV reverse primer and probe has very little ΔG, in the range of -0.1 to -0.4 $\frac{kcal}{mol}$, making binding unlikely. Table 19 and Table 20 shows the analyses of each oligonucleotide used in the viral assay and the matrix of heterodimers between them respectively.

Table 19: List of primers for the viral assay along with the respective properties. Analysis was done using Primer3Plus.

Target	Name	Sequence	Type	T_m	GC%	ΔG ($\frac{kcal}{mol}$)	
						Homodimer	Temp
DENV & JEV	DJW3UTR_CDC_SWmod-F	AAGGACTAGAGGTTAGAGGAGAC	Forward	59.8°C	47.8%	N/A	N/A
DENV	Den_Wu_SWmod-R1	GCGTTCTGTGCCTGGAATG	Reverse	60.1°C	57.9%	N/A	N/A
	Den_Wu_SWmod-R2	CGCTCTGTGCCTGGATTG	Reverse	61.3°C	61.1%	-0.144	39.5°C
	DenWHmod_SWmod-P	GGGARAGACCAGAGATCCTGCTGTCTC	Probe	60.3°C	57.4%	-5.690	25.6°C
JEV	Jap3UTR_SW-R	ATACTTCGGCGCTCTGTG	Reverse	59.5°C	55.6%	-6.3	8.3°C
	Jap3UTR_SW-P	GACACCTGGGAATAGACTGGGAGATCTTC	Probe	58.9°C	51.7%	N/A	N/A
ZIKV	ZikE_JT-F	CGCCCAATTCACCAAGAGC	Forward	60.6°C	57.9%	N/A	N/A
	ZikE_JT-R1	GCATGTGCGTCCTTGAACTC	Reverse	60.1°C	55.0%	N/A	N/A
	ZikE_JT-R2	GCATGKGCATCCTTGAACTC	Reverse	61.3°C	52.5%	-0.404	41.0°C
	ZikE_JT-Pr	GGAGTTCCGGTGTCTGCCCCAGC	Probe	63.4°C	69.6%	-0.193	40.5°C
CHIKV	ChiE1_Pas_WiHmod-F	CTCCGCGTCCTTTACCAAG	Forward	61.6°C	57.9%	-5.756	5.6°C
	ChiE1_Pas_WiHmod-R	CCAAATTGTCCTGGTCTTCCTG	Reverse	59.2°C	50.0%	-0.152	34.8°C
	ChiE1_Pas_WiHmod-PR	CAAAAGGTGTCCAGGCTGAAGACATTGGC	Probe	62.1°C	51.7%	-7.285	24.9°C

Table 20: Matrix of the Gibbs free energy of heterodimers and their T_m between oligonucleotides from the viral PCR primers and probes, as analysed in Primer3Plus.

ΔG ($\frac{kcal}{mol}$)	**DENV/ JEV-F**	**DENV-R1**	**DENV-R2**	**DENV-P**	**JEV-R**	**JEV-P**	**ZIKV-F**	**ZIKV-R1**	**ZIKV-R2**	**ZIKV-P**	**CHIKV-F**	**CHIKV-R**	**CHIKV-P**
DENV/JEV-F	-												
DENV-R1	-	-											
DENV-R2	-3.51 1.0°C	-	-										
DENV-P	-	-	-	-									
JEV-R	-	-	-	-5.198 2.5°C	-								
JEV-P	-	-3.832 2.6°C	-	-4.977 19.4°C	-	-							
ZIKV-F	-	-	-5.063 7.2°C	-	-5.396 4.3°C	-4.766 6.0°C	-						
ZIKV-R1	-5.385 3.8°C	-	-3.413 2.5°C	-	-	-	-	-					
ZIKV-R2	-	-4.048 11.0°C	-	-3.997 0.0°C	-	-	-6.454 7.4°C	-	-				
ZIKV-P	-	-	-	-6.271 12.8°C	-3.936 4.5°C	-6.386 17.5°C	-	-5.036 3.9°C	-7.164 26.1°C	-			
CHIKV-F	-4.639 9.9°C	-	-	-	-	-4.278 12.5°C	-	-	-	-5.756 5.6°C	-		
CHIKV-R	-	-	-	-7.786 25.4°C	-	-3.327 6.9°C	-	-	-	-	-	-	
CHIKV-P	-	-8.636 24.2°C	-8.685 24.7°C		-6.227 11.6°C	-6.684 12.1°C	-4.548 10.5°C	-	-6.52 18.6°C	-4.355 15.1°C	-	-5.818 10.4°C	-

3.2.3. CHIKV assay optimisation

In optimising the final CHIKV oligonucleotides in real-time RT-PCR, the Cq values decreases as the annealing temperature decreases. However, only the reaction with 56.2°C was able to detect the 10^{-4} dilution of CHIKV genomic RNA and was chosen when the multiplex assay was assembled (Figure 12).

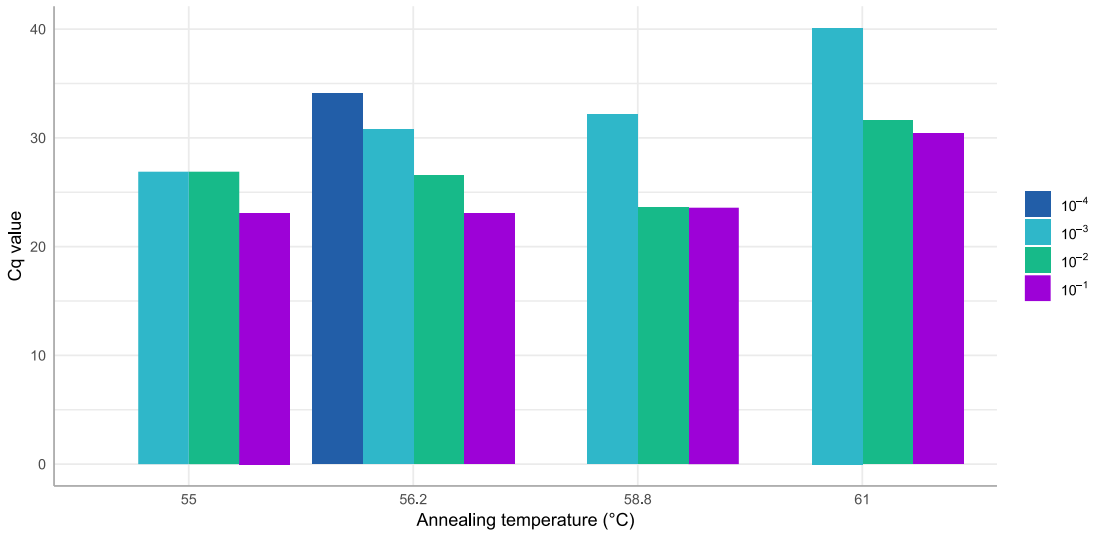

Figure 12: Cq values of the CHIKV singleplex real-time PCR assay using serially diluted CHIKV genomic RNA as template at different annealing temperatures. The 10^{-4} dilution was not detected at annealing temperatures of 55, 58.8, and 61°C.

After varying the primers' concentrations, the condition with the lowest Cq value was using 6 pmol/µL forward primer, 2 pmol/µL reverse primer, and 2 pmol/µL probe (Figure 13).

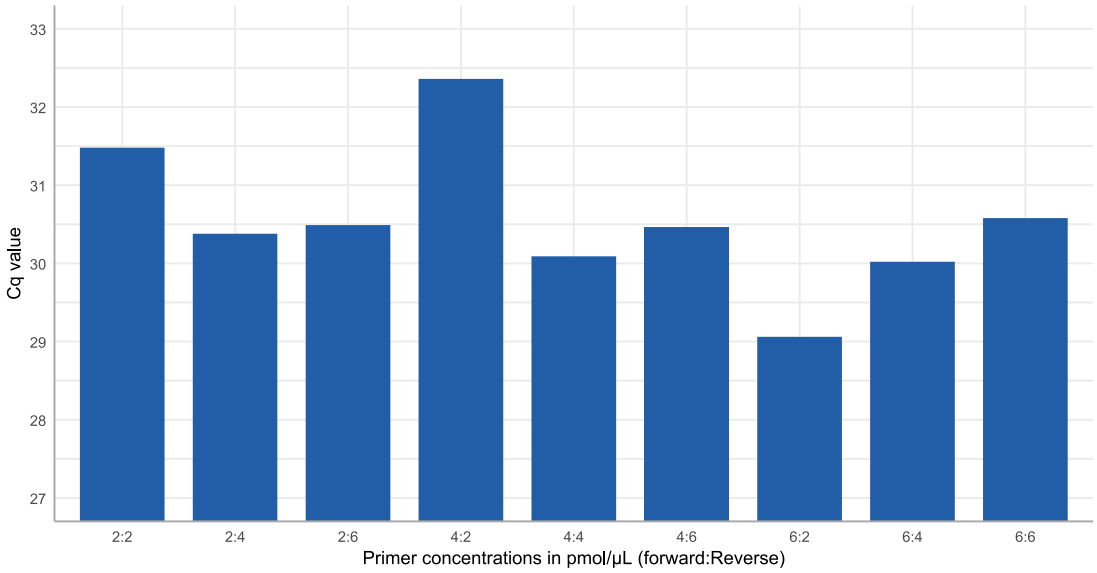

Figure 13: Cq values of the CHIKV assay from varying the ratios of the forward and reverse primers. The ratio that produces the lowest and highest Cq values are 6:2 and 4:2. The probe's concentration is 2 pmol/µL in all conditions.

After these optimisations, the *Rickettsia* and CHIKV oligonucleotides were further taken to be combined with the remaining oligonucleotides to create the multiplex bacterial and viral assays respectively by the other members of the laboratory. In assembling the assays, the annealing temperatures and oligonucleotide concentrations were further adjusted to find the compromise between the various oligonucleotide sets that have to be used in to same reaction.

3.3. Discussions

3.3.1. Real-time PCR assays

In this chapter, two sets of oligonucleotides were designed for multiplex real-time PCR assays to detect bacterial and viral pathogens in whole blood specimens. While many PCR primers and probes exists in literature, most of them are either for singleplex assays or are not specific to variants in South and Southeast Asia. As the assay developed from this project will be used in SEACTN on patient samples across South and Southeast Asia, being able to detect variants found in these areas is crucial to prevent false negatives.

Multiplexing the assay also reduces the cost as well as the required volume of the sample for the assay by reducing the number of reactions required to only two to detect reactions for eight

targets whereas in a conventional singleplex assay, each target would require separate reaction. This is very beneficial to screening applications such as for AUFs as there are a wide range of possible pathogens. Other flaviviruses including West Nile virus (WNV), yellow fever virus (YFV) as well as alphaviruses such as Mayaro virus (MAYV), Semliki Forest virus (SFV), and Sindbis virus (SINV) were also considered to be used as targets, creating a broader pan-flavivirus target and a pan-alphavirus target. These targets were ultimately dropped as not only do they complicate the oligonucleotide design process by adding more variations across the sequence alignment but also because they are not endemic to South and Southeast Asia (194, 195). This was the reason why the probes for JEV and ZIKV shares the same fluorescent dye, as they were originally intended to be combined into the pan-flavivirus target. As of writing, new sets of oligonucleotides has been ordered which labels these two probes with different fluorescent dyes, FAM and HEX for JEV and ZIKV respectively.

The two assays were designed using different tools, IDT's OligoAnalyzer for the bacterial assay and Primer3Plus for the viral assay with both tools having its own advantages and disadvantages. OligoAnalyzer is the more user-friendly option with simple and intuitive user interface. Because it only analyses the oligonucleotides, it only requires the sequence of the oligonucleotide of interest (and a second sequence for analysing heterodimers). It also accepts degenerate bases in the sequence and has condition pre-sets for endpoint as well as real-time PCR. The most convenient feature of OligoAnalyzer is the batch mode which allows multiple sequences to be analysed simultaneously, albeit each oligonucleotide is analysed separately so heterodimers still have to be done manually. However, it is limited in customisability, with only the concentrations of the oligonucleotides, monovalent cations (Na^{+}), divalent cations (Mg^{++}), and dNTPs being adjustable. Because it doesn't require the template sequence, it does not take into consideration the binding to the target, only analysing each oligonucleotide in isolation.

Primer3Plus is a much more in-depth tool with adjustments available for virtually every parameter in the reaction although the UI is much less intuitive as a result. It also requires the template sequence and at least a complete primer pair for analysis. This allows for outputs such as the binding score which calculates the percentage of primers that will bind to the template at the

primer's annealing temperature, if the primer and the template is at equal concentrations. As mentioned, Primer3Plus also calculates the T_m of each dimer. With this information, some primers with very low ΔG can be usable in the reaction if it has sufficiently low T_m, as the dimer will still dissociate during the PCR reaction. An analysis of the bacterial assay was re-done using Primer3Plus to assess the properties of each oligonucleotide (Table 21 and Table 22). In the new analysis, similar trends are observed in that oligonucleotides with low ΔG have low Tm and those with high ΔG has high ΔG which is preferable. It is noteworthy that the ΔG if each dimer is different between OligoAnalyzer and Primer3Plus which is most likely due to different calculation algorithms and different pre-set conditions.

Table 21: Re-analysis of the bacterial assay oligonucleotides using Primer3Plus.

Target	Name	Sequence	T_m	GC%	ΔG ($\frac{kcal}{mol}$)	
					Homodimer	Temperature
Rickettsia spp.	Forward	ATCGAGGATATGATATTAAAGACTTA	55.4°C	26.9%	N/A	N/A
	Reverse	GCAAGCATAATAGCCATAGGA	57.4°C	42.9%	0.110	35°C
	Probe	ACTAATGMATGATGAGCAAYCT	68.8°C*	40.9%	-0.765	47.4°C
O. tsutsugamushi	Forward	CCCATCAGTACGGAATAACA	56.4°C	45.9%	N/A	N/A
	Reverse	CTCTCAGACCAGCTACAGATCACA	63.3°C	50.0%	N/A	N/A
	Probe	GCGGCAGATTAGGTAGTTGGTAAGGT	66.4°C	50.0%	N/A	N/A
Leptospira spp.	Forward	CCCGCGYCCGATTAG	58.5°C	73.3%	-0.3	37.1°C
	Reverse	GTCTCAGTTCCATTGTGGC	58.0°C	52.6%	-0.112	38.8°C
	Probe	CTCACCAAGGCGACGATCGGTAGC	69.1°C	62.5%	-7.884	21.9°C
Eubacteria	Forward	TRCGGGRGGCWGCA	62.5°C	78.6%	-4.805	1.1°C
	Reverse	CTACCRGGGTATCTAATCC	55.0°C	52.6%	-6.203	7.0°C
	Probe	GTGCCAGCAGCCG	67.6°C*	76.9%	-0.325	43.6°C

*These oligonucleotides were modified with ZNA® to increase their T_m.

Table 22: Re-analysis of the Gibbs free energy of heterodimers between oligonucleotides in the bacterial assay using Primer3Plus.

ΔG ($\frac{kcal}{mol}$)	***Rickettsia*-F**	***Rickettsia*-R**	***Rickettsia*-P**	**OT-F**	**OT-R**	**OT-P**	***Leptospira*-F**	***Leptospira*-R**	***Leptospira*-P**	**Eubacteria-F**	**Eubacteria-R**	**Eubacteria-P**
***Rickettsia*-F**	0											
***Rickettsia*-R**		0										
***Rickettsia*-P**			0									
***O. tsutsugamushi*-F**				0								
***O. tsutsugamushi* -R**					0							
***O. tsutsugamushi* -P**		-3.606 5.4°C			-6.600 15.2°C	0						
***Leptospira*-F**							0					
***Leptospira*-R**			-1.640 3.7°C					0				
***Leptospira*-P**			-3.937 4.6°C		-7.364 21.8°C	-4.553 6.1°C	-6.117 13.2°C		0			
Eubacteria-F					-4.430 5.0°C	-5.467 0.3	-7.866 20.2°C			0		
Eubacteria-R		-3.692 1.4°C				-4.240 0.5°C	-5.924 2.2°C		-5.748 6.4°C		0	
Eubacteria-P					-3.467 7.8°C	-5.901 2.8°C				-8.122 21.9°C		0

While this thesis is only concerned with the design of the oligonucleotides used in the assays, laboratory testing was still required to complete it. Once sequences were obtained, optimisation was done to determine the final conditions of the reactions. This includes assessing the appropriate cycling temperatures of the PCR program as well as the appropriate concentrations of each oligonucleotide per reaction. The need for different concentrations of each oligonucleotide is likely due to secondary structures or potential dimers formations that decreases the efficiency of a certain oligonucleotide in binding with its target. Increasing the concentration of these oligonucleotides can mitigate this. A case-control was also done by the laboratory using positive samples previously collected in order to verify the sensitivities and specificities of the two assays. These tests were done with patient whole blood samples previously collected for the Spot Sepsis

3.3.2. Limitations

One difficulty encountered during development of this assay is increasing the T_m of oligonucleotides in low-GC loci. The method used was to modify these oligonucleotides with ZNA®. While this does adequately increase the T_m, it significantly increases the cost of the oligonucleotides as well as limits the vendor to just Metabion. For countries outside Europe, shipping will add to the cost and time between order and delivery.

Another limitation is that the sequences used to design the oligonucleotides are not only predominantly originating from South and Southeast Asia, but also focuses only on pathogens known to be found in this area. This makes this assay most effective within South and Southeast Asia. If this assay is to be adapted to other regions of the world, it might not be specific to the local variants or strains of each pathogen. There are also potentially other pathogens that is omitted from this assay entirely such as YFV and WNV.

3.3.3. Conclusion

Oligonucleotides were designed for use in real-time PCR assays to detect common bacterial and viral pathogens in South and Southeast Asia. Laboratory work was done to optimise and verify the assays. As of writing, both assays have been used to detect pathogens in patient whole blood for Spot Sepsis as well as being used in SEACTN. While it is designed with whole

blood as the specimen, these assays are useful for other media such as plasma, serum, and DBS. The viral assay is used as the reference test for the DPP® Fever Panel II Asia systems as well as the basis for the DBS assay for this thesis.

CHAPTER 4

Development of CRISPR diagnostics for bloodborne viral pathogens

This chapter describes the development of a CRISPR assay to detect CHIKV, DENV, and ZIKV in whole blood specimens. The aim of this assay is the application in a POC setting and the extraction, amplification, and detection of viral RNA are designed to be conducted with minimal equipment.

4.1. Methods

4.1.1. Optimisation of rapid nucleic acid extraction from whole blood specimens

Initial testing of rapid extraction used whole blood spiked with *E. coli* containing pCR®2.1-TOPO plasmids which were cloned with the amplicon of an influenza A (Flu A) PCR assay based on a protocol for detecting respiratory pathogens by the Hamilton Regional Laboratory Medicine Program (HRLMP). Once the DENV assay was developed, the whole blood used was then spiked with pET-21a(+) subcloned to contain the DENV assay's amplicon. In later testing, whole blood and plasma was spiked with CHIKV culture. In all cases, the ratio of the spiking agent to whole blood or plasma was 1:10 (v/v). After extraction, the products were detected with their respective PCR assays and visualised by gel electrophoresis.

During the first tests healthy whole blood samples were extracted using Lucigen's QuickExtract DNA extraction solution, initially testing both the manufacturer's protocol as well as SHERLOCK testing in one pot's (STOP) protocol (196). Samples were extracted with the MagNA Pure 24 instrument and detection was performed through real-time PCR, detecting the human *rnaseP* gene, and visualised on agarose gel, as the CRISPR assay was not developed yet. The ratio of whole blood to QuickExtract DNA extraction solution was varied between 1:1, 4:5, 3:5, 2:5, and 1:5 (v/v).

The manufacturer's technical support (Lucigen at the time) was contacted for suggestions specifically on extracting whole blood. Tests were done accordingly to the suggestions which were to prepare three 100 μL aliquots of the QuickExtract DNA extraction solution and add 1, 3 and 10 μL of blood in each tube before extracting with the manufacturer's protocol described above. A serial dilution in sterile water down to 10^{-5} was then done on the 10:100 sample after extraction before the amplicons were detected with real-time PCR. In these tests, plasmids containing Flu A amplicon were spiked into the blood.

Later tests involved serially diluting freshly drawn EDTA whole blood spiked with CHIKV culture at a 1:10 dilution. The blood sample was also left on ice for approximately 30 minutes until plasma separated out and was collected to assess whether the haem in whole blood

was affecting the assay. Each sample was serially diluted in the QuickExtract DNA extraction solution from 10^{-1} to 10^{-5} (Figure 14). The extracted products were either used in the amplification reaction directly or further manually purified with AMPure XP beads (Chapter 2.3.3). For these samples, the manufacturer's protocol was used. In these tests, the extracted CHIKV RNA was amplified by RT-PCR and detected with CRISPR. The two most concentrated whole blood and plasma samples not magnetically purified were also amplified with RAA before performing the CRISPR assay. Positives are called if the end relative fluorescence unit (RFU) is at least twice that of the PCR negative control (the no template control [NTC] of the PCR assay). Table 23 shows the different reaction mixtures and incubation conditions used.

Table 23: Reaction mixtures and incubation conditions of the extraction methods. *Post-extraction products were further diluted in sterile water.

Protocol	**Reaction mixture**		**Incubation condition**
	Whole blood	**Extraction solution**	
Manufacturer's protocol	1 drop	0.5 mL	
Lucigen's suggestion 1	1 μL	100 μL	1) 65°C for 6 minutes
Lucigen's suggestion 2	3 μL	100 μL	2) 98°C for 2 minutes
Lucigen's suggestion 3*	10 μL	100 μL	
STOP protocol 1	0.5 mL	0.5 mL	95°C for 5 minutes
STOP protocol 2	0.5 mL	0.5 mL	60°C for 10 minutes

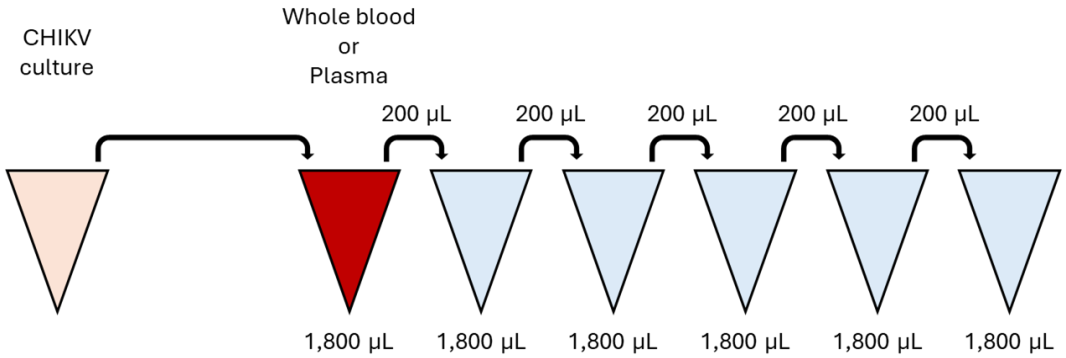

Figure 14: Serial dilutions of whole blood and plasma in QuickExtract DNA extraction solution. Extraction was done using manufacturer's protocol.

4.1.2. Isothermal amplification

LAMP primers used for testing were designed by Seok et.al as shown in Table S 2 (197). The first iteration of the CHIKV RAA primer were based on oligonucleotide sequences from Patel et. al. with modifications to remove any degenerate bases (198). The DENV and ZIKV RAA primers were newly designed using alignments from the real-time RT-PCR assay in 0. The criteria for designing RAA primers are identical to RPA primers as described in Chapter 1.3.4. In brief, a conserved regions of at least 30 nucleotides were identified. Once two conserved regions that are roughly 100 - 200 nucleotide apart have been identified, the sequences of those regions were then analysed using IDT's OligoAnalyzer tool to make sure the ΔG of hairpins, homodimers- and heterodimers do not exceed the criteria of -3 $\frac{kcal}{mol}$ and -6 $\frac{kcal}{mol}$ respectively. The list of RAA primers and their sequences is shown in Table S 4.

Initial testing compared the performance of LAMP and RAA using CHIKV genomic RNA as the template. CHIKV genomic RNA was serially diluted in sterile water was used containing 2×10^7, 2×10^6, 2×10^5copies/µL with equal amounts (2 µL) used for both the LAMP and RAA reactions, alongside a positive control in the RAA reaction supplied in the RAA kit. During these tests, incubation for RAA was done at 37°C as recommended in the product's manual, rather than 39°C as described in Chapter 2.2.3. In later tests, the RAA primer concentrations were also varied between 0.2, 0.4, and 0.6 µM to determine the optimum condition.

The forward primer containing a T7 promotor was then used to assess whether it will affect the assay. To assess the effect of the presence of the T7 promotor toward RAA efficiency, two reactions were prepared, one using the forward primer without the promotor, and one with the promotor. The products were visualised on a 4% agarose gel. The temperature of the RAA reaction was also varied, testing 39°C and 42°C. The final protocol for RAA is shown in Chapter 2.2.3.

4.1.3. CRISPR detection

LwaCas13a crRNA was designed with the cas13design online tool (199). The amplicons of each target were used as the input and the top 5 suggested sequences ranked by predicted efficiency were ordered both as ssRNA, and as ssDNA containing a T7 promotor in case the crRNA needed to be synthesised in-house (Table S 6).

Initial testing of the CRISPR detection was done using CHIKV genomic RNA amplified by RAA with a slightly different protocol as shown in Table 24. Briefly, a master mix was first prepared as shown in Table 24 before 17 μL of the master mix gets aliquoted into separate wells on a 96-well plate. 1 μL of 10 ng/μL crRNA and 2 μL of the template was then added at this point. The thermal cycler was also setup differently, incubating at 37°C and reading the plate every 5 minutes over the course of 3 hours.

Table 24: Master mix reaction component used for initial CRISPR detection tests.

Component	Volume for 1 reaction
Sterile water	5.67 μL
1 M HEPES	0.4 μL
1 M $MgCl_2$	0.18 μL
ATP	1.5 μL
GTP	1.5 μL
UTP	1.5 μL
CTP	1.5 μL
63.3 μg/mL LwaCas13a	2 μL
4 μL poly-U reporter	1.25 μL
50 U/μL T7 polymerase	1.5 μL
Total	17 μL

Troubleshooting the assay was done at the School of Biomolecular Science and Engineering (BSE) at the Vidyasirimedhi Institute of Science and Technology (VISTEC), Rayong, Thailand. Tests were performed with protocols developed by VISTEC as described in Chapter 2.5 except the detection which was done on an Infinite® 200 PRO (Tecan, Männedorf, Switzerland). The components tested were the crRNA, RAA amplicon, and reaction reagents.

The first test was done by switching to VISTEC's protocol while using the same crRNA, amplicons, and reagents as in the previous test. VISTEC's in-house assay targeting *Mycobacterium tuberculosis* and a CHIKV assay developed for Siriraj hospital were used as positive control.

To confirm that the lack of signal is due to the crRNA and not the reagent, the VISTEC-prepared reagents and the previously used MORU-prepared reagents were compared by running the *M. tuberculosis* assay, with the respective crRNA and amplicon on both sets of reagents. Two concentrations of *M. tuberculosis* genomic DNA were used as template, a 1:10 dilution, and a 1:50

dilution from stock. Fresh crRNA was also prepared from frozen stock in the case that the working stock has degraded due to thawing from transportation.

The concentration of the CHIKV crRNA was also varied to 2X and 4X of the standard protocol (1 and 2 ng/μL in the final reaction respectively) to assess whether this specific target require higher crRNA concentrations than the standard protocol. Two different aliquots of the CHIKV template were also used in case one of them has degraded. The *M. tuberculosis* assay was used as the positive control for all reagents. Finally, fresh *in vitro* transcribed crRNA was also prepared and tested after it was discovered that the initial batch of synthesised crRNA contains thymine rather than uracil.

To verify the CHIKV genomic RNA used, the stock RNA was used with Siriraj's primers/crRNA and using Siriraj's CHIKV stock with the developed primers/crRNA. CHIKV genomic RNA was also used in the CRISPR reaction bypassing amplification, in case the amplicons produced have incorrect sequences.

Once a working CHIKV assay was developed, testing on DENV was done on each serotype initially with PCR-amplified templates. RAA-amplified templates were then also tested. ZIKV testing was done similarly with two concentrations of the template (10^7 and 10^6 copies per μL) amplified with RAA and detected with CRISPR.

The LODs of the CRISPR assays were tested by serially diluting each virus's genomic RNA to 10^4 to 10^0 copies per μL. Cross-reactivities were also tested similarly by cross-checking each target's amplicon with each CRISPR assay. Due to a redesign in the DENV RAA forward primer, the DENV assay's LOD was re-evaluated using DENV1 and DENV2 genomic RNA serially diluted from 10^4 to 10^1 copies per μL.

Finally, to assemble each step of the assay together, 200 μL CHIKV culture was spiked into 1,800 μL of either freshly drawn whole blood or plasma and serially diluted in QuickExtract DNA extraction solution by adding 200 μL spiked whole blood or the previous dilution into 1800 μL QuickExtract DNA extraction solution to a dilution of 10^{-5}. Each dilution was rapidly extracted

by incubation at 65°C for 6 minutes then 98°C for 2 minutes. The products were amplified by RT-PCR and RAA before detection by CRISPR.

4.2. Results

This section presents the result of testing and optimising each step of the CRISPR assay to detect CHIKV, DENV, and ZIKV. These processes are nucleic extraction, isothermal amplification, and CRISPR detection.

4.2.1. Rapid nucleic acid extraction

Initial testing of the QuickExtract DNA extraction solution was performed using both manufacturer's and STOP's protocols to assess the ability of the buffer to extract total nucleic acid (TNA) from whole blood. Both methods showed no signal from real-time PCR of the *rnaseP* gene when compared to the positive control sample extracted by MagNA Pure 24 which has a Cq value of 24.77 as analysed with a baseline threshold, the level of fluorescence signal that distinguishes true signal from background noise, of 60. Furthermore, the sample using 1:1 whole blood to QuickExtract solution and incubated at 95°C expectedly solidified due to the high heat and high blood concentration.

Next, the ratios between whole blood and the QuickExtract DNA extraction solution were varied: 1:1, 4:5, 3:5, 2:5, and 1:5. None of the dilutions were able to extract enough DNA to produce any signal. Furthermore, all samples with 3:5 ratio of blood to QuickExtract DNA extraction solution and higher solidified when incubated at 95°C. The Cq value for the MagNA Pure 24 extracted sample is 24.07. By visualising the amplified products with agarose gel electrophoresis, a faint band could be seen around 100 bp in the MagNA Pure 24 extracted sample (expected band size 80 bp) but not in any of the QuickExtract samples (Figure 15).

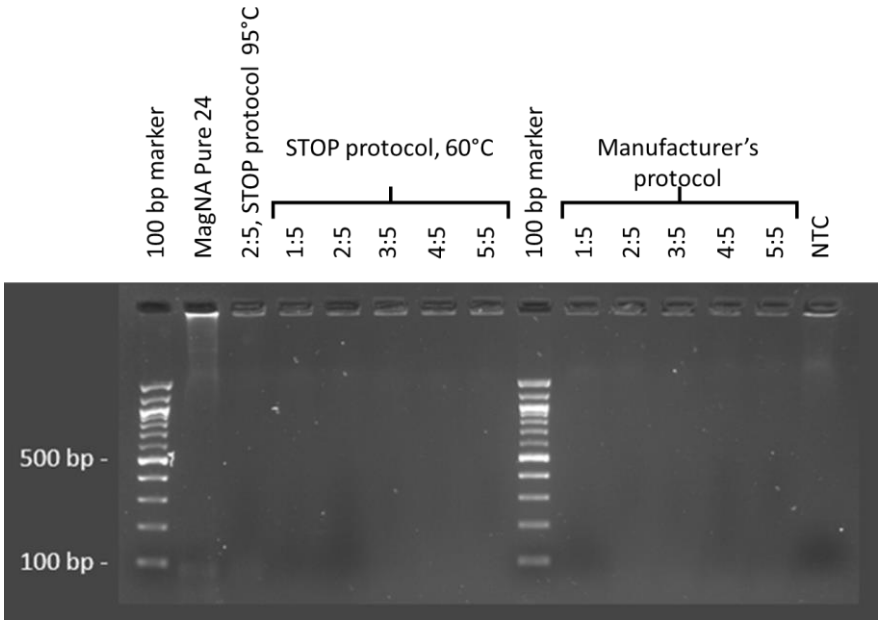

Figure 15: Agarose gel showing PCR products from templates extracted from whole blood with Lucigen's QuickExtract DNA extraction solution using three different protocols: manufacturer's protocol, STOP's protocol at 60°C and STOP's protocol at 95°C. An extraction using the Roche MagNA Pure 24 was done as control.

Following the manufacturer's suggestions, the extraction was repeated with 1:100, 3:100, and 10:100 ratios of whole blood to QuickExtract DNA signal from the spiked plasmid was seen in the samples of 1, 3, and 10 μL blood in 100 μL QuickExtract solution, as well as the first two dilutions of the 10:100 sample. However, only the diluted samples show signal for *rnaseP* (Table 25). Diluting that by 1:10 in sterile water post-extraction as it gives the lowest Cq value for the spiked plasmids out of the two sample that also have the *rnaseP* signal present.

Table 25: Cq values of whole blood samples spiked with plasmid containing Flu A amplicons using protocol suggested by Lucigen's technical support team. All samples were diluted in 100 µL QuickExtract solution.

Whole blood	Post-extraction dilution	Cq values	
		Spiked plasmid (HEX)	*rnaseP* (Cy5)
1 µL	-	29.03	-
3 µL	-	28.89	-
10 µL	-	30.85	-
10 µL	10^{-1}	31.72	37.38
10 µL	10^{-2}	33.65	42.01
10 µL	10^{-3}	-	-
10 µL	10^{-4}	-	-
10 µL	10^{-5}	-	-
NTC	-	-	-

4.2.2. Isothermal amplification

Detection of CHIKV with LAMP showed products in all three concentrations tested. However, the results were inconsistent, with the sample containing 10^7 genomic copies/µL producing a fainter than the sample containing 10^6 genomic copies/µL. Furthermore, there is a faint band, comparable to the sample containing 10^7 genomic copies/µL in the NTC. RAA was only able to clearly detect the two most concentrated samples and also with a faint band in the NTC although this could be from primer-dimers, as the NTC of the RAA positive control also shows a faint band (Figure 16).

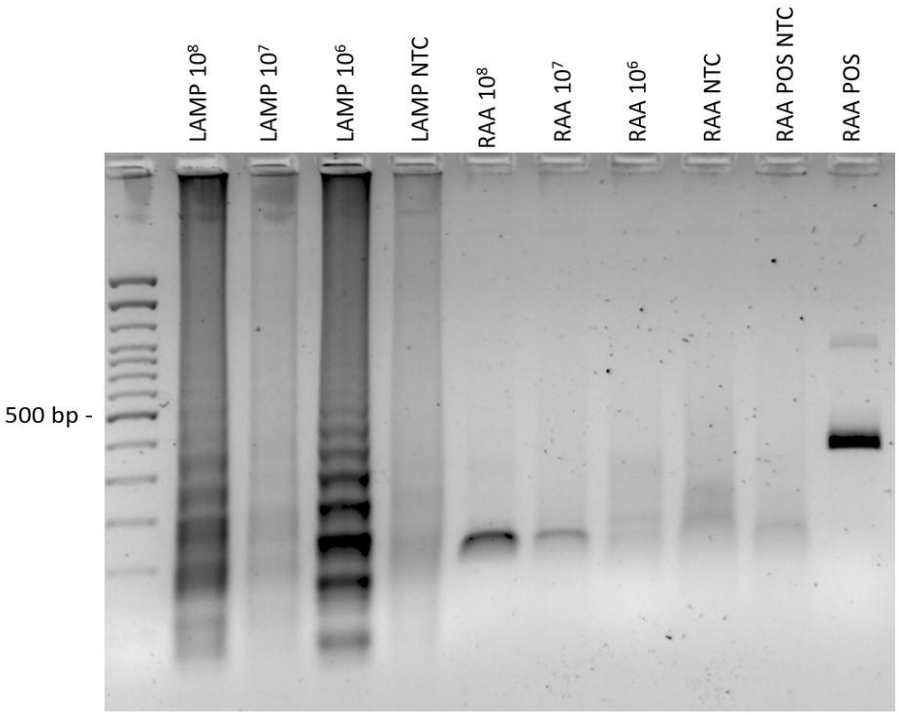

Figure 16: Agarose gel show LAMP and RAA products from serially diluted CHIKV genome. Lanes 1 – 4 shows products of the LAMP reaction. Lanes 5 – 8 shows products of the RAA reaction with CHIKV genome as template. Lanes 9 – 10 shows product of the RAA reaction's positive control as provided by the manufacturer.

Upon varying the concentration of the RAA primers, while every concentration (0.2, 0.4, and 0.6 μM) showed products, using 0.2 μM primers shows the most intense band (Figure 17A). Furthermore, using the forward primer with a T7 promotor does not affect amplification, and a product is still produced (Figure 17B). The presence of the T7 promotor can be seen by the presence of a different size band when compared to the non-T7 promotor in the 4% agarose gel (Figure 17C).

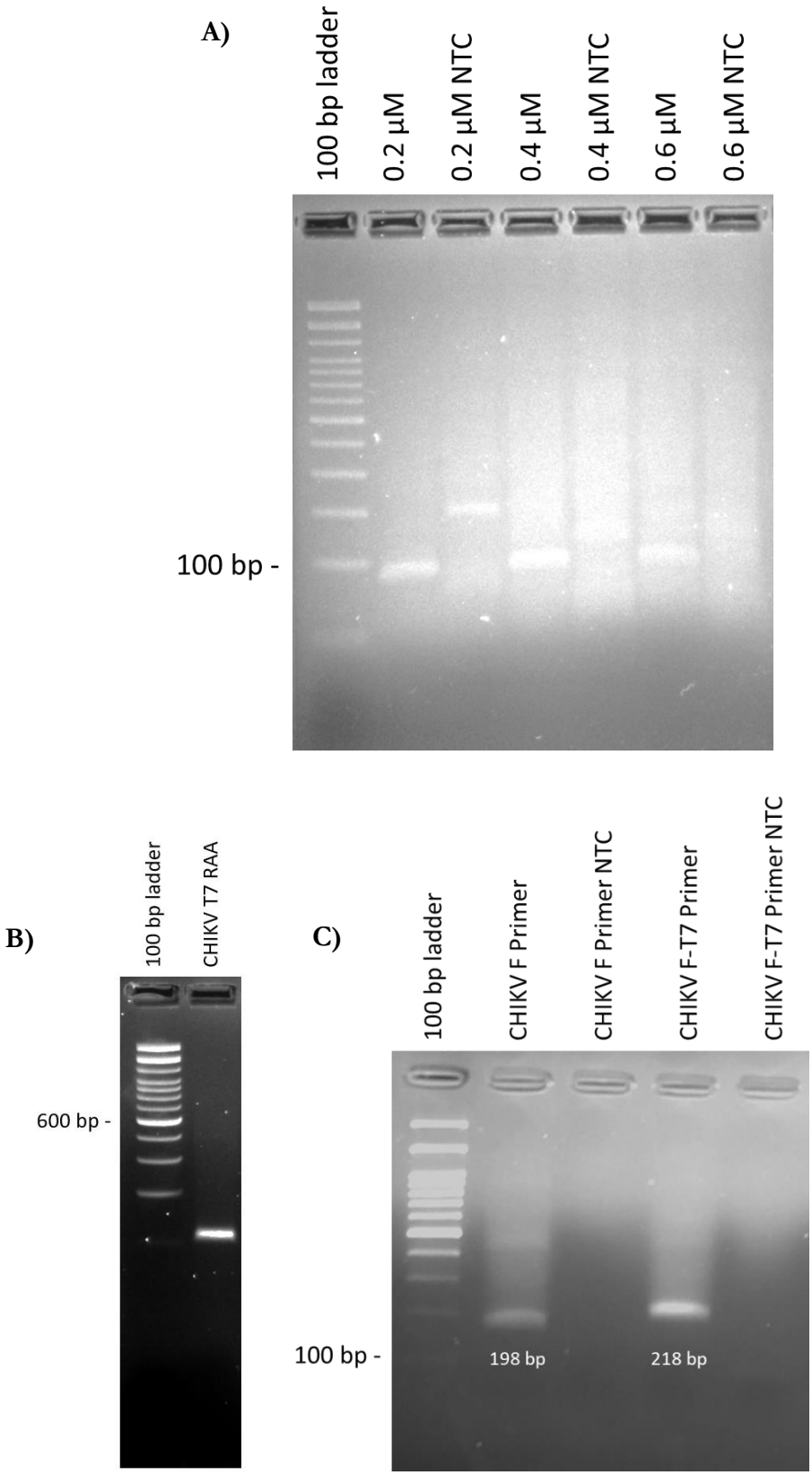

Figure 17: Agarose gels showing the products of CHIKV RAA reactions with A) varying primer concentrations, along with each respective NTC and B) using the forward primer with a T7 promotor. C) Comparison between the products of RAA reactions using forward primers with and without a T7 promotor.

Two temperatures were tested for the RAA reaction incubation. RAA reaction at different temperatures shows bands at 39°C, but not at 42°C (Figure 18).

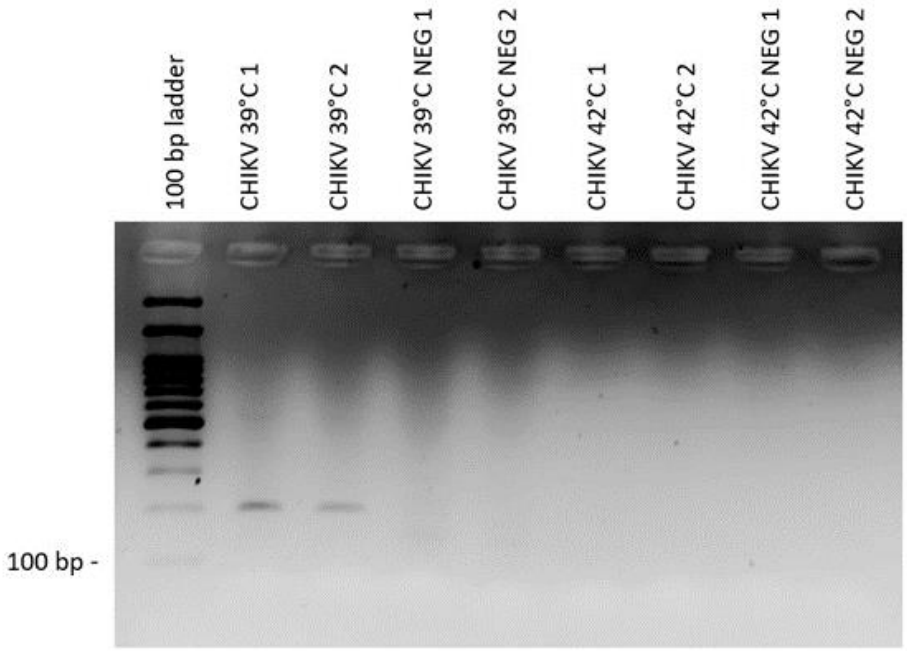

Figure 18: Agarose gel showing the product of amplifying CHIKV genomic RNA using RAA at different temperatures; 39°C, and 42°C.

4.2.3. CRISPR detection

The top five crRNA sequences with the highest scores as given by cas13design for each target were obtained and the LwaCas13a direct repeat was added onto the 5' end of each sequence before being sent for synthesis as ssRNA. The top-ranking sequences for each target were used with the remaining stored at -80°C as backups. The sequence of the gRNA used, along with the direct repeat are shown in Table 26

Table 26: Sequences of the top-ranking crRNA sequences for CHIKV, DENV, and ZIKV, as well as the LwaCas13a direct repeat sequence.

Target	crRNA sequence (5' - 3')
CHIKV	CACCUCAAACAUGGGGUACGCAC
DENV	AGUCCUUUCAGUGAGACUACAGC
ZIKV	GAACAAAUGGCAUUGGCCAUCAG
LwaCas13a direct repeat	GAUUUAGACUACCCCAAAAACGAAGGGGACUAAAAC

4.2.3.1. CHIKV detection

Initial testing at MORU was performed done on CHIKV RNA using the protocol described in Chapter 4.1.3 was not able to produce any signal. Switching to VISTEC's protocol, a fluorescent signal can be seen in the RAA-amplified products, however the highest signal peaked at around 500 RFU which is low. The increase in signal is also much more gradual than a typical CRISPR-Cas13a reaction in which the signal rapidly increases in intensity and plateau after roughly 30 minutes of incubation. When compared to the RAA-amplified *M. tuberculosis* positive control which goes up to around 7000 RFU (Figure 19).

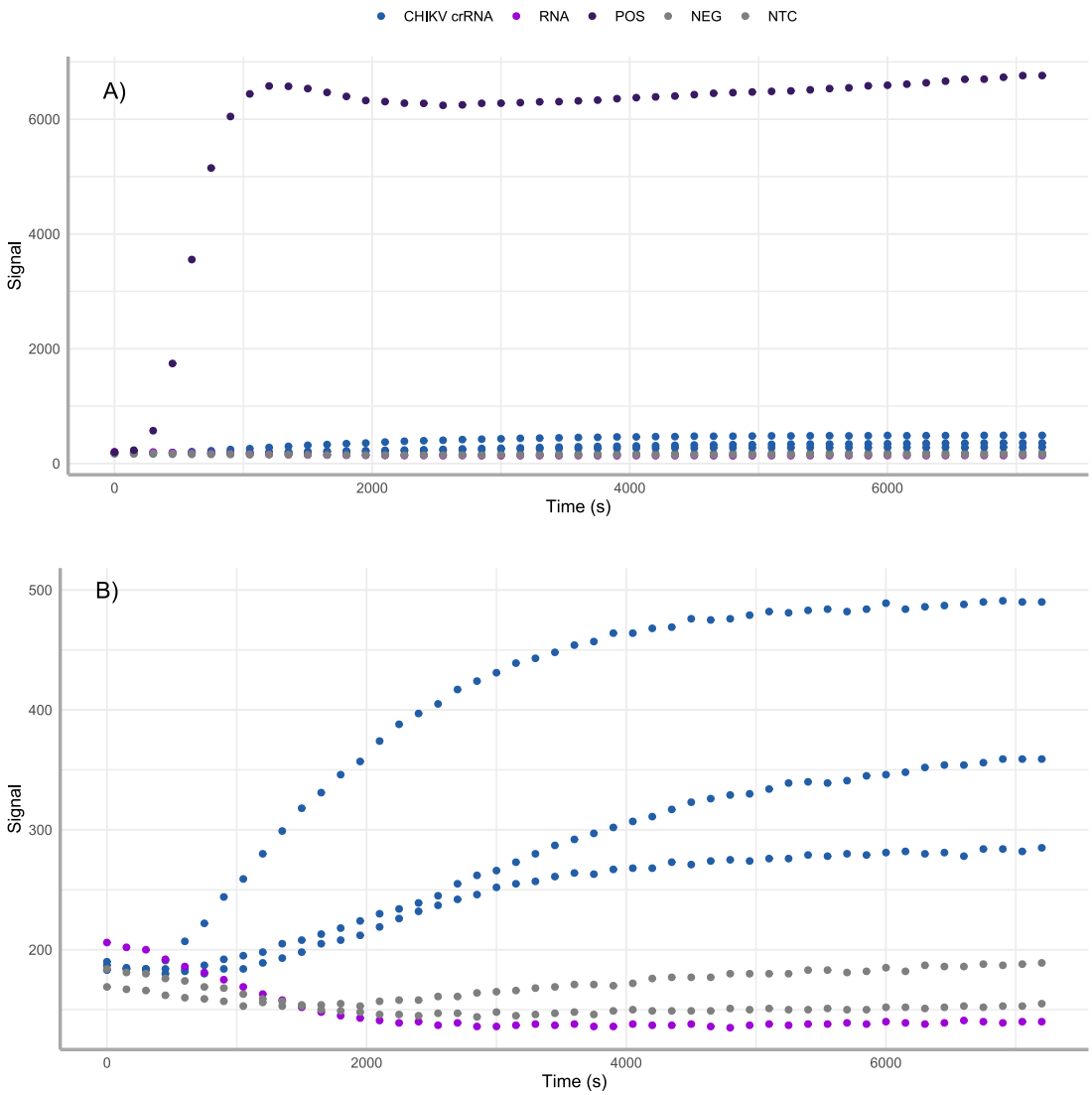

Figure 19: Fluorescence signals from CRISPR-Cas13a detection reactions of A) RAA-amplified CHIKV products along with M. tuberculosis as positive control and B) The RAA-amplified CHIKV products without M. tuberculosis control. The CHIKV CRISPR were done in triplicates. Un-amplified CHIKV RNA is shown in purple, RAA and CRISPR NTC are shown in grey.

The CHIKV assay was run with 2X and 4X the concentration of crRNA compared to earlier tests to determine whether this target require higher crRNA concentrations than expected (Figure 20). A low signal is seen in the negative samples of the reactions using 2X the crRNA concentration while an even weaker signal is also seen in the NTC. Neither aliquot of the CHIKV template was detected by the assay.

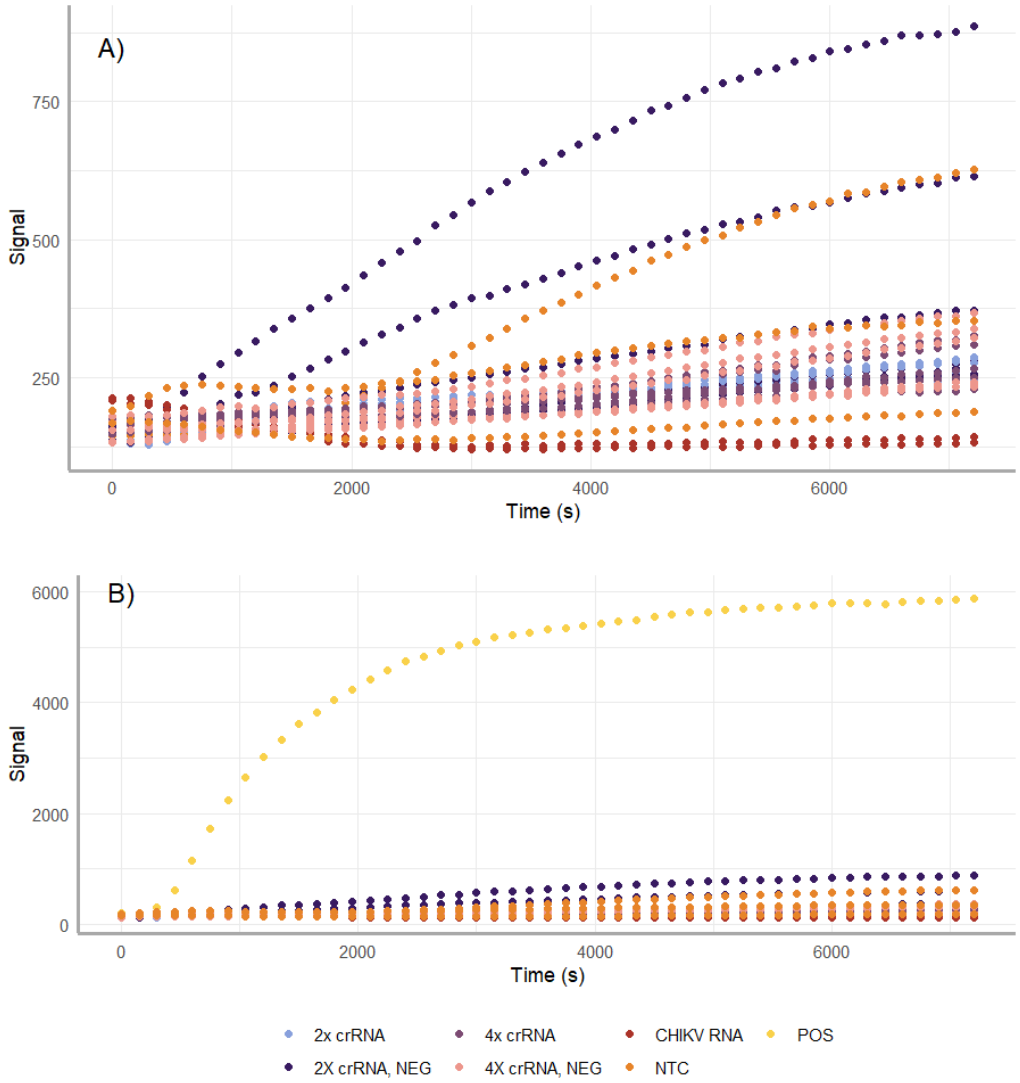

Figure 20: Fluorescence signals from using 2X and 4X the crRNA concentration in a CRISPR reaction A) with and B) without the M. tuberculosis positive control. Two different aliquots of CHIKV template were used, along with un-amplified CHIKV genomic RNA.

Upon review of the crRNAs, it was found that they were synthesised with thymine instead of uracil. This causes the Cas13 proteins to not recognise the direct repeat of the crRNA. Using the *in vitro* transcribed crRNA produced a signal with both PCR and RAA-amplified CHIKV templates. However, a high signal was also produced in the negative control for both amplification methods (Figure 21).

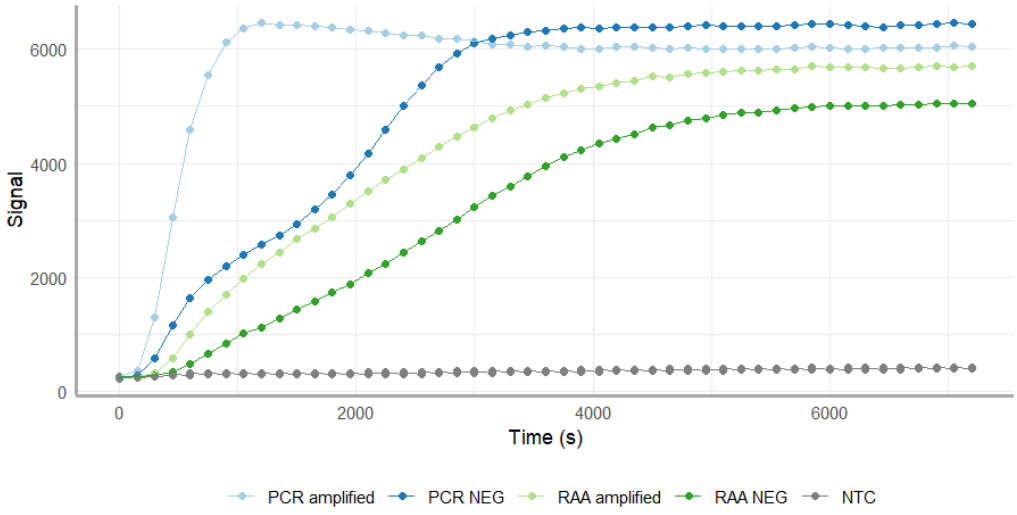

Figure 21: Fluorescence signal from CRISPR reactions using in vitro transcribed crRNA with CHIIKV template amplified by both PCR and RAA, along with the NTC of the CRISPR reaction.

The crRNA and RAA primers sequences were then reviewed again. An issue was found in that the crRNA target region is inside the forward RAA primer, which contains the T7 promotor and can be translated to RNA. This means the forward primer acts as the template for the crRNA regardless of the presence of the RAA template. This issue arises because the entire amplicon was used as input into the cas13design tool, allowing for it to target the primer sequences. To address this, the forward primer was moved further to the front of the crRNA target. The initial and revised designs of the RAA primers is shown in Figure 22.

A)

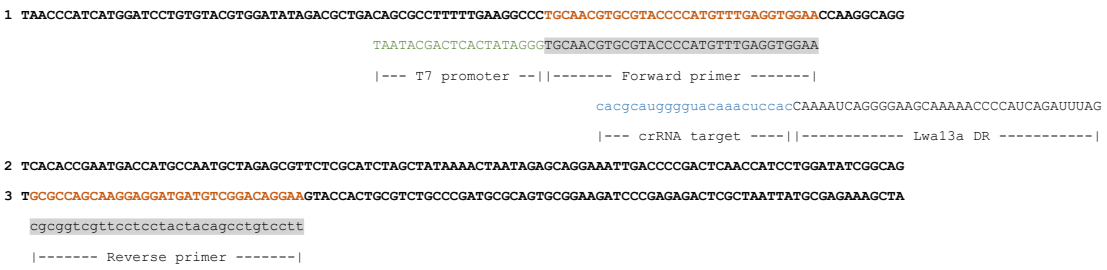

B)

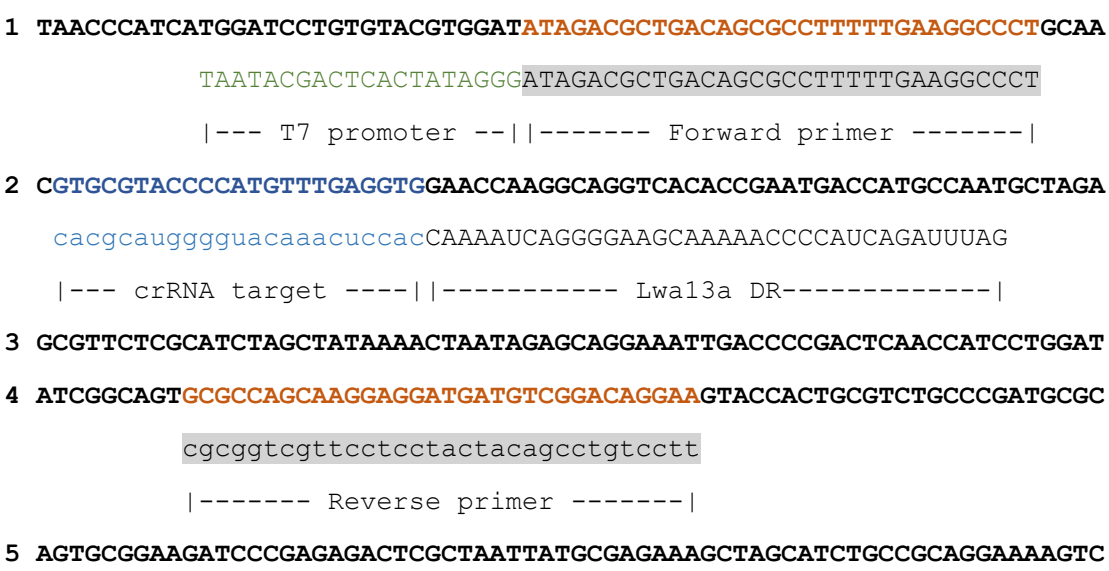

Figure 22: Location of the A) first iteration and B) revised version of RAA primers and crRNA for CHIKV target.

Once the redesigned primer was obtained, a repeat of the assay done at VISTEC was performed at MORU to verify that the assay can be repeated using the new primers and using the Bio-Rad CFX Opus 96 Real-Time PCR System. Strong fluorescence signals can be detected in the PCR-amplified CHIKV template without signal from the negative control or the NTC (Figure 23).

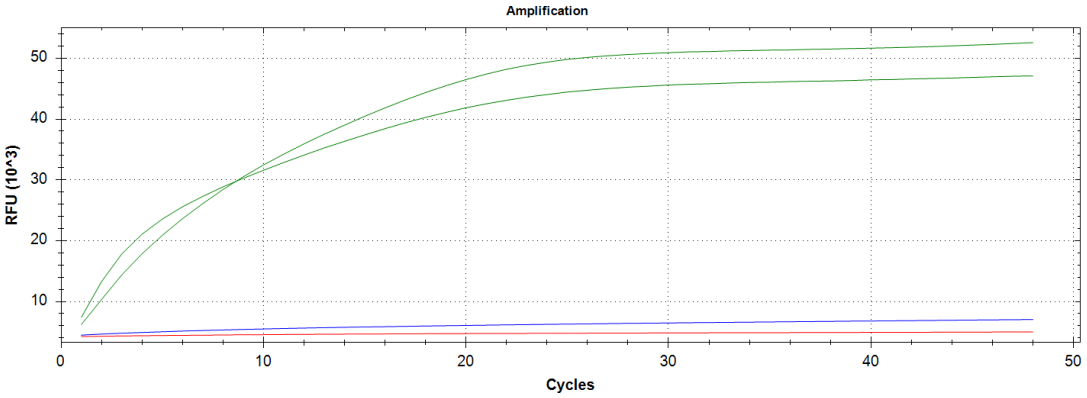

Figure 23: Fluorescence signal from CRISPR assay detecting PCR-amplified CHIKV template using redesigned RAA primers. CHIKV samples were done in duplicates. Positive control is shown in blue and the negative control is shown in red.

4.2.3.2. DENV detection

Testing with PCR-amplified DENV shows the highest fluorescence signal in DENV3, followed by DENV2 and DENV1, and DENV4. However, the signal from the negative control is relatively high. To call a sample positive or negative in VISTEC's protocol, samples must have at least twice the signal intensity of that of the negative control to be called positive, in which case only DENV1-3 are considered positive. When amplified with RAA, none of the samples were able to produce high enough signal to be called positive. Figure 24 and Table 27 shows the signal of each DENV serotypes as amplified by PCR and RAA.

A)

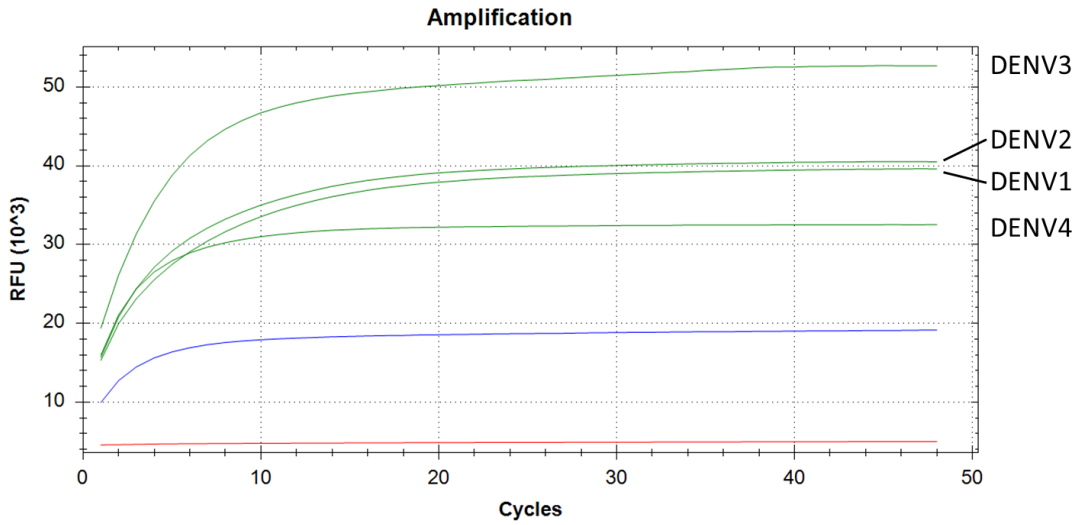

B)

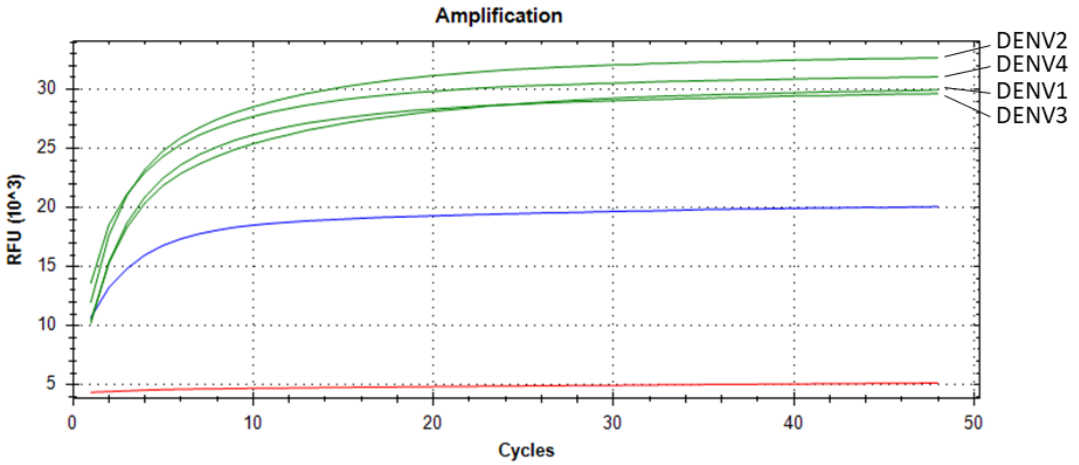

Figure 24: Fluorescence signals from all four serotypes of DENV in CRISPR assays as amplified by A) RT-PCR and B) RAA. Amplification negative is shown in blue and the NTC is shown in red.

Table 27: List of fluorescence signal from DENV templates in CRISPR reaction as amplified by both RT-PCR and RAA. The RFU values are the average of the last 5 cycles. Samples are called positives if their signal is greater than twice the signal of the negative control.

Amplification	Template	RFU	Call
RT-PCR	DENV1	39,594	Positive
	DENV2	40,517	Positive
	DENV3	52,687	Positive
	DENV4	32,519	Negative
	Negative control	19,117	N/A
	NTC	4,996	N/A
RAA	DENV1	29,902	Negative
	DENV2	32,637	Negative
	DENV3	29,606	Negative
	DENV4	31,022	Negative
	Negative control	20,049	N/A
	NTC	5,145	N/A

During the design of the primers, three conserved loci were identified in the 3'UTR and used as the RAA primers and crRNA sequences. Upon reviewing the sequences, the loci used for the forward RAA primer and crRNA contain repeat sequences which leads to the crRNA being able to bind to the forward primer, giving rise to the fluorescence signal in the negative control samples of the amplification reaction.

To resolve this, the forward primer was re-designed by moving the target sequence upstream to a relatively conserved region. Although this new locus does contain multiple SNPs, looking at the sequence alignment and geographic distribution, the sequences can be divided into two populations in Southeast Asia: DENV2, and the remaining serotypes. As such, two primers were designed, one for each population with four nucleotide differences for the SNPs (Figure 25). Nextstrain real-time tracking of dengue evolution was used to confirm that the SNPs are consistent

across the two populations throughout Southeast Asia (200, 201). Table 28 shows the sequences of the new forward primers.

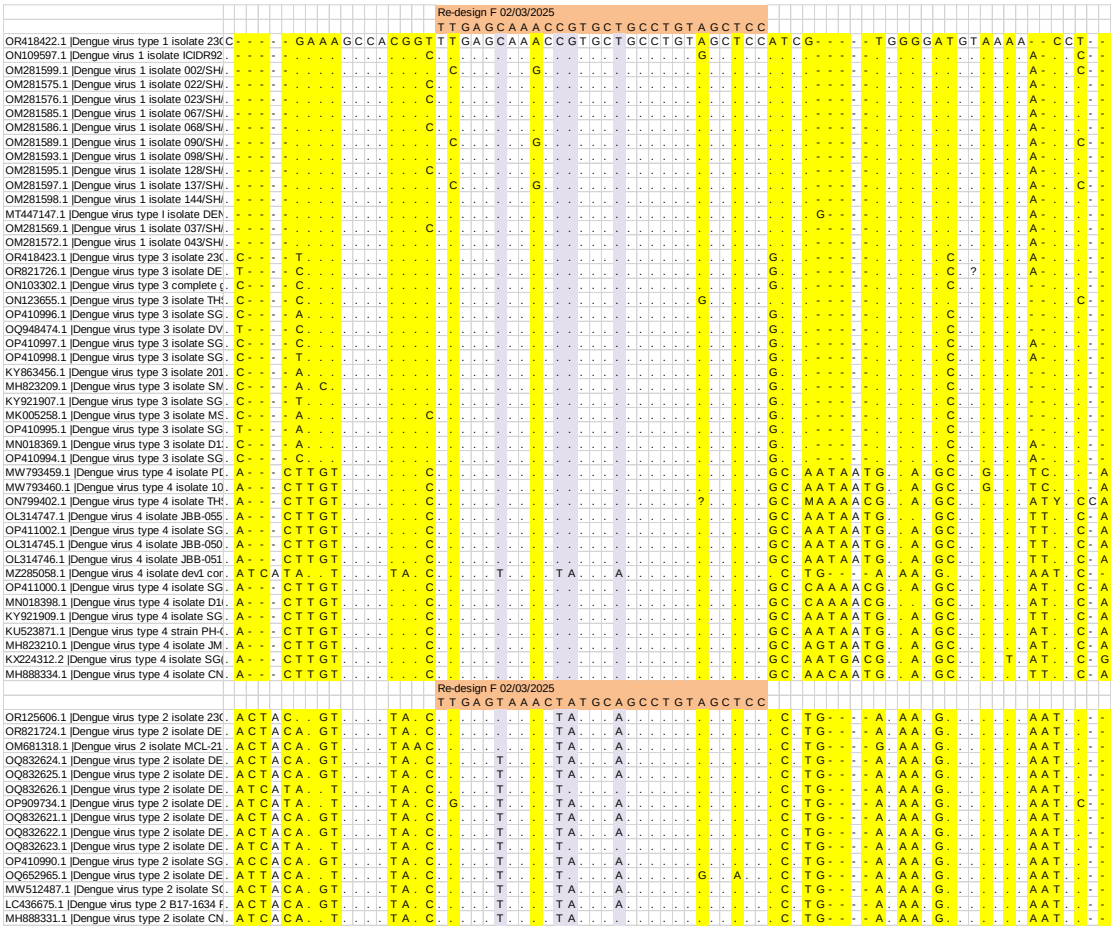

Figure 25: Alignment of DENV genome for the new DENV forward RAA primers. The sequences are divided into serotypes with DENV1, 3, and 4 on the top and DENV2 on the bottom. The primers' loci and sequences are highlighted in orange with the SNPs contributing to the different primer sequences highlighted in purple. Other SNPs are highlighted in yellow.

Table 28: Sequences of the new DENV RAA forward primers. The T7 promotor is denoted in lowercase and the SNPs within the sequences are denoted in bold.

Name	Sequence
WH_DENV134-F	taatacgactcactatagggTTGAG**C**AAAC**CG**TGC**T**GCCTGTAGCTCC
WH_DENV2-F	taatacgactcactatagggTTGAG**T**AAAC**TA**TGC**A**GCCTGTAGCTCC

Two serotypes, DENV1 and DENV2, were used to test the new primer to represent the two forward primers. By amplifying with RT-PCR, both targets show high fluorescence signal while

the amplification negative control no longer shows a high signal. The signal from the CRISPR reaction as well as the RFU of each sample is shown in Figure 26 and Table 29.

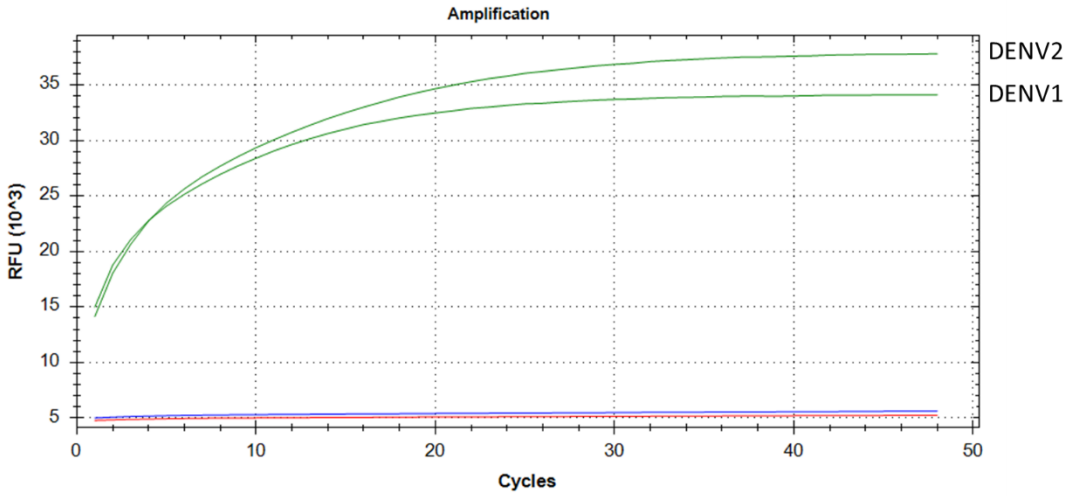

Figure 26: Fluorescence signals from DENV1 and DENV2 using the newly designed forward primers as amplified by RT-PCR. The negative control (NTC of the RAA reaction) is shown in blue and the NTC is shown in red.

Table 29: List of fluorescence signal from DENV1 and DENV2 using the newly design forward primers. The RFU values are the average of the last 5 cycles. Samples are called positives if their signal is greater than twice the signal of the negative control.

Amplification	Template	RFU	Call
RT-PCR	DENV1	34113	Positive
	DENV2	37788	Positive
	Negative control	5615	Negative
	NTC	5247	Negative

4.2.3.3. ZIKV detection

The ZIKV assay shows similar patterns to that of the DENV assay as the CRISPR assay was able to detect the PCR-amplified template but not the RAA-amplified ones. While a higher signal is seen in the RAA-amplified template compared to the negative control, it is not high enough to call it as positive. Figure 27 and Table 30 shows the signal of the ZIKV templates as amplified by both PCR and RAA.

A)

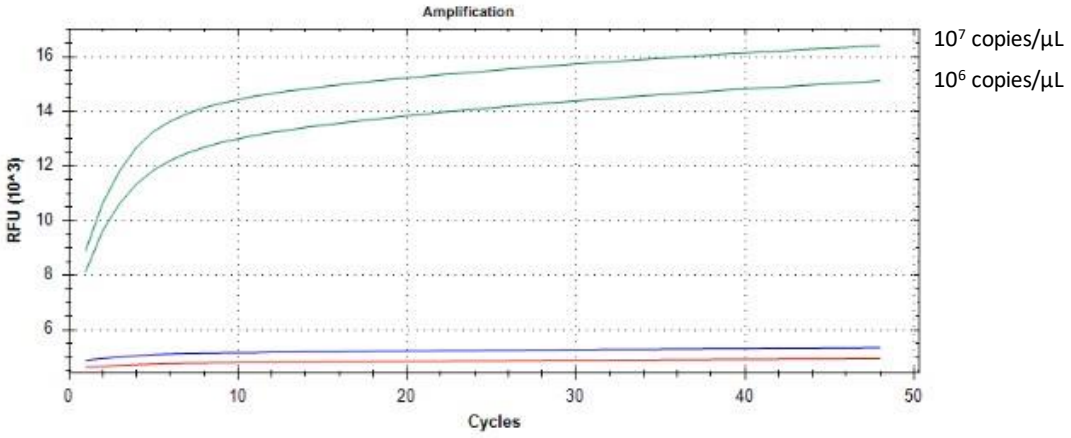

B)

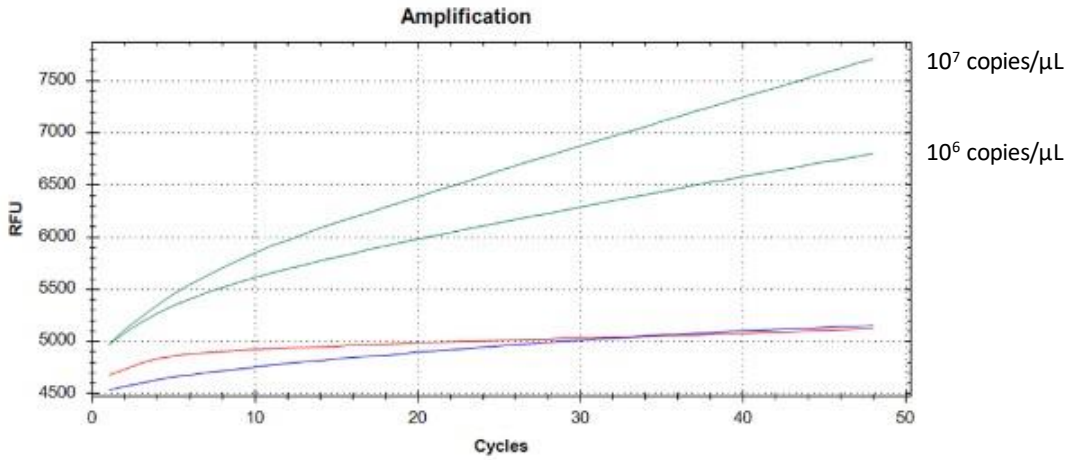

Figure 27: Fluorescence signals from two dilutions of ZIKV in CRISPR assays as amplified by A) RT-PCR and B) RAA. Amplification negative is shown in blue and the NTC is shown in red.

Table 30: List of fluorescence signal from ZIKV templates in CRISPR reaction as amplified by both RT-PCR and RAA. The RFU values are the average of the last 5 cycles. Samples are called positives if their signal is greater than twice the signal of the negative control

Amplification	Template	RFU	Call
PCR	ZIKV 10^7 copies/μL	16352	Positive
	ZIKV 10^6 copies/μL	15050	Positive
	Negative control	5341	N/A
	NTC	4944	N/A
RAA	ZIKV 10^7 copies/μL	6749	Negative
	ZIKV 10^6 copies/μL	7621	Negative
	Negative control	5141	N/A
	NTC	5113	N/A

4.2.3.4. Limit of detection

The LOD of the CRISPR assays as amplified by PCR were found to be 10^2 and 10^3 copies per reaction for CHIKV and ZIKV respectively. During the first test, the LOD of the DENV assay could not be accurately assessed as the negative control showed very high signal intensity, rendering the assay invalid. The results of the CRISPR assays are shown in Table 31.

Table 31: End relative fluorescence unit (RFU) of serial dilutions of CHIKV and ZIKV. The thresholds for calling a sample positive are 11,074 for CHIKV and 11,034 for ZIKV.

Sample	Concentration (copies/μL)	End RFU	Call
CHIKV	10^4	47190	Positive
	10^3	47993	Positive
	10^2	45900	Positive
	10^1	5615	Negative
	10^0	5475	Negative
	Negative control	5537	Negative
	No template control	5207	Negative
ZIKV	10^4	20249	Positive
	10^3	21155	Positive
	10^2	5462	Negative
	10^1	5535	Negative
	10^0	5381	Negative
	Negative control	5517	Negative
	No template control	5074	Negative

After the redesign of the DENV forward primer, the assay was able to detect down to 10^2 and 10^3 copies per μL of DENV1 and DENV2 respectively (Table 32).

Table 32: End relative fluorescence unit (RFU) of serial dilutions of DENV1 and DENV2 genomic RNA. The threshold for calling a sample positive is 11,182.

Sample	Concentration (copies/µL)	End RFU	Call
DENV1	10^4	34069	Positive
	10^3	30640	Positive
	10^2	19889	Positive
	10^1	5651	Negative
DENV2	10^4	37687	Positive
	10^3	28686	Positive
	10^2	5646	Negative
	10^1	5677	Negative
	Negative control	5591	Negative
	No template control	5229	Negative

4.2.3.5. Full process testing

To test the full process, CHIKV culture spiked in either whole blood or plasma and serially diluted in the QuickExtract DNA extraction solution before extraction by incubation. The extraction product was either used directly as template for amplification or was purified using AMPure XP beads (Chapter 2.3.3). After amplification by RAA and PCR, the products were detected with CRISPR. A positive result was obtained in two of the five dilutions amplified by PCR. CHIKV in un-purified plasma was detected down to the 10^{-4} dilution except for 10^{-3} while purified plasma was able to detect all four dilutions. Only the highest CHIKV concentration spiked in plasma was detected if amplified by RAA (Table 33).

Table 33: End relative fluorescence unit (RFU) of CHIKV RNA in whole blood and plasma samples extracted using QuickExtract DNA extraction solution, amplified by PCR, and detected by CRISPR. The RFU values are the average of the last 5 cycles. Samples are called positives if their signal is greater than twice the signal of the negative control.

Sample	Dilution	Amplification	End RFU	Call
Whole blood	10^{-1}	PCR	32193	Positive
	10^{-2}		53705	Positive
	10^{-3}		5426	Negative
	10^{-4}		5454	Negative
	10^{-5}		5354	Negative
Whole blood	10^{-1}	RAA	7671	Negative
	10^{-2}		6036	Negative
Whole blood, purified	10^{-1}	PCR	54062	Positive
	10^{-2}		55221	Positive
	10^{-3}		47455	Positive
	10^{-4}		5332	Negative
	10^{-5}		5341	Negative
Plasma	10^{-1}	PCR	56861	Positive
	10^{-2}		57755	Positive
	10^{-3}		5349	Negative
	10^{-4}		57478	Positive
	10^{-5}		5352	Negative
Plasma	10^{-1}	RAA	13179	Positive
	10^{-2}		6225	Negative
Plasma, purified	10^{-1}	PCR	59214	Positive
	10^{-2}		57007	Positive
	10^{-3}		55163	Positive
	10^{-4}		51731	Positive

10^{-5}	5289	Negative
PCR Negative control	5424	N/A
RAA Negative control	5985	N/A
NTC	5137	N/A

4.3. Discussion

4.3.1. The developed assay

In this chapter, an assay to rapidly extract, amplify, and detect bloodborne pathogens has been developed using CHIKV and ZIKV as proof-of-concept, with a working detection assay for DENV. Using the QuickExtract DNA extraction solution, RAA, and CRISPR detection, the assay was able to detect CHIKV virus spiked in plasma. When using real-time RT-PCR for amplification, CHIKV was able to be detected from spiked whole blood samples.

Extraction was able to be performed crudely by simply diluting whole blood in QuickExtract DNA extraction buffer and incubating at two different temperatures. Nucleic acid extraction is very important to molecular tests because many proteins in blood act as PCR inhibitors and lowers the efficiency of the reaction if present (202). Many DNA extraction protocols, while producing clean products, require specific instruments such as a centrifuge for spin columns, or potentially hazardous chemicals, such as guanidinium thiocyanate. The method used here, while not as clean as the other methods mentioned, is able to produce clean enough products to be further amplified and detected. Another advantage of this method is that it requires less volume of blood which can be obtained by finger prick. This is ideal in POC situations where there are no personnel trained in venepuncture and also in helping with patient compliance as it is less invasive.

Isothermal amplification was successfully performed with both RAA and LAMP in CHIKV and DENV although ZIKV was only tested with RAA, as detected on agarose gel. RAA was ultimately used for CRISPR detection. LAMP and RAA both have their advantages and disadvantages. The former is cheaper, more readily available, and has been shown to be more

sensitive than RPA/RAA (203). However, LAMP is more susceptible to false positives and operates at a higher temperature range, 60 - 65°C. Moreover, because the primer design for LAMP requires at least six conserved regions, designing assays for a target with high variation such as a pan-DENV assay is much more challenging. RAA on the other hand is much simpler to design for, only requiring 2 primers as with conventional PCR. This, and the fact that the operating temperature is much lower, at the point of body heat, makes RAA a very attractive technology. Because detection is done by CRISPR, not RAA, there is more tolerance for non-specific amplification as only the correct amplicon will be detected by CRISPR, not any non-specific amplification products which could cause false positives.

The CRISPR assay was able to consistently detect viral RNA extracted from viral culture and amplified by RT-PCR. The methods presented here incubated the assay for two hours but in practice, only 30 minutes is required to detect a positive signal as the fluorescence signal sharply increases during incubation and plateauing around 30 minutes. Detection of RAA-amplified samples has shown to be unreliable although RAA amplicons can be detected by gel-electrophoresis. Currently, amplification for the assembled assay relies on PCR for the target to be detected by CRISPR with the sensitivities of 10^2 copies/μL, for CHIKV which is comparable to real-time PCR using SYBR green. However, with probe-based real-time PCR, the limit of detection can be as low as 10^0 copies/μL (204). Similar ranges were reported for ZIKV and DENV using real-time RT-PCR as well (205, 206).

The fully assembled assay with CHIKV was able to detect the spiked virus in plasma if amplified by RAA and in both plasma and whole blood if amplified by RT-PCR. CHIKV viral load in acute febrile patients can reach 10^8 genome copies/mL of whole blood, this assay should be able to detect the pathogens in highly viraemic patients, as this assay can theoretically detect down to 10^6 genome copies/mL in whole blood samples (207). However, with viruses such as ZIKV with lower viral loads, around 10^5 copies/mL in blood, this assay would not be able to detect them in the current form (208). This is also true for bacteraemia as bacterial loads are generally much lower than viral loads. *O. tsutsugamushi* for instance, has median bacterial load in the 10^3 copies/mL range

(209). There is also the potential loss of yield from extraction that could lower the sensitivity of the assay.

Adding a nucleic acid purification step using AMPure XP beads was able to increase the sensitivity of the assembled assay in whole blood by tenfold despite not specifically made for RNA purification and an RNA-specific product such as the RNAClean XP Bead-Based Reagent (A66514, Beckman Coulter, Indianapolis, IN, US) would likely produce a better yield. This is most likely due to the removal of proteins and other amplification inhibitors present in whole blood such as haem (202). This is corroborated in the higher sensitivity in plasma compared to whole blood. While purification improves the assay's sensitivity, it contributes to additional costs and labour in performing the assay.

A potential way to overcome the inhibitors in whole blood is to use alternative samples. As demonstrated above, using plasma can increase the sensitivity of the assay, enough to increase the detection from 10^{-2} to 10^{-4} dilutions. However, obtaining plasma requires either centrifugation of whole blood or using plasma collection tubes that doesn't contain anticoagulants. Both of these options require venepuncture which is a procedure not always available, especially in a POC situation. Saliva and urine are two sample types that are non-invasive and easily collected. DENV, CHIKV, and ZIKV are detectable in these matrices with viral load roughly the same as whole blood (210-212). It has also been shown that these samples retain viruses for longer than whole blood, with DENV being detectable up to 7 days in saliva and 14 days in urine (213).

Many CRISPR-based diagnostics rely on using urine or saliva as sample. One such assay for DENV detection processes the samples using Heating Unextracted Diagnostic Sample to Obliterate Nucleases (HUDSON) which involve heating the samples twice at two temperatures to inactivate any nuclease and virus in the sample before adding the product into an RPA reaction directly (214). Another assay was able to use whole blood as the sample to detect African swine fever (ASF) in plasmid-spiked samples as well as PCR positive swine blood sample. However, whole blood extraction was done using a spin column extraction kit which requires a centrifuge (215).

4.3.2. Limitations

The major limitation of the developed assay is the need for conventional PCR amplification as RAA amplification was not able to be used for reliable detection due to low yields. In contrast, the Taq polymerase used for the PCR reaction remains stable long after its expiration date. If this is the case, applying assays such as this in a real-world setting would have to be conscious of the conditions that the reagents need to be stored. The LwaCas13a proteins would particularly be difficult as although the working stock can be stored at 4°C, the stock is stored at -80°C. More tests with additional replicates should also be performed to assess the consistency of the results of both PCR and RAA.

Even if RAA proves to be reliable, this assay would still require multiple temperatures across the different steps. The extraction step alone requires two temperatures; 60°C and 98°C while the RAA and CRISPR assays require slightly different and much lower temperatures: 39°C and 37°C. Although for the latter point, the operational temperature of RAA has high enough tolerance that using the same temperature as the CRISPR reaction would still work. So, while a thermal cycler is not required, multiple heat sources are still required. Realistically, the number of heat sources can be minimised to two, mainly for the extraction step as the samples must be immediately moved from 60°C to 98°C. The heat sources can then be set to 39°C and 37°C for the amplification and detection steps while keeping the samples on ice.

Another limitation of this assay is the need for specific reagents. The QuickExtract DNA extraction solution, RAA reagents, and LwaCas13a are not widely available. The requirement of crRNA and RNA reporters also increases the cost, especially since the reporters have to be labelled with fluorescent dyes. While LwaCas13a and crRNA can be synthesised at a lower cost in-house from plasmids and ssDNA respectively, the process of doing so is intensive and require skilled laboratory workers.

4.3.3. Conclusion

The singleplex assays developed are able to detect CHIKV, DENV, and ZIKV from whole blood by rapid extraction, isothermal amplification, and CRISPR. The assay can detect virus

concentrations typical of highly viraemic patients. Extraction was done by diluting blood in QuickExtract DNA extraction solution and heating. Isothermal amplification was done with RT-PCR, then detection with CRISPR at 37°C. Using RAA for amplification was also able to detect the targets although less consistently. The entire assembled assay can be done in roughly two hours from extraction to detection with RT-PCR and as short as one and a half hour if using RAA. The sensitivity of the assay can be further improved if an additional purification step is done. If RAA can be optimised for this assay, it could be able to be performed without any specialised equipment such as centrifuges and thermal cyclers which would make it ideal for rural areas where hospital access is limited.

CHAPTER 5

Development of an automated real-time PCR assay for detecting bloodborne viral pathogens from dried blood spot specimens

This chapter describes the development and optimisation for a real-time PCR assay to detect bloodborne viral pathogens from DBS specimens. The assay encompasses elution of DBS and automatic extraction and molecular detection using the BD MAX™ system.

5.1. Methods

5.1.1. Optimisation of dried blood spot elution

Before extraction, DBS need to be eluted to remove the genetic material from the filter paper as well as to resuspend the sample for further processing. The general protocol for elution is to immerse each spot in a buffer for a fixed amount of time before collecting the supernatant. The blood spot itself can be excised from the paper in a number of ways including using DBS punching machines and manually cutting with scissors. Initially, the BSD600 DBS puncher (BSD, Brendale, Australia) was used to punch three to four 6.0 mm per blood spot, depending on the radius of each spot, into a deep-well 96 well plate and covered with an adhesive seal. Later, manually cutting each spot with scissors was the chosen method.

Different dilutions of the pET-21a(+) plasmid transformed with CHIKV PCR amplicon were spiked into healthy whole blood and dropped onto filter paper. Plasmids were chosen as the target in lieu of viral RNA as it can be produced in-house and can be accurately quantified. The human *rnaseP* gene was used as the internal control. Extraction controls used were whole blood from healthy volunteers that was either spiked with plasmids or used as healthy whole blood.

Three different elution solutions were tested; 500 µL BD MAX™ Sample Buffer Tube (SBT) buffer, 500 µL BD MAX™ SBT buffer with approximately 80 µL acid-washed 425-600 µm glass beads, and 500 µL MagNA Pure LC Total Nucleic Acid Isolation Kit (03246779001, Roche) lysis/binding buffer. Addition of glass beads was done to assess whether additional agitation of the DBS can increase the yield. Other factors were also varied such as buffer volume (500, 1500, and 3000 µL) and elution time (1 and 3 hours). Other more esoteric procedures were also tested to assess whether the saturation of the buffer is slowing down the elution process. These methods are adding 500 µL of buffer every 30 minutes over 3 hours and eluting with 500 µL buffer for 30 minutes before replacing with fresh buffer while pooling the used buffer over 3 hours (Figure 28). All testing was done using separate extraction only and PCR only protocols of the BD MAX™ instrument in order to include the positive standards in the PCR assays. These standards are the pET-21a(+) plasmids with CHIKV amplicons, diluted between 10^5 to 10^0 CHIKV amplicon copies

per µL. The final protocol used for elution going forward is shaking DBS in 1500 µL SBT buffer at 1100 rpm for 3 hours.

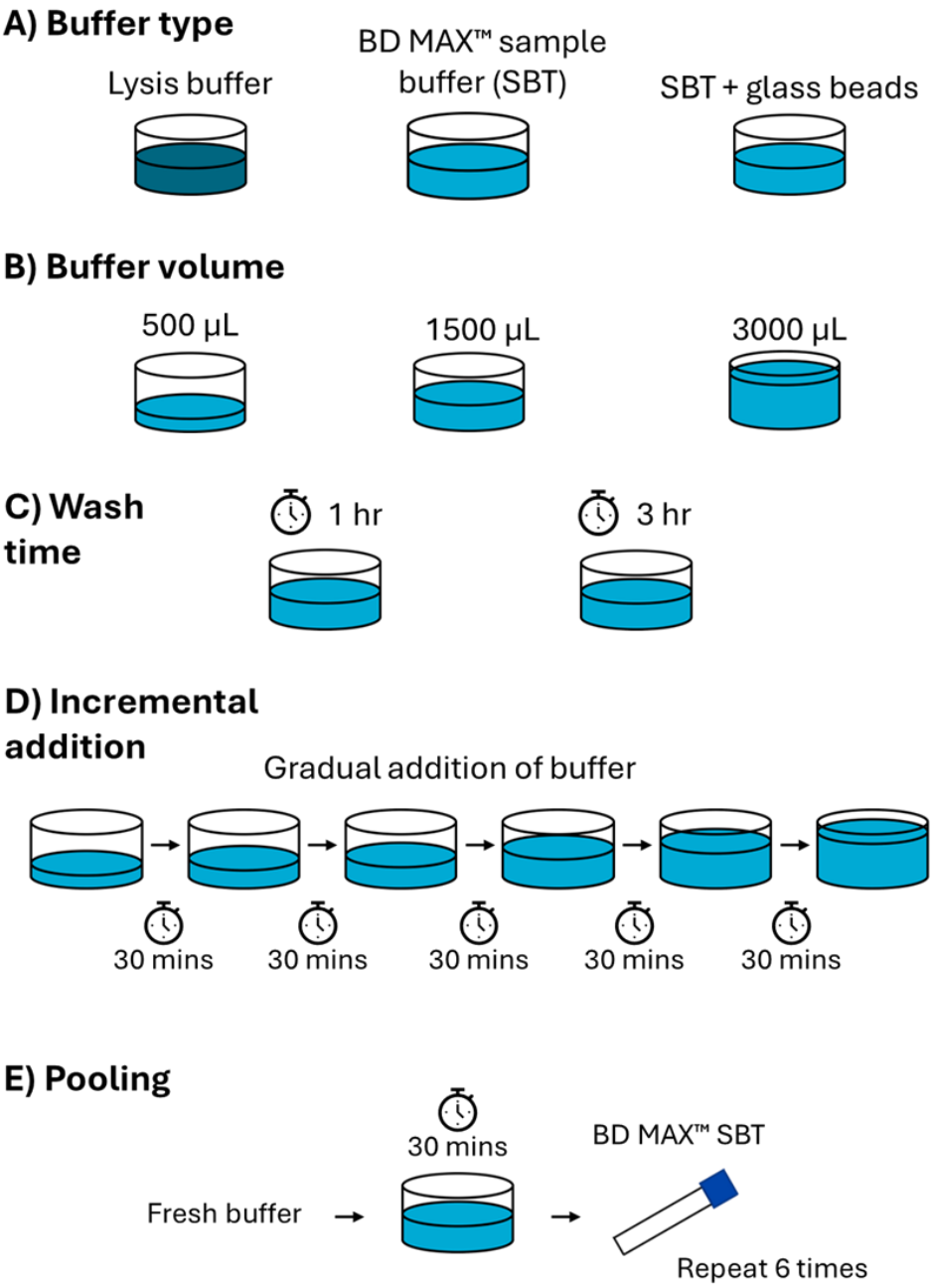

Figure 28: Different factors tested for eluting DBS. A) Different elution buffers B) Varying the buffer volume C) Varying the elution time D) Incrementally adding buffer over time E) 'Pooling' the buffer. Fresh buffer was added to be shaken and removed into a BD MAX™ SBT. Additional fresh buffer was added and pooled into the same SBT.

To assess the amount of blood eluted compared to whole blood, 50, 25, 12.5, and 6.25 µL of whole blood was used as control alongside the DBS. Any inhibitory effect the filter paper might have on the assay was also assessed by performing a mock elution of clean filter paper before 50 µL whole blood was added. In these tests, only the *rnaseP* target was used.

5.1.2. Optimisation of the automated dried blood spot real-time PCR assay

To optimise the fully automated DBS assay on the BD MAX™ instrument, a comparison was done between extraction only and PCR only (half process) against a BD MAX™ full process run (Figure 29). This was done to ensure there is no difference between the two methods as optimisation was done primarily using the half process run as it allows for two PCR reactions per sample. These runs were performed using DBS from whole blood spiked with CHIKV culture at 10^{0} and 10^{-1} dilutions. Healthy whole blood was used for both elution and extraction controls. 50 µL of whole blood was added into either 1500 µL SBT buffer in a 12-well plate to be shaken or directly into an SBT tube as elution and extraction control respectively. A duplex assay targeting CHIKV and the human *rnaseP* gene was used for this test, with three replicates per sample.

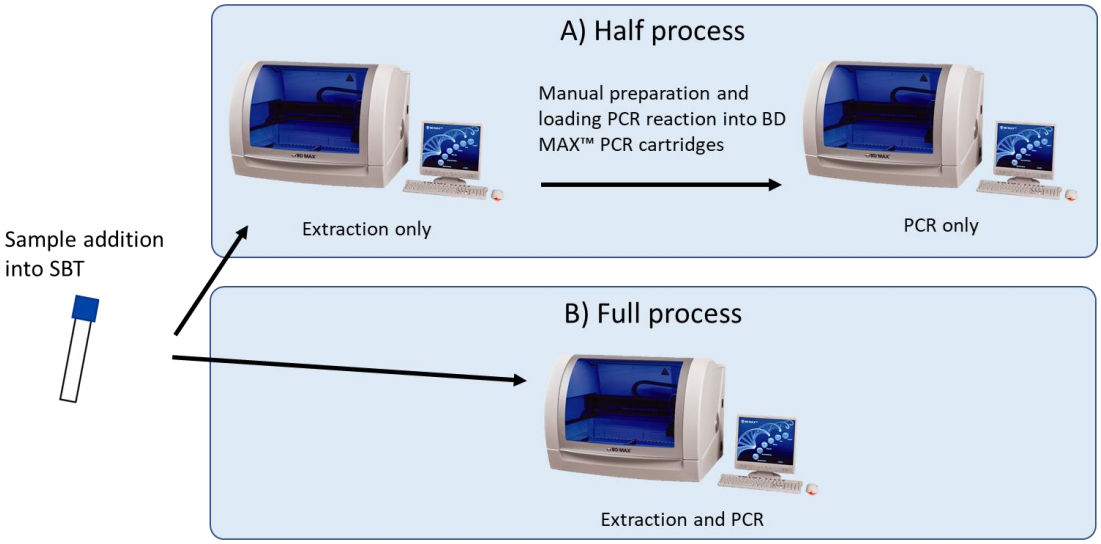

Figure 29: Two methods of running the BD MAX instrument. A) Half process with separate, manual extraction and PCR steps. B) Full process with fully automatic extraction and PCR steps.

To assess the consistency of the assay between runs, three runs were planned to be performed on three separate days. These tests only used healthy whole blood and thus only the

rnaseP target. DBS and 50 μL whole blood were used as the samples in full process runs with three replicates per sample. Six replicates were done per sample type.

Optimising the PCR assay was done by varying the *rnaseP*-specific primers and probe concentrations between 0.03, 0.06, 0.09, and 0.114 pmol/μL. The whole blood control uses the 0.03 pmol/μL primers and probe. To assess the consistency between runs, three runs using DBS, 50 μL whole blood, and 5 μL whole blood were again performed over three days from elution to detection with freshly prepared primer mixes.

The CHIKV target was added to create a duplex. Two groups of reactions were prepared; one using a duplex mix and another using the same template for two singleplex mixes (CHIKV and *rnaseP*) via the dual master mix protocol of the BD MAX™. This allows for direct comparison between the signals of the duplex and singleplex assays.

5.1.3. Assessment of temperature on the storage of viral RNA in dried blood spots

DBS were prepared by serially diluting fresh CHIKV culture in PBS (from 10^{0} to 10^{-5}) and spiking each dilution into freshly drawn whole blood giving dilutions of 10^{-1} to 10^{-6}. These DBS were divided into four groups to be stored at different conditions for two months. The first three groups were stored at room temperature, -20°C, and -80°C respectively for the entirety of two months. The last group was stored at room temperature for one month before being moved to -20°C for another month. This was done to simulate the typical storage condition of DBS in the field, as many DBS sample will remain at ambient temperature for a prolonged period of time before being stored at -20°C at the site. After two months, all samples were stored at -80°C until use. The spiked whole blood was also stored at -80°C to be used as control.

For detection, each DBS sample was eluted using the protocol developed in this chapter. Then each sample, along with spiked whole blood and healthy whole blood were extracted using the extraction only program on the BD MAX™. Real-time PCR was done on the Bio-Rad CFX Opus 96 Real-Time PCR System to be able to run every sample simultaneously. The condition used is the viral assay developed in 0.

5.2. Results

5.2.1. Dried blood spot elution

In optimising the elution of DBS, each spot must be excised from the filter paper to be immersed in an elution buffer. Initial testing with the BSD600 DBS puncher is less laborious than manual cutting. However, this method proved to be problematic when the seal was removed for further processing. Due to the static electricity, some of the punched-out spots were attracted to the seal as it was being removed causing some spots to jump and adhere to the seal while others jumped into adjacent wells, mixing up the contents. Furthermore, because the assay to be used with these samples are qualitative, the goal of elution is to get the maximum amount of genetic material from each sample and punching DBS leaves behind much blood on the filter paper. Because of this, the method of cutting out blood spots changed to excising the whole spot.

5.2.1.1. Comparison of buffer types

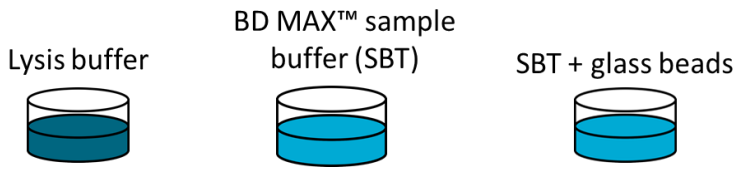

Figure 30: Comparison between different buffer conditions for the elution of DBS.

Three different conditions for eluting DBS: MagNA Pure lysis/binding buffer, BD MAX™ SBT buffer, and BD MAX™ SBT buffer with glass beads, were compared in elution across three time periods. Among the three elution solutions, the BD MAX™ SBT buffer without glass beads gave the highest relative yield at longer incubation times, from approximately 88,488.89 µL CHIKV plasmid copies per reaction after incubating for 90 minutes and up to 796,804.25 copies per reaction after incubating overnight. Adding glass beads to the SBT buffer does not show much difference in the 30-minute elution with the yield between SBT buffer alone is very similar but gave less yield at longer incubations, with a maximum yield of 109,460.17 copies per reaction after incubating overnight. The MagNA Pure lysis/binding buffer shows very consistent yield across all incubation times. Between 30 to 90 minutes of incubation, the MagNA Pure lysis/binding buffer

shows very similar yields between 30,552.86 and 37,793.69 copies per reaction respectively. The SBT was chosen as the buffer to use because while the MagNA Pure lysis/binding buffer shows consistency across the incubation times, it does not have the increase in yield in the 90-minute incubation as the SBT buffer does (Figure 31). It is also preferable as the buffer if the BD MAX™ instrument is to be used for the assay for economic reasons as the SBT buffer is required to run the BD MAX™ and is included with the ExK™ TNA-2 kits.

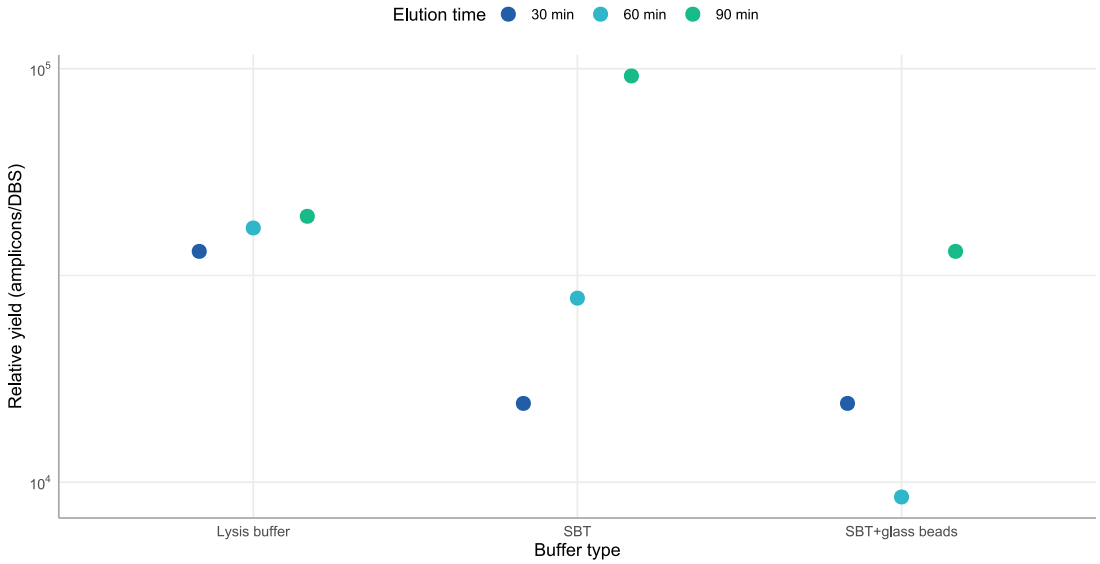

Figure 31: Relative yields of DBS spiked with CHIKV plasmids by eluting with different buffers for different durations. All samples were eluted with 500 µL of the respective buffers and shaken at 1100 rpm.

5.2.1.2. Comparison of elution duration

Figure 32: Comparison between different elution duration of DBS.

Once the buffer was chosen, a comparison was done on the elution duration, between one and three hours, using the SBT buffer. As seen in Figure 33, longer incubation times directly correlates with higher relative elution yield. The average yields from a one-hour incubation are 1,130.40 and 200.96 CHIKV plasmid copies per reaction for a 10^{-2} and 10^{-3} dilution respectively

while the average yields of a 3-hour incubation are 2,583.09 and 279.04 copies per reaction respectively. Three-hour elution was chosen for the protocol because of the higher yield.

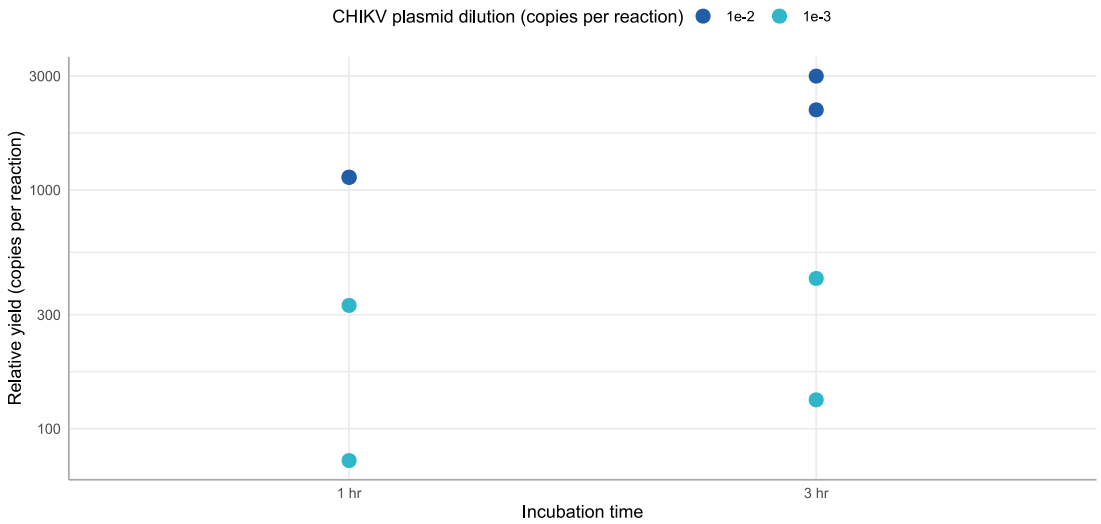

Figure 33: Relative yields of DBS spiked with serially diluted CHIKV plasmids at different incubation times. All samples were eluted with 500 µL SBT buffer. Samples were tested in duplicates.

5.2.1.3. Comparison of elution times

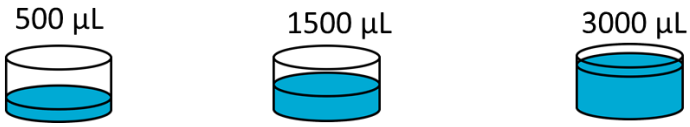

Figure 34: Comparison between different buffer volumes.

Three volumes (500 µL, 1,500 µL, and 3,000 µL) of buffer was compared using the previously established condition: three-hour elution in SBT buffer. 1,500 µL buffer resulted in the highest yield, up to 9,674.90 copies per reaction, followed by 3,000 µL and 500 µL respectively. However, it is noteworthy that using 1,500 and 3,00 µL buffer shows a high variation across replicates, with some having yields of 589.77 copies per reaction (Figure 35). 1,500 µL buffer was chosen as it has the highest yield and because each SBT tube contains 1,500 µL SBT buffer so each sample uses exactly one SBT tube.

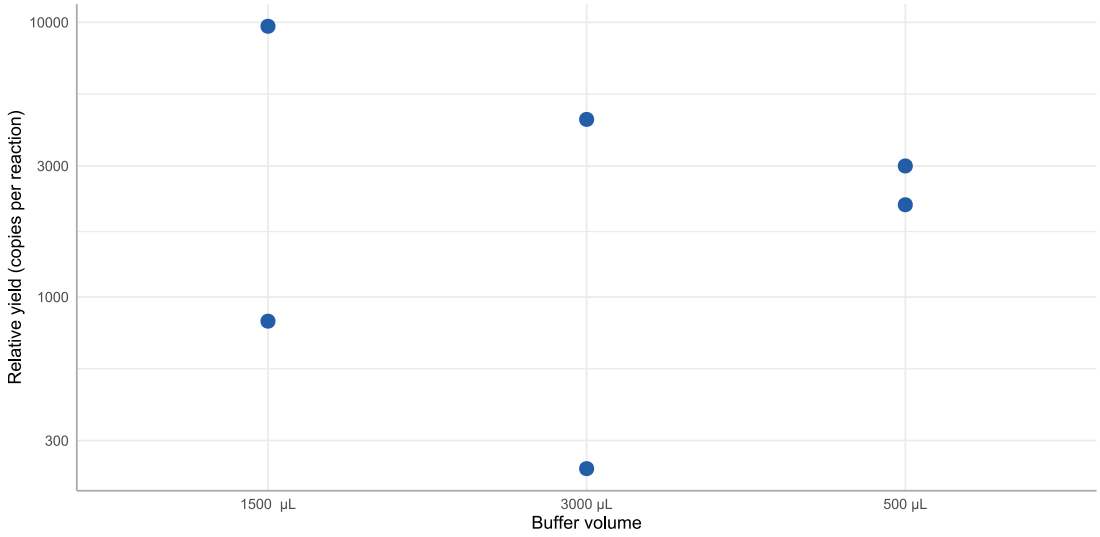

Figure 35: Relative yields of DBS at different elution buffer (SBT) volumes. All samples were spiked with CHIKV plasmids diluted to 10^{-2} from stock and eluted by shaking at 1100 rpm for 3 hours. Samples were tested in duplicates.

5.2.1.4. Assessing alternative methods of elution

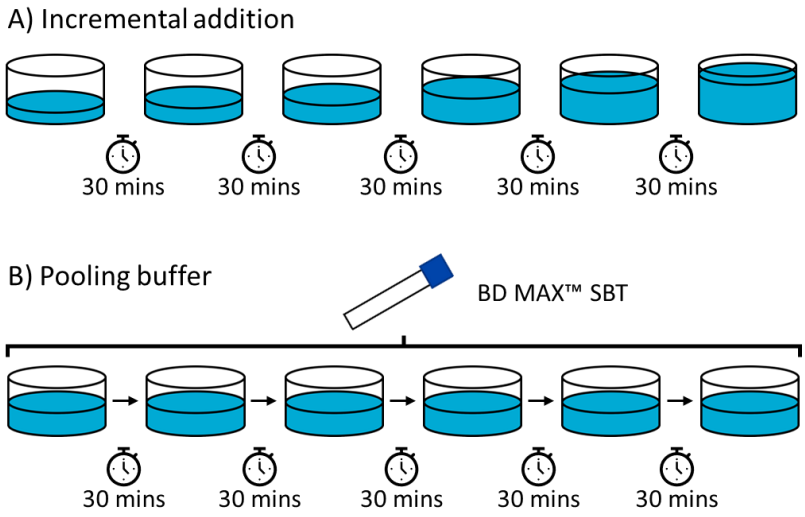

Figure 36: Comparison of alternative elution methods. A) Incremental addition of buffer B) Pooling buffer

Other alternative methods of elution were compared including incrementally adding fresh buffer into each well and pooling multiple washes of the same sample into the same tube. These alternate methods do not have a significant improvement in detection over adding the complete volume at the start of elution. Both incrementally adding buffer and repeatedly replacing the buffer

with fresh buffer and pooling the result have maximum yields of 5,749 and 9,674 copy numbers per reaction respectively from a template dilution of 10^{-2}. While the two alternative methods, especially pooling, seem more consistent across different replicates, the overall yield is not significantly higher than the methods used before (Figure 37). Because of this, and because these methods are more complicated to perform, they were dropped in favour of the more straightforward methods of eluting each DBS in a fixed amount of buffer for a fixed amount of time.

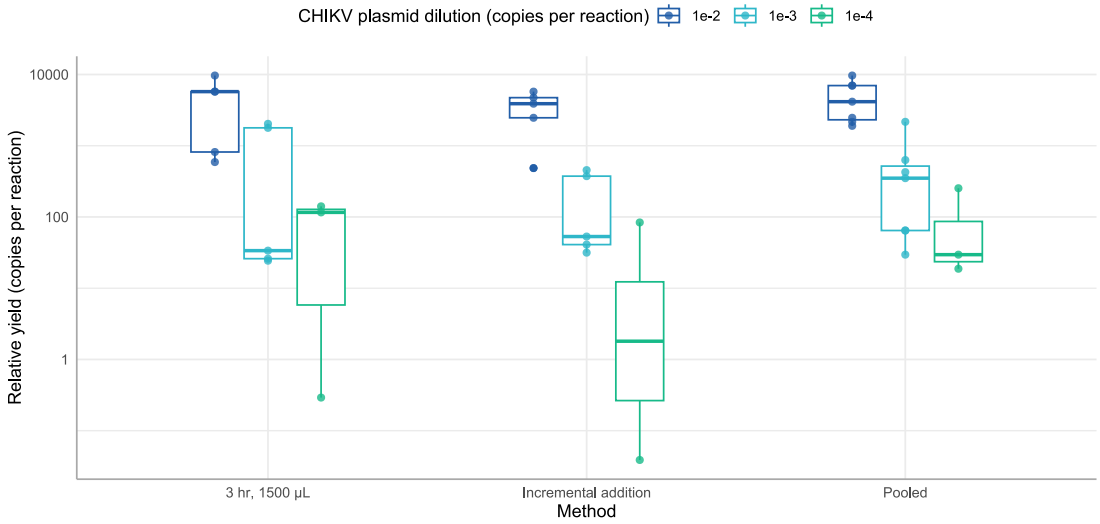

Figure 37: Yield of DBS from alternative methods of elution; incrementally adding buffer over time and replacing the buffer with fresh buffer over time while pooling the used buffer. The yields of eluting DBS in 1,500 µL SBT buffer for three hours from previous experiments are shown for comparison. A total of 4 replicates was performed.

5.2.1.5. Comparison between DBS and whole blood

Here, Cq values of 50 µL DBS and different volumes of whole blood sample are compared to assess what volume of whole blood is equivalent to 50 µL DBS. DBS sample has higher Cq values than any of the whole blood samples, slightly higher than 6.25 µL whole blood with Cq values upward of 36.6. This shows that there is a significant loss of detectable yield between the two specimen types. Furthermore, one of the DBS replicates does not show any signal showing that the reaction is not optimised enough to consistently detect *rnaseP*. For the other dilutions of whole blood, there are little variations and the Cq values all are between 26.8 and 30.6. Having the

filter paper also does not seem to have any inhibitory effect on the assay, with Cq values between 27.6 and 29, comparable to the values of whole blood without filter paper (Figure 38).

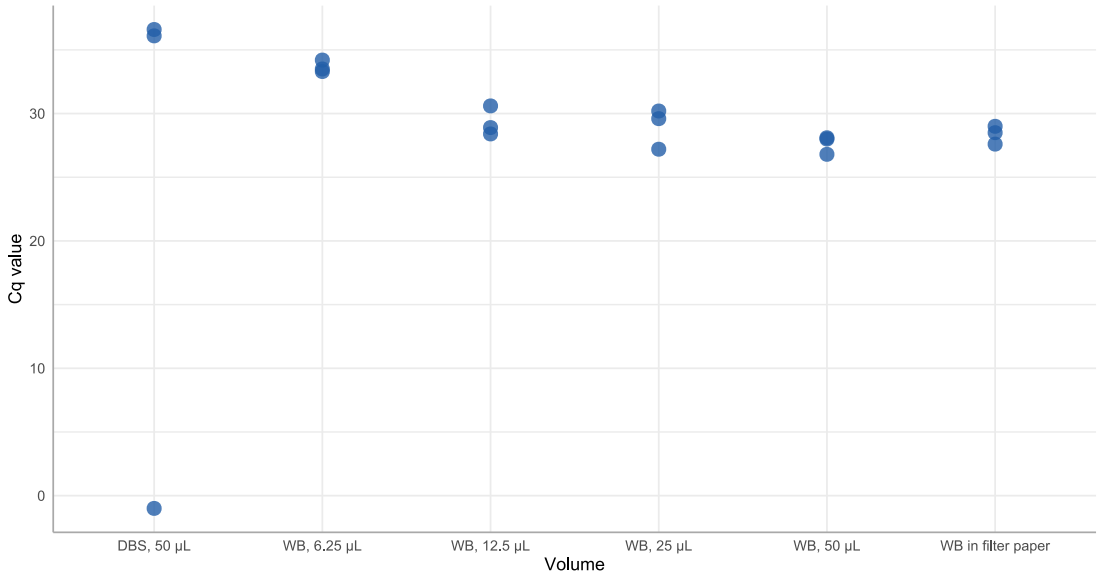

Figure 38: Comparison of Cq values for the rnaseP gene between DBS and various dilutions of healthy whole blood (WB). A mock elution (WB in filter paper) was done by adding 50 µL whole blood into a well containing a clean filter paper. A total of 3 replicates was performed.

5.2.2. Automated dried blood spot real-time PCR

Comparing the separate extraction only/PCR only run against the BD MAX™ full process run shows very similar Cq values. For the CHIKV target, the Cq values between DBS and whole blood were very similar with a range between 18.5 to 21.0 for the undiluted samples and between 22.6 and 23.9 for most of the 10^{-1} samples. The mock eluted whole blood shows slightly lower Cq values in both dilutions, ranging between 17.2 to 18.6 in the undiluted samples, and between 20.3 and 21.7 in the 10^{-1} samples. There is also an outlier in one of the replicates in the 10^{-1} DBS sample which has a Cq value of 31.9.

The *rnaseP* target also shows similar Cq values between the half and full BD MAX™ processes. The Cq values between the whole blood and mock eluted whole blood samples are in the same range, between 26.1 and 32.4. However, the differences between DBS and whole blood are significant, as seen in previous tests with the DBS samples having Cq values in the range between 34.8 and 40 with three samples not being detected at all. One of these is a replicate of the

full process run of the undiluted sample while the other two were replicates from the 10^{-1} dilution using half process. In general, there is no negative effect in using the BD MAX™ full process, compared to the half process. The comparison for both CHIKV and *rnaseP* is shown in Figure 39.

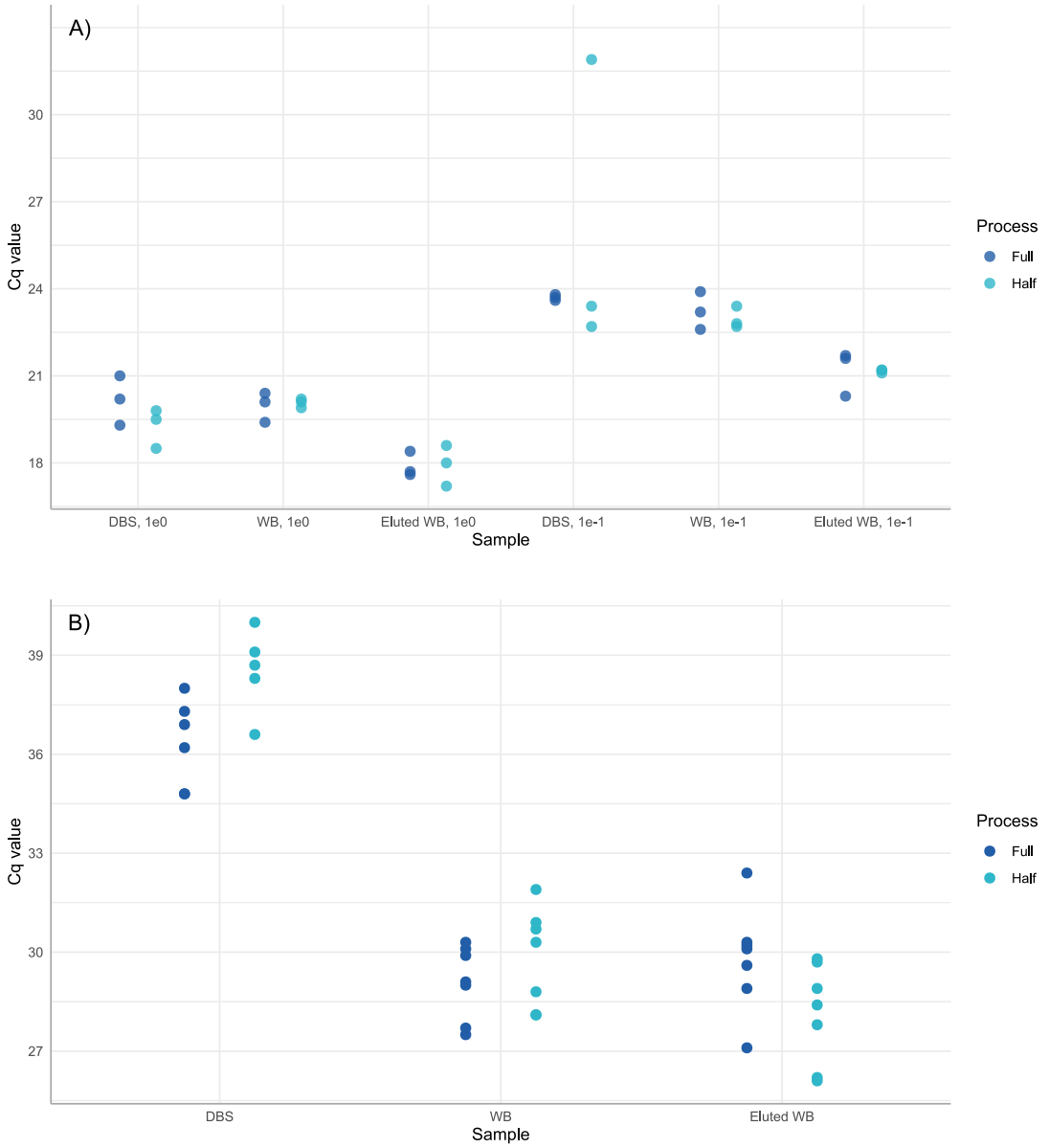

Figure 39: Cq values in the comparison between BD MAX™ full and half processes with DBS, whole blood (WB), and mock eluted whole blood (Eluted WB). A) shows the signals for the CHIKV target at different dilutions and B) shows the signal of the rnaseP target. rnaseP signal was not detected in three DBS samples and are omitted from this plot.

While performing the first of three runs to determine consistency between runs, the DBS samples already show inconsistency within the same run. Three out of six DBS replicates were not

detected and the test was halted with priority shifted to optimising the *rnaseP* real-time PCR assay for DBS as the *rnaseP* oligonucleotide condition used so far was based on the whole blood assay.

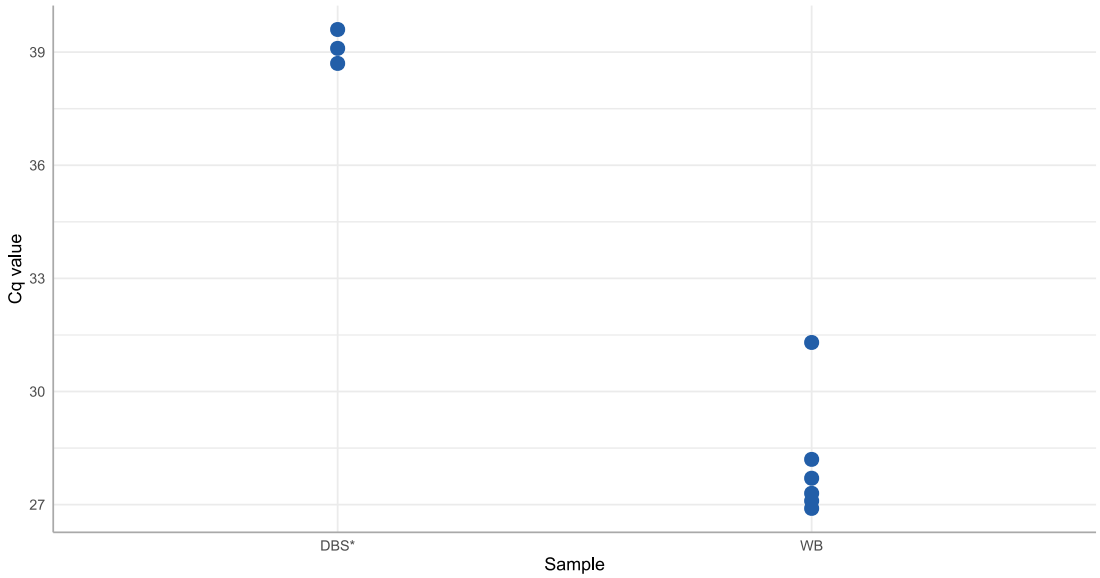

Figure 40: Testing the consistency of the DBS assay using both DBS and whole blood (WB) across six replicates. DBS samples were not detected in three replicates and are omitted from this plot.

Optimising the *rnaseP* oligonucleotides for DBS was mainly done by increasing the concentration of each oligonucleotide to be able to detect the lower concentration of DBS yield compared to whole blood. After varying the concentrations of the *rnaseP* oligonucleotides, the condition with the most consistency is 0.09 pmol/µL with a Cq value range of between 31.5 and 32.0. The 0.06 pmol/µL condition have a much more scattered range, with a replicate having a Cq value as high as 39.4. The range here is similar to the range of 5 µL whole blood controls, albeit the latter was not able to detect one of the replicates. The 0.114 pmol/µL expectedly has the lowest Cq, but one replicate was not able to be detected. The previously used condition of 0.03 pmol/µL was not able to detect any of the replicates (Figure 41).

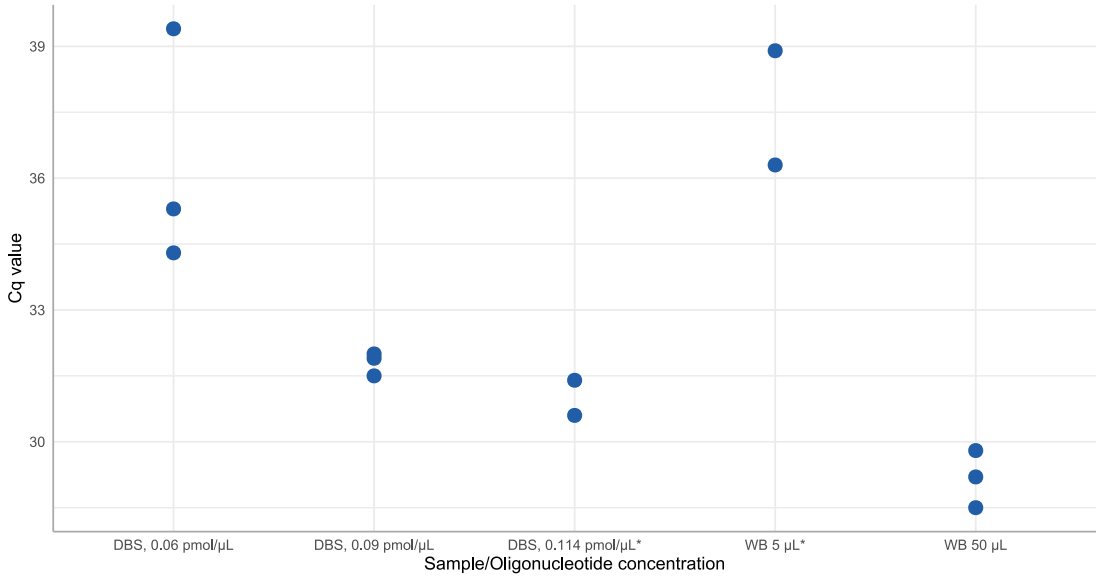

Figure 41: Cq values of rnaseP PCR from varying the concentrations of the oligonucleotides in DBS with whole blood (WB) as controls. *These conditions were not able to detect one of the thee replicates. Both whole blood samples used oligonucleotide concentrations of 0.06 pmol/µL.

The optimised concentration of 0.09 pmol/µL *rnaseP* oligonucleotides was used to determine the replicability for the assay over multiple days. Across the three days, Cq values of the DBS samples remain within 29.5 and 32.0. However, the whole blood samples show much higher variabilities, with the 5 µL whole blood having a Cq value range of between 25.0 to 38.9. One replicate on day one was also not able to be detected. The 50 µL whole blood samples, while having some variation, have a smaller range of Cq values of between 22.3 and 29.8 (Figure 42).

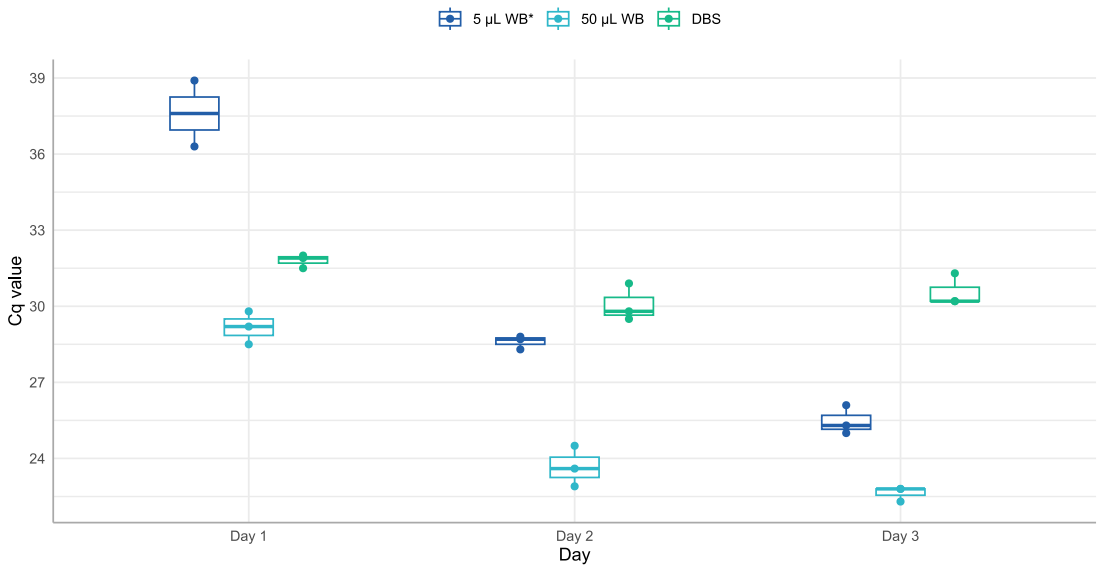

Figure 42: Cq values of testing consistency of the DBS assay on DBS and two different volumes, 5 and 50 µL, of whole blood (WB) across three days. Each sample was tested in triplicates in each day. *One 5 µL whole blood replicate was not detected on day 1.

5.2.3. Dried blood spot storage

rnaseP detection was performed on the DBS samples spiked with CHIKV and stored at different conditions to check for any differences between Cq values caused by samples storage condition. Samples constantly stored at freezing temperatures have roughly the same Cq values with averages of 28.26 and 30.49 for samples stored at -80°C and -20°C respectively. Samples stored at room temperature for 1 and 2 months show higher Cq values with averages of 31.99 and 32.63 respectively. This shows that *rnaseP* is stable at sub-zero conditions but not when exposed to ambient temperature. The loss of yield is also proportional to the duration the sample is left at room temperature. The amplification curves as well as the summaries of the different conditions are shown in Figure 43 and Table 34 respectively.

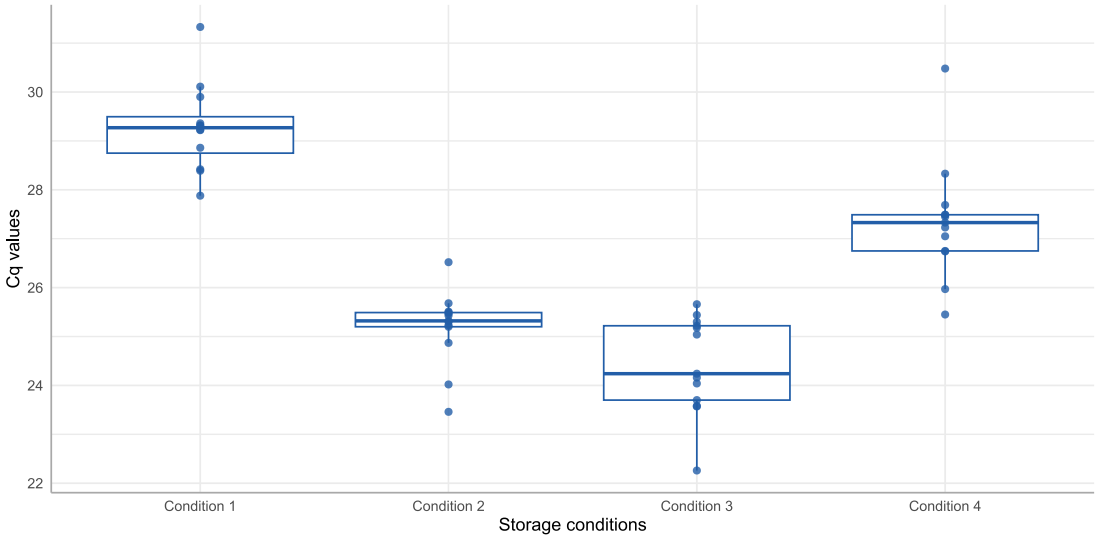

Figure 43: Cq values of the rnaseP target (Cy5) for the DBS samples stored at different conditions. Condition 1: two months at room temperature, condition 2: two months at -20°C, condition 3: two months at -80°C, condition 4: one month at room temperature and one month at -20°C. All samples were stored at -80°C after two months onwards.

Table 34: Summary of storage conditions of DBS samples.

Condition	Month 1	Month 2	Onwards
Condition 1	Room temperature		-80°C
Condition 2	-20°C		
Condition 3	-80°C		
Condition 4	Room temperature	-20°C	

For the CHIKV target, the only signals detected by the assay in the DBS samples were non-specific signals in the form of rising signals towards the end of the cycling program. This shows that the viral RNA in the DBS is susceptible to degradation as the spiked whole blood sample was able to be detected by the assay. The amplification curves are shown in Figure 44.

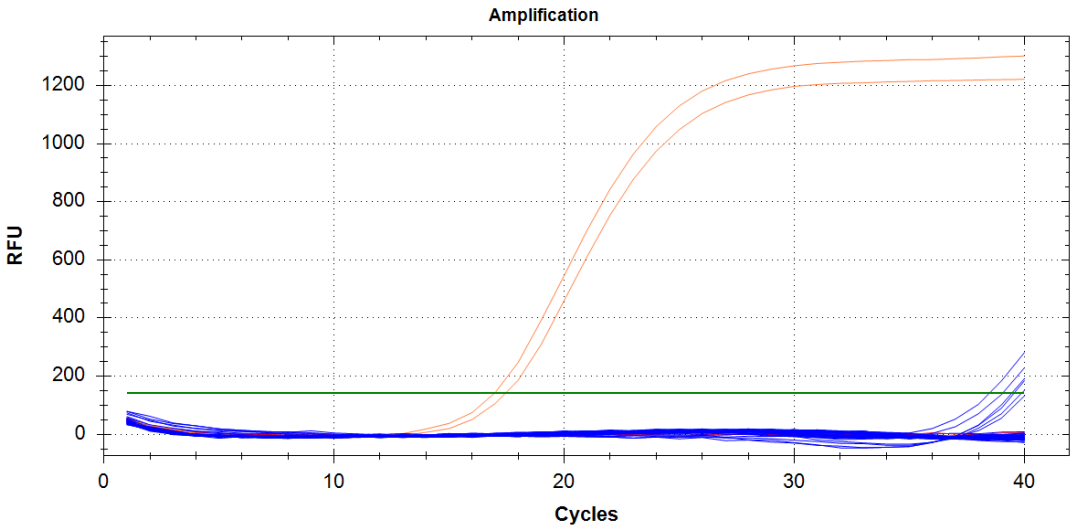

Figure 44: Amplification curves of CHIKV target (Cy5.5) in the DBS samples stored at different conditions shown in Table 34. All DBS samples are shown in blue and the spiked whole blood is shown in orange. The NTC is shown in red in both figures.

5.3. Discussion

5.3.1. Developed assay

In this chapter, an assay was developed for detecting viral pathogens in DBS specimens from elution to extraction and molecular detection using the automated BD MAX™ system. CHIKV was used as the target as proof-of-concept but the assay will be adapted for DENV, JEV, and ZIKV as well. Detection was done using real-time RT-PCR with the oligonucleotides developed in 0.

Much work was done on the elution process of the DBS because with the high number of specimens SEACTN has collected, the method used have to be relatively simple and fast. Most protocols for DBS elution requires the blood spots to be punched out into small discs no more than a centimetre in diameter (216). The method developed here used the entire blood spot not only to reduce the workload, but also to elute as much material from each DBS as possible. Note that this can be done as the assay will be used qualitatively. If the quantifying the pathogen is of interest such as in cases of paired samples, using punches will be preferred because it will consistently produce the same volume of sample whereas whole blood spots have varying volumes.

The final method of immersing entire blood spots in the BD MAX™ SBT buffer and shaking at 1,100 rpm for three hours at room temperature removes the need of an incubator and cuts down on time, as many protocols advise overnight incubation. The speed of the plate shaker was chosen as it is the maximum speed that can be used while the shaker is sat in the BSC as higher speeds cause the shaker to wander around and risk spilling the contents of the 12-well plates. Because elution was done in 12-well plates, the throughput limit is the number of plates that can be shaken at the same time. The buffer used is the SBT buffer from the BD MAX™ ExK™ TNA-2 which is used for the extraction and detection steps. While the buffer is proprietary and the composition is not available, it most likely stabilises the sample without lysis, as a separate lysis buffer is present in the BD MAX™ URS. This cuts down on cost and simplifies the process as there is no need to acquire and prepare another buffer specifically for the elution process. With the current setup in the lab, up to four plates (48 samples) can be shaken simultaneously. This correlates to one PCR run of the BD MAX™ instrument.

What makes this assay possible to be done automatically is the BD MAX™ Open-System. Many automated detection systems such as the BioFire® FilmArray® Torch only supply users with pre-made reagents for targets as selected by the manufacturer. The BD™ Open-System provide kits only containing necessary reagents for extraction and consumables for real-time PCR. This gives the versatility for users to apply their own oligonucleotides and enzymes. It is noteworthy that the ExK™ TNA-2 kits used in this assay is not specifically designed for DBS nor whole blood, rather it is designed for dry swabs and cerebrospinal fluid (CSF). The reason this kit was chosen is because BD does not produce any kit specific for whole blood. While there is a kit specific for plasma, serum, or urine (ExK™ DNA-1), it is specifically for DNA targets. The ExK™ TNA-2 has also been previously shown to be able to detect ZIKV in plasma samples (217).

The range of Cq values across different storage temperatures shows the stability of DBS as a sample collection method. DNA is shown to be more difficult to detect when stored at room temperature unlike at freezing temperature, regardless of whether it is stored at -80°C or -20°C. This could be due to degradation or issues with recovery of the DNA from filter paper. This means that sites aiming to collect DBS for DNA detection should prepare -20°C freezers to store the

samples and minimise the time each sample spends at room temperature. This could possibly be exacerbated in tropical regions where ambient temperature exceeds 30°C.

The lack of RNA detection could be due to degradation in two places: storage and elution. In the former case, storage of RNA on DBS will lead to degradation regardless of the temperature. This is unlikely as in a study on HIV, viral RNA in DBS has been shown to be stable at both room temperature and -70°C for an extended period of time (149). In this study, DBS was eluted in 9 mL of lysis buffer for 2 hours at room temperature, as opposed to this study, in which the SBT buffer is a sample preservation buffer rather than a lysis buffer. This would support that the RNA was degraded during the elution process as many commercial lysis buffers would include chemicals such as guanidium thiocyanate to inhibit nucleases by denaturation. This is critical for blood samples as blood and its components contain high concentrations of RNases. RNases are also very stable, being able to retains enzymatic activity after freeze-drying, with the rate of RNase degradation proportional to level of moisture in the sample. The higher the moisture, the higher degradation rate (218).

There are more experiments that were not able to be done in the time of this thesis to further assess the conditions necessary for detecting RNA in DBS samples. Experiments are planned to assess the rate of viral RNA degradation from RNases in DBS by adding virus culture directly into the 12-well plate during DBS elution to remove desiccation as a factor. Using a dedicated TNA extraction instrument such as the Roche MagNA Pure 24 in tandem with conventional real-time PCR is also being considered. This would improve the extraction capabilities as the MagNA Pure 24 allows for adjustments of many parameters such as sample and eluate volumes and would increase the throughput as conventional PCR in a 96-well plate significantly increases the number of reactions that can be done per run. However, this would increase the workload in the overall assay as there would be three separate process to perform (elution, extraction, PCR) as opposed to two with the BD MAX™ instrument (elution, automatic extraction and PCR).

5.3.2. Limitations

The main limitation of this assay is the throughput. With the protocol developed, only 48 samples can be eluted simultaneously over 3 hours. While a larger plate shaker can increase the number of samples that can be eluted, the BD MAX™ instrument is still limited to 24 samples per extraction run. A feature that speeds this up is that the BD MAX™ can be opened after a batch of extraction is completed to start the next batch while the samples from the first is moved into PCR reactions.

Using DBS reduces the sensitivity of the assay compared to whole blood specimens, as can be seen in the Cq values between the two types of specimens. Whole blood samples consistently produce Cq values roughly ten cycles less than those of the DBS. This loss is most likely due to the storage temperature of DBS. This is exacerbated in RNA samples as RNA is much less stable than DNA. A Previous study has shown RNA degraded much more quickly than DNA when stored in DBS for a long period of time (219). If compared to conventional real-time PCR assays, the volume of blood used in DBS is also significantly less. This can pose a problem this this assay is to be adapted for pathogens with lower concentrations in blood.

While running the assay is relatively simple, preparing the reagents for the run required a more experienced laboratory technician and is very time consuming. First the PCR premix containing the primers, probes, and enzyme had to be prepared and aliquoted into the BD MAX™ conical tubes which are then sealed. On a large scale, this process can take multiple technicians multiple hours to complete. A potential solution that is being considered is to send the conical tubes to the oligonucleotides' manufacturer to synthesise lyophilised oligonucleotides inside the tubes. This way, a lyophilised primers and probes protocol could be used in the BD MAX™ instrument and the only required preparation would be to aliquot and seal the enzymes.

As stated above, the ExK™ TNA-2 kits used in this assay are not designed for DBS nor any blood-related specimens. While the real-time PCR uses an in-house assay, the extraction step is entirely dependent on the kits. This can potentially cause the extraction to not be as efficient compared to a blood-specific extraction protocol. Because of this, the protocols developed here

do have to be strictly adhered to for the best results. For example, it is critical that the samples are adequately vortexed in the SBTs before being loaded onto the racks as the instrument does not use all of the volume in the SBTs. Having the most homogeneous sample mixture ensures the maximum amount of sample is used for extraction.

5.3.3. Conclusion

The assay developed here is aimed to detect bloodborne viruses from DBS samples using the automated BD MAX™ instrument. Much work was done on elution of the DBS using plasmids containing the CHIKV amplicon. As a consequence, the developed protocol is much more suited to DNA targets rather than RNA targets. The stability of DNA on DBS is also demonstrated here, with the difficulty of detection increasing with the amount of time spent at room temperature, exacerbated by the higher-than-average room temperature in the tropics compared to the rest of the world.

More work is being done to elute viral RNA using whole blood spiked with viral culture. The assay is also being developed for the remaining targets: DENV, JEV, and ZIKV. The fully developed assay will be used to detect these pathogens in patient DBS in WP-A of SEACTN. DBS are economical options for collecting and processing patient specimens albeit with the trade-off of lower sensitivity compared to assays using whole blood. The ability of the BD MAX™ Open-System to accept in-house real-time PCR assays gives the potential to substitute the targets with other pathogens and for the assay to be adapted for use in other regions of the world.

CHAPTER 6

Validation of the CHEMBIO DPP® Fever Panel II Asia antigen and IgM antibody systems

The DPP® Fever Panel II Asia systems are potentially powerful tests for a POC setting. It includes 9 targets, blood borne bacteria and viruses, across two tests, antigen and IgM antibody. This chapter describes testing the DPP® Fever Panel II Asia antigen and IgM antibody systems in the laboratory and in the field with the aim of validating the assays as well as determining the appropriate threshold value for each target. By using it in the field, the usability can also be assessed in a POC setting.

6.1. Methods

The DPP® Fever Panel II Asia systems were evaluated first using previously collected EDTA whole blood stored at -80°C in a laboratory setting then with fresh capillary blood in a POC setting. This allows for assessing the effect of EDTA and freezing on the performance of the Fever Panel II systems.

6.1.1. Reference tests

The real-time RT-PCR assay developed in Chapter 3 was used as the reference test. EDTA Whole blood samples from patients were collected as part of SEACTN's WP-B. Extraction was done with the Roche MagNA Pure instrument (Chapter 2.3.1) and real-time PCR was done on the Bio-Rad CFX Opus Real-Time PCR System (Chapter 2.2.1).

6.1.2. Data analysis

Statistical analysis was done in the R programming language (R 4.2.3). The `pROC` and `ggplot2` packages were used to create the ROC curve, as well as to calculate the AUC (220). The `caret` package was also used to create the confusion matrix and determine the sensitivity and specificity of the assay (221). The Youden Index was calculated for each potential threshold value from receiver operating characteristic (ROC) curve analysis as detailed in Chapter 1.3.5. The threshold value with the maximum Youden index was chosen as the optimal value.

6.2. Results

6.2.1. Laboratory-based testing of the Chembio DPP® Fever Panel II Asia systems

Laboratory testing with the DPP® Fever Panel II Asia systems was performed on 216 venous EDTA whole blood specimens. Using previously collected whole blood stored at -80°C for no longer than one year proved to be very problematic, especially for the antigen panel. For many samples, once blood was dropped onto the cassettes, it was not able to get absorbed through the membranes. As a result, blood pooled in well 2 of these cassettes and the test was not able to be completed. In most of the cassettes that were able to absorb the blood, the LFT strips were coloured red due to haemolysis which made discerning the bands visually difficult.

Only 71 samples could be successfully tested on the antigen panel, so the decision was made to use the already commercially available DPP® ZCD IgM/IgG system to test the remaining 168 samples as a reference test. Interestingly, neither the IgM antibody panel nor the ZCD IgM/IgG system suffered from clotting or the red colour. Figure 45 shows example pictures of invalid antigen cassettes alongside a valid IgM antibody cassette.

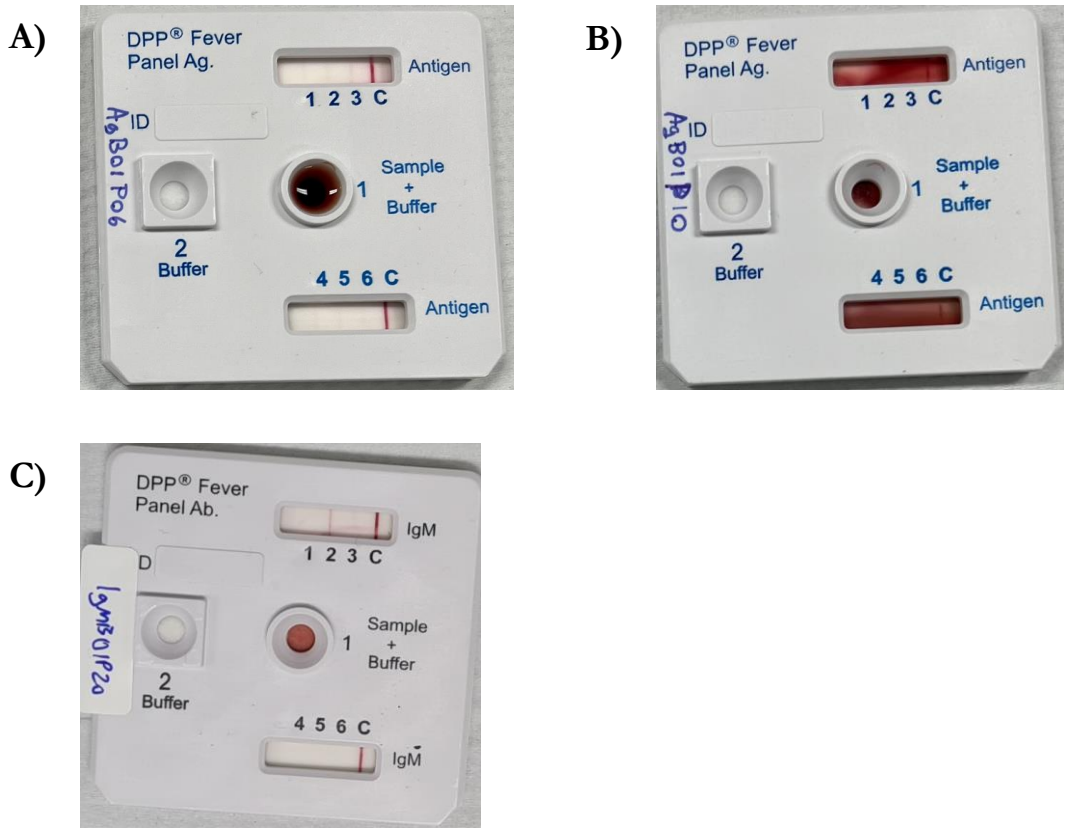

Figure 45: DPP® Fever Panel II Asia System cassettes. A) Invalid antigen cassette due to blood pooling in the sample well. B) Invalid antigen cassette due to haemolysis which caused the LFT strips to turn red. C) Example of a valid strip (IgM antibody cassette).

A control experiment was performed using healthy whole blood to assess whether freezing whole blood caused the clogging issue. Collected whole blood, even after freezing and thawing, did not have the same clotting effect as the patient specimens pointing to the importance of blood collection technique and thorough mixing of blood with EDTA.

Because of the blood clogging issue, data for the antigen panel contains much fewer results than the IgM antibody panel. Out of the samples that were successfully tested on the antigen panel, the background signal of each target seems to be high or has a very broad range, particularly in the

CHIKV, DENV, and pan-*Plasmodium* target. Only one sample showed a significantly higher signal than the other in the CHIKV target with a signal of 69. Figure 46A shows the results of the DPP® Fever Panel II Asia antigen panel for the 71 successful samples.

The DPP® Fever Panel II Asia IgM antibody system overall has much higher signals than any antigen system as read on the DPP® Micro Reader 2 (Figure 46B). Multiple samples show significantly high signals with the highest in ZIKV (245), followed by two in DENV (158, 132), and one in CHIKV (121) that could perhaps be counted as positive results. Similar to the antigen panel, many targets have very wide ranges of background signal, especially leptospirosis which has a range of between 1 and 101. The *O. tsutsugamushi* and *R. typhi* targets however have generally very low and consistent signals.

The ZCD IgM/IgG panel shows samples with high signals in both antigen and IgM assays (Figure 46C and D). It is noteworthy that by the time testing was done, the ZCD kits are approximately three months expired, which could have lowered the intensity of the signals but was done as these are the only kits immediately available. The IgM tests detected one sample with a high ZIKV signal (150) and one with a high CHIKV signal (86). The IgG test detected one sample with a high DENV signal (53). The ZCD panels have narrower and lower background signals compared to either of the Fever Panel II Asia systems.

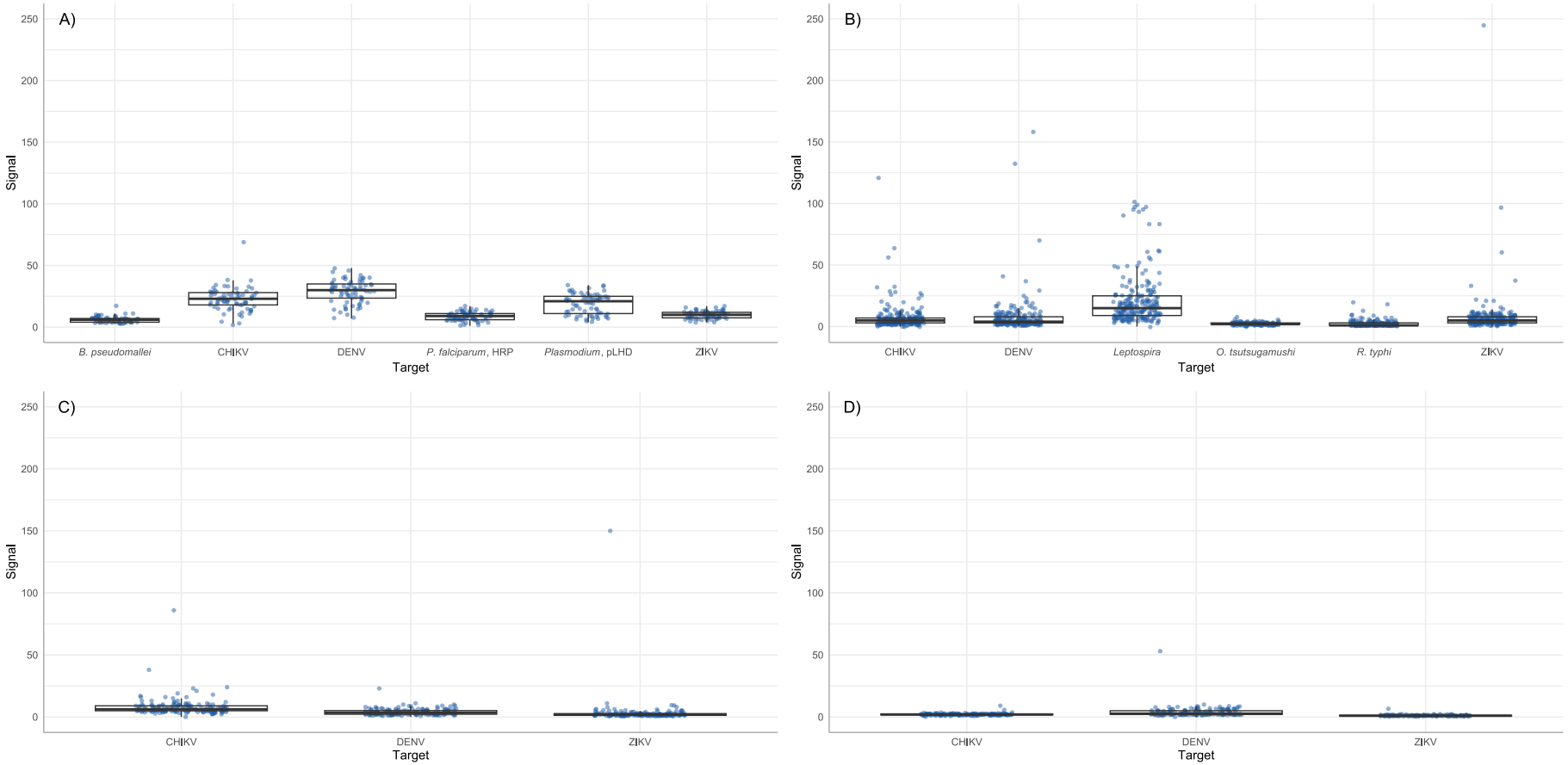

Figure 46: Signals from the DPP® Fever Panel II Asia A) antigen and B) IgM antibody panels as well as the DPP® ZCD C) IgM and D) IgG panel from laboratory testing.

The real-time PCR data did not correlate with the Fever Panel II Asia antigen panel data. This could be due to the difference in sensitivities between real-time PCR and the DPP® antigen panel. Of the 71 samples tested, the only sample with a positive PCR test is for *R. typhi* which is not a target on the antigen cassette. None of the samples with high values in the IgM panel tested positive on PCR in the respective targets.

Figure 47 shows a scatterplot comparing the signals from the CHIKV, DENV, and ZIKV targets of the IgM antibody detection between the Fever Panel II Asia system and the ZCD panel. In the CHIKV and ZIKV targets, one sample shows high signal in both systems. In the DENV target however, the high signals, up to 150, are only found in the Fever Panel II Asia system with a maximum signal on the ZCD panel of 23 (R2 = 0.1882).

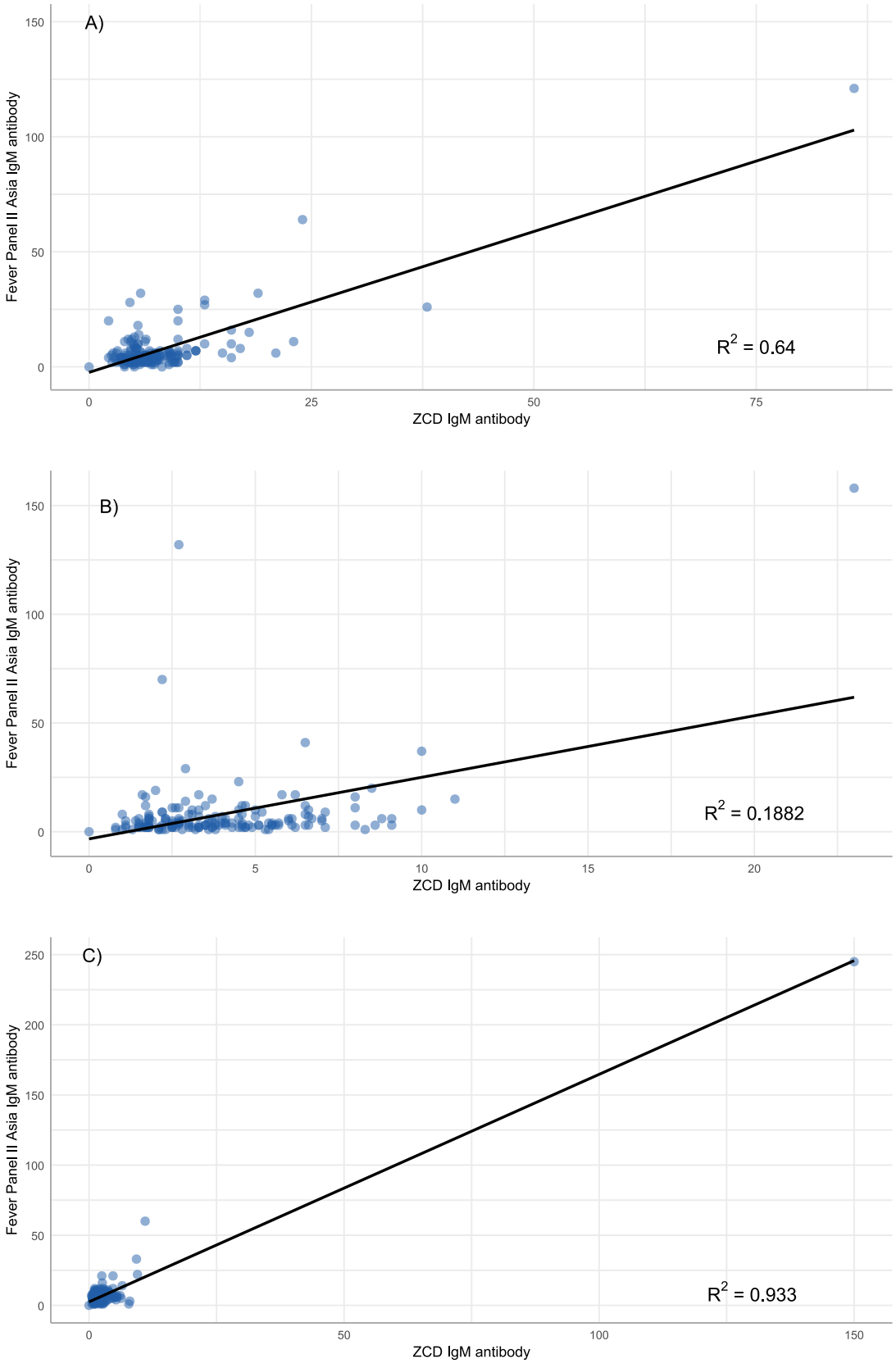

Figure 47: Comparison between the signal intensities of the IgM tests of the Fever Panel II and the ZCD Panel. A) CHIKV B) DENV C) ZIKV. Note the difference in axis scales in different plots. The DENV target generally has very low signal in the ZCD antibody panel with the highest at 23 compared to 86 and 150 in the CHIKV and ZIKV target.

6.2.2. Field testing of the Chembio DPP® Fever Panel II Asia systems

The DPP® Fever Panel II Asia systems were tested on 534 patients across the two sites: 269 in Mae Chan Hospital and 265 in Mae Suai Hospital with 30 samples discarded as a digital data entry was not present (12 from Mae Chan Hospital and 18 from Mae Suai Hospital). Using capillary blood resulted in no clotting in either of the Fever Panel II cassettes. By following the protocol provided, no other issue was reported and the research nurses all filled in the booklets as instructed, and reported the data online.

The results of the antigen and IgM panels are shown in Figure 48. The signals of samples from field testing have much broader ranges than those from laboratory testing, specifically in the DENV targets of both panels with a range of between 4 and 271 in the antigen panel and between 0 and 322 in the IgM antibody panel. The targets here also do not separate into clear populations, instead showing a wide range which makes calling positives difficult although some targets contain a small number of samples with extreme outliers. These are the *B. pseudomallei* and ZIKV targets in the antigen panel and the *O. tsutsugamushi* and ZIKV targets in the IgM antibody panel. The background signals of the DENV and leptospirosis targets also seem relatively wide, the latter of which was also observed in the laboratory test as described earlier.

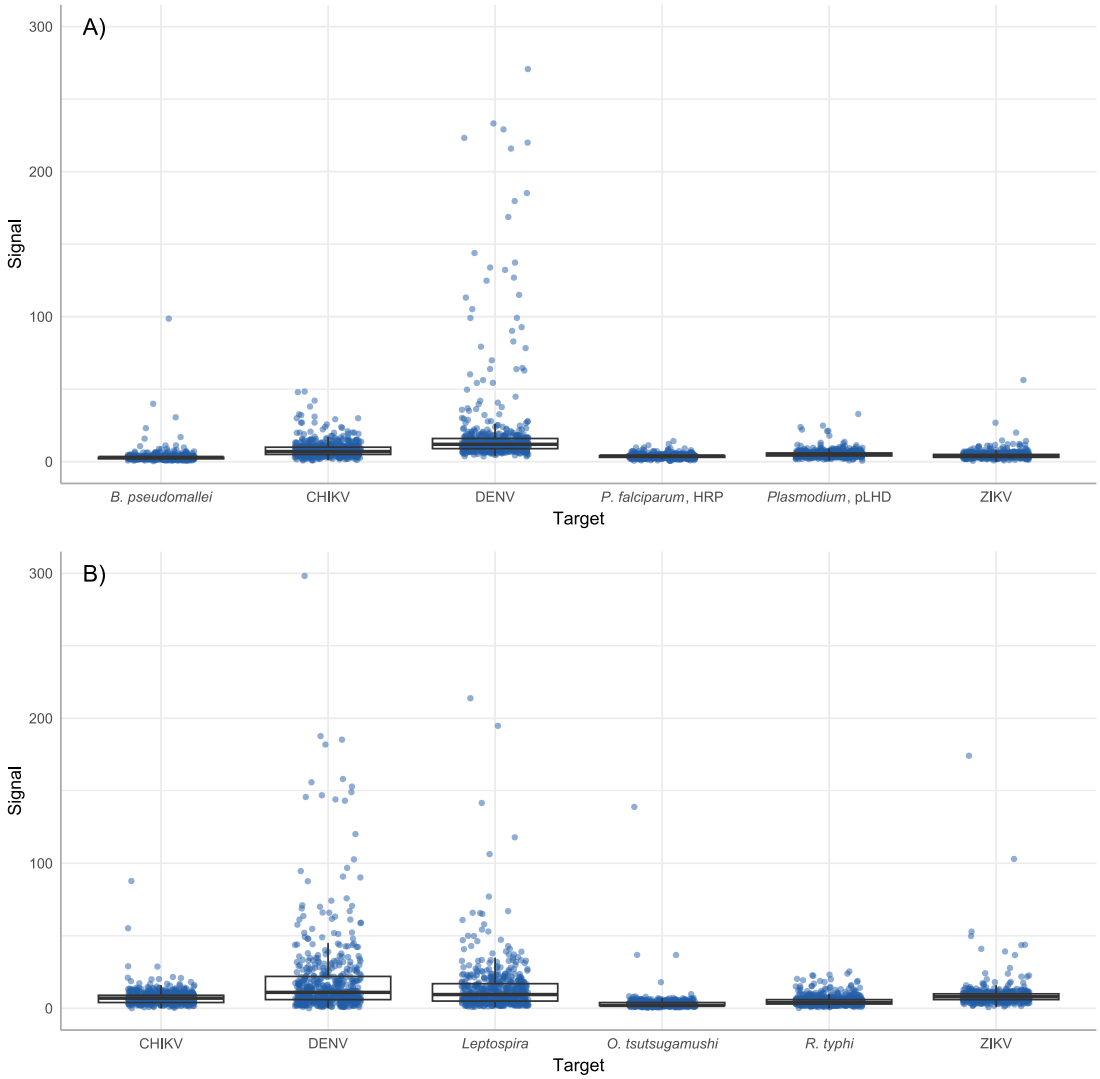

Figure 48: Signals from the DPP® Fever Panel II Asia A) antigen and B) IgM antibody systems from patients in Chiang Rai.

Looking at the real-time PCR results, out of 534 samples, there are 26 DENV positives, 13 *O. tsutsugamushi* positives, 1 *R. typhi* positive, and 1 *Leptospira* spp. positive. Comparing the DENV target in the antigen and IgM antibody panels against real-time PCR, the former shows some correlation as the samples with the highest signals are all PCR positive. The opposite is seen in the IgM antibody panel as PCR-positive samples have relatively low signals (Figure 49).

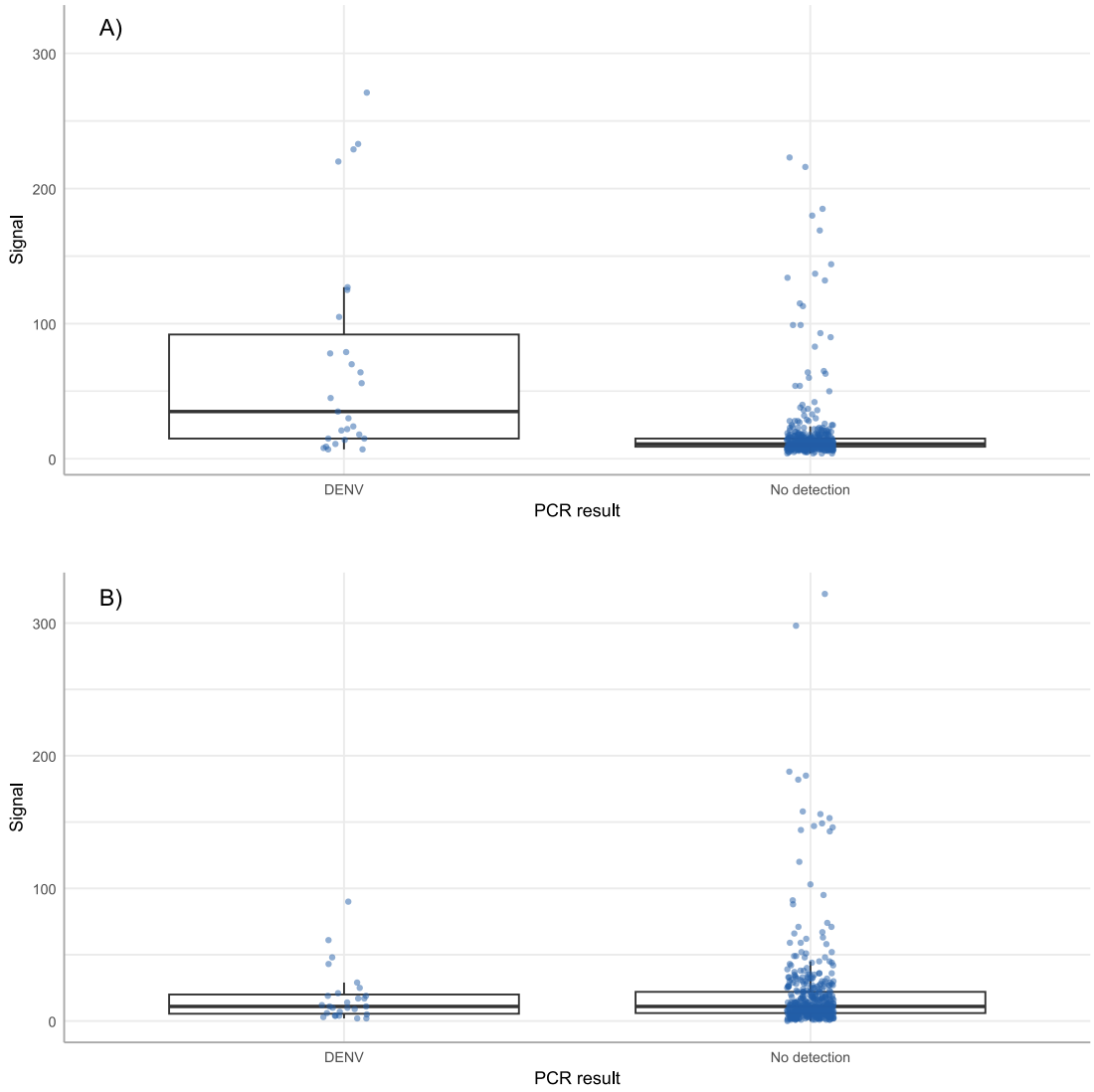

Figure 49: Distribution of signal intensities in the DPP® Fever Panel II Asia A) antigen and B) IgM antibody systems against real-time PCR for DENV.

The PCR-positive *R. typhi* and *Leptospira* spp. samples, both correspond to relatively low signals in the DPP® panels with signals of 23 and 5 respectively. The bacterial loads of these samples are quite low as their Cq values are very high, with the *R. typhi*-positive sample at 41.9 and the leptospirosis-positive sample at 36.3.

Comparing between the Fever Panel II Asia antigen panel and real-time PCR for the DENV target, all samples with signals of more than 150 are PCR positives although many samples with low signals are also shown to be PCR positive, giving the wide range of signals with a mean

of 76.92. The DENV PCR negative samples had a lower and narrower spread although there are three samples with quite high signals at 144, 99, and 65. In comparing the Fever Panel II Asia IgM antibody system with PCR, little correlation is seen. Most samples with high IgM antibody panel signal are PCR negative. Figure 49 shows the distribution of signals of the DENV targets in the antigen and IgM antibody panels as separated by the real-time PCR results.

Figure 50 shows the ROC curve and area under curve of DENV detection in the antigen panel using real-time RT-PCR as the reference test. The area under curve was determined to be 0.7909 and the optimal threshold value, calculated using the Youden Index, is 20.5. This would give the assay a sensitivity of 24.32% and a specificity of 97.55%.

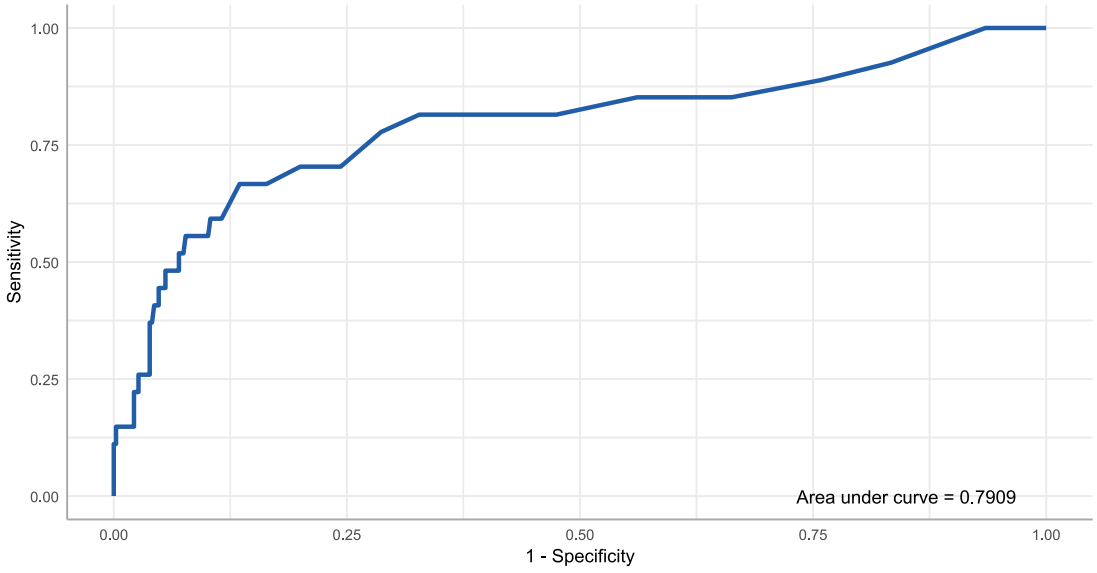

Figure 50: The ROC curve of the DENV target in the DPP® Fever Panel II Asia antigen system compared to DENV real-time RT-PCR.

Using the calculated threshold, a comparison could be made between the Fever Panel II Asia antigen system and the DENV RT-PCR as given in Table 35. Using the threshold calculated with the Youden Index, there are 18 true positives, 9 false positives, and 56 false negatives.

Table 35: Confusion matrix of the DENV target of the DPP® Fever Panel II Asia antigen system against the PCR results using threshold value as calculated from the Youden Index.

		PCR results	
		Positive	**Negative**
Antigen panel	**Positive**	18 (4.1%)	9 (2.0%)
	Negative	56 (12.7%)	359 (81.2%)

Comparing between the real-time PCR Cq values against the signal in the DENV target of the Fever Panel II Asia antigen system, samples with high signal in the antigen panel all have low Cq values (28.0, 23.3, 28.6, and 28.0). However, the majority of PCR positive samples have low signal in the antigen panel, many with low Cq values (R^2 = 0.06891).

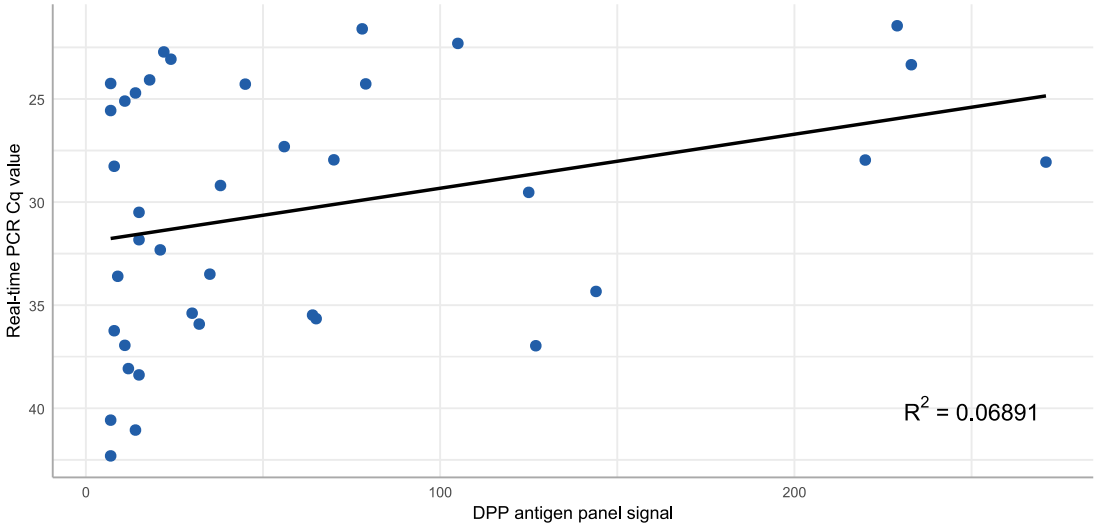

Figure 51: Comparison between the Cq values DENV PCR positive samples against the signal in the DENV signal in the DPP® Fever panel II Asia antigen panel.

For the *O. tsutsugamushi* target, the distribution between the PCR-positive and negative samples is similarly narrow (Figure 52). The highest signal is found in the PCR positive sample, with a signal of 139 and a PCR Cq value of 34.3. The samples with high signals in the IgM panel (37, 37, and 18) are all PCR negatives.

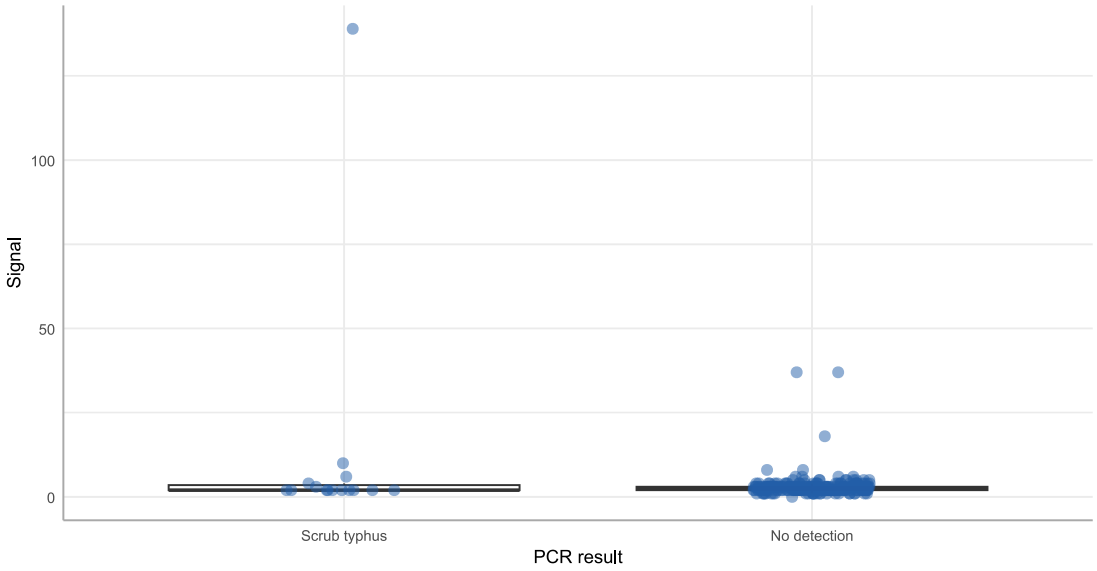

Figure 52: Distribution of signals in the DPP® Fever Panel II Asia IgM antibody panel against real-time PCR for scrub typhus.

To assess cross-reactivity, correlation matrices were created to compare each target of the two panels (Figure 53). As is the case for many POC tests, there was a cross-reaction between the two flavivirus targets in the IgM antibody panel. Interestingly, there was an unexpected cross-reaction between *O. tsutsugamushi* and CHIKV in the IgM antibody panel. There are also cross-reactions between the pan-*Plasmodium* and both the DENV and CHIKV targets in the antigen panel. It is possible that the patients do have co-infections rather than a cross-reaction of the Fever Panel II Asia systems.

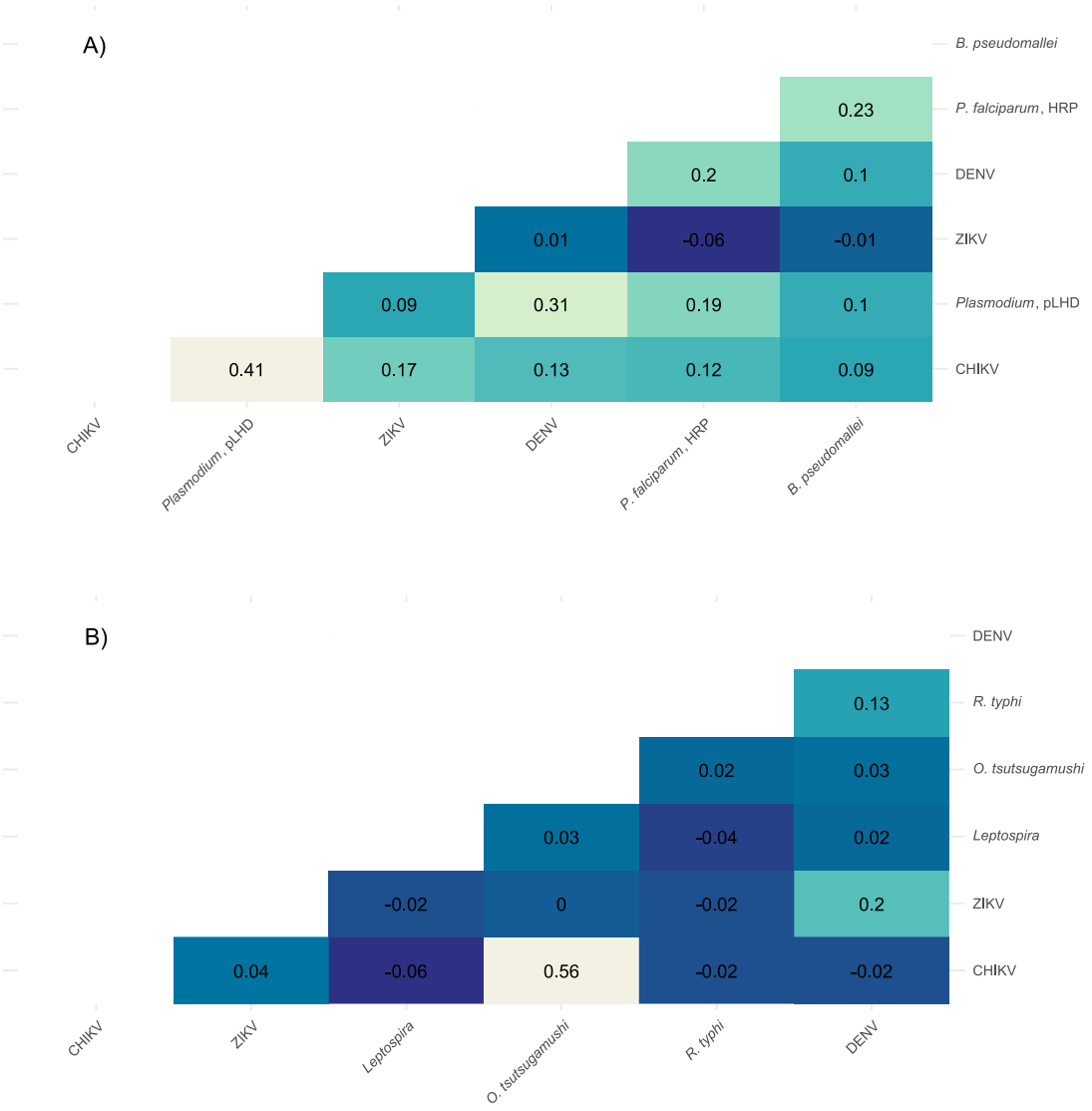

Figure 53: Heatmaps showing the cross-reactivities between each target of the DPP® Fever Panel II Asia A) antigen and B) IgM antibody systems.

A previous study on the DPP® Fever Panel II Asia systems determined threshold values for the targets that gives specificities of at least 95% (142). Using these thresholds, significantly more samples are called positives with every target across the two panels containing positives. Table 36 and Figure 54 shows the threshold used as well as the positive and negative counts.

Table 36: Thresholds as reported by Amornchai et.al. and the positive and negative counts for the DPP® Fever Panel II Asia systems (142).

Test	Target	Threshold	Positives
Antigen	CHIKV	≥12	93/534 (17.4%)
	Plasmodium pLDH	≥19	6/534 (1.1%)
	DENV	≥22	70/534 (13.1%)
	ZIKV	≥11	15/534 (2.8%)
	P. falciparum HRPII	≥9	8/534 (1.5%)
	B. pseudomallei	≥8	15/534 (2.8%)
IgM Antibody	CHIKV	≥21	7/534 (1.3%)
	ZIKV	≥18	19/534 (3.5%)
	Leptospira spp.	≥36	28/534 (5.2%)
	O. tsutsugamushi	≥7	18/534 (3.4%)
	R. typhi	≥10	55/534 (10.3%)
	DENV	≥56	37/534 (6.9%)

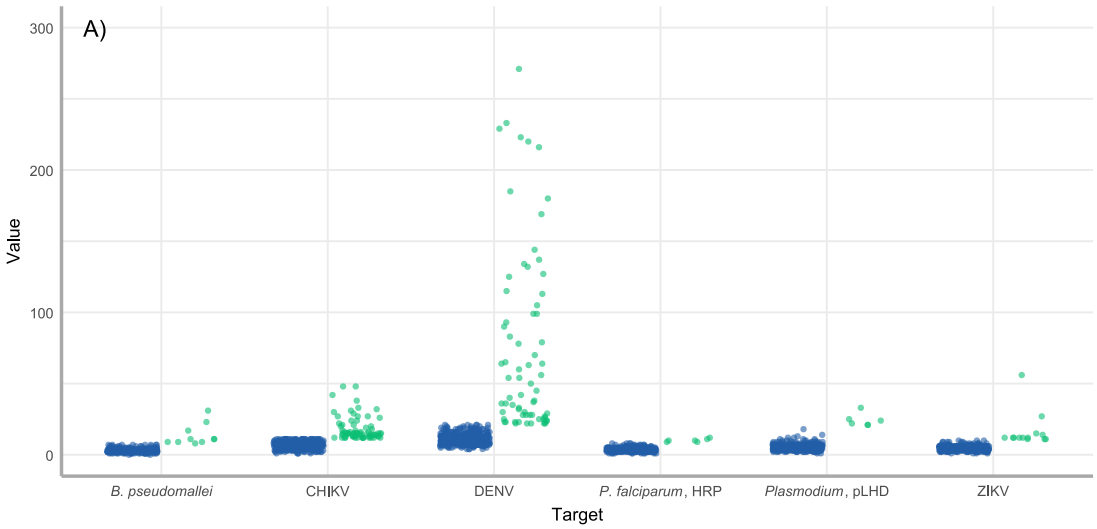

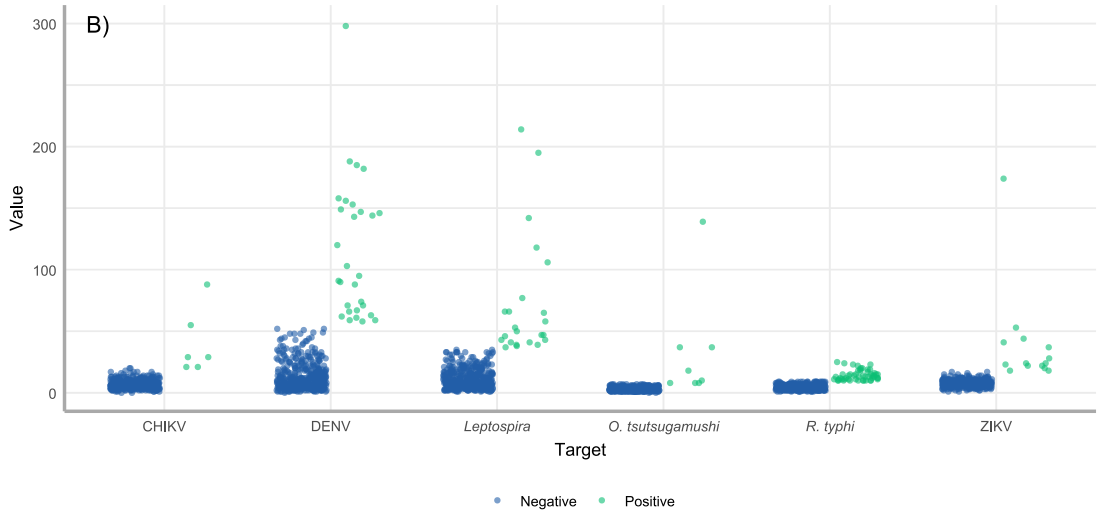

Figure 54: Signals from the DPP® Fever Panel II Asia A) antigen and B) IgM antibody systems with positives as called by thresholds previously reported by Amornchai et al. (142).

Comparing the DENV positives using this threshold from the antigen panel with this threshold against the DENV PCR positive samples, the assay has 11 false positive samples and 48 false negative samples (Table 37). This gives the assay a sensitivity and a specificity of 25.0% and 97.09% respectively.

Table 37: Confusion matrix of the DENV target of the DPP® Fever Panel II Asia antigen system against the PCR results using threshold value as reported by Amornchai et al. (142).

		PCR results	
		Positive	**Negative**
Antigen panel	**Positive**	16 (3.6%)	11 (2.5%)
	Negative	48 (10.9%)	367 (83.0%)

As part of SEACTN, information on the number of days since illness onset at the time of sample collection is recorded. Mapping this data against the signal intensities of each of the targets on the DPP® Fever Panel II Asia system shows several patterns as shown in Figure 55 and Figure 56. Samples with the highest signal intensities in the IgM antibody panel are collected from patients

after 6 - 7 days since the onset of the illness. On the antigen panel, high signal intensities can be observed from sample collected as early as 2 days after the onset of illness but wanes after day 6 as seen in Figure 55.

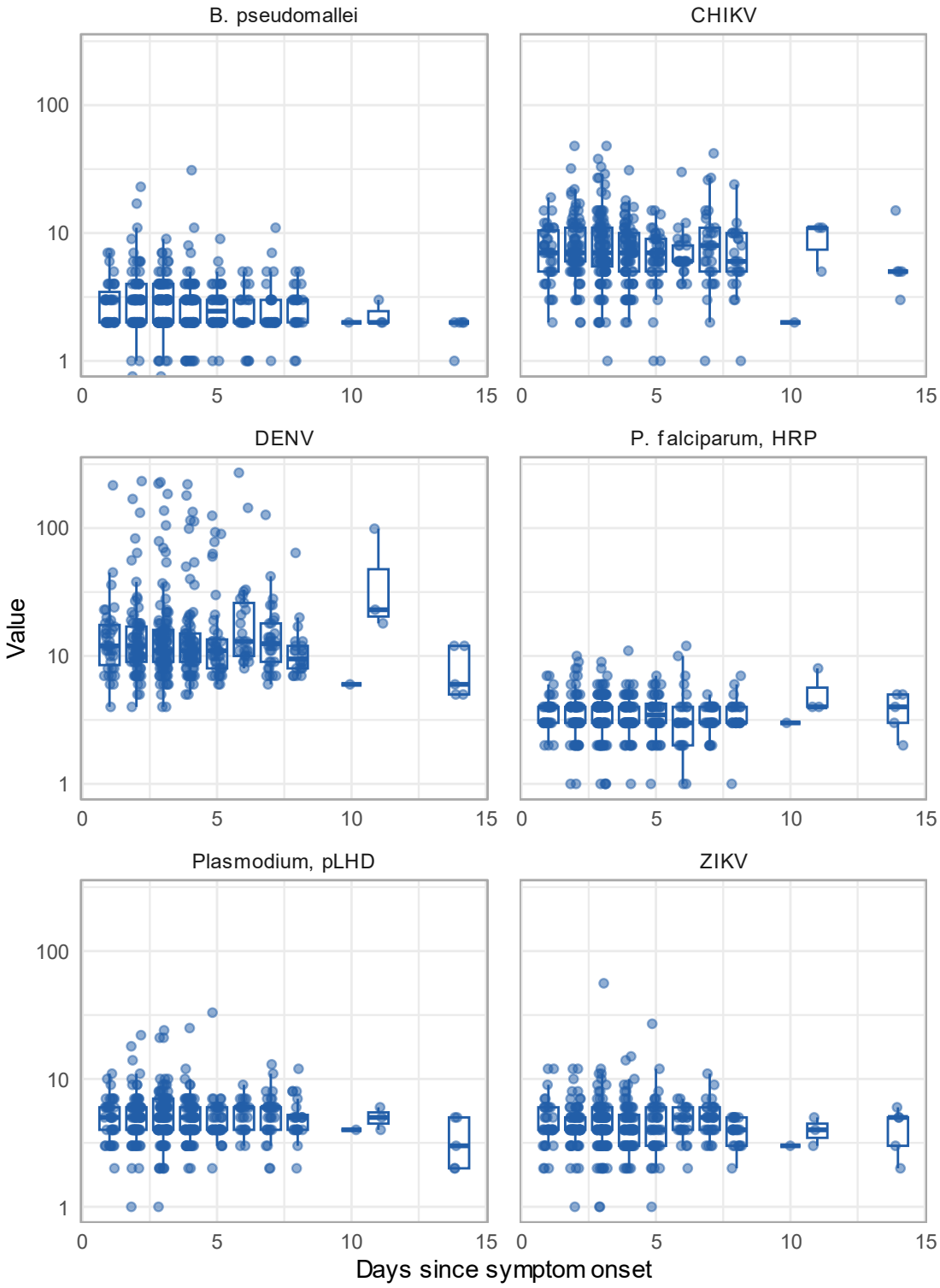

Figure 55: Signal intensities of each target of the DPP® Fever Panel II Asia antigen system with respect to the duration of illness.

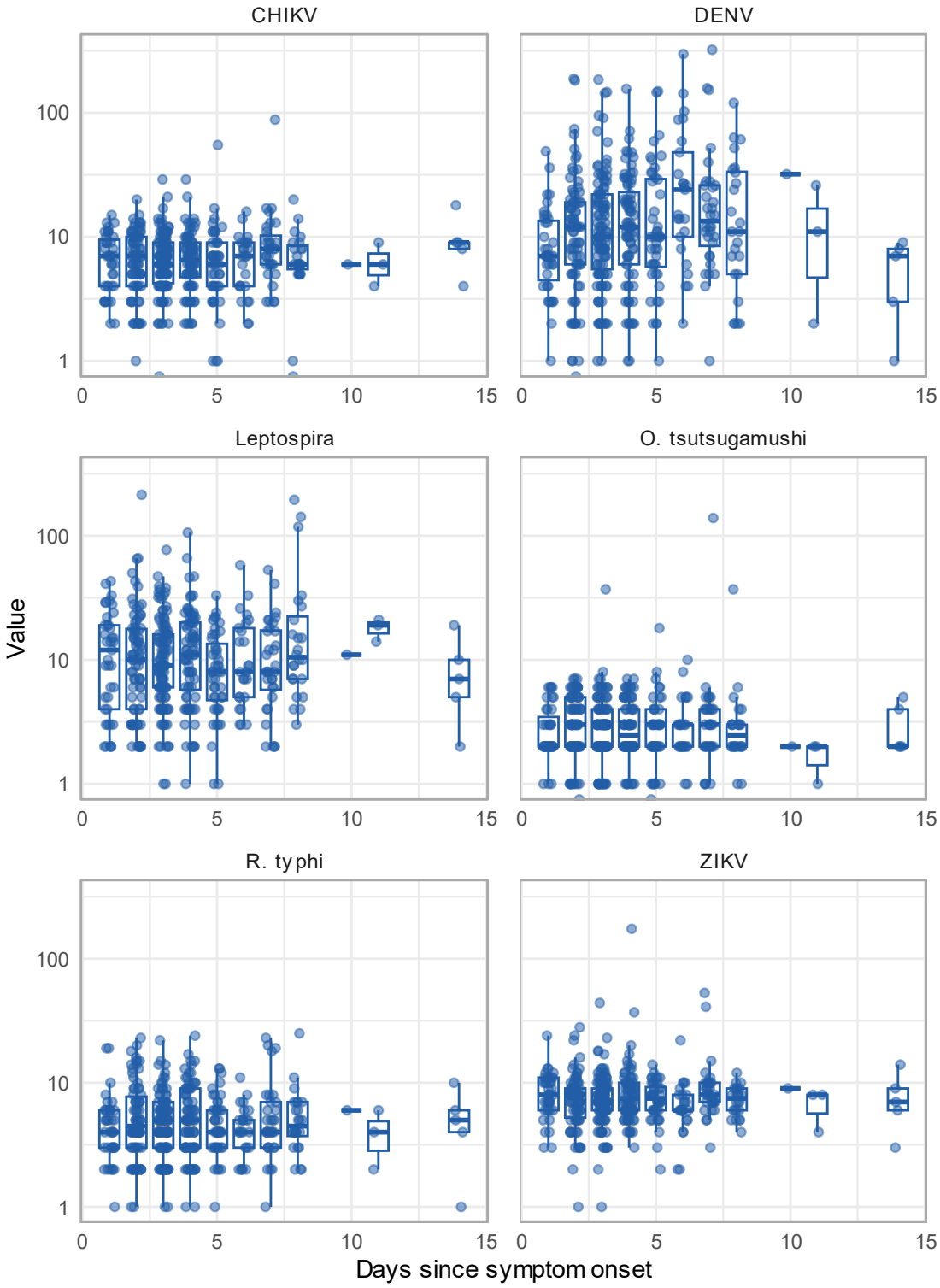

Figure 56: Signal intensities of each target of the DPP® Fever Panel II Asia IgM antibody system with respect to the duration of illness.

A similar trend can be seen in the DENV PCR-positive samples in which most positive samples are found on days 3 and 4 after symptom onset as shown in Figure 57.

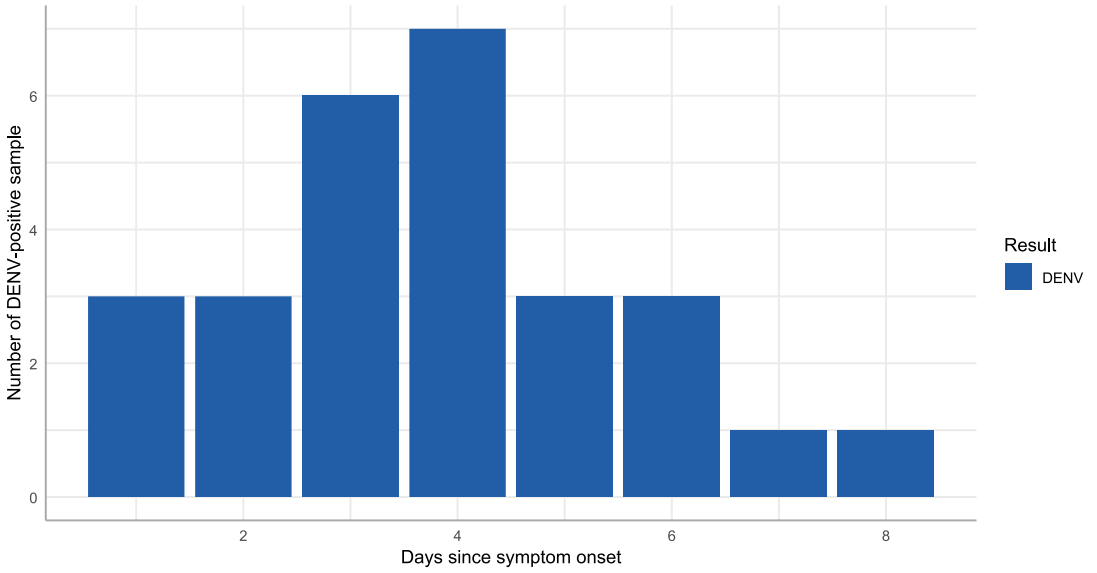

Figure 57: Number of DENV-positive samples (count) as detected by PCR from each duration of illness.

6.3. Discussion

6.3.1. Performance of the Chembio DPP® Fever Panel II Asia systems

The DPP® Fever Panel II Asia system is potentially a very powerful POC test. With the inclusion of the viral targets, DENV, CHIKV, and ZIKV in both the antigen and IgM panels, the window of time for diagnosis is able to be widened. In primary infections antigen detection is most accurate when done within the first 5 days of symptom onset while the IgM level typically rises 5 to 7 days after symptom onset (222). Having both targets also has the potential to differentiate between primary and secondary infections of as IgM levels can persist in patients for many months after infection so that simultaneously high signal intensities in both antigen and IgM antibody panels early on after onset of symptoms could be indicative of a previous but recent infection. Furthermore, IgM levels are typically much lower in secondary infections compared to primary infections (223). Previous studies have established that the performance of the Fever Panel II Asia systems is comparable to the RDTs for each respective target (142, 143). The main advantage of the Fever Panel II Asia systems over the other RDTs is that they can perform the diagnosis of multiple diseases simultaneously using low-volume samples in the same cassette. However, the studies mentioned above were performed in a laboratory setting with previously collected whole

blood or serum samples. Here, the DPP® Fever Panel II Asia systems were tested from collected patient EDTA whole blood as well as capillary blood collected from patients on-site.

Using the panels with previously collected EDTA whole blood samples proved to be difficult for a number of reasons. Most prominently, the filter on the lateral flow test strips inside the DPP® cassettes is very sensitive to blood clot. Samples that were improperly collected, such as insufficient mixing of whole blood and EDTA after venepuncture, can cause the anticoagulant to not fully dissolve in the whole blood, allowing for clots. In the WHO Guideline for Drawing Blood (2010), it is recommended to invert tubes with additives such as EDTA a certain number of times as required before dispatching the sample (224). The samples collected from Bangladesh that were used for laboratory testing were suspected to clog the DPP® cassettes due to insufficient mixing with EDTA. Not only does this invalidates the test, but it also poses a safety hazard. This was supported by our own test of preparing EDTA whole blood and ensuring proper mixing (20 inversions) before freezing which did not cause any clots. It is noteworthy that the clogging was only observed in the antigen cassettes, and not in either the Fever Panel II Asia IgM antibody system or the ZCD system. This is most likely due to the inclusion of a pre-dilution step in the antibody panels that is absent in the antigen panel. Another issue with frozen blood is haemolysis. In many samples, the LFT strips turned red and the test bands were noticeably darker. Because these tests rely on a reader for analysis, this can skew the results by interfering with the intensities of the gold nanoparticle bands. For this test to be used in a laboratory setting, much care will need to be put into sample preparation and storage to mitigate these issues.

Testing the kits in the field was more successful with no report of any clotting, unlike in the laboratory tests. By far the target with the highest signal is DENV in both panels, followed by leptospirosis and ZIKV in the IgM antibody panel. Malaria was not detected at all, which corresponds to the decreasing number of cases in Thailand with efforts being put into eliminating malaria within the country by 2024 (225). However, the lack of *O. tsutsugamushi* and *Rickettsia* is unexpected as both pathogens are endemic in many northern provinces of Thailand including Chiang Rai (226, 227).

The overall spread of signals in each target makes discerning where an appropriate threshold difficult. Ideally, the signals from a diagnostic test would be bimodal, grouping the positives and negative samples together with the threshold in between. While some of the targets have samples with extreme outliers, the low number of these samples makes it difficult to distinguish whether they belong to a separate group in a bimodal distribution or just a high background signal.

Out of all the targets across the Fever Panel II Asia systems, DENV is the target with the most real-time PCR-positive samples. Comparing the signal intensity of the antigen system with the Cq value shows that these are inversely correlated in that samples with low Cq values having high signal intensity in the Fever Panel II Asia antigen system with the highest signal in the antigen panel having Cq values of 28.0, 23.3, 28.6, and 28.0. This is expected as the lower the Cq value, the higher the viral load and vice versa, and antigen detection is less sensitive than real-time PCR.

Using the PCR-positive samples as reference, the calculated threshold for the DENV target in the antigen panel, 20.5, is lower than a previous study on the Fever Panel II Asia systems which used threshold values of 22 (142). Compared to that study, the sensitivity is slightly higher at 97.55% compared to 95%, but with a much lower specificity at 24.32% compared to 55%. The specificity in particular is low in the Fever Panel Asia II systems as there are many samples with extremely high signals that are PCR-negative, which could result in false positives. Using the Youden Index does result in a threshold that only takes two factors into consideration, sensitivity and specificity, omitting other factors such as prevalence and cost-effectiveness (228). It also treats sensitivity and specificity with equal importance which might not be true for certain diseases in practice.

The pattern that emerged from mapping the signal intensities of each panel to the duration of illness shows the highest signals early on in the antigen panel and much later in the IgM antibody panel. This is expected as viral antigen levels are highest around the time of symptom onset, while IgM antibodies are generally produced from day 5 of illness.

One common pitfall in serological tests is cross-reactivity such as between DENV and ZIKV, which share approximately 55.6% common amino acid sequences (229). The Fever Panel II Asia IgM antibody system also exhibited these cross-reativities. Many of the other cross-reactivity found in both panels are more surprising, with the two targets coming from very different groups. These are *O. tsutsugamushi* and CHIKV IgM antibody (bacteria and virus), and pan-*Plasmodium* against DENV and CHKV antigen (parasite and virus). It is possible that the correlation between the CHIKV and pan-*Plasmodium* targets to come from residual IgM levels after a previous infection. Without a reference test to detect antibodies, this could not be confirmed. Cross-reactivity between the two panels was also assessed, but no significant correlation was found.

Using thresholds previously reported by Amornchai et al., the remaining targets can also be called positive or negative (Figure 54). Positives are found in every target across the two systems with this method, including the targets that have no PCR positives. This is likely because these thresholds were determined from serum samples and are not well suited for this application, as the whole blood samples used here could have a higher background signal compared to serum. This would be expected however, as antigen-based detection is less sensitive than PCR-based detection. To adjust the assay for whole blood use, the thresholds would have to be increased as the current values would result in high false-positives as seen in the DENV target in the antigen panel.

The presence of real-time PCR negative samples with high signal in the Fever Panel II Asia IgM antibody system is most likely due to the timing of sample collection, with this sample being collected on day 7 after symptom onset. At this time, pathogen loads would have declined and IgM levels would have risen.

6.3.2. Limitations

The main limitation of this study is that only real-time RT-PCR was used as the reference test, which leaves the IgM antibody panel without an appropriate reference test. Added to this is the small sample size, which resulted in a small number of positive samples. IgM antibodies arises later in the course of the infection, generally after the detectable phase for NAATs. This means a patient is usually positive for either IgM antibodies or NAATs depending on when the testing is

done. While serological testing was done for SEACTN on both acute and convalescent samples, the results were unfortunately unavailable at the time of writing this thesis. Analytical validation of the antibody panel will later be carried out by comparing the intensity levels with those measured with the Luminex™ xMAP™ INTELLIFLEX® System (APX2020, Thermo Fisher Scientific, Waltham, MA, US), as well as clinical validation focusing on the sensitivity and specificity of the test using both serology (including convalescence samples) and molecular reference assays.

Another related limitation is the lack of positives. The only target with positive samples in the antigen panel is DENV; as such the performances of the other targets of the DPP® Fever Panel II Asia could not be assessed. Because samples used were collected from recruited patients, there is no way to screen or select for patients with specific diseases. While patient EDTA whole blood samples that are PCR-confirmed for selected pathogens could be used, freeze-thawing could affect the performance of the panels.

6.3.3. Conclusion

The DPP® Fever Panel II Asia system is a powerful POC diagnostic tool in development that can be easily performed and require minimal equipment. Here, we were able to use the DPP® kits on patient samples in a hospital setting. Using the real-time PCR assay developed in 0 as the reference test, we were able to determine a new threshold for the DENV target in the Fever Panel II Asia antigen system which has a higher sensitivity than a previous study. While data for only a portion of the available targets on the Fever Panel II Asia systems were available, once the results of the serology reference assays are available, analysis for the threshold values for the other targets should be possible. Future studies could expand to more sites with higher patient numbers to be able to maximise the chances of detecting more pathogens.

CHAPTER 7

Discussion

This chapter presents the discussion of the various assays developed or evaluated in this thesis and their implications on AUF diagnostics in rural South and Southeast Asia alongside limitations and future works.

The main theme of this thesis is in the development and evaluation of diagnostics for common AUF-causing bloodborne pathogens in South and Southeast Asia specifically regarding rural areas and the challenges. Three tests were developed and one evaluated:

1. Oligonucleotides were designed for real-time (RT-)PCR assays detecting bacterial (*Rickettsia* spp., *Leptospira* spp., *O. tsutsugamushi*, and pan-Eubacteria) and viral (CHIKV, DENV, JEV, and ZIKV) pathogens from whole blood specimens
2. CRISPR-based assays for rapid detection of CHIKV, DENV, and ZIKV aimed for use as POC tests
3. Automated real-time RT-PCR assay for detecting viral pathogens in DBS specimens with CHIKV as proof-of-concept
4. Evaluation of the Chembio DPP® Fever Panel II Asia Antigen and IgM Antibody systems in a POC setting on whole blood specimens

The multiplex real-time (RT-)PCR tests are aimed to be more economical by being able to use only one whole blood aliquot across two tests for eight different targets. An additional benefit is the ability to sequence the amplicon of the *Rickettsia* target for species identification if needed. Not only does this test have potential for use as a diagnostic test for clinical and research purposes, it also useful as a reference test for other diagnostic tests in development. It is also the basis of the DBS assay of this thesis. As of writing, the assays have been further optimised and verified by the Molecular Microbiology Laboratory for Diagnosis and Epidemiology (MoMiLDE) at MORU and has been used for the Spot Sepsis project. However, the same limitations as with any other real-time PCR assay applies with the high equipment cost and requirement of a laboratory so while this it is more economical than singleplex assays, it is not suited for POC settings.

The CRISPR assay developed here is aimed specifically for POC settings. The typically labour-intensive processes of nucleic acid extraction and amplification is replaced by simpler methods. The extraction process here only involves mixing sample with buffer and incubation. Although the amplification method successfully used in the assembled assay is RT-PCR, RAA shows promise as a simpler and less laborious method. More work must be done to adapt it to the

CRISPR detection as while RAA does produce amplicons, the CRISPR reaction was not able to detect them and the complete assay has a high limit of detection. RAA would be the preferable amplification method as it is done at a single, relatively low temperature and is commercially available in a lyophilised form.

The CRISPR detection itself is also done at a single temperature, very close to the temperature that the amplification reaction is performed. While the reactions here are performed over two hours, a positive or negative result can generally be detected in only about 30 minutes. The detection here is done via fluorescence using a real-time PCR instrument.

To further adapt this assay to the field, more developments could be done including multiplexing, colorimetric detection, and LFT detection. Multiplexing a CRISPR assay is able to be done because as mentioned in Chapter 1.5.2, each Cas protein ortholog has different preferences to what bystander molecule it cleaves. A study was done using four Cas protein orthologs along with four different reporter molecules, modified with different fluorescent dyes, as well as four crRNA specific for each Cas protein to detect four different targets (164). Table 38 shows the Cas orthologs used and their respective reporter molecules. To adapt the assay developed in this thesis for multiplex, the crRNA for each target must have direct repeats specific to different Cas orthologs. The respective reporter will also be pooled and used in the same reaction. However, fluorescence readout would be necessary, as there are no commercially available LFT strips that supports three targets, not including the control band. The hypothetical crRNA sequences for each target are shown in Table 39.

Table 38: List of Cas protein orthologs and their respective reporter molecules for a multiplexed CRISPR detection assay.

Cas ortholog	Organism of origin	Reporter sequence (5' - 3')	Reporter molecule	Fluorescent dye
PsmCas13b	*Prevotella* sp. MA2016	AAAAA	RNA	FAM
LwaCas13a	*Leptotrichia wadei*	AU	RNA	TEX
CcaCas13b	*Capnocytophaga canimorsus*	UA	RNA	Cy5
AsCas12a	*Acidaminococcus* sp. BV3L6	TTATT	DNA	HEX

Table 39: Hypothetical crRNA sequences for a multiplex CRISPR detection assay.

Target	Cas ortholog	crRNA sequence
CHIKV	LwaCas13a	gauuuagacuaccccaaaaacgaaggggacuaaaacCACCUCAAACAUGGGGUACGCAC
DENV	PsmCas13b	guuguagaagcuuaucguuuggauagguaugacaacGUCUCCUCUAACCUCUAGUCCUU
ZIKV	CcaCas13b	guuggaacugcucucauuuuggaggguaaucacaacUGUUCAUCUGUGCCAGUUGACUGG

A colorimetric readout would allow for visualisation under the naked eye with the ability to multiplex. By modifying different reporters for different Cas proteins with FAM or ROX, fluorescence can be induced under specific LED lights (blue or white) and different excitation/emission filters. The resulting fluorescence of each modification have different colour patterns and can be differentiated under the naked eye (168). The resulting fluorescence can simply be recorded by taking a picture on any smartphone.

To adapt the assay to LFTs, only the reporter molecule needs to be modified (230). Instead of a fluorescent dye and a quencher, the reporter would be modified with FAM (or FITC) at one end, and biotin at the other. This would make it compatible with commercially available LFT strips such as the HybriDetect - Universal Lateral Flow Assay Kit (MGHD 1, Milenia Biotec GmbH, Gießen, Germany). These strips contain gold nanoparticles with anti-FAM polyclonal rabbit antibodies that will mix with the sample and bind to FAM. Further down the strip are two bands, one with streptavidin which binds to biotin, and another with anti-rabbit polyclonal goat antibodies which binds to the rabbit antibodies. The CRISPR reaction can be directly added to the LFT strips.

Once the reaction is added to the LFT strips, the gold nanoparticles will bind to the FAM. If the target is not present in the CRISPR reaction and the reporters remain intact, the entire molecule will be captured by the streptavidin and only the first band will be visible. If the target is present and the reporters are cleaved, the biotin and FAM-gold nanoparticle complex will be captured by streptavidin and the anti-rabbit antibodies. As only the latter contains the gold nanoparticles, only the second band will be visible. However, because not all reporter molecules are cleaved, especially at lower target concentration, there can be a visible streptavidin band albeit fainter. Generally, the test is considered positive if both or only the anti-rabbit antibody band is visible and negative if only the streptavidin band is visible. Figure 58 shows the mechanism of applying CRISPR detection assays to LFTs.

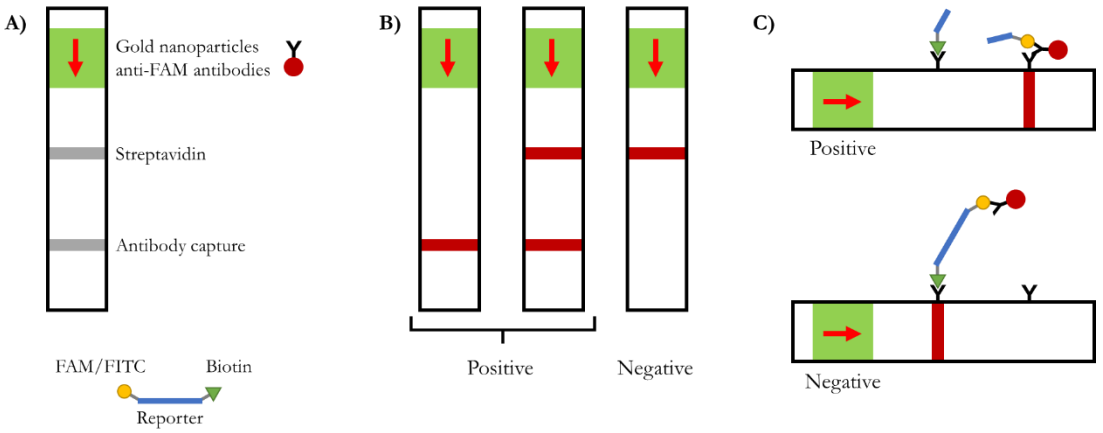

Figure 58: Applying CRISPR detection assay to LFTs. A) Layout of a LFT strip and CRISPR reporter molecule. B) Conditions to call positives and negatives. C) Mechanisms of the reporter on the LFT strip in positive and negative samples.

A potential way to improve the assay is to include a nucleic acid purification step, either after extraction or after amplification. This process removes extraneous proteins such as enzymes from the sample which could potentially inhibit or interfere with the amplification or detection reactions. Typically, this step would significantly add to the cost of the assay as it would require more reagents including magnetic beads such as the AMPure XP beads as well as a magnetic rack which are commercially available but generally costly.

One solution for this is the use of modern fabrication techniques, namely 3D printing. 3D printing is an additive manufacturing process that is able to fabricate complicated models using plastics relatively cheaply and quickly. The most widespread type of 3D printing is fused deposition modelling (FDM) in which plastic filaments are fed into a hotend that melts and deposits it onto a print bed. Computer controlled motors move the nozzle in such a way that a model is created layer by layer, as dictated by the 3D model loaded.

As a proof-of-concept, a magnetic stand was fabricated from a design available on bomb.bio (231). However, the design was found to be problematic in practice, especially if it is to be used in a POC situation, as the specific size of magnet needed is not commonly available in Thailand, and a smaller magnet was used instead. This not only lessen the magnetic pull, it also causes the magnets to be situated further away from the tubes, lessening the pull even further. The

openings for each tube were also much wider than the tube's diameter, allowing the tubes to spin inside which makes handling much more difficult. A prototype magnetic stand was designed and fabricated to address these issues. These would potentially reduce the cost of performing purification. Because of the design, using them would be less laborious than commercial magnetic stand as well. Renders of the magnetic stand and the fabricated version are shown in Figure 59.

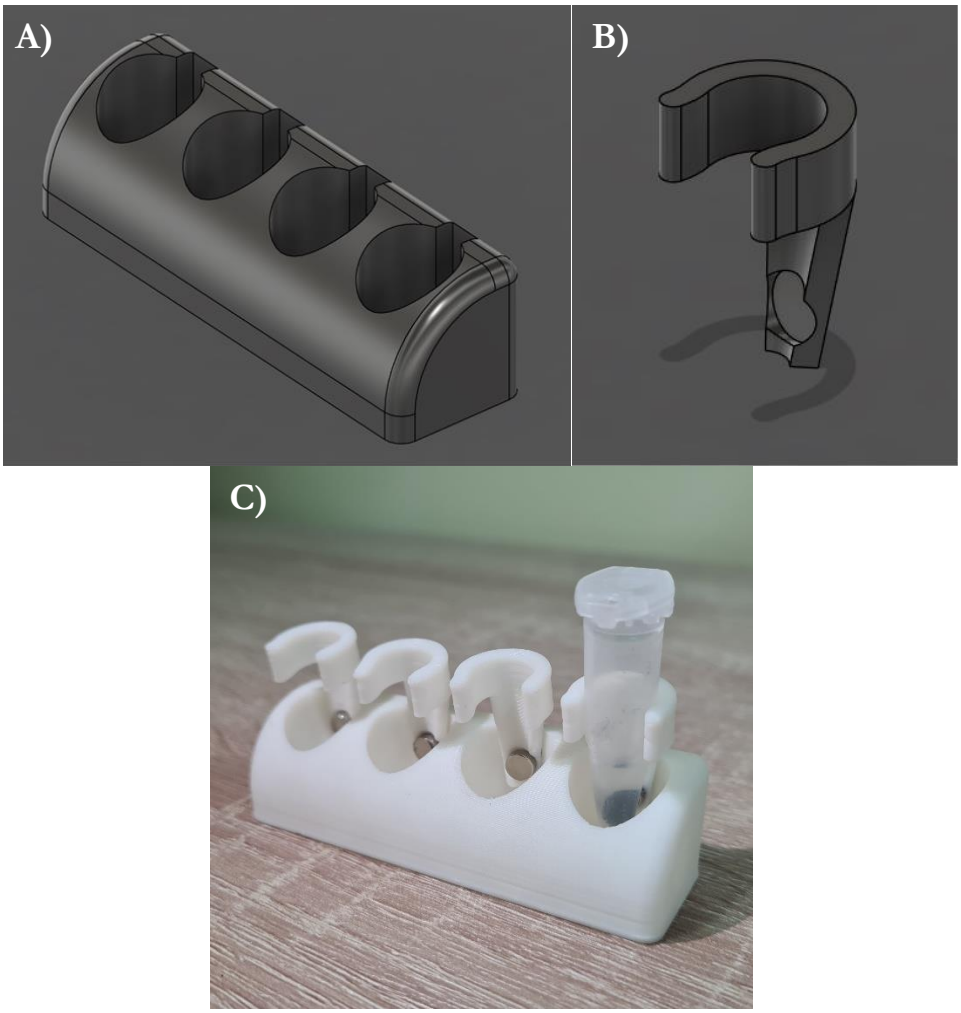

Figure 59: Autodesk Fusion 360 renders of the designed magnetic stand composed of A) base and B) clip for nucleic acid purification. C) shows the fabricated magnetic stand.

The automated real-time RT-PCR assay developed here is able to detect DNA targets from DBS specimens with an economical elution method. The buffer used for elution is the same buffer as the one required for the extraction process, cutting down on the need of an additional buffer. The protocol is also done over three hours, not overnight, allowing for multiple batches per day. Any eluted sample that is not used can be safely stored in the SBT at -80°C.

Using the BD MAX™ instrument simplifies the assay significantly by automating the extraction and detection process inside one instrument. Not only does less laboratory work need to be done by workers, but the lab work in running the assay needs less training than manual extraction and detection. By using batch-prepared reagents that are separately sealed in individual tubes, work during each run only include assembling each component and loading them into the instrument.

Data analysis is also somewhat simplified as the BD MAX™ instrument allows for pre-setting criteria for detection of each target. It also has an auto-analysis function that conditionally call each target for each sample depending on pre-set criteria. In this case, a target is called positive only if both the respective target and the *rnaseP* control are detected. If only the *rnaseP* target is detected, the sample is negative. If the *rnaseP* target is not detected, the sample is marked as inconclusive regardless of the other targets. When exported, both the Cq values, the amplification curves and the results as analysed by the instrument are all given. In this way, any laboratory technician can export the results and get preliminary data while a more experienced technician can inspect the Cq and amplification curve for a more detailed analysis. Added to this, being an automated instrument, the extraction and PCR are very consistent as there is virtually no manual handling throughout the process. Also, unlike many automated instruments, the BD MAX™ instrument uses separate consumables for each of the 24 samples, lessening the risk of cross-contaminations from shared reagent pools. This also means the instrument can be run with less than 24 samples without leaving partially used reagent containers. In contrast, the MagNA Pure 24 stores all reagents in a tank that is shared across the samples. If less than 24 samples are used, the reagent tank can be stored at 4°C but needs to be used within a timeframe of roughly 1 week. This can be an issue if samples arrive in small batches spread out across weeks as once the reagents have passed the expiry timeframe, the instrument will reject it, requiring a new tank to be used which can be costly.

The BD MAX™ instrument does have some drawbacks however. The maximum 24 samples per batch, while sufficient for most applications, is a limiting factor if used for a larger study such as SEACTN with upwards of 10,000 DBS samples to be processed. Furthermore, unlike

most real-time PCR instruments, the BD MAX™ instrument's tests require users to set the threshold, and cycles of the PCR program to analyse which cannot be changed post-run. This means optimising the instrument is better initially done on a conventional real-time instrument that allows for changing these parameters post-run to determine the appropriate values to use on the BD MAX. Lastly, while the PCR is automated, preparation of the primer and probe mix needs to be done manually. This involves mixing the PCR pre-mix as in conventional PCR, aliquoting the mix into individual 0.6 μL conical tubes and sealing them. This can become laborious if a large number of mixes are being prepared in a big batch.

Currently, the assay is being optimised also for the remaining viral targets of the assay (DENV, JEV, and ZIKV) and will be used for detection of pathogens from DBS specimens in SEACTN. The assay itself has the potential to be adapted for the detection of other bloodborne pathogens in DBS specimens.

The use of DBS makes this assay more applicable to rural areas and areas with limited access to hospitals compared to assays that uses whole blood, plasma, or serum. For patients, DBS are much less invasive than whole blood collection with less volume taken. For healthcare workers, DBS require less equipment to collect as well as less training to be properly done. For the laboratory, DBS can be stored and transported much easier than whole blood. Combined with the automated system, this assay could potentially be ideal for provincial-level hospitals or secondary healthcare centres that could house a laboratory with a BD MAX™ and sufficiently trained technicians to run it. Although direct access to household level is more limited, the ability to easily store and transport specimens means patients do not need to personally travel to the hospital.

However, being able to recover RNA in DBS has proven to be an issue due to the degradation of RNA, the rate of which is proportional to the time spend at ambient temperature. A possible explanation is that the RNases in whole blood are able to recover after rehydration and were able to degrade the eluted RNA in the elution process. Currently, work is being done testing out the effects of different sample and lysis buffers specifically on the degradation of viral RNA.

Nonetheless, the protocol developed here would be suited to detecting DNA targets such as bacteria, parasites, or DNA viruses.

A potential pitfall for the DBS assay is the detection of pathogens with low concentrations in blood if the assay is to be adapted for them. The acute phase of viraemia generally sees high concentrations of virus in patient bloodstream. For example, DENV infections can have viral loads of up to 10^{10} copies/mL (232). Meanwhile, bacteria such as *Leptospira* spp. can cause severe disease even with as low as 10^4 bacteria/mL (233). This can be even as low as 10^2 bacteria/mL in other bacteria (234). In DBS, however, because the targets are DNA, the storage stability is much better compared to RNA, which could compensate for the low concentration.

The DPP® Fever Panel II Asia systems have the potential to be incredibly useful as a POC test. Its main advantage is the number of targets that can be tested for with very little blood and the inclusion of both antigen and IgM antibody detection which gives a broader time period to detect those targets that are included in both tests such as DENV.

The tests are relatively user friendly, and were able to be performed on patients alongside other tests in the field. However, laboratory testing is very much dependent on the quality of the collected specimens if whole blood is used. Inadequately collected whole blood can cause clogs that render the tests invalid. This makes the DPP® Fever Panel II Asia system potentially less useful for studies in which whole blood samples are required to be cryogenically frozen for later testing. As they are currently in development and not commercially available, the threshold values for the different targets and tests are not yet given by the manufacturer, and this work demonstrates the difficulty in determining an appropriate threshold value and reference test.

One obstacle in serological tests is the background seropositivity. Different populations can have different background seropositivity for different pathogens due to exposures to the pathogen itself or related organisms (235). For example, healthy samples from northeast Thailand had higher seropositivity of the *B. pseudomallei* haemolysin-coregulated protein 1 (Hcp1) antigen compared to healthy US donors (141). This means the threshold values of a serological test ideally would need to differ depending on the population it is being used on.

While the assays are very simple and can be done with minimal equipment or training, there are some aspects that could be better designed for user experience. The main aspect that was found to be potentially problematic is the fact that between the two systems, there are four reagent bottles, a sample and running buffer for each system. However, the bottles are only colour-coded for the test they are used in; blue caps for the antigen system and black caps for the IgM antibody system. It is very possible for a worker to mistakenly use a sample buffer instead of the running buffer and vice versa. For the protocol used in this project, research nurses were instructed to label the sample buffer with a brightly coloured sticker to prevent this (see Chapter 9.2). Another aspect that affects user experience is that there are many components and consumables used in the assays such as Pasteur pipettes and tubes. Without a tube rack, workers have to either hold on to the tubes or place them on a table, both of which is a safety hazard. For this project, paper tube racks were obtained from used MagNA Pure 24 kits and provided to each site. This is a viable solution for those already with access to these racks although paper racks are not durable and will weaken over time.

To address this, bases were designed for each DPP® Fever Panel II Asia system with the goal of providing a secure place to put each component of the assays as well as arrange them in a way that each component has an unambiguous location. Each base accommodates one DPP® cassette and its respective components (buffer bottles, tube, and pipettes) with the name of the test clearly labelled in the centre. This would prevent confusion between the buffers by fixing each bottle's location. The tube and pipette holders also free up workers' hands while providing a secure rack to place the items. Many commonly available filaments such as PLA, acrylonitrile butadiene styrene (ABS), and Polyethylene terephthalate glycol (PETG) are also reasonably resistant to ethanol, troclosene sodium and UV light, allowing for easy disinfection. However, these bases were not fabricated in time to be used in this project. Renders of the bases are shown in Figure 60.

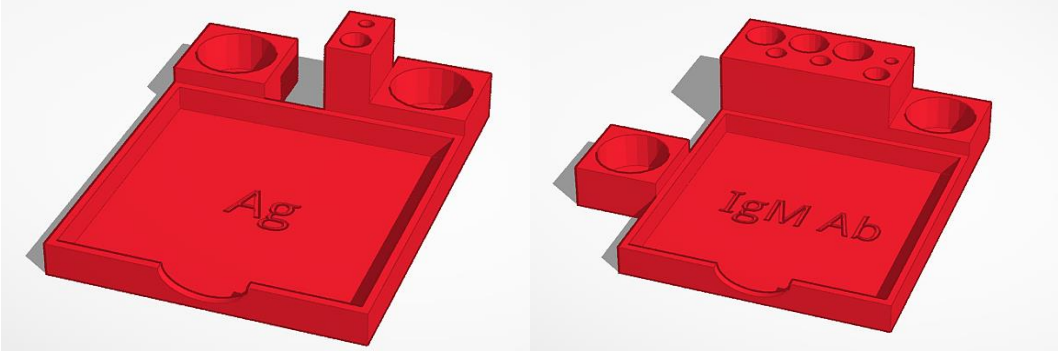

Figure 60: Tinkercad renders of bases designed for the DPP® Fever Panel II Asia antigen (left) and IgM antibody (right) systems.

Many of the assays developed in this thesis will be used in the SEACTN project. The multiplex real-time (RT-)PCR assay is currently in use in WP-B. The DBS assay will continue to be developed for the other viral targets, DENV, JEV, and ZIKV to be used with WP-A. Many further developments could be made on the CRISPR assay, with the most interesting being to adapt the assay onto a LFT readout. Developing a multiplex version of the assay is also appealing, especially in adding a human housekeeping gene for the assay to have an internal control. Lastly, the DPP® Fever Panel II Asia System as mentioned, is still in development and will require further validation on other populations to assess the appropriate thresholds for different areas.

To summarise, this thesis has explored different diagnostics for AUFs in rural South and Southeast Asia. This includes laboratory tests fit for higher-level healthcare facilities such as the real-time (RT-)PCR assays for whole blood specimens and DBS which are aimed to be more economical by reducing the required specimen volume as well as maximising the number of targets that can be detected simultaneously. Diagnostics aimed towards POC settings are also investigated with the development of a rapid CRISPR-based molecular diagnostic for whole blood and evaluation of the Chembio DPP® Fever Panel II Asia Systems for detection of antigen and IgM antibody of selected pathogens.

With the prevalence of AUFs across resource-limited areas in LMICs, it is important for new diagnostics to be more accessible and economical. Bringing diagnostics to patient bedside as

well as the ability to screen for a broad range of pathogens have the potential to benefit patient and reduce mortality in areas that laboratory tests are unavailable otherwise.

CHAPTER 8

References

1. Mittal G, Ahmad S, Agarwal RK, Dhar M, Mittal M, Sharma S. Aetiologies of Acute Undifferentiated Febrile illness in Adult Patients - an Experience from a Tertiary Care Hospital in Northern India. J Clin Diagn Res. 2015;9(12):DC22-4.

2. World Health O. Guidelines for the treatment of malaria. 3rd ed ed. Geneva: World Health Organization; 2015 2015.

3. Acestor N, Cooksey R, Newton PN, Ménard D, Guerin PJ, Nakagawa J, et al. Mapping the Aetiology of Non-Malarial Febrile Illness in Southeast Asia through a Systematic Review—Terra Incognita Impairing Treatment Policies. PLOS ONE. 2012;7(9):e44269.

4. Mayxay M, Castonguay-Vanier J, Chansamouth V, Dubot-Peres A, Paris DH, Phetsouvanh R, et al. Causes of non-malarial fever in Laos: a prospective study. Lancet Glob Health. 2013;1(1):e46-54.

5. Wangdi K, Kasturiaratchi K, Nery SV, Lau CL, Gray DJ, Clements ACA. Diversity of infectious aetiologies of acute undifferentiated febrile illnesses in south and Southeast Asia: a systematic review. BMC Infect Dis. 2019;19(1):577.

6. Crump JA, Gove S, Parry CM. Management of adolescents and adults with febrile illness in resource limited areas. BMJ. 2011;343:d4847.

7. Gandra S, Alvarez-Uria G, Turner P, Joshi J, Limmathurotsakul D, van Doorn HR. Antimicrobial Resistance Surveillance in Low- and Middle-Income Countries: Progress and Challenges in Eight South Asian and Southeast Asian Countries. Clin Microbiol Rev. 2020;33(3).

8. Simmons CP, Farrar JJ, Nguyen v V, Wills B. Dengue. N Engl J Med. 2012;366(15):1423-32.

9. Wood CL, McInturff A, Young HS, Kim D, Lafferty KD. Human infectious disease burdens decrease with urbanization but not with biodiversity. Philos Trans R Soc Lond B Biol Sci. 2017;372(1722).

10. Innovations Flagships: funded projects: UK WellcomeTrust; [Available from: https://wellcome.org/grant-funding/funded-people-and-projects/innovations-flagships.

11. Chandna A, Chew R, Shwe Nwe Htun N, Peto TJ, Zhang M, Liverani M, et al. Defining the burden of febrile illness in rural South and Southeast Asia: an open letter to announce the launch of the Rural Febrile Illness project. Wellcome Open Res. 2021;6:64.

12. Htun NSN, Perrone C, Phyo AP, Sen A, Phommasone K, Vanna M, et al. Ethical and cultural implications for conducting verbal autopsies in South and Southeast Asia: a qualitative study. BMJ Glob Health. 2023;8(12).

13. Zhang M, Htun NSN, Islam S, Sen A, Islam A, Neogi AK, et al. Defining the hidden burden of disease in rural communities in Bangladesh, Cambodia and Thailand: a cross-sectional household health survey protocol. BMJ Open. 2024;14(3):e081079.

14. Weaver SC, Forrester NL. Chikungunya: Evolutionary history and recent epidemic spread. Antiviral Res. 2015;120:32-9.

15. Vairo F, Haider N, Kock R, Ntoumi F, Ippolito G, Zumla A. Chikungunya: Epidemiology, Pathogenesis, Clinical Features, Management, and Prevention. Infect Dis Clin North Am. 2019;33(4):1003-25.

16. Solignat M, Gay B, Higgs S, Briant L, Devaux C. Replication cycle of chikungunya: a re-emerging arbovirus. Virology. 2009;393(2):183-97.

17. Althouse BM, Guerbois M, Cummings DAT, Diop OM, Faye O, Faye A, et al. Role of monkeys in the sylvatic cycle of chikungunya virus in Senegal. Nat Commun. 2018;9(1):1046.

18. Sourisseau M, Schilte C, Casartelli N, Trouillet C, Guivel-Benhassine F, Rudnicka D, et al. Characterization of reemerging chikungunya virus. PLoS Pathog. 2007;3(6):e89.

19. Silva JVJ, Jr., Ludwig-Begall LF, Oliveira-Filho EF, Oliveira RAS, Duraes-Carvalho R, Lopes TRR, et al. A scoping review of Chikungunya virus infection: epidemiology, clinical characteristics, viral co-circulation complications, and control. Acta Trop. 2018;188:213-24.

20. Cunha RVD, Trinta KS. Chikungunya virus: clinical aspects and treatment - A Review. Mem Inst Oswaldo Cruz. 2017;112(8):523-31.

21. Capeding MR, Chua MN, Hadinegoro SR, Hussain IIHM, Nallusamy R, Pitisuttithum P, et al. Dengue and Other Common Causes of Acute Febrile Illness in Asia: An Active Surveillance Study in Children. PLOS Neglected Tropical Diseases. 2013;7(7):e2331.

22. Rahman M, Yamagishi J, Rahim R, Hasan A, Sobhan A. East/Central/South African Genotype in a Chikungunya Outbreak, Dhaka, Bangladesh, 2017. Emerg Infect Dis. 2019;25(2):370-2.

23. Schwartz O, Albert ML. Biology and pathogenesis of chikungunya virus. Nat Rev Microbiol. 2010;8(7):491-500.

24. Simon F, Javelle E, Cabie A, Bouquillard E, Troisgros O, Gentile G, et al. French guidelines for the management of chikungunya (acute and persistent presentations). November 2014. Med Mal Infect. 2015;45(7):243-63.

25. Waymouth HE, Zoutman DE, Towheed TE. Chikungunya-related arthritis: case report and review of the literature. Semin Arthritis Rheum. 2013;43(2):273-8.

26. Huang YJ, Hsu WW, Higgs S, Vanlandingham DL. Temperature Tolerance and Inactivation of Chikungunya Virus. Vector Borne Zoonotic Dis. 2015;15(11):674-7.

27. Li YG, Siripanyaphinyo U, Tumkosit U, Noranate N, A An, Tao R, et al. Chikungunya virus induces a more moderate cytopathic effect in mosquito cells than in mammalian cells. Intervirology. 2013;56(1):6-12.

28. Chusri S, Siripaitoon P, Silpapojakul K, Hortiwakul T, Charernmak B, Chinnawirotpisan P, et al. Kinetics of chikungunya infections during an outbreak in Southern Thailand, 2008-2009. Am J Trop Med Hyg. 2014;90(3):410-7.

29. Huits R, Okabayashi T, Cnops L, Barbe B, Van Den Berg R, Bartholomeeusen K, et al. Diagnostic accuracy of a rapid E1-antigen test for chikungunya virus infection in a reference setting. Clin Microbiol Infect. 2018;24(1):78-81.

30. Litzba N, Schuffenecker I, Zeller H, Drosten C, Emmerich P, Charrel R, et al. Evaluation of the first commercial chikungunya virus indirect immunofluorescence test. J Virol Methods. 2008;149(1):175-9.

31. Prat CM, Flusin O, Panella A, Tenebray B, Lanciotti R, Leparc-Goffart I. Evaluation of commercially available serologic diagnostic tests for chikungunya virus. Emerg Infect Dis. 2014;20(12):2129-32.

32. Natrajan MS, Rojas A, Waggoner JJ. Beyond Fever and Pain: Diagnostic Methods for Chikungunya Virus. J Clin Microbiol. 2019;57(6).

33. Tian N, Zheng JX, Guo ZY, Li LH, Xia S, Lv S, et al. Dengue Incidence Trends and Its Burden in Major Endemic Regions from 1990 to 2019. Trop Med Infect Dis. 2022;7(8).

34. Westaway EG, Brinton MA, Gaidamovich S, Horzinek MC, Igarashi A, Kaariainen L, et al. Flaviviridae. Intervirology. 1985;24(4):183-92.

35. Bhatt S, Gething PW, Brady OJ, Messina JP, Farlow AW, Moyes CL, et al. The global distribution and burden of dengue. Nature. 2013;496(7446):504-7.

36. Shepard DS, Undurraga EA, Halasa YA. Economic and Disease Burden of Dengue in Southeast Asia. PLOS Neglected Tropical Diseases. 2013;7(2):e2055.

37. Chambers TJ, Hahn CS, Galler R, Rice CM. Flavivirus genome organization, expression, and replication. Annu Rev Microbiol. 1990;44:649-88.

38. Back AT, Lundkvist A. Dengue viruses - an overview. Infect Ecol Epidemiol. 2013;3.

39. Wu SJ, Grouard-Vogel G, Sun W, Mascola JR, Brachtel E, Putvatana R, et al. Human skin Langerhans cells are targets of dengue virus infection. Nat Med. 2000;6(7):816-20.

40. Kou Z, Quinn M, Chen H, Rodrigo WW, Rose RC, Schlesinger JJ, et al. Monocytes, but not T or B cells, are the principal target cells for dengue virus (DV) infection among human peripheral blood mononuclear cells. J Med Virol. 2008;80(1):134-46.

41. Willey S, Aasa-Chapman MM, O'Farrell S, Pellegrino P, Williams I, Weiss RA, et al. Extensive complement-dependent enhancement of HIV-1 by autologous non-neutralising antibodies at early stages of infection. Retrovirology. 2011;8:16.

42. Takada A, Feldmann H, Ksiazek TG, Kawaoka Y. Antibody-dependent enhancement of Ebola virus infection. J Virol. 2003;77(13):7539-44.

43. Krilov LR, Anderson LJ, Marcoux L, Bonagura VR, Wedgwood JF. Antibody-mediated enhancement of respiratory syncytial virus infection in two monocyte/macrophage cell lines. J Infect Dis. 1989;160(5):777-82.

44. Tamura M, Webster RG, Ennis FA. Subtype cross-reactive, infection-enhancing antibody responses to influenza A viruses. J Virol. 1994;68(6):3499-504.

45. Schieffelin JS, Costin JM, Nicholson CO, Orgeron NM, Fontaine KA, Isern S, et al. Neutralizing and non-neutralizing monoclonal antibodies against dengue virus E protein derived from a naturally infected patient. Virol J. 2010;7:28.

46. Flipse J, Wilschut J, Smit JM. Molecular mechanisms involved in antibody-dependent enhancement of dengue virus infection in humans. Traffic. 2013;14(1):25-35.

47. Sridhar S, Luedtke A, Langevin E, Zhu M, Bonaparte M, Machabert T, et al. Effect of Dengue Serostatus on Dengue Vaccine Safety and Efficacy. N Engl J Med. 2018;379(4):327-40.

48. Thomas SJ, Yoon IK. A review of Dengvaxia(R): development to deployment. Hum Vaccin Immunother. 2019;15(10):2295-314.

49. Patel SS, Rauscher M, Kudela M, Pang H. Clinical Safety Experience of TAK-003 for Dengue Fever: A New Tetravalent Live Attenuated Vaccine Candidate. Clin Infect Dis. 2023;76(3):e1350-e9.

50. Biswal S, Reynales H, Saez-Llorens X, Lopez P, Borja-Tabora C, Kosalaraksa P, et al. Efficacy of a Tetravalent Dengue Vaccine in Healthy Children and Adolescents. N Engl J Med. 2019;381(21):2009-19.

51. Angelin M, Sjolin J, Kahn F, Ljunghill Hedberg A, Rosdahl A, Skorup P, et al. Qdenga(R) - A promising dengue fever vaccine; can it be recommended to non-immune travelers? Travel Med Infect Dis. 2023;54:102598.

52. Rigau-Perez JG, Clark GG, Gubler DJ, Reiter P, Sanders EJ, Vorndam AV. Dengue and dengue haemorrhagic fever. Lancet. 1998;352(9132):971-7.

53. Jagadishkumar K, Jain P, Manjunath VG, Umesh L. Hepatic involvement in dengue Fever in children. Iran J Pediatr. 2012;22(2):231-6.

54. Gubler DJ. Dengue and dengue hemorrhagic fever. Clin Microbiol Rev. 1998;11(3):480-96.

55. Harapan H, Michie A, Sasmono RT, Imrie A. Dengue: A Minireview. Viruses. 2020;12(8).

56. Lum L, Ng CJ, Khoo EM. Managing dengue fever in primary care: A practical approach. Malays Fam Physician. 2014;9(2):2-10.

57. Organization WH. Dengue haemorrhagic fever: diagnosis, treatment, prevention and control: World Health Organization; 1997.

58. Kuo MC, Lu PL, Chang JM, Lin MY, Tsai JJ, Chen YH, et al. Impact of renal failure on the outcome of dengue viral infection. Clin J Am Soc Nephrol. 2008;3(5):1350-6.

59. Wali JP, Biswas A, Chandra S, Malhotra A, Aggarwal P, Handa R, et al. Cardiac involvement in Dengue Haemorrhagic Fever. Int J Cardiol. 1998;64(1):31-6.

60. Rajapakse S. Dengue shock. J Emerg Trauma Shock. 2011;4(1):120-7.

61. Medina F, Medina JF, Colon C, Vergne E, Santiago GA, Munoz-Jordan JL. Dengue virus: isolation, propagation, quantification, and storage. Curr Protoc Microbiol. 2012;Chapter 15:Unit 15D 2.

62. Johnson BW, Russell BJ, Lanciotti RS. Serotype-specific detection of dengue viruses in a fourplex real-time reverse transcriptase PCR assay. J Clin Microbiol. 2005;43(10):4977-83.

63. Dussart P, Labeau B, Lagathu G, Louis P, Nunes MRT, Rodrigues SG, et al. Evaluation of an Enzyme Immunoassay for Detection of Dengue Virus NS1 Antigen in Human Serum. Clinical and Vaccine Immunology. 2006;13(11):1185-9.

64. Chen L, Wang H, Guo T, Xiao C, Liu L, Zhang X, et al. A rapid point-of-care test for dengue virus-1 based on a lateral flow assay with a near-infrared fluorescent dye. J Immunol Methods. 2018;456:23-7.

65. Dick GW, Kitchen SF, Haddow AJ. Zika virus. I. Isolations and serological specificity. Trans R Soc Trop Med Hyg. 1952;46(5):509-20.

66. Li MI, Wong PS, Ng LC, Tan CH. Oral susceptibility of Singapore Aedes (Stegomyia) aegypti (Linnaeus) to Zika virus. PLoS Negl Trop Dis. 2012;6(8):e1792.

67. Foy BD, Kobylinski KC, Chilson Foy JL, Blitvich BJ, Travassos da Rosa A, Haddow AD, et al. Probable non-vector-borne transmission of Zika virus, Colorado, USA. Emerg Infect Dis. 2011;17(5):880-2.

68. Lanciotti RS, Lambert AJ, Holodniy M, Saavedra S, Signor Ldel C. Phylogeny of Zika Virus in Western Hemisphere, 2015. Emerg Infect Dis. 2016;22(5):933-5.

69. Haddow AD, Schuh AJ, Yasuda CY, Kasper MR, Heang V, Huy R, et al. Genetic characterization of Zika virus strains: geographic expansion of the Asian lineage. PLoS Negl Trop Dis. 2012;6(2):e1477.

70. Wang A, Thurmond S, Islas L, Hui K, Hai R. Zika virus genome biology and molecular pathogenesis. Emerg Microbes Infect. 2017;6(3):e13.

71. Musso D, Nilles EJ, Cao-Lormeau VM. Rapid spread of emerging Zika virus in the Pacific area. Clin Microbiol Infect. 2014;20(10):O595-6.

72. Sudulagunta SR, Sodalagunta MB, Sepehrar M, Khorram H, Bangalore Raja SK, Kothandapani S, et al. Guillain-Barre syndrome: clinical profile and management. Ger Med Sci. 2015;13:Doc16.

73. Cao-Lormeau VM, Blake A, Mons S, Lastere S, Roche C, Vanhomwegen J, et al. Guillain-Barre Syndrome outbreak associated with Zika virus infection in French Polynesia: a case-control study. Lancet. 2016;387(10027):1531-9.

74. Noronha L, Zanluca C, Azevedo ML, Luz KG, Santos CN. Zika virus damages the human placental barrier and presents marked fetal neurotropism. Mem Inst Oswaldo Cruz. 2016;111(5):287-93.

75. Landry ML, St George K. Laboratory Diagnosis of Zika Virus Infection. Arch Pathol Lab Med. 2017;141(1):60-7.

76. Petersen LR, Jamieson DJ, Powers AM, Honein MA. Zika Virus. New England Journal of Medicine. 2016;374(16):1552-63.

77. Waggoner JJ, Gresh L, Mohamed-Hadley A, Ballesteros G, Davila MJ, Tellez Y, et al. Single-Reaction Multiplex Reverse Transcription PCR for Detection of Zika, Chikungunya, and Dengue Viruses. Emerg Infect Dis. 2016;22(7):1295-7.

78. Griffin I, Martin SW, Fischer M, Chambers TV, Kosoy O, Falise A, et al. Zika Virus IgM Detection and Neutralizing Antibody Profiles 12-19 Months after Illness Onset. Emerg Infect Dis. 2019;25(2):299-303.

79. Priyamvada L, Quicke KM, Hudson WH, Onlamoon N, Sewatanon J, Edupuganti S, et al. Human antibody responses after dengue virus infection are highly cross-reactive to Zika virus. Proc Natl Acad Sci U S A. 2016;113(28):7852-7.

80. Vatti A, Monsalve DM, Pacheco Y, Chang C, Anaya JM, Gershwin ME. Original antigenic sin: A comprehensive review. J Autoimmun. 2017;83:12-21.

81. Lanciotti RS, Kosoy OL, Laven JJ, Velez JO, Lambert AJ, Johnson AJ, et al. Genetic and Serologic Properties of Zika Virus Associated with an Epidemic, Yap State, Micronesia, 2007. Emerging Infectious Disease journal. 2008;14(8):1232.

82. Kelly DJ, Fuerst PA, Ching WM, Richards AL. Scrub typhus: the geographic distribution of phenotypic and genotypic variants of Orientia tsutsugamushi. Clin Infect Dis. 2009;48 Suppl 3:S203-30.

83. Phasomkusolsil S, Tanskul P, Ratanatham S, Watcharapichat P, Phulsuksombati D, Frances SP, et al. Influence of Orientia tsutsugamushi infection on the developmental biology of Leptotrombidium imphalum and Leptotrombidium chiangraiensis (Acari: Trombiculidae). J Med Entomol. 2012;49(6):1270-5.

84. Enatsu T, Urakami H, Tamura A. Phylogenetic analysis of Orientia tsutsugamushi strains based on the sequence homologies of 56-kDa type-specific antigen genes. FEMS Microbiol Lett. 1999;180(2):163-9.

85. Peter JV, Sudarsan TI, Prakash JA, Varghese GM. Severe scrub typhus infection: Clinical features, diagnostic challenges and management. World J Crit Care Med. 2015;4(3):244-50.

86. Varghese GM, Dayanand D, Gunasekaran K, Kundu D, Wyawahare M, Sharma N, et al. Intravenous Doxycycline, Azithromycin, or Both for Severe Scrub Typhus. N Engl J Med. 2023;388(9):792-803.

87. Jang WJ, Huh MS, Park KH, Choi MS, Kim IS. Evaluation of an immunoglobulin M capture enzyme-linked immunosorbent assay for diagnosis of Orientia tsutsugamushi infection. Clin Diagn Lab Immunol. 2003;10(3):394-8.

88. Singh OB, Panda PK. Scrub Typhus. StatPearls. Treasure Island (FL) companies. Disclosure: Prasan Panda declares no relevant financial relationships with ineligible companies.2024.

89. Parola P, Paddock CD, Socolovschi C, Labruna MB, Mediannikov O, Kernif T, et al. Update on tick-borne rickettsioses around the world: a geographic approach. Clin Microbiol Rev. 2013;26(4):657-702.

90. Merhej V, Raoult D. Rickettsial evolution in the light of comparative genomics. Biol Rev Camb Philos Soc. 2011;86(2):379-405.

91. Walker DH, Ismail N. Emerging and re-emerging rickettsioses: endothelial cell infection and early disease events. Nat Rev Microbiol. 2008;6(5):375-86.

92. Silva-Pinto A, Santos Mde L, Sarmento A. Tick-borne lymphadenopathy, an emerging disease. Ticks Tick Borne Dis. 2014;5(6):656-9.

93. Alvarez-Hernandez G, Roldan JFG, Milan NSH, Lash RR, Behravesh CB, Paddock CD. Rocky Mountain spotted fever in Mexico: past, present, and future. Lancet Infect Dis. 2017;17(6):e189-e96.

94. Helmick CG, Bernard KW, D'Angelo LJ. Rocky Mountain spotted fever: clinical, laboratory, and epidemiological features of 262 cases. J Infect Dis. 1984;150(4):480-8.

95. Galanakis E, Bitsori M. Rickettsioses in children: a clinical approach. Adv Exp Med Biol. 2011;719:145-62.

96. Labruna MB, Santos FC, Ogrzewalska M, Nascimento EM, Colombo S, Marcili A, et al. Genetic identification of rickettsial isolates from fatal cases of Brazilian spotted fever and comparison with Rickettsia rickettsii isolates from the American continents. J Clin Microbiol. 2014;52(10):3788-91.

97. Biggs HM, Behravesh CB, Bradley KK, Dahlgren FS, Drexler NA, Dumler JS, et al. Diagnosis and Management of Tickborne Rickettsial Diseases: Rocky Mountain Spotted Fever and Other Spotted Fever Group Rickettsioses, Ehrlichioses, and Anaplasmosis - United States. MMWR Recomm Rep. 2016;65(2):1-44.

98. Paris DH, Dumler JS. State of the art of diagnosis of rickettsial diseases: the use of blood specimens for diagnosis of scrub typhus, spotted fever group rickettsiosis, and murine typhus. Curr Opin Infect Dis. 2016;29(5):433-9.

99. Regan JJ, Traeger MS, Humpherys D, Mahoney DL, Martinez M, Emerson GL, et al. Risk factors for fatal outcome from rocky mountain spotted Fever in a highly endemic area-Arizona, 2002-2011. Clin Infect Dis. 2015;60(11):1659-66.

100. Costa F, Hagan JE, Calcagno J, Kane M, Torgerson P, Martinez-Silveira MS, et al. Global Morbidity and Mortality of Leptospirosis: A Systematic Review. PLoS Negl Trop Dis. 2015;9(9):e0003898.

101. Thibeaux R, Iraola G, Ferres I, Bierque E, Girault D, Soupe-Gilbert ME, et al. Deciphering the unexplored Leptospira diversity from soils uncovers genomic evolution to virulence. Microb Genom. 2018;4(1).

102. Spichler A, Athanazio D, Seguro AC, Vinetz JM. Outpatient follow-up of patients hospitalized for acute leptospirosis. Int J Infect Dis. 2011;15(7):e486-90.

103. Turner LH. Leptospirosis. II. Serology. Trans R Soc Trop Med Hyg. 1968;62(6):880-99.

104. Karpagam KB, Ganesh B. Leptospirosis: a neglected tropical zoonotic infection of public health importance-an updated review. Eur J Clin Microbiol Infect Dis. 2020;39(5):835-46.

105. Thaipadungpanit J, Chierakul W, Wuthiekanun V, Limmathurotsakul D, Amornchai P, Boonslip S, et al. Diagnostic accuracy of real-time PCR assays targeting 16S rRNA and lipL32 genes for human leptospirosis in Thailand: a case-control study. PLoS One. 2011;6(1):e16236.

106. Haake DA, Levett PN. Leptospirosis in humans. Curr Top Microbiol Immunol. 2015;387:65-97.

107. Acestor N, Cooksey R, Newton PN, Menard D, Guerin PJ, Nakagawa J, et al. Mapping the aetiology of non-malarial febrile illness in Southeast Asia through a systematic review--terra incognita impairing treatment policies. PLoS One. 2012;7(9):e44269.

108. White NJ. Melioidosis. Lancet. 2003;361(9370):1715-22.

109. McRobb E, Sarovich DS, Price EP, Kaestli M, Mayo M, Keim P, et al. Tracing melioidosis back to the source: using whole-genome sequencing to investigate an outbreak originating from a contaminated domestic water supply. J Clin Microbiol. 2015;53(4):1144-8.

110. Basu S, Shetty A. Laboratory Diagnosis of Tropical Infections. Indian J Crit Care Med. 2021;25(Suppl 2):S122-S6.

111. Burrell CJ, Howard CR, Murphy FA. Laboratory Diagnosis of Virus Diseases. Fenner and White's Medical Virology. 2017:135-54.

112. Alcon S, Talarmin A, Debruyne M, Falconar A, Deubel V, Flamand M. Enzyme-linked immunosorbent assay specific to Dengue virus type 1 nonstructural protein NS1 reveals circulation of the antigen in the blood during the acute phase of disease in patients experiencing primary or secondary infections. J Clin Microbiol. 2002;40(2):376-81.

113. Bosch I, de Puig H, Hiley M, Carre-Camps M, Perdomo-Celis F, Narvaez CF, et al. Rapid antigen tests for dengue virus serotypes and Zika virus in patient serum. Sci Transl Med. 2017;9(409).

114. Machado BAS, Hodel KVS, Barbosa-Junior VG, Soares MBP, Badaro R. The Main Molecular and Serological Methods for Diagnosing COVID-19: An Overview Based on the Literature. Viruses. 2020;13(1).

115. Rogers R, O'Brien T, Aridi J, Beckwith CG. The COVID-19 Diagnostic Dilemma: a Clinician's Perspective. J Clin Microbiol. 2020;58(8).

116. Mullis KB, Faloona FA. Specific synthesis of DNA in vitro via a polymerase-catalyzed chain reaction. Methods Enzymol. 1987;155:335-50.

117. Waggoner JJ, Ballesteros G, Gresh L, Mohamed-Hadley A, Tellez Y, Sahoo MK, et al. Clinical evaluation of a single-reaction real-time RT-PCR for pan-dengue and chikungunya virus detection. J Clin Virol. 2016;78:57-61.

118. Valones MA, Guimaraes RL, Brandao LA, de Souza PR, de Albuquerque Tavares Carvalho A, Crovela S. Principles and applications of polymerase chain reaction in medical diagnostic fields: a review. Braz J Microbiol. 2009;40(1):1-11.

119. Spiegelman S, Haruna I, Holland IB, Beaudreau G, Mills D. The synthesis of a self-propagating and infectious nucleic acid with a purified enzyme. Proc Natl Acad Sci U S A. 1965;54(3):919-27.

120. Walker GT, Little MC, Nadeau JG, Shank DD. Isothermal in vitro amplification of DNA by a restriction enzyme/DNA polymerase system. Proc Natl Acad Sci U S A. 1992;89(1):392-6.

121. Barreda-Garcia S, Miranda-Castro R, de-Los-Santos-Alvarez N, Miranda-Ordieres AJ, Lobo-Castanon MJ. Helicase-dependent isothermal amplification: a novel tool in the development of molecular-based analytical systems for rapid pathogen detection. Anal Bioanal Chem. 2018;410(3):679-93.

122. Notomi T, Okayama H, Masubuchi H, Yonekawa T, Watanabe K, Amino N, et al. Loop-mediated isothermal amplification of DNA. Nucleic Acids Res. 2000;28(12):E63.

123. Nagamine K, Hase T, Notomi T. Accelerated reaction by loop-mediated isothermal amplification using loop primers. Mol Cell Probes. 2002;16(3):223-9.

124. Tomita N, Mori Y, Kanda H, Notomi T. Loop-mediated isothermal amplification (LAMP) of gene sequences and simple visual detection of products. Nat Protoc. 2008;3(5):877-82.

125. Panno S, Matic S, Tiberini A, Caruso AG, Bella P, Torta L, et al. Loop Mediated Isothermal Amplification: Principles and Applications in Plant Virology. Plants (Basel). 2020;9(4).

126. Piepenburg O, Williams CH, Stemple DL, Armes NA. DNA detection using recombination proteins. PLoS Biol. 2006;4(7):e204.

127. Crannell ZA, Rohrman B, Richards-Kortum R. Equipment-free incubation of recombinase polymerase amplification reactions using body heat. PLoS One. 2014;9(11):e112146.

128. Lillis L, Lehman D, Singhal MC, Cantera J, Singleton J, Labarre P, et al. Non-instrumented incubation of a recombinase polymerase amplification assay for the rapid and sensitive detection of proviral HIV-1 DNA. PLoS One. 2014;9(9):e108189.

129. Kersting S, Rausch V, Bier FF, von Nickisch-Rosenegk M. Rapid detection of Plasmodium falciparum with isothermal recombinase polymerase amplification and lateral flow analysis. Malar J. 2014;13:99.

130. Rohrman B, Richards-Kortum R. Inhibition of recombinase polymerase amplification by background DNA: a lateral flow-based method for enriching target DNA. Anal Chem. 2015;87(3):1963-7.

131. Li Y, Yu Z, Jiao S, Liu Y, Ni H, Wang Y. Development of a recombinase-aided amplification assay for rapid and sensitive detection of porcine circovirus 3. J Virol Methods. 2020;282:113904.

132. Yimer SA, Booij BB, Tobert G, Hebbeler A, Oloo P, Brangel P, et al. Rapid diagnostic test: a critical need for outbreak preparedness and response for high priority pathogens. BMJ Glob Health. 2024;9(4).

133. Land KJ, Boeras DI, Chen XS, Ramsay AR, Peeling RW. REASSURED diagnostics to inform disease control strategies, strengthen health systems and improve patient outcomes. Nat Microbiol. 2019;4(1):46-54.

134. Organization WH. World malaria report 2023. 2023.

135. Chappuis F, Alirol E, d'Acremont V, Bottieau E, Yansouni CP. Rapid diagnostic tests for non-malarial febrile illness in the tropics. Clin Microbiol Infect. 2013;19(5):422-31.

136. Allan-Blitz LT, Klausner JD. A Real-World Comparison of SARS-CoV-2 Rapid Antigen Testing versus PCR Testing in Florida. J Clin Microbiol. 2021;59(10):e0110721.

137. Gaspar-Castillo C, Rodriguez MH, Ortiz-Navarrete V, Alpuche-Aranda CM, Martinez-Barnetche J. Structural and immunological basis of cross-reactivity between dengue and Zika infections: Implications in serosurveillance in endemic regions. Front Microbiol. 2023;14:1107496.

138. Masyeni S, Santoso MS, Widyaningsih PD, Asmara DW, Nainu F, Harapan H, et al. Serological cross-reaction and coinfection of dengue and COVID-19 in Asia: Experience from Indonesia. Int J Infect Dis. 2021;102:152-4.

139. Nahm FS. Receiver operating characteristic curve: overview and practical use for clinicians. Korean J Anesthesiol. 2022;75(1):25-36.

140. Youden WJ. Index for rating diagnostic tests. Cancer. 1950;3(1):32-5.

141. Phokrai P, Karoonboonyanan W, Thanapattarapairoj N, Promkong C, Dulsuk A, Koosakulnirand S, et al. A Rapid Immunochromatography Test Based on Hcp1 Is a Potential Point-of-Care Test for Serological Diagnosis of Melioidosis. J Clin Microbiol. 2018;56(8).

142. Amornchai P, Hantrakun V, Wongsuvan G, Boonsri C, Yoosuk S, Nilsakul J, et al. Sensitivity and specificity of DPP(R) Fever Panel II Asia in the diagnosis of malaria, dengue and melioidosis. J Med Microbiol. 2022;71(8).

143. Dhawan S, Dittrich S, Arafah S, Ongarello S, Mace A, Panapruksachat S, et al. Diagnostic accuracy of DPP Fever Panel II Asia tests for tropical fever diagnosis. PLoS Negl Trop Dis. 2024;18(4):e0012077.

144. Lee RA. Clinical performance evaluation of the BioFire Joint Infection Panel. J Clin Microbiol. 2024;62(11):e0102224.

145. De Jesus VR, Mei JV, Bell CJ, Hannon WH. Improving and assuring newborn screening laboratory quality worldwide: 30-year experience at the Centers for Disease Control and Prevention. Semin Perinatol. 2010;34(2):125-33.

146. Mei J. Dried Blood Spot Sample Collection, Storage, and Transportation. Dried Blood Spots2014. p. 21-31.

147. Kivuyo SL, Johannessen A, Troseid M, Kasubi MJ, Gundersen SG, Naman E, et al. p24 antigen detection on dried blood spots is a feasible and reliable test for infant HIV infection in rural Tanzania. Int J STD AIDS. 2011;22(12):719-21.

148. Andersen NJ, Mondal TK, Preissler MT, Freed BM, Stockinger S, Bell E, et al. Detection of immunoglobulin isotypes from dried blood spots. J Immunol Methods. 2014;404:24-32.

149. Brambilla D, Jennings C, Aldrovandi G, Bremer J, Comeau AM, Cassol SA, et al. Multicenter evaluation of use of dried blood and plasma spot specimens in quantitative assays for

human immunodeficiency virus RNA: measurement, precision, and RNA stability. J Clin Microbiol. 2003;41(5):1888-93.

150. Demirev PA. Dried blood spots: analysis and applications. Anal Chem. 2013;85(2):779-89.

151. Mojica FJ, Diez-Villasenor C, Garcia-Martinez J, Soria E. Intervening sequences of regularly spaced prokaryotic repeats derive from foreign genetic elements. J Mol Evol. 2005;60(2):174-82.

152. Makarova KS, Haft DH, Barrangou R, Brouns SJ, Charpentier E, Horvath P, et al. Evolution and classification of the CRISPR-Cas systems. Nat Rev Microbiol. 2011;9(6):467-77.

153. Amitai G, Sorek R. CRISPR-Cas adaptation: insights into the mechanism of action. Nat Rev Microbiol. 2016;14(2):67-76.

154. Sapranauskas R, Gasiunas G, Fremaux C, Barrangou R, Horvath P, Siksnys V. The Streptococcus thermophilus CRISPR/Cas system provides immunity in Escherichia coli. Nucleic Acids Res. 2011;39(21):9275-82.

155. Jinek M, Chylinski K, Fonfara I, Hauer M, Doudna JA, Charpentier E. A programmable dual-RNA-guided DNA endonuclease in adaptive bacterial immunity. Science. 2012;337(6096):816-21.

156. Gratz SJ, Cummings AM, Nguyen JN, Hamm DC, Donohue LK, Harrison MM, et al. Genome engineering of Drosophila with the CRISPR RNA-guided Cas9 nuclease. Genetics. 2013;194(4):1029-35.

157. Cisneros-Aguirre M, Ping X, Stark JM. To indel or not to indel: Factors influencing mutagenesis during chromosomal break end joining. DNA Repair (Amst). 2022;118:103380.

158. Jasin M, Rothstein R. Repair of strand breaks by homologous recombination. Cold Spring Harb Perspect Biol. 2013;5(11):a012740.

159. Chang N, Sun C, Gao L, Zhu D, Xu X, Zhu X, et al. Genome editing with RNA-guided Cas9 nuclease in zebrafish embryos. Cell Res. 2013;23(4):465-72.

160. Abudayyeh OO, Gootenberg JS, Konermann S, Joung J, Slaymaker IM, Cox DB, et al. C2c2 is a single-component programmable RNA-guided RNA-targeting CRISPR effector. Science. 2016;353(6299):aaf5573.

161. Chen JS, Ma E, Harrington LB, Da Costa M, Tian X, Palefsky JM, et al. CRISPR-Cas12a target binding unleashes indiscriminate single-stranded DNase activity. Science. 2018;360(6387):436-9.

162. East-Seletsky A, O'Connell MR, Knight SC, Burstein D, Cate JH, Tjian R, et al. Two distinct RNase activities of CRISPR-C2c2 enable guide-RNA processing and RNA detection. Nature. 2016;538(7624):270-3.

163. Gootenberg JS, Abudayyeh OO, Lee JW, Essletzbichler P, Dy AJ, Joung J, et al. Nucleic acid detection with CRISPR-Cas13a/C2c2. Science. 2017;356(6336):438-42.

164. Gootenberg JS, Abudayyeh OO, Kellner MJ, Joung J, Collins JJ, Zhang F. Multiplexed and portable nucleic acid detection platform with Cas13, Cas12a, and Csm6. Science. 2018;360(6387):439-44.

165. Joung J, Ladha A, Saito M, Segel M, Bruneau R, Huang MW, et al. Point-of-care testing for COVID-19 using SHERLOCK diagnostics. medRxiv. 2020.

166. Teng F, Cui T, Feng G, Guo L, Xu K, Gao Q, et al. Repurposing CRISPR-Cas12b for mammalian genome engineering. Cell Discov. 2018;4:63.

167. Patchsung M, Jantarug K, Pattama A, Aphicho K, Suraritdechachai S, Meesawat P, et al. Clinical validation of a Cas13-based assay for the detection of SARS-CoV-2 RNA. Nat Biomed Eng. 2020;4(12):1140-9.

168. Patchsung M, Homchan A, Aphicho K, Suraritdechachai S, Wanitchanon T, Pattama A, et al. A Multiplexed Cas13-Based Assay with Point-of-Care Attributes for Simultaneous COVID-19 Diagnosis and Variant Surveillance. CRISPR J. 2023;6(2):99-115.

169. Chung CT, Miller RH. [43] Preparation and storage of competent Escherichia coli cells. In: Wu R, editor. Methods in Enzymology. 218: Academic Press; 1993. p. 621-7.

170. R Core Team. R: A Language and Environment for Statistical Computing_. Vienna, Austria: R Foundation for Statistical Computing; 2025.

171. Wickham H. Reshaping Data with the reshape Package. Journal of Statistical Software; 2007.

172. Wickham H, Vaughan D, Girlich M. tidyr: Tidy Messy Data. 1.3.1 ed2024.

173. Wickham H, Averick M, Bryan J, Chang W, McGowan L, François R, et al. Welcome to the tidyverse.: _Journal of Open Source Software_; 2019.

174. Wickham H, François R, Henry L, Müller K, Vaughan D. dplyr: A Grammar of Data Manipulation. 2023.

175. M G. stringi: Fast and portable character string processing in R.: _Journal of Statistical Software_; 2022.

176. Grolemund G, Wickham H. Dates and Times Made Easy with lubridate. Journal of Statistical Software; 2011.

177. Wickham H. ggplot2: Elegant Graphics for Data Analysis. pringer-Verlag New York; 2016.

178. Sonthayanon P, Chierakul W, Wuthiekanun V, Phimda K, Pukrittayakamee S, Day NP, et al. Association of high Orientia tsutsugamushi DNA loads with disease of greater severity in adults with scrub typhus. J Clin Microbiol. 2009;47(2):430-4.

179. Smythe LD, Smith IL, Smith GA, Dohnt MF, Symonds ML, Barnett LJ, et al. A quantitative PCR (TaqMan) assay for pathogenic Leptospira spp. BMC Infect Dis. 2002;2:13.

180. Su W, Jiang L, Lu W, Xie H, Cao Y, Di B, et al. A Serotype-Specific and Multiplex PCR Method for Whole-Genome Sequencing of Dengue Virus Directly from Clinical Samples. Microbiol Spectr. 2022;10(5):e0121022.

181. Kumar S, Stecher G, Li M, Knyaz C, Tamura K. MEGA X: Molecular Evolutionary Genetics Analysis across Computing Platforms. Mol Biol Evol. 2018;35(6):1547-9.

182. Stoddard RA, Gee JE, Wilkins PP, McCaustland K, Hoffmaster AR. Detection of pathogenic Leptospira spp. through TaqMan polymerase chain reaction targeting the LipL32 gene. Diagn Microbiol Infect Dis. 2009;64(3):247-55.

183. Loyola S, Torre A, Flores-Mendoza C, Kocher C, Salmon-Mulanovich G, Richards AL, et al. Molecular Characterization by Multilocus Sequence Typing and Diversity Analysis of Rickettsia asembonensis in Peru. Vector Borne Zoonotic Dis. 2022;22(3):170-7.

184. Blanton LS. The Rickettsioses: A Practical Update. Infect Dis Clin North Am. 2019;33(1):213-29.

185. Helminiak L, Mishra S, Kim HK. Pathogenicity and virulence of Rickettsia. Virulence. 2022;13(1):1752-71.

186. Perini M, Piazza A, Panelli S, Di Carlo D, Corbella M, Gona F, et al. EasyPrimer: user-friendly tool for pan-PCR/HRM primers design. Development of an HRM protocol on wzi gene for fast Klebsiella pneumoniae typing. Sci Rep. 2020;10(1):1307.

187. Klindworth A, Pruesse E, Schweer T, Peplies J, Quast C, Horn M, et al. Evaluation of general 16S ribosomal RNA gene PCR primers for classical and next-generation sequencing-based diversity studies. Nucleic Acids Res. 2013;41(1):e1.

188. Sonthayanon P, Chierakul W, Wuthiekanun V, Blacksell SD, Pimda K, Suputtamongkol Y, et al. Rapid diagnosis of scrub typhus in rural Thailand using polymerase chain reaction. Am J Trop Med Hyg. 2006;75(6):1099-102.

189. Pastorino B, Bessaud M, Grandadam M, Murri S, Tolou HJ, Peyrefitte CN. Development of a TaqMan RT-PCR assay without RNA extraction step for the detection and quantification of African Chikungunya viruses. J Virol Methods. 2005;124(1-2):65-71.

190. Xu Z, Peng Y, Yang M, Li X, Wang J, Zou R, et al. Simultaneous detection of Zika, chikungunya, dengue, yellow fever, West Nile, and Japanese encephalitis viruses by a two-tube multiplex real-time RT-PCR assay. J Med Virol. 2022;94(6):2528-36.

191. Wu W, Wang J, Yu N, Yan J, Zhuo Z, Chen M, et al. Development of multiplex real-time reverse-transcriptase polymerase chain reaction assay for simultaneous detection of Zika, dengue, yellow fever, and chikungunya viruses in a single tube. J Med Virol. 2018;90(11):1681-6.

192. Untergasser A, Cutcutache I, Koressaar T, Ye J, Faircloth BC, Remm M, et al. Primer3--new capabilities and interfaces. Nucleic Acids Res. 2012;40(15):e115.

193. Noir R, Kotera M, Pons B, Remy JS, Behr JP. Oligonucleotide-oligospermine conjugates (zip nucleic acids): a convenient means of finely tuning hybridization temperatures. J Am Chem Soc. 2008;130(40):13500-5.

194. Azar SR, Campos RK, Bergren NA, Camargos VN, Rossi SL. Epidemic Alphaviruses: Ecology, Emergence and Outbreaks. Microorganisms. 2020;8(8).

195. Pierson TC, Diamond MS. The continued threat of emerging flaviviruses. Nat Microbiol. 2020;5(6):796-812.

196. Joung J, Ladha A, Saito M, Kim NG, Woolley AE, Segel M, et al. Detection of SARS-CoV-2 with SHERLOCK One-Pot Testing. N Engl J Med. 2020;383(15):1492-4.

197. Seok Y, Batule BS, Kim MG. Lab-on-paper for all-in-one molecular diagnostics (LAMDA) of zika, dengue, and chikungunya virus from human serum. Biosens Bioelectron. 2020;165:112400.

198. Patel P, Abd El Wahed A, Faye O, Pruger P, Kaiser M, Thaloengsok S, et al. A Field-Deployable Reverse Transcription Recombinase Polymerase Amplification Assay for Rapid Detection of the Chikungunya Virus. PLoS Negl Trop Dis. 2016;10(9):e0004953.

199. Wessels HH, Mendez-Mancilla A, Guo X, Legut M, Daniloski Z, Sanjana NE. Massively parallel Cas13 screens reveal principles for guide RNA design. Nat Biotechnol. 2020;38(6):722-7.

200. Sagulenko P, Puller V, Neher RA. TreeTime: Maximum-likelihood phylodynamic analysis. Virus Evol. 2018;4(1):vex042.

201. Hadfield J, Megill C, Bell SM, Huddleston J, Potter B, Callender C, et al. Nextstrain: real-time tracking of pathogen evolution. Bioinformatics. 2018;34(23):4121-3.

202. Sidstedt M, Hedman J, Romsos EL, Waitara L, Wadso L, Steffen CR, et al. Inhibition mechanisms of hemoglobin, immunoglobulin G, and whole blood in digital and real-time PCR. Anal Bioanal Chem. 2018;410(10):2569-83.

203. Diagne CT, Faye M, Lopez-Jimena B, Abd El Wahed A, Loucoubar C, Fall C, et al. Comparative Analysis of Zika Virus Detection by RT-qPCR, RT-LAMP, and RT-RPA. Methods Mol Biol. 2020;2142:165-79.

204. Esposito DLA, Fonseca B. Sensitivity and detection of chikungunya viral genetic material using several PCR-based approaches. Rev Soc Bras Med Trop. 2017;50(4):465-9.

205. Gurukumar KR, Priyadarshini D, Patil JA, Bhagat A, Singh A, Shah PS, et al. Development of real time PCR for detection and quantitation of Dengue Viruses. Virol J. 2009;6:10.

206. Barnard TR, Wang AB, Sagan SM. A highly sensitive strand-specific multiplex RT-qPCR assay for quantitation of Zika virus replication. J Virol Methods. 2022;307:114556.

207. Sagar R, Raghavendhar S, Jain V, Khan N, Chandele A, Patel AK, et al. Viremia and clinical manifestations in acute febrile patients of Chikungunya infection during the 2016 CHIKV outbreak in Delhi, India. Infect Med (Beijing). 2024;3(1):100088.

208. Santiago GA, Sharp TM, Rosenberg E, Sosa C, II, Alvarado L, Paz-Bailey G, et al. Prior Dengue Virus Infection Is Associated With Increased Viral Load in Patients Infected With Dengue but Not Zika Virus. Open Forum Infect Dis. 2019;6(7).

209. Wang G, Fu R, Zhang L, Xue L, Al-Mahdi AY, Xie X, et al. Genomic bacterial load associated with bacterial genotypes and clinical characteristics in patients with scrub typhus in Hainan Island, Southern China. PLoS Negl Trop Dis. 2023;17(4):e0011243.

210. Poloni TR, Oliveira AS, Alfonso HL, Galvao LR, Amarilla AA, Poloni DF, et al. Detection of dengue virus in saliva and urine by real time RT-PCR. Virol J. 2010;7:22.

211. Musso D, Teissier A, Rouault E, Teururai S, de Pina JJ, Nhan TX. Detection of chikungunya virus in saliva and urine. Virol J. 2016;13:102.

212. da Conceicao PJP, de Carvalho LR, de Godoy BLV, Nogueira ML, Terzian ACB, de Godoy MF, et al. Detection of DENV-2 and ZIKV coinfection in southeastern Brazil by serum and urine testing. Med Microbiol Immunol. 2023;212(3):193-201.

213. Mizuno Y, Kotaki A, Harada F, Tajima S, Kurane I, Takasaki T. Confirmation of dengue virus infection by detection of dengue virus type 1 genome in urine and saliva but not in plasma. Trans R Soc Trop Med Hyg. 2007;101(7):738-9.

214. Myhrvold C, Freije CA, Gootenberg JS, Abudayyeh OO, Metsky HC, Durbin AF, et al. Field-deployable viral diagnostics using CRISPR-Cas13. Science. 2018;360(6387):444-8.

215. Wu J, Mukama O, Wu W, Li Z, Habimana JD, Zhang Y, et al. A CRISPR/Cas12a Based Universal Lateral Flow Biosensor for the Sensitive and Specific Detection of African Swine-Fever Viruses in Whole Blood. Biosensors (Basel). 2020;10(12).

216. Gruner N, Stambouli O, Ross RS. Dried blood spots--preparing and processing for use in immunoassays and in molecular techniques. J Vis Exp. 2015(97).

217. Zimmerman C, J S, M D, C S, S S, Winegar R, et al. Real-Time RT-PCR Diagnostic Assay for the Detection of the Zika Virus (ZIKV) in Febrile Patients Using the BD Max™ System2016.

218. Townsend MW, DeLuca PP. Stability of ribonuclease A in solution and the freeze-dried state. J Pharm Sci. 1990;79(12):1083-6.

219. Li J, Ulloa GM, Mayor P, Santolalla Robles ML, Greenwood AD. Nucleic acid degradation after long-term dried blood spot storage. Mol Ecol Resour. 2024;24(6):e13979.

220. Robin X, Turck N, Hainard A, Tiberti N, Lisacek F, Sanchez J-C, et al. pROC: an open-source package for R and S+ to analyze and compare ROC

curves. BMC Bioinformatics; 2011.

221. Kuhn M. Building Predictive Models in R Using the caret Package. Journal of Statistical Software; 2008.

222. Mardekian SK, Roberts AL. Diagnostic Options and Challenges for Dengue and Chikungunya Viruses. Biomed Res Int. 2015;2015:834371.

223. Guzman MG, Halstead SB, Artsob H, Buchy P, Farrar J, Gubler DJ, et al. Dengue: a continuing global threat. Nat Rev Microbiol. 2010;8(12 Suppl):S7-16.

224. WHO Guidelines on Drawing Blood: Best Practices in Phlebotomy. WHO Guidelines Approved by the Guidelines Review Committee. Geneva2010.

225. Shah JA. Learnings from Thailand in building strong surveillance for malaria elimination. Nat Commun. 2022;13(1):2677.

226. Linsuwanon P, Auysawasdi N, Wongwairot S, Leepitakrat S, Rodkhamtook W, Wanja E, et al. Assessing scrub typhus and rickettsioses transmission risks in the Chiang Rai province of northern Thailand. Travel Med Infect Dis. 2021;42:102086.

227. Wangrangsimakul T, Elliott I, Nedsuwan S, Kumlert R, Hinjoy S, Chaisiri K, et al. The estimated burden of scrub typhus in Thailand from national surveillance data (2003-2018). PLoS Negl Trop Dis. 2020;14(4):e0008233.

228. Indrayan A, Malhotra RK, Pawar M. Use of ROC curve analysis for prediction gives fallacious results: Use predictivity-based indices. J Postgrad Med. 2024;70(2):91-6.

229. Chang HH, Huber RG, Bond PJ, Grad YH, Camerini D, Maurer-Stroh S, et al. Systematic analysis of protein identity between Zika virus and other arthropod-borne viruses. Bull World Health Organ. 2017;95(7):517-25I.

230. Kellner MJ, Koob JG, Gootenberg JS, Abudayyeh OO, Zhang F. SHERLOCK: nucleic acid detection with CRISPR nucleases. Nat Protoc. 2019;14(10):2986-3012.

231. Baden T, Chagas AM, Gage GJ, Marzullo TC, Prieto-Godino LL, Euler T. Open Labware: 3-D printing your own lab equipment. PLoS Biol. 2015;13(3):e1002086.

232. Pathak B, Chakravarty A, Krishnan A. High viral load positively correlates with thrombocytopenia and elevated haematocrit in dengue infected paediatric patients. J Infect Public Health. 2021;14(11):1701-7.

233. Segura ER, Ganoza CA, Campos K, Ricaldi JN, Torres S, Silva H, et al. Clinical spectrum of pulmonary involvement in leptospirosis in a region of endemicity, with quantification of leptospiral burden. Clin Infect Dis. 2005;40(3):343-51.

234. Ezenarro JJ, Mas J, Muñoz-Berbel X, Uria N. Advances in bacterial concentration methods and their integration in portable detection platforms: A review. Anal Chim Acta. 2022;1209:339079.

235. Cheng AC, Peacock SJ, Limmathurotsakul D, Wongsuvan G, Chierakul W, Amornchai P, et al. Prospective evaluation of a rapid immunochromogenic cassette test for the diagnosis of melioidosis in northeast Thailand. Trans R Soc Trop Med Hyg. 2006;100(1):64-7.

CHAPTER 9

Appendices

9.1. Supplementary tables

Table S 1: List of PCR oligonucleotides.

Target organism	Gene	Type	3' modification	Sequence (5'-3')	5' modification
Homo sapiens	RNase P3	Forward		CCAAGTGTGAGGGCTGAAAAG	
		Reverse		TGTTGTGGCTGATGAACTATAAAAGG	
		Probe	BHQ-2	CCCCAGTCTCTGTCAGCACTCCCTTC	Cy5
Rickettsia spp.	Citrate synthase (gltA)	Forward		ATCGAGGATATGATATTAAAGACTTA	
		Reverse		GCAAGCATAATAGCCATAGGA	
		Probe	ZNA-4-BHQ-1	ACTAATGMATGATGAGCAAYCT	6-FAM
O. tsutsugamushi	16S rDNA	Forward		CCCATCAGTACGGAATAACA	
		Reverse		CTCTCAGACCAGCTACAGATCACA	
		Probe	BHQ-1	GCGGCAGATTAGGTAGTTGGTAAGGT	HEX
Leptospira spp.	16S rDNA	Forward		CCCGCGYCCGATTAG	
		Reverse		GTCTCAGTTCCATTGTGGC	
		Probe	BHQ-2	CTCACCAAGGCGACGATCGGTAGC	Cy5.5
Eubacteria	16S rDNA	Forward		TRCGGGRGGCWGCA	
		Reverse		CTACCRGGGTATCTAATCC	

		Probe	ZNA-2-BHQ-2	GTGCCAGCAGCCG	Texas Red
DENV/JEV	3'UTR	Forward		AAGGACTAGAGGTTAGAGGAGAC	
DENV	3'UTR	Reverse		GCGTTCTGTGCCTGGAATG	
		Reverse		CGCTCTGTGCCTGGATTG	
		Probe	BHQ-2	GGGARAGACCAGAGATCCTGCTGTCTC	Texas Red
JEV	3'UTR	Reverse		ATACTTCGGCGCTCTGTG	
		Probe	BHQ-1	GACACCTGGGAATAGACTGGGAGATCTTC	6-FAM
ZIKV	E	Forward		CGCCCAATTCACCAAGAGC	
		Reverse		GCATGTGCGTCCTTGAACTC	
		Reverse		GCATGKGCATCCTTGAACTC	
		Probe	BHQ-1	GGAGTTCCGGTGTCTGCCCCAGC	6-FAM
CHIKV	E1	Forward		CTCCGCGTCCTTTACCAAG	
		Reverse		CCAAATTGTCCTGGTCTTCCTG	
		Probe	BHQ-2	CAAAAGGTGTCCAGGCTGAAGACATTGGC	Cy5.5

Table S 2: List of LAMP primers. The T7 promotor sequence is denoted in lowercase.

Target organism	Gene	Type	Sequence (5'-3')
CHIKV	E2	F3	TCCCGACTGTGGAGAAGG
		B3	CGTACACGGTGCTGATGTTC
		FIP	CCGATTTGCAAGGAGACCTGGAAGTCCCGTAGCACTAGAACG
		BIP	GACGGATGACAGCCACGATTGGAAATAGCCCCGCCCTCTC
		LF	CGTCTGTCGCTTCATTTCTGATG
		LB	CACATGCCAGCAGACGCA
		FIP with T7 promotor	taatacgactcactatagAGTCCCGTAGCACTAGAACG
DENV	Polyprotein	F3	ACCTACACCCAGGATCGG
		B3	GGCGTGACACATAAGGTCAA
		FIP	GTGGGAGCTAGAACTAGCGTGCTACCTTCCAGCCATAGTCCG
		BIP	CTCTGAAATGGCAGAGGCGCTCCTTTCCCGTGTGTTCACTC
		LF	GCAGCTTTCTTTTTATGGCCTCA
		LB	CAAGGGAATGCCAATAAGGTATCA

Table S 3: List of RAA primers The T7 promoter sequence is denoted in lowercase.

Name	Target organism	Gene	Type	Sequence (5'-3')
CHIKV-Fv1			Forward	taatacgactcactatagggTGCAACGTGCGTACCCCATGTTTGAGGTGGAA
CHIKV-F-v2	CHIKV	nsP1	Forward	taatacgactcactatagggATAGACGCTGACAGCGCCTTTTTGAAGGCCCT
CHIKV-R			Reverse	TTCCTGTCCGACATCATCCTCCTTGCTGGCGC
DENV-F1	DENV	3'UTR	Forward	taatacgactcactatagggKYRGACTAGYGGTTAGAGGAGACCCCTCCC
WH_DENV134-F	DENV1, 3, 4		Forward	taatacgactcactatagggTTGAGCAAACCGTGCTGCCTGTAGCTCC
WH_DENV2-F	DENV2		Forward	taatacgactcactatagggTTGAGTAAACTATGCAGCCTGTAGCTCC
DENV-R	DENV		Reverse	GATCTCTGGTCTYTCCCAGCGTCAATATGCTG
ZIKV-F	ZIKV	Polyprotein	Forward	taatacgactcactatagggGCTCCTTTATTTCCACAGAAGGGACCTCCG
ZIKV-R			Reverse	TGGTCGTTCTCCTCAATCCACACTCTGTTCCA

Table S 4: List of the first iteration of RAA primers for CHIKV.

Target	Name	Sequence
CHIKV	WH_CHInsP1-RF	TGCAACGTGCGTACCCCATGTTTGAGGTGGAA
	WH_CHInsP1-RF-T7	taatacgactcactatagggTGCAACGTGCGTACCCCATGTTTGAGGTGGAA
	WH_CHInsP1-RR	TTCCTGTCCGACATCATCCTCCTTGCTGGCGC

Table S 5: List of LwaCas13a crRNA. The LwaCas13a direct repeat sequence is denoted in lowercase.

Target organism	Sequence (5'-3')
CHIKV	gauuuagacuaccccaaaaacgaaggggacuaaaacCACCUCAAACAUGGGGUACGCAC
DENV	gauuuagacuaccccaaaaacgaaggggacuaaaacGUCUCCUCUAACCUCUAGUCCUU
ZIKV	gauuuagacuaccccaaaaacgaaggggacuaaaacUGUUCAUCUGUGCCAGUUGACUGG

Table S 6: List of crRNA sequences containing T7 promotors to synthesise crRNA in-house. The T7 promotor is shown in lowercase and the LwaCas13a direct repeat is shown in bold.

Target	Strand	Sequence (5' - 3')
CHIKV	Sense	taatacgactcactatagg**GATTTAGACTACCCCAAAAACGAAGGGGACTAAAAC**CACCTCAAACATGGGGTACGCAC
		taatacgactcactatagg**GATTTAGACTACCCCAAAAACGAAGGGGACTAAAAC**CCACCTCAAACATGGGGTACGCA
		taatacgactcactatagg**GATTTAGACTACCCCAAAAACGAAGGGGACTAAAAC**ACCTCAAACATGGGGTACGCACG
		taatacgactcactatagg**GATTTAGACTACCCCAAAAACGAAGGGGACTAAAAC**TTTATAGCTAGATGCGAGAACGC
		taatacgactcactatagg**GATTTAGACTACCCCAAAAACGAAGGGGACTAAAAC**CCTCAAACATGGGGTACGCACGT
	Antisense	ACGTGCGTACCCCATGTTTGAGG**GTTTTAGTCCCCTTCGTTTTTGGGGTAGTCTAAATC**cctatagtgagtcgtatta
		GCGTTCTCGCATCTAGCTATAAA**GTTTTAGTCCCCTTCGTTTTTGGGGTAGTCTAAATC**cctatagtgagtcgtatta
		CGTGCGTACCCCATGTTTGAGGT**GTTTTAGTCCCCTTCGTTTTTGGGGTAGTCTAAATC**cctatagtgagtcgtatta
		TGCGTACCCCATGTTTGAGGTGG**GTTTTAGTCCCCTTCGTTTTTGGGGTAGTCTAAATC**cctatagtgagtcgtatta
		GTGCGTACCCCATGTTTGAGGTG**GTTTTAGTCCCCTTCGTTTTTGGGGTAGTCTAAATC**cctatagtgagtcgtatta
DENV	Sense	taatacgactcactatagg**GATTTAGACTACCCCAAAAACGAAGGGGACTAAAAC**AGTCCTTTCAGTGAGACTACAGC
		taatacgactcactatagg**GATTTAGACTACCCCAAAAACGAAGGGGACTAAAAC**TCATCTCACCTTGGGCCCCCATT
		taatacgactcactatagg**GATTTAGACTACCCCAAAAACGAAGGGGACTAAAAC**TTCATCTCACCTTGGGCCCCCAT
		taatacgactcactatagg**GATTTAGACTACCCCAAAAACGAAGGGGACTAAAAC**GGGCCCCCATTGTTGCTGCGATT
		taatacgactcactatagg**GATTTAGACTACCCCAAAAACGAAGGGGACTAAAAC**CATCTCACCTTGGGCCCCCATTG

Antisense	CAATGGGGGCCCAAGGTGAGATG**GTTTTAGTCCCCTTCGTTTTTGGGGTAGTCTAAATC**cctatagtgagtcgtatta
	AATCGCAGCAACAATGGGGGCCC**GTTTTAGTCCCCTTCGTTTTTGGGGTAGTCTAAATC**cctatagtgagtcgtatta
	ATGGGGGCCCAAGGTGAGATGAA**GTTTTAGTCCCCTTCGTTTTTGGGGTAGTCTAAATC**cctatagtgagtcgtatta
	AATGGGGGCCCAAGGTGAGATGA**GTTTTAGTCCCCTTCGTTTTTGGGGTAGTCTAAATC**cctatagtgagtcgtatta
	GCTGTAGTCTCACTGAAAGGACT**GTTTTAGTCCCCTTCGTTTTTGGGGTAGTCTAAATC**cctatagtgagtcgtatta

Table S 7: List of concentrations used in the PCR assay.

Assay	Target	Oligonucleotide	Final reaction concentration
RELO/JeCDZ	RNase P3	Forward	0.0125 pmol/µL
		Reverse	0.0125 pmol/µL
		Probe	0.0125 pmol/µL
RELO	*Rickettsia* spp.	Forward	0.20 pmol/µL
		Reverse	0.20 pmol/µL
		Probe	0.20 pmol/µL
	O. tsutsugamushi	Forward	0.20 pmol/µL
		Reverse	0.20 pmol/µL
		Probe	0.15 pmol/µL
	Leptospira spp.	Forward	0.05 pmol/µL
		Reverse	0.05 pmol/µL
		Probe	0.075 pmol/µL
	Eubacteria	Forward	0.30 pmol/µL
		Reverse	0.30 pmol/µL
		Probe	0.20 pmol/µL
JeCDZ	DENV/JEV	Forward	0.448 pmol/µL
	DENV	Reverse	0.288 pmol/µL
		Reverse	0.288 pmol/µL
		Probe	0.409 pmol/µL
	JEV	Reverse	0.273 pmol/µL
		Probe	0.0275 pmol/µL
	ZIKV	Forward	0.248 pmol/µL
		Reverse	0.11 pmol/µL
		Reverse	0.11 pmol/µL
		Probe	0.358 pmol/µL
	CHIKV	Forward	0.22 pmol/µL
		Reverse	0.22 pmol/µL
		Probe	0.275 pmol/µL

Table S 8: List of cycling programs for real-time PCR and CRISPR detection reactions.

Program	Temperature	Time
WBBac01		
1)	95.0°C	2 minutes
2)	95.0°C	5 seconds
3)	58.0°C	30 seconds
4)	Read signal from all channels	
5)	Go to step 2) 44 times	
6)	25.0°C	5 minutes
WBVir00		
1)	55.0°C	20 minutes
2)	95.0°C	2 minutes
3)	95.0°C	12 seconds
4)	63.5°C	45 seconds
5)	Read signal from all channels	
6)	Go to step 2) 44 times	
7)	25.0°C	5 minutes
CRISPR-Cas13		
1)	37.0°C	2:30 minutes
2)	Read signal from all channels	
3)	Go to 1) 47 times	
crRNA_AMP		
1)	98°C	30 seconds
2)	98°C	30 seconds
3)	58°C	30 seconds
4)	72°C	20 seconds/kb
5)	Go to step 2) 33 times	
6)	72°C	5 minutes
7)	12°C	Hold

Table S 9: List of Rickettsia species used in primer design.

Group	Species	Strain	Accession
Spotted fever group	*R. conorii*	Malish 7	NC_003103.1
	R. heilongjiangensis	54	NC_015866.1
		CH8-1	NZ_AP019862.1
		HCN-13	NZ_AP019863.1
		Sendai-29	NZ_AP019864.1
		Sendai-58	NZ_AP019865.1
	R. honei	NTT-118	U59726.1
		N/A	AF018074.1
		N/A	AF022817.1
	R. japinoca	HH07167	NZ_AP017576.1
		MZ08014	NZ_AP017577.1
		Nakase	NZ_AP017578.1
		Tsuneishi	NZ_AP017581.1
		YH_M	NZ_AP017602.1
	R. rickettsii	Sheila Smith	NC_009882.1
		Brazil	NC_016913.1
		Arizona	NC_016909.1
		Iowa	NZ_CP018913.1
		Iowa	NZ_CP018914.1
Typhus	*R. prowazekii*	Madrid E	NC_017048.1
		GvV257	NC_017049.1
		Chernikova	NC_017050.1
		Katsinyian	NC_017056.1
		BuV67-CWPP	NC_017057.1
		RpGvF24	NC_017560.1
		Rp22	NC_020992.1

		NMRC Madrid E	NC_020993.1
		Breinl	NZ_CP014865.1
		Naples-1	NC_017048.1
	R. typhi	Wilmington	NC_006142.1
		B9991CWPP	NC_017062.1
		TH1527	NC_017066.1
		TM2540	NZ_LS992663.1
Transitional	*R. felis*	URRWXCal2	CP000053.1
		LI16	JN375498.1
		URRWXCal2	NC_007109.1

Table S 10: List of O. tsutsugamushi strains used in primer design.

***O. tsutsugamushi* strain/isolate**	**Accession numbers**
07-280	HM352765.1
Boryong	NC_009488.1
Gilliam	D38622.1, NZ_LS398551.1, U17256.1
Ikeda	NC_010793.1
Karp	D38623.1, NR_025860.1, NR_118785.1, NZ_LS398548.1, U17257.1
Kato	D38624.1, NZ_LS398550.1
Kawasaki	D38625.1
Kuroki	D38626.1
Shimokoshi	D38627.1
UT176	NZ_LS398547.1
UT76	NZ_LS398552.1
Wuj/2014	NZ_CP044031.1

Table S 11: List of Leptospira species used in primer design.

***Leptospira* species**	**Accession numbers**
L. adleri	MK688976.1
L. alexanderi	NR_043047.1
L. alstonii	MK720176.1
L. baratonii	MK791625.1
L. biflexa	NR_043043.1
L. borgpertersenii	NR_043259.1, NR_114969.1
L. broomi	NR_043200.1
L. dzianensis	MN060986.1
L. ellinghausenii	NPEH01000112.1, NPEF01000404.1
L. fainei	NR_043049.1
L. inadai	NR_115269.1
L. interrogans	NR_114968.1, NR_116542.1
L. johnsonii	LC196061.1
L. kirschneri	NR_043051.1
L. kmetyi	NR_041544.1
L. licerasiae	NR_044310.1
L. mayottensis	NR_134067.1
L. nogushii	NR_043050.1, NR_115926.1
L. putramalaysiae	MN062724.1
L. saintgironsiae	MN047234.1
L. santarosai	NR_043048.1
L. sarikeiensis	MN062730.1
L. selangorensis	MN062732.1
L. stimsonii	QHCS01000002.1, QHCT01000027.1
L. tipperaryensis	CP015217.1
L. venezuelensis	MK688379.1

L. weilii	NR_118435.1, NR_119300.1, NR_043044.1
L. wolffii	NR_044042.1
L. yasudae	QHCR01000024.1, QHCU01000018.1

Table S 12: List of Eubacteria species used in primer design.

Eubacteria species	Strain	Gram type	Accession number
Acinetobacter calcoaceticus	NCCB 22016	Gram-negative	NR_042387.1
Actinomyces israelii	D5aditya	Gram-positive	LC810201.1
Actinomyces meyeri	Prevot 2477B	Gram-positive	NR_029286.1
Bacteroides fragilis	NCTC 9343	Gram-negative	NR_074784.2
Burkholderia pseudomallei	ATCC 23343	Gram-negative	NR_043553.1
Clostridium botulinum	ELTDK 103	Gram-positive	NR_029157.1
Clostridium difficile	5 N-1	Gram-positive	NR_197708.1
Clostridium septicum	Pasteur III	Gram-positive	NR_026020.1
Corynebacterium jeikeium	A376/84	Gram-positive	NR_037035.1
Enterobacter aerogenes	KCTC 2190	Gram-negative	NR_102493.2
Enterococcus faecalis	JCM 5803	Gram-positive	NR_040789.1
Enterococcus faecium	LMG 11423	Gram-positive	NR_042054.1
Enterococcus gallinarum	NBRC 100675	Gram-positive	NR_113924.1
Escherichia coli	U 5/41	Gram-negative	NR_024570.1
Faecalibacterium prausnitzii	ATCC 27768	Gram-positive	NR_028961.1
Filifactor alocis	ATCC 35896	Gram-positive	NR_074645.1
Francisella tularensis	B-38	Gram-negative	NR_029362.1
Fusobacterium naviforme	ATCC 25832	Gram-negative	AF342840.1
Fusobacterium necrophorum	ATCC 25286	Gram-negative	NR_042365.1
Fusobacterium nucleatum	ATCC 25586	Gram-negative	NR_074412.1
Fusobacterium periodonticum	EK1-15	Gram-negative	NR_026085.1
Fusobacterium sulci	ATCC 35585	Gram-negative	NR_025289.1

Haemophilus aphrophilus	CCUG 32956	Gram-negative	DQ223313.1
Haemophilus ducreyi	CIP 54.2	Gram-negative	NR_044741.1
Haemophilus parahaemolyticus	536	Gram-negative	NR_025938.1
Haemophilus paraphrophilus	180703ADIE	Gram-negative	AY360333.1
Haemophilus pittmaniae	HK85	Gram-negative	NR_025423.1
Klebsiella pneumoniae	DSM 30104	Gram-negative	NR_036794.1
Leptospira interrogans	RGA	Gram-negative	NR_029361.1
Listeria grayi	KKP 1070	Gram-positive	ON799416.1
Listeria monocytogenes	NCTC 10357	Gram-positive	NR_044823.1
Moraxella catarrhalis	Ne 11	Gram-negative	NR_028669.1
Mycobacterium avium	5617	Gram-positive	NR_026082.1
Mycobacterium fortuitum	M213	Gram-positive	GU142933.1
Mycobacterium gordonae	ATCC 14470	Gram-positive	NR_044812.1
Mycobacterium intracellulare	FI-0169	Gram-positive	NR_029003.1
Mycobacterium kansasii	ATCC 12478	Gram-positive	NR_121712.2
Mycobacterium scrofulaceum	ATCC 19981	Gram-positive	NR_025237.1
Neisseria gonorrhoeae	NCTC 8375	Gram-negative	NR_026079.2
Neisseria lactamica	NCTC 10617	Gram-negative	NR_028899.1
Neisseria Mucosa	N16	Gram-negative	NR_117696.1
Nocardia brasiliensis	DSM 43758	Gram-positive	NR_041860.1
Nocardia pseudobrasiliensis	DSM 44290	Gram-positive	NR_041864.1
Oligella urethralis	Brest	Gram-negative	MH285271.1
Orientia tsutsugamushi	Karp	Gram-negative	NR_025860.1
Parvimonas micra	3119B	Gram-positive	NR_036934.1
Plesiomonas shigelloides	NCIMB 9242	Gram-negative	NR_044827.1
Proteus mirabilis	NCTC 11938	Gram-negative	NR_043997.1
Proteus vulgaris	ATCC 29905	Gram-negative	NR_115878.1
Pseudomonas aeruginosa	DSM 50071	Gram-negative	NR_026078.1

Pseudomonas stutzeri	NBRC 14165	Gram-negative	AB680573.1
Rhodococcus equi	084-07	Gram-positive	EF680931.1
Rickettsia rickettsii	R	Gram-negative	NR_028018.1
Salmonella paratyphi A	ATCC 9150	Gram-negative	AF057361.1
Serratia marcescens	KRED	Gram-negative	NR_036886.1
Shigella boydii	P288	Gram-negative	NR_104901.1
Shigella dysenteriae	ATCC 13313	Gram-negative	NR_026332.1
Staphylococcus caprae	ATCC 35538	Gram-positive	NR_024665.1
Staphylococcus equorum	PA 231	Gram-positive	NR_027520.1
Staphylococcus haemolyticus	SM 131	Gram-positive	NR_036955.1
Staphylococcus hominis	DM 122	Gram-positive	NR_036956.1
Staphylococcus lugdunensis	ATCC 43809	Gram-positive	NR_024668.1
Staphylococcus schleiferi	DSM 4807	Gram-positive	NR_037009.1
Staphylococcus simulans	MK 148	Gram-positive	NR_036906.1
Staphylococcus warneri	AW 25	Gram-positive	NR_025922.1
Streptococcus agalactiae	ATCC 13813	Gram-positive	NR_040821.1
Streptococcus aureus	JP080	Gram-positive	AP017922.1
Streptococcus gordonii	SK3	Gram-positive	NR_028666.1
Streptococcus intermedius	1877	Gram-positive	NR_028736.1
Streptococcus pneumoniae	ATCC 33400	Gram-positive	NR_028665.1
Streptococcus pyogenes	I-273	Gram-positive	NR_028598.1
Streptococcus salivarius	ATCC 7073	Gram-positive	NR_042776.1
Streptococcus suis	S735	Gram-positive	NR_036918.1
Streptococcus uberis	JCM 5709	Gram-positive	NR_040820.1
Vibrio cholerae	RC782	Gram-negative	NR_044050.1
Viridans streptococci	ATCC 19258	Gram-positive	NR_042778.1
Yersinia enterocolitica	ATCC 9610	Gram-negative	NR_041832.1

Table S 13: List of sequences used for the viral real-time RT-PCR assay primer design.

Virus	Accession numbers
CHIKV	MW349426.1, OK316990.1, LC664154.1, LC664159.1, OL705486.1, OL979153.1, MW574902.1, MT495605.1, MN974208.1, MN974220.1
DENV1	LC652827.1, LC652828.1, MW396465.1, MW828678.1, OK448162.1
DENV2	MW512341.1, NC001474.2, OK605760.1, ON123651.1, ON398847.1
DENV3	LC436676.1, MN018375.1, NC001475.2, OK605763.1, OK605764.1
DENV4	MW793459.1, MZ285058.1, OK605599.1, OK605771.1, ON123668.1
JEV	LC461958.1, LC461960.1, LC461961.1, LC687612.1, LC708273.1, MK495877.1, MT134112.1, MT232844.1, MT859415.1, OK423757.1
ZIKV	KU955593.1, KX051561.1, KX601167.1, MH158236.1, MT377500.1, MT377502.1, MW015936.1, MW680969.1, MZ008356.1, OK054351.1, OL414716.1, AY632535.2, MN101548.1, KU321639.1

9.2. Design of the magnetic stand for nucleic acid purification

The magnetic stand was designed in Fusion 360 (Autodesk, San Francisco, CA, US) not only to address these problems, but also to improve the user experience in both usage and fabrication. The stand is composed of two parts; the base and the tube clips. The base acts as a tube rack with four slots for four tubes. The back of each slot was designed with a groove that accommodates a 10 x 5 x 2 mm magnet per slot to hold each clip in place. Each tube clip was designed to mechanically snap onto standard 1.5 mL tubes and contain an indent that hold a ø5 x 2 mm cylindrical magnet that would not only attract the magnetic beads inside the tube, but enables the clips to snap into the slots in the base. This allows for the users to handle the tubes more freely while the magnet is actively pulling on the magnetic beads. With this clip, removing the supernatant can be as simply done as inverting the tube over a waste bin, as the magnetic beads are constantly pulled against the magnet. Having separate magnets for each tube also allows for multiple users to perform purification on multiple tubes simultaneously. All parts were fabricated from polylactic acid (PLA) filaments at a total cost of 5.01 THB per base and 0.32 THB per one clip. The magnets were commercially available neodymium magnets costing 2.0 and 1.2 THB per bar magnet cylindrical magnet respectively. Thus, the total cost of the entire stand for four sample is 19.09 THB (roughly 0.40 GBP).

The bases for the DPP® Fever Panel II Asia system was designed using the free online program Tinkercad (Autodesk, San Francisco, CA, US). The cost of fabrication is 9.03 THB (0.21 GBP) and 12.30 (0.28 GBP) for the antigen and IgM antibody systems.

All fabrication was done using a personal machine, a modified Ender-3 v2 (Creality, Shenzhen, China). The models were designed specifically for 3D printing to be easily printed on any machine without supports.

9.3. DPP® Fever II Asia System booklet

MoMiLDE MORU Tropical Health Network

Source Data for Chembio DPP® Fever Panel II Asia IgM Antibody and Antigen Systems

Date: _____ Time: _____

Patient ID: _____ Performer: _____

DPP antigen system

	Band present		☐ Pass	☐ Fail
	Yes	No	Target	Values
1	☐	☐	CHIK	
2	☐	☐	pLDH	
3	☐	☐	DEN	
C	☐	☐		
4	☐	☐	ZIKA	
5	☐	☐	HRP II	
6	☐	☐	BURK	
C	☐	☐		
Note:				

DPP IgM antibody system

	Band present		☐ Pass	☐ Fail
	Yes	No	Target	Values
1	☐	☐	CHIK	
2	☐	☐	ZIKA	
3	☐	☐	LEPTO	
C	☐	☐		
4	☐	☐	OT	
5	☐	☐	RT	
6	☐	☐	DEN	
C	☐	☐		
Note:				

Checklist

Fill in google form and upload images

DPP® Fever Panel II Asia Antigen System

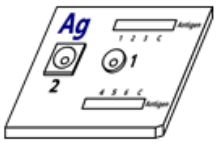

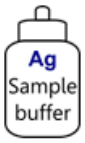

DPP® Fever Panel II Asia IgM Antibody System

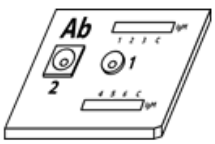

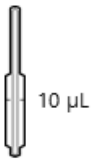

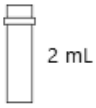

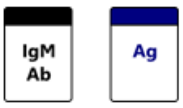

RFID cards

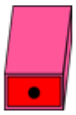

Lancet

Cotton ball

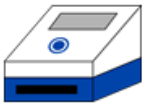

Recommended timer app: **MultiTimer**

Preparations

1 ☐ Put stickers on the caps of the **sample buffers**

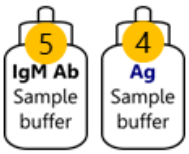

2 ☐ 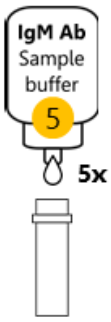

3 ☐ 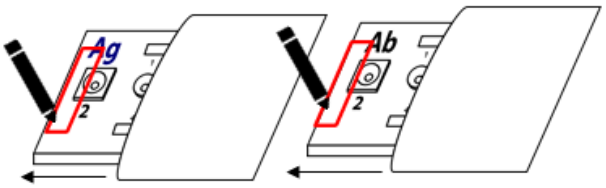

Remove cassettes from packaging and label patient ID along the left edge

4 ☐ Perform finger prick

5 ☐ 

Add blood to the Ab sample buffer

Squeeze out blood from the tube

Set aside until **step B1**

6 ☐ Prepare 4 timers

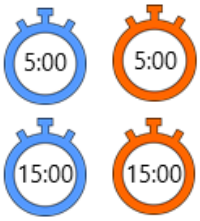

DPP Antigen System

A1 ☐ 

A2 ☐ 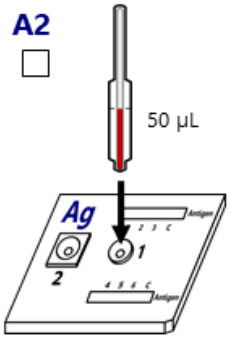

! Immediately move to **step A3** !

A3 ☐ 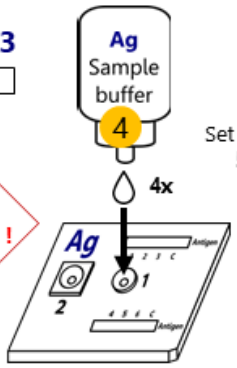

Set first timer for **5 minutes**

A5 ☐ 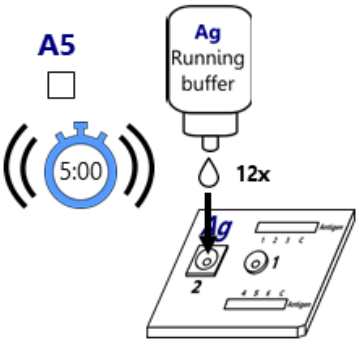

Set first timer for **15 minutes**

Set aside until **step C2**

MoMiLDE MORU Tropical Health Network

DPP IgM Antibody System

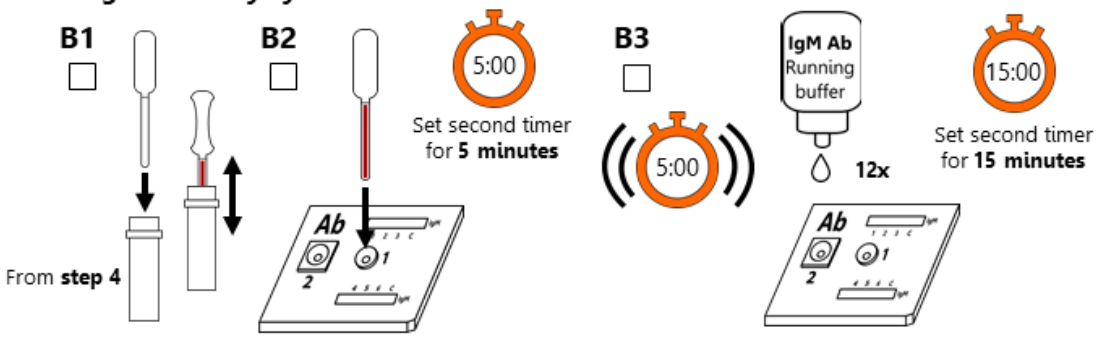

Mix IgM Ab sample buffer and blood well with 100 µL transfer pipette

Set aside until **step C2-2**

Micro Reader 2

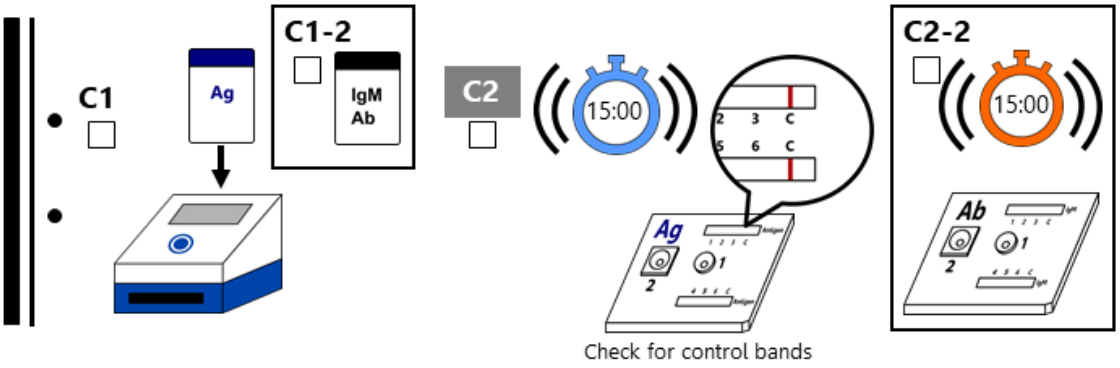

Check for control bands

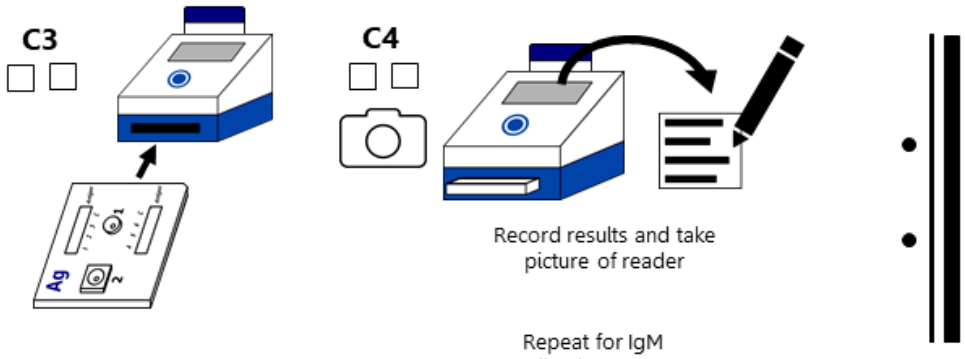

Record results and take picture of reader

Repeat for IgM antibody cassette

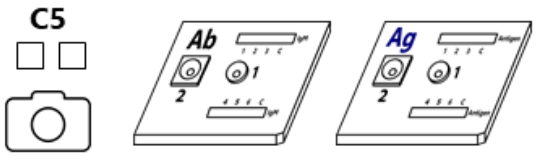

Take pictures of each cassettes and collect the cassettes for return

Results

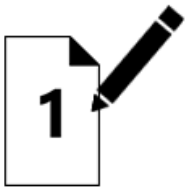

Record the results on **page 1**

Enter data and upload pictures onto google form

Reader sample image

Make sure the values and patient ID are visible

For any questions or issues, contact Witchayoot Huangsuranun
witchayoot@tropmedres.ac
or official line group